

Ruprecht-Karls-Universität Heidelberg
Fakultät für Biowissenschaften

PhD Thesis

**High-confidence fusion gene detection in
different tumor entities & biomarker discovery
in breast cancer**

Zhiqin Huang

January, 2016

Referees

Prof. Dr. Benedikt Brors

Prof. Dr. Peter Lichter

Huang, Zhiqin:

*High-confidence fusion gene detection in different tumor entities
& biomarker discovery in breast cancer*

PhD Thesis Bioinformatics

Ruprecht-Karls-Universität Heidelberg

Thesis period: 08.2012 – 01.2016

INAUGURAL DISSERTATION

submitted to the

Combined Faculties for Natural Sciences and for Mathematics
of the Ruperto-Carola University of Heidelberg, Germany
for the degree of
Doctor of Natural Sciences

presented by

Zhiqin Huang, M.Sc.
born in Guangxi, China

Date of oral examination: March 21, 2016

High-confidence fusion gene detection in different tumor entities & biomarker discovery in breast cancer

Referees

Prof. Dr. Benedikt Brors

Prof. Dr. Peter Lichter

Acknowledgements

First and foremost I would like to thank Prof. Dr. Peter Licher, who was my supervisor, for giving me the opportunity to do this thesis project. I really appreciate the challenges that were given to me during this thesis.

I would also like to thank Dr. Marc Zapatka for his advice and supervision during this project. I am very thankful to Prof. Dr. Benedikt Brors and Dr. Jan Korbel as my thesis advisory members for providing necessary guidance.

I sincerely express heartfelt thanks to Dr. David T.W. Jones, Dr. Yonghe Wu, Dr. Barbara Worst, Dr. Andrius Serva, Dr. Verena Thewes, Dr. Michael Fletcher and Dr. Wei Wang for helping me and sharing their valuable experience. I also thank Achim Stephan for technical assistance. Huge thanks to Dr. Zuguang Gu and Dr. Volker Hovestadt for valuable discussion and sharing experience in bioinformatics. With your great help, the project became much more easier and was finished successfully.

I am also grateful to cooperation partners in Prof. Dr. Benedikt Brors's group, Prof. Dr. Thorsten Zenz's group, Prof. Dr. med. Reiner Siebert's group, Prof. Dr. Holger Sültmann's group, Prof. Dr. med. Stefan Pfister's group and Prof. Dr. Roland Eils's group. Thanks a lot for sharing their data and giving bioinformatic support. I also thank Prof. Dr. med. Peter Sinn, Prof. Dr. Barbara Burwinkel and Prof. Dr. med. Andreas Schneweiss for providing patient samples and clinical data. I felt very happy in working on these different projects involved in German Cancer Research Center (Deutsches Krebsforschungszentrum, DKFZ) and National Center for Tumor Diseases (Nationale Centrum für Tumorerkrankungen, NCT) in Heidelberg.

Finally, I would like to express my gratitude to my parents (Yongsen Huang & Yuying Chen) and members in my whole family who have supported me in every possible way.

Herzlichen Dank für Ihre Hilfe und Unterstützung.

首先，衷心感谢我的父母（陈玉英和黄永森），感谢他们孜孜不倦的教诲，感谢他们无时无刻的关怀和支持。同时，也衷心感谢所有曾经给予我帮助和关心的亲戚们，朋友们，同学们和老师们。最后，衷心祝愿您们有一个美好的明天和一个美满的生活！

黄智勤，2016年1月于海德堡

Abstract

Fusion genes play an important role in the tumorigenesis of many cancers. Next generation sequencing (NGS) methods such as RNA-seq provide accurate, high-resolution data, which makes unbiased fusion detection much more feasible. Most fusion detection tools based on RNA-seq data report a great number of candidates (mostly false positives), making it hard to prioritize candidates for validation. I therefore developed confFuse, a scoring algorithm to reliably select high-confidence fusion genes which are likely to be biologically relevant.

Compared with alternative tools based on 96 published RNA-seq samples from six different tumor entities, confFuse dramatically reduces the number of fusion candidates (301 high-confidence from 8083 predicted fusion genes, ~3.7%) and retains high detection accuracy (recovery rate 85.7% of previously validated fusions). Another analysis of 27 unpublished tumors of various origins, results in a recovery rate of ~93% (25/27). Furthermore, a screen of 22 GBM tumors shows 242 high-confidence fusions from 6,018 candidates (~4%), of which ~62% (150/242) were previously validated or harbor supporting reads in DNA-seq. Similarly, in 11 published prostate cancer tumors ~72% high-confidence fusions (17/24 from 849 predictions) have supporting evidence. Validation of 18 high-confidence fusions detected in three primary breast tumor samples resulted in a 100% true positive rate. When applying confFuse on three CLL samples, 15 of 18 candidates were successfully validated. In summary, confFuse can reliably select high-confidence fusion genes that are more likely to be biologically relevant, achieving both high validation rate and high detection accuracy, while reducing the number of candidates to a restricted number for validation.

A genetic analysis of primary and refractory breast cancer tumors identified different aberrations in CNVs, SNVs/Indels and rearrangements. Mutations of microtubule-associated serine-threonine kinase (MAST) and 1-phosphatidylinositol-4,5-bisphosphate phosphodiesterase beta (PLCB) gene family members were only detected in refractory tumors (3/50 and 4/50, respectively). Mutations of members of the calcium channel, voltage-dependent, alpha (CACNA) gene family members, which are involved in the MAPK signalling pathway, are highly prevalent in refractory tumors (24%, 12/50) compared to primary tumors (~2%, 1/46). Rearrangements of CACNA were also identified in one primary and two refractory tumors, and PLCB in three

refractory tumors. This suggests that mutations of MAST, CACNA or PLCB gene families may be a novel acquired resistance mechanism in addition to ESR1 mutation.

Hundreds of known or novel fusion genes were identified by confFuse in seven unpublished tumor cohorts, including more than 60 highly reliable fusion proteins in breast cancer. Furthermore, different chromosome-wide enrichments of fusion genes were identified across tumor entities. Overall, a comprehensive landscape of fusion genes in different tumor entities was provided to give an insight for biomarker discovery, especially in breast cancer.

Zusammenfassung

Fusionsgene spielen eine wichtige Rolle in der Tumorgenese von vielen Krebsarten. Next Generation Sequencing (NGS) Methoden wie RNA-Sequenzierung erlauben die Erfassung von genauen Expressionsprofilen und ermöglichen die genomweite Erkennung von exprimierten Fusionsgenen. Die meisten Algorithmen, die Fusionengene auf Basis von RNA-Sequenzierungsdaten erkennen, identifizieren eine große Anzahl von Kandidaten (vermutlich meist falsch positive), was es erschwert, Kandidaten für die Validierung zu priorisieren. Ich entwickelte deshalb confFuse, einen Algorithmus zur Bewertung von Fusionsgenen, um zuverlässig solche zu identifizieren, die voraussichtlich biologisch relevant sind.

Basierend auf 96 veröffentlichten und validierten Fusionsgenen aus sechs Tumorentitäten wurde confFuse mit alternativen Algorithmen verglichen. Es kann die Anzahl der Fusionsgenkandidaten drastisch reduzieren (Reduktion von 8083 Fusionsgenkandidaten auf 301, ~3.7%) und trotzdem eine hohe Sensitivität erreichen (Identifikation von 85,7% der validierten Fusionsgene). Eine weitere Analyse von 27 unveröffentlichten Tumoren verschiedenen Ursprungs, resultierte in einer Identifikation von 93% validierbaren Fusionsgenen (25/27). Eine Untersuchung von 22 GBM Tumoren ergab eine Reduktion von 6018 Kandidaten auf 242 (~4%), von denen ~62% (150/242) experimentell validiert werden konnten oder auch in der DNA-Sequenzierung detektiert werden. In elf Prostatakarzinomen konnten ebenfalls ~72% der getesteten Fusionsgenkandidaten verifiziert werden (17/24 validiert aus 849 Kandidaten). In Brustkrebstumoren konnten alle 18 getesteten, mittels confFuse identifizierten Fusionen, experimentell validiert werden. Bei der Untersuchung von drei CLL Proben wurden 15 von 18 Kandidaten erfolgreich validiert. Zusammenfassend kann confFuse zuverlässig Fusionsgene identifizieren, die sich experimentell validieren lassen und reduziert die Anzahl der Fusionsgenkandidaten auf eine realistische Anzahl für die Validierung.

Eine genetische Analyse der Kopienzahlveränderungen, Mutationen und Insertionen/Deletionen von primären und refraktären Brustkrebstumoren ergab verschiedene Veränderungen. Mutationen der Mikrotubuli-assoziierten Serin-Threoninkinase (MAST) und der 1-Phosphatidylinositol-4,5-bisphosphat-Phosphodiesterase beta (PLCB) Gene Familie wurden nur in refraktären Tumoren (3/50 und 4/50) detektiert. Mutationen der Gene Familie des span-

nungsabhängigen Kalzium-Kanals alpha (CACNA), die am MAPK-Signalweg beteiligt ist, sind häufiger in refraktären Tumoren (24%, 12/50) als in primären ($\sim 2\%$, 1/46). DNA-Struktur-Umlagerungen von CACNA wurden in einem primären und zwei refraktären Tumoren, sowie für PLCB in drei refraktären Tumoren identifiziert. Diese Veränderungen in MAST, CACNA oder PLCB Familie Genes könnten neben der Mutation von ESR1 ein weiterer Resistenzmechanismus sein.

Es wurden hunderte von bekannten oder neuen Fusionsgenen durch confFuse in sieben unveröffentlichten Kohorten, darunter mehr als 60 Fusionsgene bei Brustkrebs identifiziert. Außerdem konnten Häufungen von Fusionsgenen auf spezifischen Chromosomen in den untersuchten Tumorentitäten identifiziert werden. Insgesamt konnten nach der Entwicklung von confFuse eine umfassende Analyse der Fusionsgene in verschiedenen Tumorentitäten durchgeführt werden und so, vor allem bei Brustkrebs, potentielle Biomarker identifiziert werden.

Contents

Acknowledgements	i
Abstract	iii
Zusammenfassung	v
1 Introduction	1
1.1 Genetics and cancer	1
1.2 Breast cancer genomics	1
1.3 Mechanisms of fusion gene generation	7
1.4 Detection of fusion genes	10
1.5 “deFuse” algorithm	15
1.6 Objectives	15
2 Material and methods	19
2.1 Material	19
2.2 NGS data analysis	20
2.2.1 Whole-genome sequencing analysis	20
2.2.2 Whole-exome sequencing analysis	20
2.2.3 RNA sequencing analysis	21
2.3 “confFuse” algorithm	23
3 Results	27
3.1 CNVs and SNVs/Indels in breast cancer	27
3.1.1 CNVs in breast cancer	27

3.1.2 Somatic mutations in breast cancer	28
3.1.3 Expression of mutant allele in breast cancer	31
3.2 ConfFuse	32
3.2.1 Generation of artefact list	32
3.2.2 Recovery rate of validated fusions	34
3.2.3 Comparison of alternative fusion detection tools	34
3.2.4 Comparison of deFuse probability and confFuse confidence score	38
3.2.5 Validation of confFuse predicted candidates	38
3.2.6 ConfFuse performance in data sets with verified fusion genes	38
3.3 Fusion genes in different tumor entities	43
3.3.1 Sarcoma	43
3.3.2 Prostate cancer	44
3.3.3 Glioblastoma multiforme	45
3.3.4 Germinal-center derived B-cell malignant lymphoma	47
3.3.5 B-cell chronic lymphocytic leukemia	52
3.3.6 Ependymoma	57
3.3.7 Breast cancer	60
3.3.7.1 Ras superfamily	61
3.3.7.2 Solute carrier family	62
3.3.7.3 HIF1 pathway	62
3.3.7.4 Notch pathway	62
3.3.7.5 TP53 pathway	62
3.3.7.6 Estrogen pathway	62
3.3.7.7 Ras pathway	63
3.3.7.8 ErbB pathway	63
3.3.7.9 PI3K-AKT-mTOR pathway	64
3.3.7.10 MAPK pathway	66
3.3.7.11 Tumor suppressor gene	66
3.3.7.12 Oncogene	66
3.3.7.13 Census gene (COSMIC)	68
3.3.7.14 Recurrent fusions	68

3.3.7.15 Fusions related to tamoxifen and estrogen metabolism	69
3.3.7.16 Potential fusion proteins	70
3.3.7.17 Fusions in paired primary-refractory breast tumors	72
3.3.8 Fusion features across entities	72
4 Discussion and outlook	77
4.1 Fusion gene detection	77
4.1.1 ConfFuse performance	77
4.1.2 Problems with deFuse	78
4.1.3 Possible improvement	79
4.2 Fusion genes in different tumor entities	79
4.3 Biomarker discovery in breast cancer	80
4.3.1 CNV	80
4.3.2 SNV/Indel	80
4.3.3 Fusion-related genes	81
4.4 Outlook	83
Supplementary	85
Bibliography	171
List of Figures	189
List of Tables	193

Chapter 1

Introduction

1.1 Genetics and cancer

Cancer is a genetic disease arising from a multistep process of sequential alterations in different types of genes, including oncogenes, tumor suppressor genes or microRNA genes [1, 2]. These alterations include germline mutations (inherited variants) and somatic mutations (also called acquired mutations). There are at least five types of somatic mutations, namely point mutations (single nucleotide substitutions), insertions, deletions, gene amplifications and gene fusions in genetic alterations. An example of somatic genetic alteration is the structural chromosome rearrangement, Philadelphia chromosome, first identified in chronic myeloid leukaemia (CML) by chromosome banding analysis [3]. After that, molecular cytogenetic techniques, such as fluorescence in situ hybridization (FISH) and high-throughput microarray-based analysis, played an important role in detecting genes associated with tumorigenesis and identified many genes involved in fusions in neoplastic disorders, such as fusions BCR:ABL1, IGH:MYC in Burkitt lymphoma and TMPRSS2:ERG in prostate cancer [3, 4].

1.2 Breast cancer genomics

Breast cancer is one of the most common cancers and occurs much more often in women than in men. It is a heterogeneous disease originating from breast tissue and counts for >1,300,000 cases and >450,000 deaths each year all over the world [5]. More than 2/3 cases express estrogen receptor- α (ER α $^+$) [6, 7] and approximately 12%-17% of cases have triple-negative breast cancer lacking expression of estrogen receptor (ER), progesterone receptor (PR) and HER2 [8]. Approximately 0.3% (\sim 1/300) women under age 40 were diagnosed with breast cancer in the world [9]. Currently, treatment of breast cancer mostly depends on biologically intrinsic

subtypes which are classified into luminal A, luminal B, HER2-enriched and triple-negative based on clinico-pathology [10]. A great many aspects of breast cancer biology have already been investigated, including copy number variants (CNVs), single nucleotide variants (SNVs), mRNA, microRNA, antisense RNA and alternative splicing RNA.

- **Copy number variants**

The copy number variants (CNVs) and single nucleotide polymorphisms (SNPs) are associated with ~40% of expressed genes based on a study cohort of ~2000 breast tumors [11]. Ten novel subgroups of breast cancer patients were classified by integrating CNVs and gene expression profiling data based on ~2000 breast tumor samples (method called intClust) [11]. These ten subgroups/subtypes have been demonstrated that they were correlated with different clinical outcomes [11].

- **Single nucleotide variants**

Four studies, in which more than 1000 whole-exome/-genome sequencing (WES/WGS) samples were totally analyzed, show different numbers of significantly mutated genes (SMGs) in breast cancer, including six SMGs of false discovery rate (FDR) <0.1 in 103 samples [12], 18 SMGs of FDR<0.26 in 79 samples [13], 35 SMGs of FDR<0.05 in 507 samples [5] and 32 SMGs of FDR<0.1 in 892 samples [14]. Four SMGs (TP53, PIK3CA, GATA3 and MAP3K1) have been identified in these four studies. In addition, analysis of 79 ER⁺ and 21 ER⁻ primary breast cancer shows driver mutations in nine cancer genes (ARID1B, CASP8, MAP3K1, MAP3K13, NCOR1, SMARCD1, CDKN1B and AKT2) [15]. A summary of somatically mutated genes in key signalling pathways in primary breast cancer is given in Figure 1.1.

Two recent studies of aromatase inhibitor-resistant metastatic breast cancers revealed a high mutation rate of ESR1, which indicates activating ESR1 mutations is a key mechanism in acquired endocrine resistance during breast cancer treatment [6, 7]. A prevalence of mutations in TP53, PIK3CA and GATA3 was comparable in both primary and relapsed breast tumors, whereas much higher mutation rate of ESR1, ERBB3 and RPTOR was observed in aromatase inhibitor-resistant relapsed breast cancers (Figure 1.2.a). Some identified ESR1 mutations are located in the functional ligand-binding domain (LBD) (Figure 1.2.c and Figure 1.3). Some of the LBD-localized ESR1 mutations can constitutively activate and continue responsiveness to anti-estrogen therapy *in vitro* [7]. Furthermore, several amplified genes such as ERBB2, CCND1 and FGFR1 were identified and these genes have been reported to be associated with hormone resistance (Figure 1.2.b) [6].

- **Messenger RNA**

Gene expression profiling by microarray has given us deep insight into understanding breast cancer and has been used to provide prognostic and predictive information, such as 50-gene PAM50 intrinsic subtypes [18, 19], 21-gene OncotypeDx assay [20, 21] and 70-gene MammaPrint

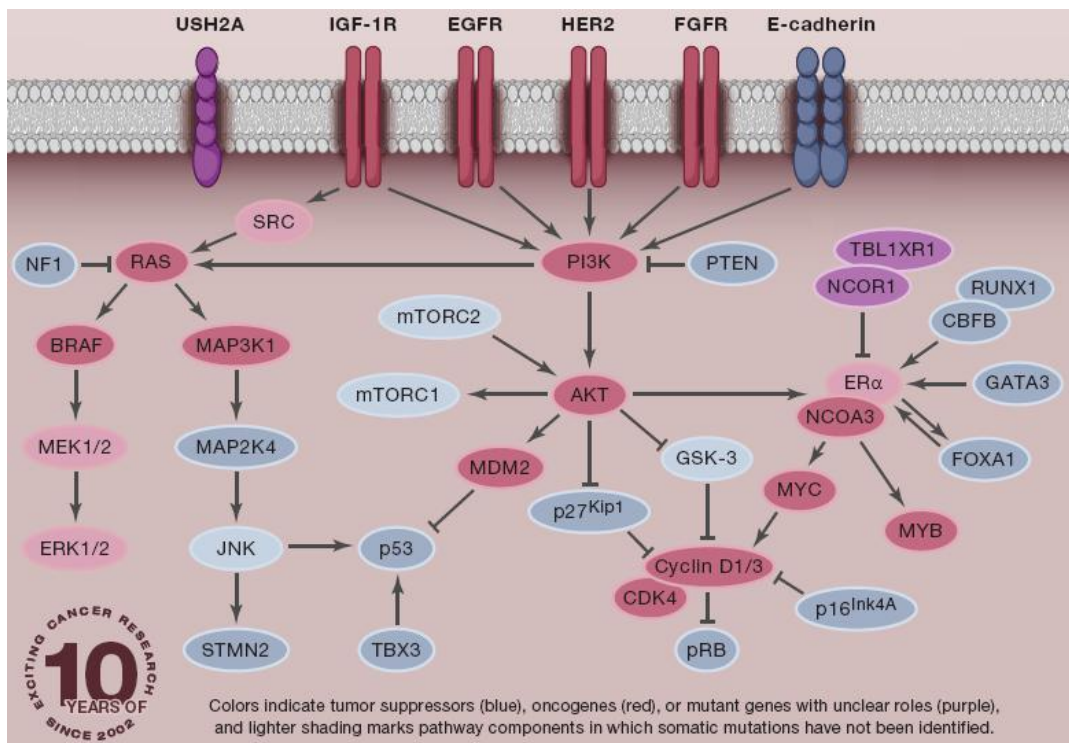


Figure 1.1: Key signalling pathways in breast cancer based on somatically mutated genes. There are four significantly mutated genes, namely TP53 (p53), PIK3CA (PI3K), GATA3 and MAP3K1, in primary breast cancer (FDR<0.1). Image source:[16].

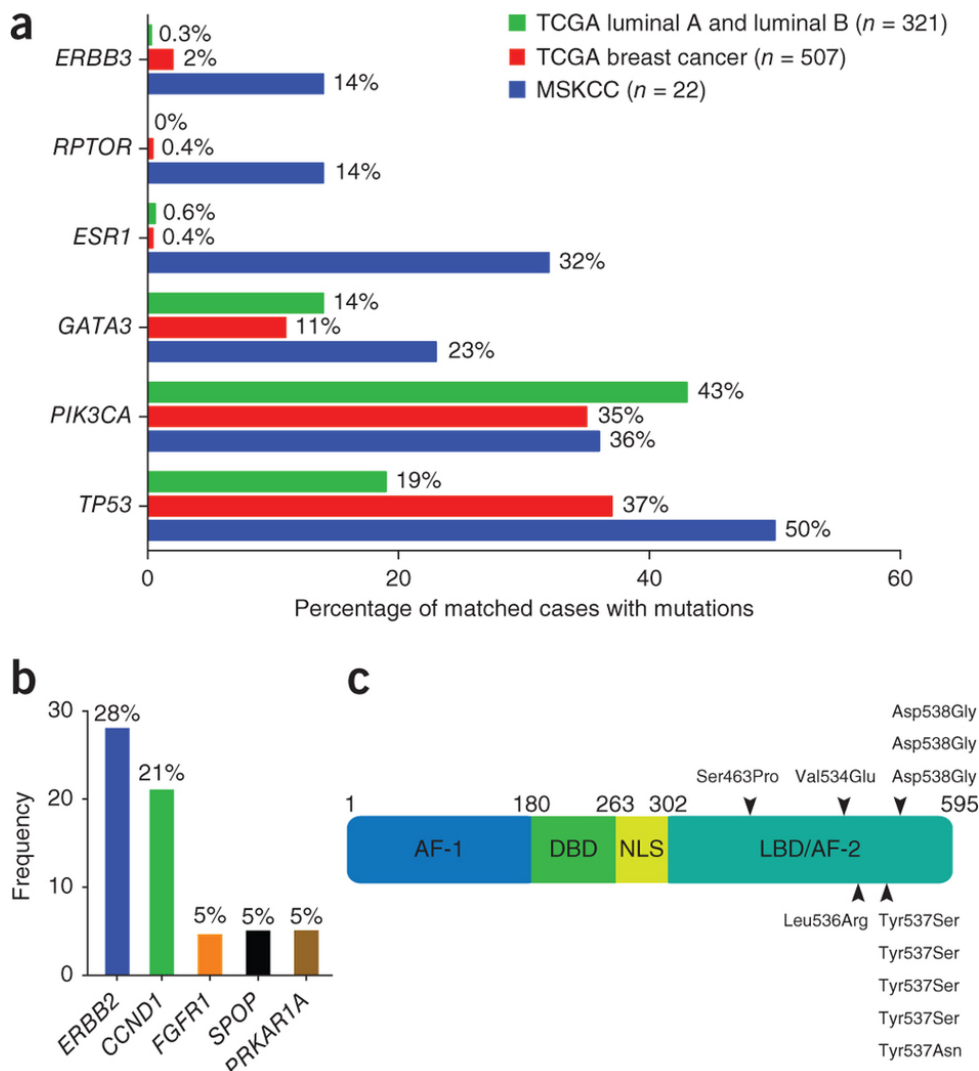


Figure 1.2: Top mutated and amplified genes in metastatic breast cancers. (a) Comparison of top 6 mutated genes in aromatase inhibitor-resistant relapsed breast cancers and the ones in primary breast cancer and luminal A & luminal B cases in TCGA data set. Mutated genes identified in more than 10% samples were shown. Three mutated genes (ESR1, RPTOR and ERBB3) are of much higher rates in relapsed samples. (b) Top amplified genes in relapsed breast cancers. Fold change of copy number in tumor and normal samples is greater than 2. (c) The structure domains of ER α and location of identified mutations in ligand-binding domains (LBD). Image source:[6].

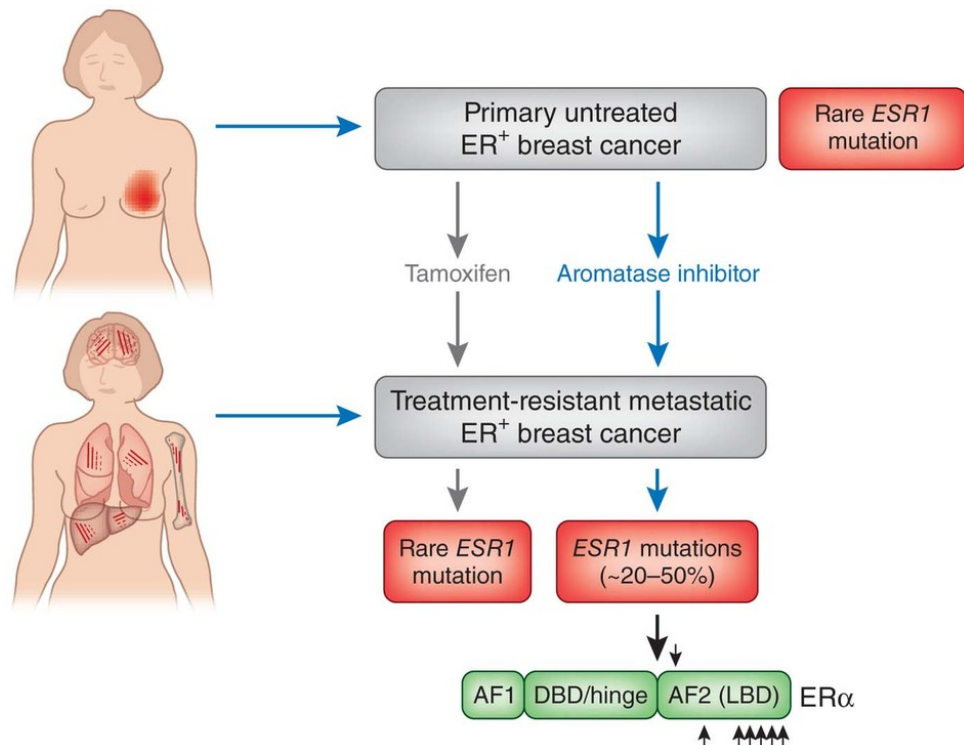


Figure 1.3: ESR1 mutation in metastatic breast cancer. Rare ESR1 mutations can be identified in primary and tamoxifen treatment-resistant metastatic ER⁺ breast cancers. The ER α structure includes activation function 1 (AF1) domain, DNA-binding domain (DBD) and activation function 2 (AF2) which contains ligand-binding domain (LBD). Most of the ER α mutations locate in LBD (small black arrows). Image source:[17].

[22, 23]. Those studies showed the correlation between gene-expression profiling and clinical outcomes as well as between gene-expression profiling and response to chemotherapy [24]. Analysis of gene-expression profiling based on DNA microarray has confirmed that “*breast cancer is not a single disease with variable morphologic features and biomarkers but, rather, a group of molecularly distinct neoplastic disorders*” [24]. A recent study has developed a novel method to classify breast cancer into ten previously validated subgroups (intClust) based on 612 gene expression profiling [25].

- **MicroRNAs**

MicroRNAs (20-23 nucleotides in length) play an important role in cell differentiation, apoptosis and cell cycle regulation [26]. There are at least three types of microRNAs, including oncogenic, tumor-suppressive and metastatic-influencing microRNAs in the pathogenesis of breast cancer [27]. For example, microRNA-10b can promote cell migration and invasion as well as initiate metastasis through targeting homeobox D10 (HOXD10) in breast cancer [28, 29]. Analysis of 1,302 breast tumors showed that microRNAs are associated with differential co-expression of mRNA and confirmed that “*miRNAs act as modulators of mRNA-mRNA interactions rather than as on-off molecular switches*” [30].

- **Antisense RNA**

Recently, a newly developed RNA-seq library protocol, strand-specific RNA-seq [31, 32], can preserve strand information of the transcript for RNA sequencing, which makes antisense gene expression detectable in the analysis of next-generation sequencing data. A study of 376 cancer samples (strand-specific RNA-seq) from nine different tissue types including breast cancer shows 44 cancer-specific antisense loci involving tumor suppressor genes or oncogenes [33]. More than 38% of annotated transcripts have consistent antisense transcript expression which is positively correlated with sense transcript expression [33]. In addition, several functional natural antisense transcripts have been identified, such as NKX2-1-AS1 which can regulate NKX2-1 oncogene and cell proliferation in lung cancer cells [33].

- **Alternative splicing RNA**

Alternative pre-mRNA splicing is a process of genetic regulation, which results in multiple proteins from a single gene [34]. In the analysis of RNA splicing alteration in breast cancer, subtype specific differentially spliced genes and spliced isoforms were identified and the predominant splice events are exon skipping and intron retention [35].

- **Targeting agents against breast cancer**

Many targeting agents against breast cancer are now under clinical development. Those agents are classified into three groups based on targeted cellular compartments including breast cancer cells, breast cancer stem cells and breast cancer microenvironment [36]. Different agents targeting functional genes in oncogenic signalling pathways are under development, including

PI3K-AKT-mTOR pathway, IGF signalling pathway, FGF signalling pathway, MET and MAPK signalling pathway (Figure 1.4) [36].

- **Reported fusions in breast cancer**

Several recurrent fusions have been identified and experimentally validated in breast cancer cells or tissues, such as MYB:NFIB in adenoid cystic carcinoma of the breast [37], ETV6:NTRK3 in secretory breast carcinomas [38], microtubule-associated serine-threonine kinase (MAST) rearrangements and Notch gene family rearrangements [39], as well as ESR1:CCDC170 in ER⁺ breast tumors [40]. Another recurrent fusion MAGI3:AKT3 has been reported in triple negative breast cancer (TNBC) which leads to constitutive activation of AKT kinase [12]. It was, however, recently amended that MAGI3:AKT3 is neither recurrent nor sub-clonal in TNBC [41].

1.3 Mechanisms of fusion gene generation

A fusion gene is typically desired from two separate genes due to genomic aberrations instead of read through co-transcript events. Fusion genes may occur as a result of interstitial deletion, chromosomal inversion, translocation or duplication (Figure 1.5) [42]. Considering whether the overall amount of genomic material is changed or not, rearrangements could be grouped into two types: balanced rearrangements (inversion or translocation) and unbalanced rearrangements (deletion or duplication). The former only changes the order of chromosomal genes/segments but does not result in loss or gain of any DNA, such as fusions IGH:BCL2 and IGH:MYC (translocation) [43], whereas unbalanced rearrangements change the total amount of genomic materials. Co-occurrence of translocations and deletions was often observed. Interestingly, fusion TMPRSS2:ERG can be produced by either translocation or interstitial deletion which were identified by array-based comparative genomic hybridization and interphase fluorescence in situ hybridization in prostate cancer [44, 45, 46].

Two different structural groups of fusion genes were observed, including fusion of a coding gene (or part of it) and a regulatory sequence such as IGH:MYC, and fusion of two different coding genes (or parts of them) such as BCR:ABL1. There are at least three categories of gene fusion effects: overexpression of an oncogene, deregulation of a suppressor gene and formation of a new functional protein [42]. First, an oncogene (3' fusion partner) can be over expressed by using highly expressed 5' fusion partner which functions as an enhancer, such as well known fusions IGH:MYC, IGH:BCL2 and TMPRSS2:ETS (E26 transformation-specific family genes). Second, a tumor suppressor gene (3' fusion partner) can be deregulated through adding/removing a frame-shifted sequence during gene fusion process. Based on FISH and reverse transcription-polymerase chain reaction (RT-PCR), fusion PPP2R2A:CHEK2 in childhood teratoma has been identified that there is an inserted fragment (class I endogenous retrovirus-

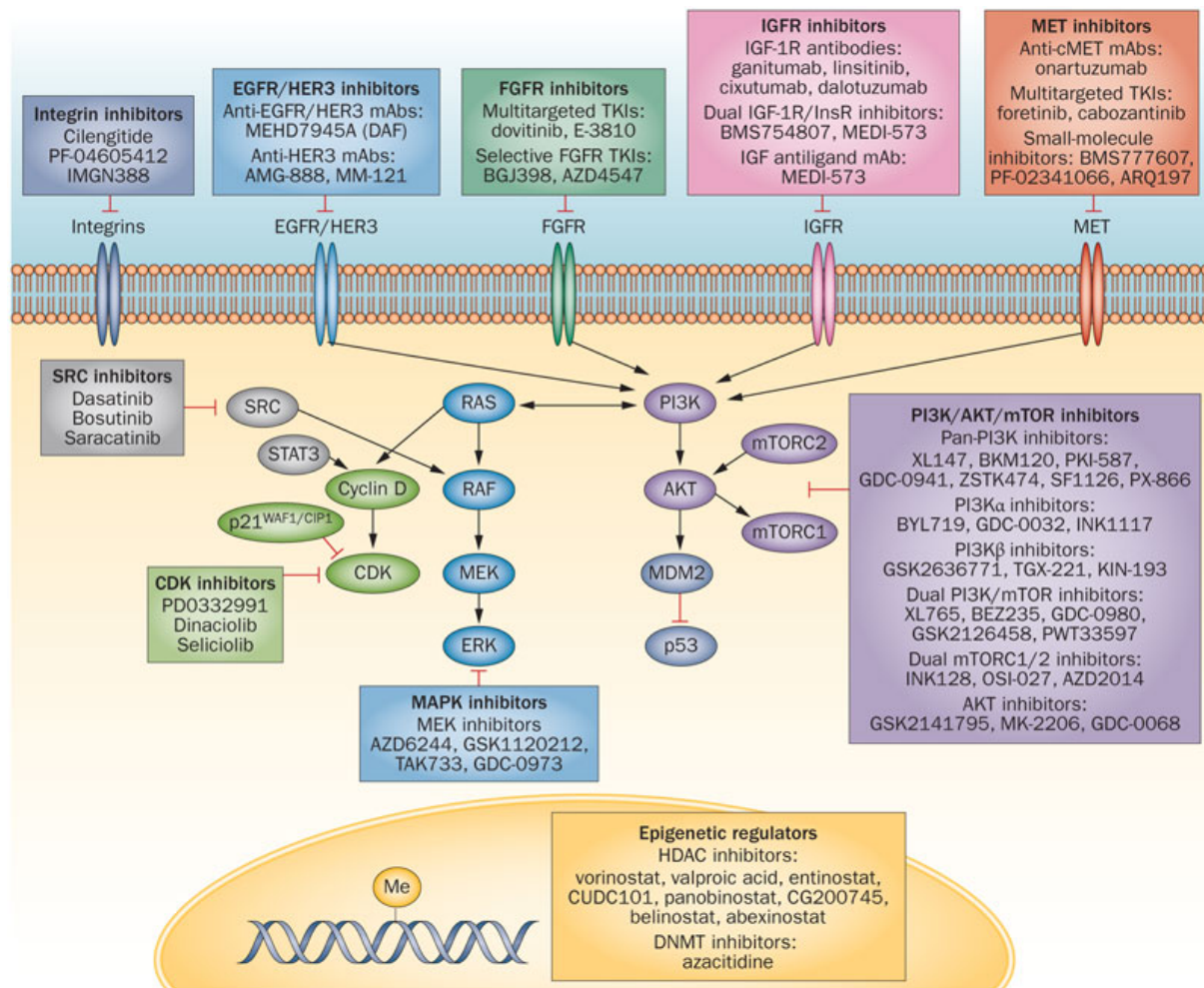


Figure 1.4: Targeting agents under clinical development. Those agents are expected to target molecular components involved in oncogenic pathways in breast cancer cell lines, including PI3K-AKT-mTOR pathway, IGF signaling pathway, MET signalling pathway, MAPK signalling pathway as well as cyclin-dependent kinases (CDKs) and epigenetic regulators. Image source:[36].

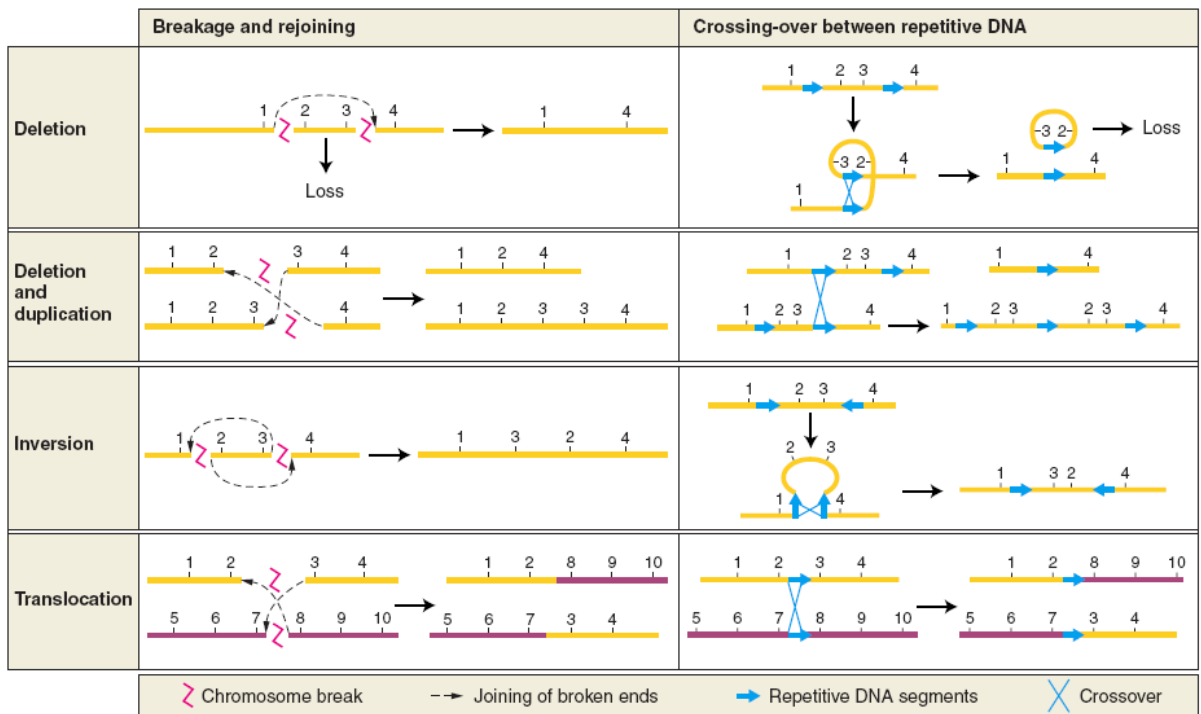


Figure 1.5: Different types of chromosomal rearrangements. Four types of chromosomal rearrangements. These rearrangements occur due to either DNA double-strand breakage and reunion or crossing-over between repetitive chromosomal segments in different regions. Image source:[47].

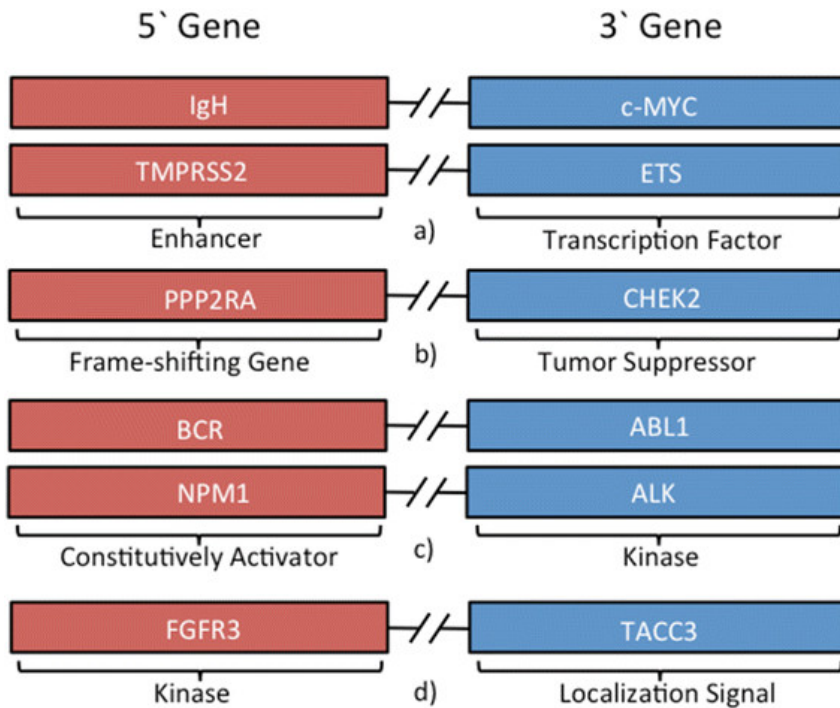


Figure 1.6: Different categories of gene fusions. (a) Enhanced overexpression of an oncogene due to high expression of 5' fusion partner (an endogenous enhancer). (b) Dere regulation of a tumor suppressor gene by introducing frame-shifted sequence to prevent formation of functional protein. (c)(d) Formation of a new functional chimeric protein. Image source:[42].

related sequences) on the fusion boundary, resulting in an out-of-frame fusion transcript [48]. Third, a new functional chimeric protein is formed by a fusion transcript which includes kinase domain, such as BCR:ABL1, NPM1:ALK and FGFR3:TACC3 (Figure 1.6) [42].

1.4 Detection of fusion genes

Several technologies have been applied for detecting chromosome alterations such as chromosome banding analysis and FISH as mentioned in Chapter 1.1. Up to date, the next-generation sequencing (NGS) technologies (also called massively parallel sequencing) such as paired-end RNA-seq and WGS provide accurate, high-resolution data in a single experiment, enabling unbiased genome-wide fusion gene detection. The first application of deep paired-end sequencing was carried out on lung cancer cell lines in 2008 [49], and these were quickly followed by a large number of investigations of tumor samples across different tumor entities, such as breast cancer [50], colon cancer [51], lymphoma [52], prostate cancer [53], thyroid cancer [54] and glioma [55], leukaemia [56], as well as kidney cancer [57] and lung cancer [58]. Currently,

whole-exome sequencing (WES) [59], whole-genome sequencing (WGS) [12, 53] and whole transcriptome sequencing (RNA-seq) [52] have already been successfully applied on fusion gene discovery in different tumor types. A great number of fusion gene detection tools have been developed to interrogate data from NGS, particularly paired-end RNA-seq (Table 1.1).

Table 1.1: An overview of different fusion detection tools based on RNA-seq data.

Tool Name	Reads	Cited	Tool Name	Reads	Cited
TopHat-Fusion [60]	Single/Paired End	116	ShortFuse [61]	Paired End	27
deFuse [50]	Paired End	108	FusionHunter [62]	Paired End	22
FusionSeq [63]	Paired End	62	FusionFinder [64]	Single/Paired End	15
FusionMap [65]	Single/Paired End	56	SOAPFuse [66]	Paired End	13
ChimeraScan [67]	Paired End	53	BreakFusion [68]	Paired End	10
SnowShoes-FTD [69]	Paired End	30	FusionAnalyser [70]	Paired End	9
			PRADA [71]	Paired End	5

Based on WEB OF SCIENCE, 2015-09-14.

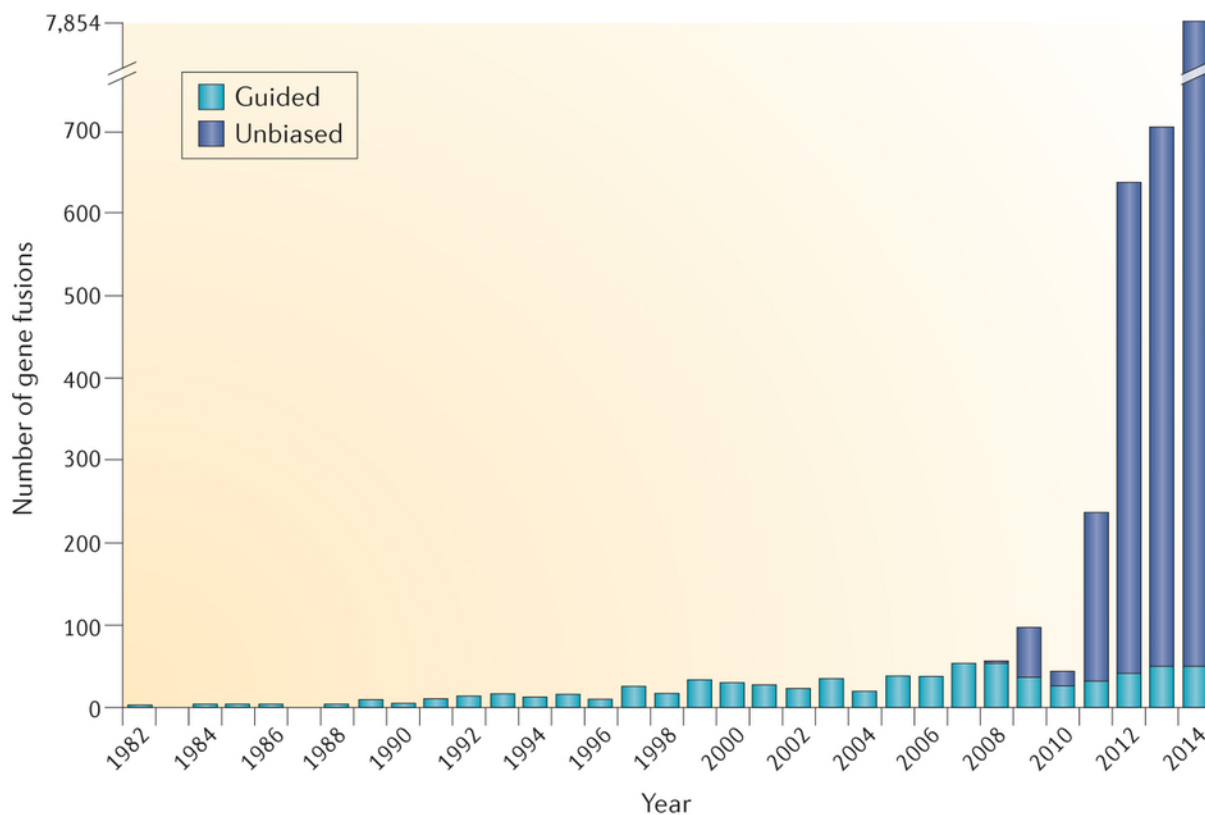
The NGS technologies can be applied on different cell lines or tumor types. Recently, a new fusion detection pipeline PRADA [71] was applied on a large cohort of transcriptomic data (4,366 neoplasms from 13 different tumor types) that had been previously studied in The Cancer Genome Atlas (TCGA) network (Table 1.2) [72]. Using stringent filtering criteria, PRADA identified more than 8,600 different fusion transcripts across 13 different cancer types, resulting in a plethora of gene fusions (>9,000) (Figure 1.7) [4, 71, 72]. The distribution of currently known/identified fusions across different neoplasia types is given in Table 1.3. More than 90% of the total 9,928 fusions were identified by NGS technologies during the past five years, of which 75% are intrachromosomal and approximately 50% are in the same chromosome band [4]. In nine of 13 tumor types from TCGA RNA-seq cohort, more than 80% of fusion transcripts were associated with DNA amplifications or deletions (Figure 1.8) [72].

RNA-seq provides a very high sensitivity in fusion gene detection. It should be noted that most of the identified/putative fusions were not experimentally validated. Even though a very stringent filtering method was used to select reliable fusion candidates, it can still not be sure that all the identified fusions are true positives. Some false positive fusion predictions may be due to sequencing/alignment artefacts or library preparation for sequencing. Different fusion detection tools perform variably in terms of sensitivity and specificity, depending on the individual algorithms and filtering methods [73]. Currently, RT-PCR followed by Sanger sequencing is a typical experimental method for validating predicted fusion genes in addition to FISH validation.

Fusion detection based on RNA-seq may lead to not only false positive but also false negative predictions, which may be a result of several aspects. First, low RNA quality of samples or sequencing errors may reduce the number and quality of sequence reads, thereby decreasing the probability of detecting fusion transcripts. For example, RNA in formalin-fixed paraffin-embedded

Table 1.2: RNA-seq data set from 13 different tumor types in TCGA. Source:[72].

Tumor type	Tumor	Normal
Bladder urothelial carcinoma (BLCA)	121	16
Breast cancer (BRCA)	1,019	110
Glioblastoma multiforme (GBM)	158	-
Head and neck squamous cell carcinoma (HNSC)	300	37
Clear cell renal cell carcinoma (KIRC)	474	71
Acute myeloid leukemia (LAML)	171	-
Low-grade glioma (LGG)	266	-
Lung adenocarcinoma (LUAD)	487	57
Lung squamous cell carcinoma (LUSC)	220	17
Ovarian serous cystadenocarcinoma (OV)	400	-
Prostate adenocarcinoma (PRAD)	178	-
Skin cutaneous melanoma (SKCM)	78	-
Thyroid carcinoma (THCA)	494	56
Total	4,366	364



Nature Reviews | Cancer

Figure 1.7: Number of newly reported fusions from 1982 to 2014. Guided fusion genes were based on cytogenetic features, FISH and high-throughput array-based analysis, whereas unbiased fusions were detected using NGS data. Most of the newly identified fusions were reported in 2014. Image source:[4].

Table 1.3: Number of known/identified gene fusions in different neoplasia subtypes. Source:[4].

Diagnosis	Number of gene fusions	
	Total	Confirmed as recurrent
<i>Haematological disorders</i>		
Undifferentiated and biphenotypic leukaemia	25	3
Acute myeloid leukaemia	302	51
Myelodysplastic syndromes	52	8
Myeloproliferative neoplasms, including chronic myeloid leukaemia	72	24
Acute lymphoblastic leukaemia	237	59
Plasma cell neoplasms	22	5
Mature B cell neoplasms	181	31
Mature T cell and natural killer cell neoplasms	28	8
Hodgkin disease	13	2
<i>Benign solid tumours</i>		
Benign epithelial tumours	14	6
Benign mesenchymal tumours	57	8
<i>Malignant solid tumours</i>		
Respiratory system	2,110	11
Digestive system	522	5
Breast	3,856	68
Female genital organs	432	0
Male genital organs	676	25
Urinary tract	626	5
Endocrine system	158	15
Nervous system	738	6
Skin	193	0
Bone	28	5
Soft tissue	104	34

The total number of known/identified fusions is 9,928, 330 of which are recurrent fusions. Haematological disorders harbor 759 fusions (157 recurrent) and 9,189 fusions (176 recurrent) were identified in solid tumors.

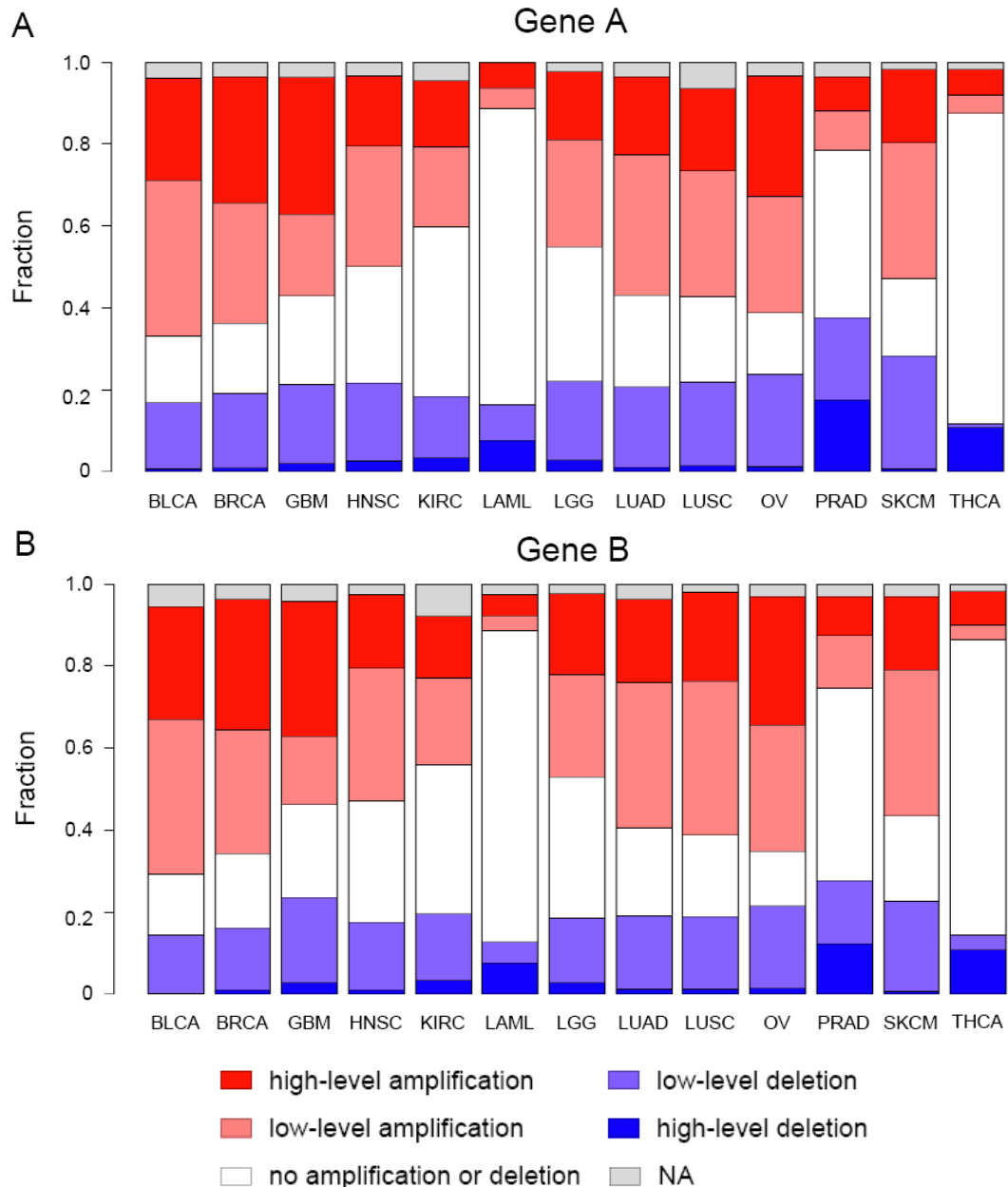


Figure 1.8: Copy number variance of each fusion partner gene identified by PRADA. Five types of copy number variance were presented in each bar plot for each tumor type. Copy number status for some genes were not available (NA) due to incompatibility of gene symbols between fusions and copy number variance. Excluding THCA, KIRC, LAML and PRAD, more than 80% of fusion transcripts were associated with copy number variance in the remaining nine tumor types. Image source:[72].

tumor tissues considered to be highly degraded and chemically modified, may not be sufficient for discovering fusions compared with RNA in fresh-frozen tissue samples. In addition, fusions with low expression or low sequencing depth may be difficult to be detected. The same may happen to sub-clonal fusion events in heterogeneous tumors [4].

1.5 “deFuse” algorithm

One of the popular fusion gene detection tools, deFuse, aims to discover fusions based on tumor paired-end RNA-seq data. DeFuse considers not only uniquely mapped alignments but also ambiguous alignments, as well as all possible locations of fusion boundaries, including end of exon and intron region. *“The central idea behind deFuse is to guide a dynamic programming-based split read analysis with discordant paired end alignments”* [50].

DeFuse consists of four main steps. The first step is to use bowtie [74] for mapping paired-end reads on a genome reference. The second step is to select the most likely discordant alignments (Figure 1.9a). Third, deFuse uses a dynamic programming based solution to identify fusion boundaries (Figure 1.9b). The fourth step is to calculate the p-value of corroborating spanning read and split read evidence (Figure 1.9c).

In the end, deFuse trains an adaboost classifier to discriminate true fusions and false positive fusions. It uses 11 features to train an adaboost classifier in order to increase the specificity (Figure 1.10). The deFuse adaboost classifier’s probability 0.81 correspond to 10% false positive rate and 82% true positive rate based on a list of 60 RT-PCR validated fusions and 61 true negative fusions from different entities (sarcomas, ovarian carcinomas, prostate cancer, chronic myelogenous leukemia and melanoma) (Figure 1.11) [50].

1.6 Objectives

Fusion genes as pathognomonic mutations have been reported to be clinically important [4]. Some fusion genes are strong driver mutations such as BCR:ABL1 and have provided an fundamental understanding of the disease mechanisms in tumorigenesis. The fusion genes observed is highly dependent on the tumor phenotype, making fusion genes good candidates for diagnostic purposes and enabling the subclassification of tumor entities [4]. Some gene fusions have been targeted in treatment and clinical outcomes have been dramatically improved [4]. Currently, published fusion gene detection tools are not good enough due to issues such as a high false-positive rate. One aim of this study was to develop an improved method or algorithm for reliable detection of fusion genes.

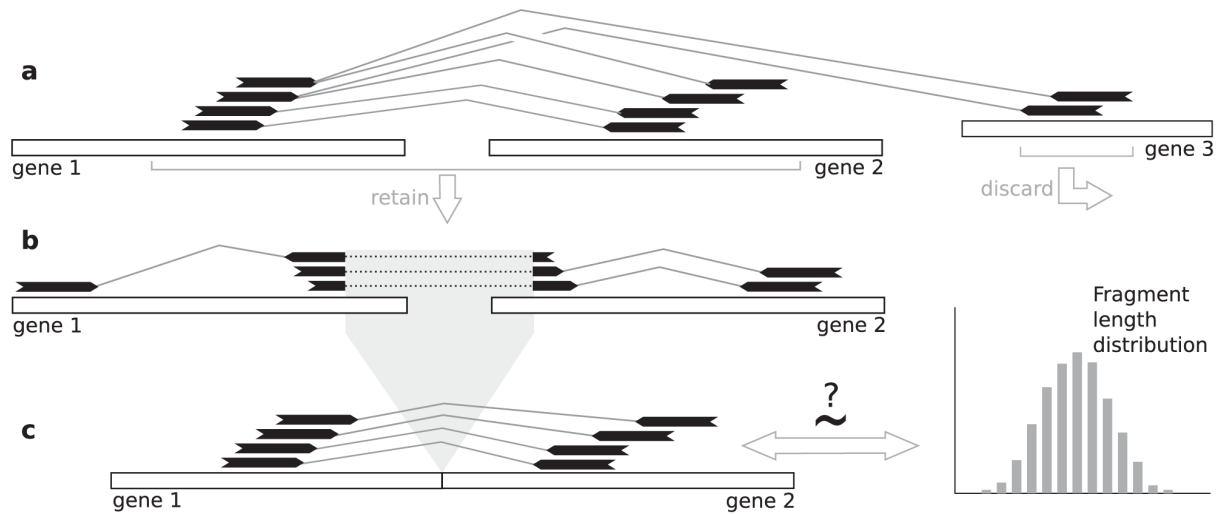


Figure 1.9: Method of fusion detection in deFuse. (a) Discordant alignments are clustered based on the spanning reads. Ambiguous alignments are assigned to the most likely set of fusion events instead of filtering them directly and the remaining ambiguous alignments are discarded. (b) DeFuse uses a dynamic programming-based method to mine split alignments for both fusion partners gene 1 and gene 2 and predicts the fusion boundary. (c) The fragment lengths of spanning reads are estimated based on the predicted fusion boundary. Then deFuse tests whether the fragment length distribution are random. Image source:[50].

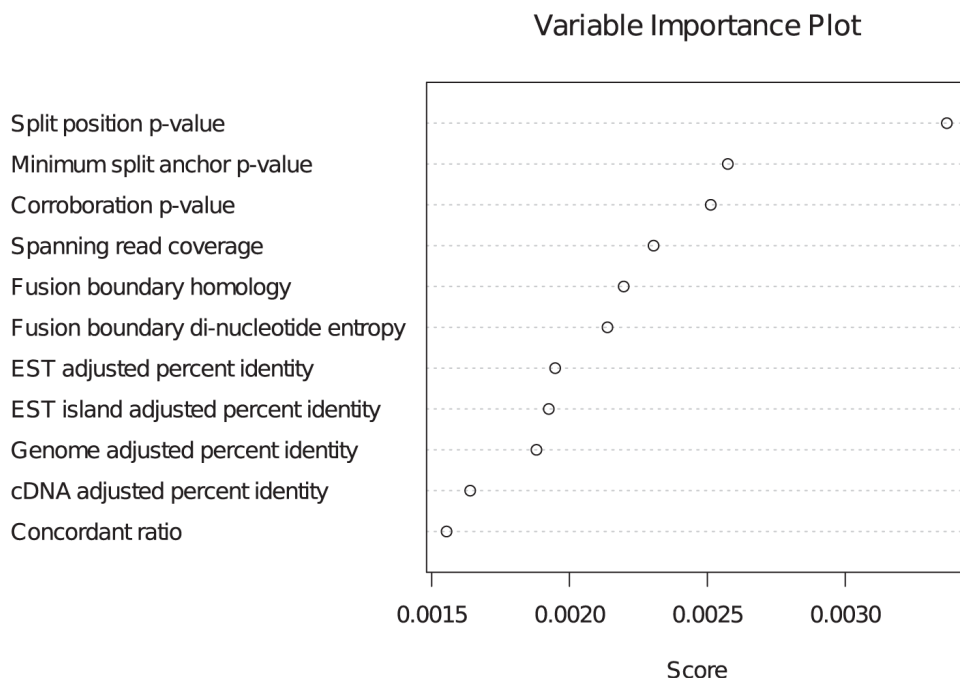


Figure 1.10: Relative importance of 11 features in deFuse adaboost classifier. Those features were used to predict true positive fusions. Image source:[50].

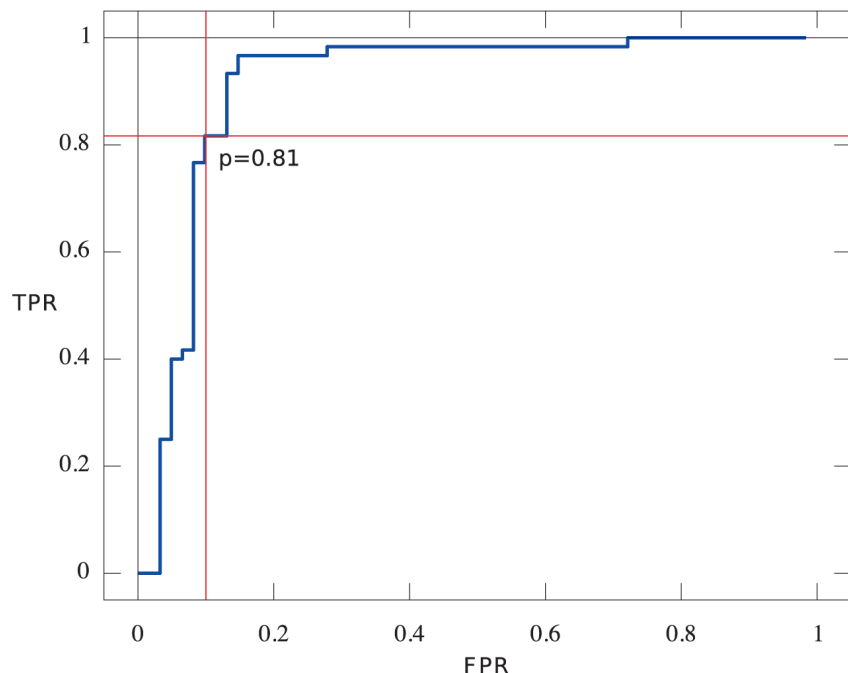


Figure 1.11: ROC curve of adaboost probability in deFuse. The area under the ROC curve (AUC) is 0.91. The adaboost probability 0.81 corresponds to a false positive rate of 10% and a true positive rate of 82%. The 60 RT-PCR validated fusion genes are from sarcomas, ovarian carcinomas, prostate cancer cell line, chronic myelogenous leukemia cell line and melanoma samples. Image source:[50].

As mentioned above (Chapter 1.2), ESR1 mutation is a major mechanism in acquired endocrine resistance during breast cancer treatment [6, 7]. Fusions of MAST kinase and Notch gene families affect the phenotype in breast epithelial cells [39]. It will be very interesting to identify novel fusion genes or biomarkers by analyzing WES and RNA-seq data in primary and refractory breast tumors in order to elucidate the resistance mechanism and contribute to individualized therapy for breast cancer patients.

In summary, the objectives of this thesis were to reliably identify fusion genes for giving a comprehensive landscape of fusion genes in different tumor entities and to identify novel molecular markers that may contribute to personalized treatment in breast cancer.

Chapter 2

Material and methods

2.1 Material

In total, 46 primary and 29 refractory breast tumor samples from HIPO-017 (Heidelberg Center for Personalized Oncology, DKFZ-HIPO) were involved for WES analysis in this thesis. The library of control and tumor samples was prepared according to Agilent SureSelect Human All Exon V5+UTRs protocol for WES. Paired-end sequencing ($2 \times 101\text{bp}$) was carried out with Illumina Hiseq-2000 instruments. Furthermore, additional 21 refractory WES data sets generated by Matthew Ellis's group were included in this thesis¹.

Paired-end RNA-sequencing library was prepared with ribosomal RNA depleted, strand-specific protocol for breast cancer samples as previous describes [31, 32]. Deep sequencing ($2 \times 101\text{bp}$) was carried out on an Illumina HiSeq-2000 platform. Totally, 98 breast tumor RNA-seq samples from HIPO-017 project were sequenced, 42 of which were refractory tumors and 46 of which were primary tumors. In addition, 24 refractory tumor RNA-seq samples generated by Matthew Ellis's group were also analyzed in this thesis².

Library preparation and sequencing of WES and RNA-seq from HIPO-017 were completed in DKFZ³. There were five primary-refractory matched-paired samples in fusion analysis, namely OE5B_T1 & T2VO_M1, QYXQ_T1 & QYXQ_M1, B2HF_T1 & B2HF_M1, 4R5V_T1 & 4R5V_M1 and DMG3_T1 & DMG3_M1.

The other unpublished RNA-seq data sets in this thesis include sarcoma generated from Benedikt Brors's group (HIPO-028), CLL from Thorsten Zenz's group (HIPO-005), gliomas from

¹In total, 46 primary WES samples were involved in SNVs and Indels analysis and 44 primary WES samples were involved in CNVs analysis. 50 refractory WES data were involved in SNVs, Indels and CNVs analysis.

²Currently, three patient samples were sequenced by WES but not by RNA-seq in Ellis's data.

³Done by core facility in DKFZ, Dr. Andrius Serva and Dr. Verena Thewes in Peter Licher's group.

Peter Lichter's group (HIPO-016), lymphomas from Reiner Siebert's group (ICGC), prostate cancer from Holger Sültmann's group (ICGC), as well as ependymoma, 22 glioblastoma multi-forme (GBM) and 27 INFORM samples (INdividualized Therapy FOr Relapsed Malignancies in Childhood) from Stefan Pfister's group. In this thesis, all raw sequencing data were not generated by myself.

2.2 NGS data analysis

2.2.1 Whole-genome sequencing analysis

25 GBM samples were prepared with paired-end DNA library and mate-pair (long-range paired-end) DNA library, according to Illumina, Inc. v2 protocol. Deep sequencing ($2 \times 101\text{bp}$) was carried out with HiSeq-2000 instruments. 22 of 25 GBM samples with previously validated fusions were selected for downstream analysis after successful deFuse run.

Structural rearrangements were identified using CREST [75] with default parameters in paired-end sequenced samples. Furthermore, another tool DELLY [76] was used for detecting structural rearrangements in mate-pair sequenced samples⁴.

2.2.2 Whole-exome sequencing analysis

Using an in-house pipeline from Roland Eils' group (B080) in German Cancer Research Center (DKFZ), sequencing reads were mapped on human genome reference assembly (hg19) with Burrows-Wheeler Aligner (BWA-v0.6.2) [77].

SNVs were then called by SAMtools mpileup (version-0.1.19) and bcftools (version-0.1.19) [78]. Furthermore, additional filtering steps were complemented in order to remove possible artefacts as previously described [79]. Only somatic mutations (non-synonymous, stop-gain or stop-loss) of high-confidence score (≥ 8) were chosen for downstream analysis. CNV calling was based on the alignment results and a tool for copy number alteration discovery, VarScan-2 [80]. Small insertions and deletions (Indels) were identified with the tool Platypus [81]. In-house pipelines from Roland Eils' group (B080) were used for CNV and SNV/Indels analysis.

⁴The structural arrangement analysis was done by David T.W. Jones *et al.*. Results of structural aberration were used to estimate a validation rate by comparing with predicted fusion genes in RNA-seq.

2.2. NGS DATA ANALYSIS

21

Total Reads

Sample	Note	Total Purity Filtered Reads Sequenced	Alternative Alignments	Failed Vendor QC Check	Read Length	Estimated Library Size
H017_7DTJ_T1_R1	ssRNA	314,132,810	32,675,104	NA	101	142,783,345

Total Purity Filtered Reads Sequenced are filtered for vendor fail flags and exclude alternative alignment reads. **Alternative Alignments** are duplicate read entries providing alternative coordinates. **Failed Vendor QC Check** are reads which have been designated as failed by the sequencer. **Read Length** is the maximum length found for all reads. **Estimated Library Size** is the number of expected fragments based upon the total number of reads and duplication rate assuming a Poisson distribution.

Mapped Reads

Sample	Note	Mapped	Mapping Rate	Mapped Unique	Mapped Unique Rate of Total	Unique Rate of Mapped	Duplication Rate of Mapped	Base Mismatch Rate	rRNA	rRNA rate
H017_7DTJ_T1_R1	ssRNA	308,249,268	0.981	188,534,232	0.600	0.612	0.388	0.001	4,221,630	0.013

Mapped reads are those that were aligned. **Mapping Rate** is per total reads. **Mapped Unique** are both aligned as well as non-duplicate reads. **Mapped Unique Rate of Total** is per total reads. **Unique Rate of Mapped** are unique reads divided by all mapped reads. **Duplication Rate of Mapped** is the duplicate read divided by total mapped reads. **Base Mismatch Rate** is the number of bases not matching the reference divided by the total number of aligned bases. **rRNA** reads are non-duplicate and duplicate reads aligning to rRNA regions as defined in the transcript model definition. **rRNA Rate** is per total reads.

Mate Pairs

Sample	Note	Mapped Pairs	Unpaired Reads	End 1 Mapping Rate	End 2 Mapping Rate	End 1 Mismatch Rate	End 2 Mismatch Rate	Fragment Length Mean	Fragment Length StdDev	Chimeric Pairs
H017_7DTJ_T1_R1	ssRNA	154,058,442	NA	0.981	0.981	0.001	0.001	494	588	1

Mapped Pairs is the total number of pairs for which both ends map. **Unpaired Reads** are the number of reads that are lacking a mate. **End 1/2 Mapping Rate** is the number of mapped divided by the total number of End1/End2 reads. **End 1/2 Mismatch Rate** is the number of End 1 and 2 bases not matching the reference divided by the total number of mapped End 1 and 2 bases. **Fragment Length Mean/StdDev** is the mean distance, standard deviation between the start of an upstream read and the end of the downstream one. Only fragments contained within single exons are used. **Chimeric Pairs** are pairs whose mates map to different genes.

Transcript-associated Reads

Sample	Note	Intragenic Rate	Exonic Rate	Intronic Rate	Intergenic Rate	Expression Profiling Efficiency	Transcripts Detected	Genes Detected
H017_7DTJ_T1_R1	ssRNA	0.953	0.783	0.170	0.046	0.768	155,849	30,708

All of the above rates are per mapped read. **Intragenic Rate** refers to the fraction of reads that map within genes (within introns or exons). **Exonic Rate** is the fraction mapping within exons. **Intronic Rate** is the fraction mapping within introns. **Intergenic Rate** is the fraction mapping in the genomic space between genes. **Expression Profile Efficiency** is the ratio of exon reads to total reads. **Transcripts/Genes Detected** is the number of transcripts/genes with at least 5 reads.

Strand Specificity

Sample	Note	End 1 Sense	End 1 Antisense	End 2 Sense	End 2 Antisense	End 1 % Sense	End 2 % Sense
H017_7DTJ_T1_R1	ssRNA	1,521,509	123,573,658	123,737,095	1,497,122	1.216	98.805

End 1/2 Sense are the number of End 1 or 2 reads that were sequenced in the sense direction. Similarly, **End 1/2 Antisense** are the number of End 1 or 2 reads that were sequenced in the antisense direction. **End 1/2 Sense %** are percentages of intragenic End 1/2 reads that were sequenced in the sense direction.

Figure 2.1: Example of quality control of an RNA-seq sample.

2.2.3 RNA sequencing analysis

- Quality control for RNA-seq data

Quality control was performed using RNA-SeQC [82] which can provide investigators with alignment rate, duplication rate, strand-specific rate, GC bias, rRNA content, regions of alignment (exon, intron and intragenic), and count of detectable transcripts. An example of strand-specific RNA-seq from breast cancer sample is given in Figure 2.1.

- Gene expression

Paired-end RNA-seq data were aligned to human reference genome hg19 with decoy sequence (Hs37D5) using STAR-2.3.0e [83]. Sequence reads mapped on each gene were counted by HTSeq-count [84] with GENCODE annotation version 19. HTSeq-count was specifically designed for gene-level count based on exon model in order to analyze differentially expressed genes. Ambiguous reads mapped on different genes were not considered for downstream analysis. Gene-level count was then quantified in terms of reads per kilobase per million mapped reads (RPKM). Gene length was calculated based on total non-redundant cumulative exon length of a gene with GENCODE annotation version 19.

- Integration of SNVs and RNA-seq data

For breast tumor samples where both WES and RNA-seq data were available, DNA variant positions (somatic mutation positions) were annotated with RNA mapped reads (RNA BAM files). RNA aligned reads containing the same variance (tumor allele) was required to call a candidate

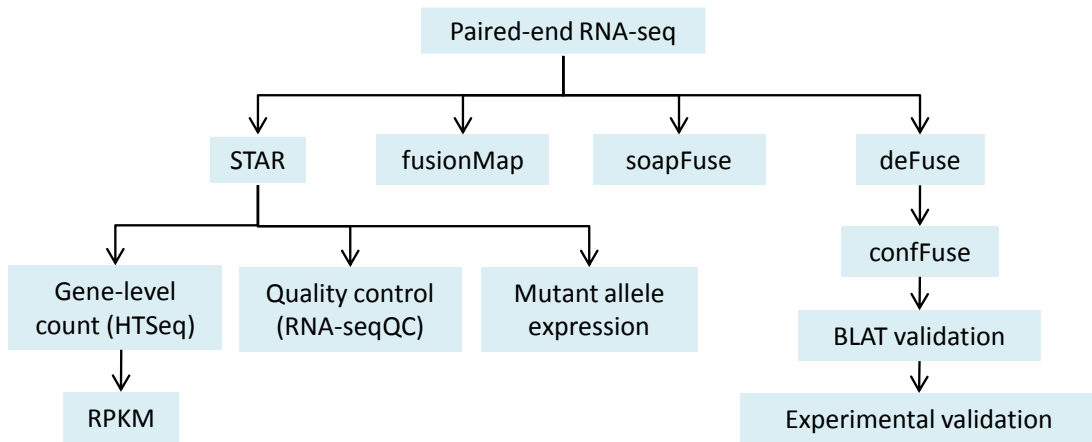


Figure 2.2: Overview of data flow in RNA-seq analysis. High-confidence fusion candidates were selected by confFuse and then validated *in silico* by BLAT, followed by experimental validation.

DNA tumor allele *expressed*. Expressed tumor alleles with less than ten RNA-sequencing reads mapped on the position were not used in further analysis.

- **Fusion gene detection and validation**

Different tools (fusionMap [65], soapFuse [66] and deFuse [50]) were used to detect fusion genes based on paired-end RNA-seq data. Versions of these tools were SOAPfuse-v1.26, deFuse-0.6.1 and FusionMap-2015-03-31. Human genome reference hg19/GRCh37 was used in deFuse and SOAPfuse. Genome reference Human.B37.3 and gene model Ensemble.R75 were used in FusionMap. In addition, I developed a new scoring algorithm, confFuse, to reliably select high-confidence fusion genes (details in next section). After validation *in silico* by BLAT, experimental validation for fusion candidates was carried out using RT-PCR followed by Sanger sequencing⁵. Primers for RT-PCR validation were designed using Primer3 [85].

- **Pathway analysis**

Gene lists in different pathways were based on KEGG (Kyoto Encyclopedia of Genes and Genomes). For fusion genes identified by confFuse, pathway figures were generated in INGENUITY pathway analysis.

- **Overview of data flow**

An overview of data flow in RNA-seq analysis is given in Figure 2.2.

⁵RT-PCR and Sanger sequencing done by Yonghe Wu and Achim Stefan for three breast tumor samples, and done by Yonghe Wu for three CLL samples .

2.3 “confFuse” algorithm

A great number of fusion gene detection tools/pipelines (Chapter 1.1) have been developed to interrogate the NGS data. Those tools/pipelines consist of three major parts: mapping based on existing alignment tools such as Bowtie and BWA; individual methods for generating fusion candidates; and filtering algorithms to remove false positive candidates. The sensitivity of fusion gene detection mainly depends on the mapping step and the specificity depends on the methods of generating fusion candidates and filtering methods.

Most of those tools/pipelines generate a large number of putative fusion transcripts even after filtering, of which most may be false positives or of low biological interest (e.g. precursor read-through transcripts), making it hard to prioritize candidates for experimental validation. Additional filtering methods were developed based on individual datasets in order to select reliable fusion candidates [52, 57]. Those individual filters, however, may have a bias towards cancer or cell type-specific artefacts. Furthermore, stringent filtering can decrease sensitivity of true fusion detection [71]. Therefore, I developed confFuse, a new scoring algorithm, which can be applied on paired-end RNA-seq across tumor entities with both high true positive rate and high detection accuracy.

ConfFuse was designed to rank fusion candidates based on deFuse output by assigning each fusion candidate a confidence score, with the aim of markedly reducing the total number of fusion candidates while retaining a high recall rate for true positives. It takes multiple features into account, including some from the standard deFuse output and also newly generated features, with each given a specific score weight. Those features are related to number and quality of reads supporting a fusion, fusion structural features and sequence motif such as gene homology. The final confidence score is the sum of the score weights of different single/combined features (initial baseline score is 10). These parameter weightings were iteratively optimized in comparison to a known validated fusion list, in order to achieve a balance between eliminating false positives whilst retaining true fusions. Fusion candidates scoring between 8 and 10 are considered as being high-confidence. The main features used to calculate the score are described below.

Split reads and spanning reads. Highly expressed fusions are easier to be detected by RNA-seq technology, resulting in more sequence reads identified by fusion detection tools. Sequencing depth is another important factor related to the number of sequence reads from fusions. High fusion expression and/or high coverage sequencing would likely result in a high number of split reads and spanning reads in fusion detection. For lowly expressed fusions with low sequencing depth, it is hard to detect them and only a few reads could probably be confirmed to support predicted fusions. Setting a number threshold to filter fusions may increase the specificity but can reduce the sensitivity. The more uniquely mapped the spanning reads are, the stronger is the evidence supporting fusions. Considering the complexity of some genome regions, multiple

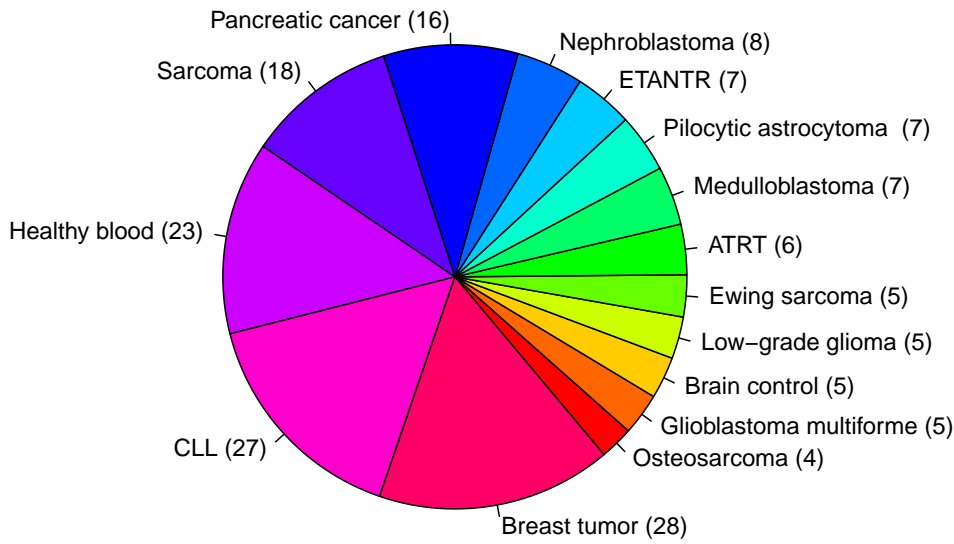


Figure 2.3: 171 paired-end RNA-seq samples from 15 different entities.

mapped reads (ambiguous alignments) can still be evidence supporting true fusions. However, spanning reads mapped on repeat regions may result in false putative fusion. ConfFuse therefore assigns a positive score to fusions with a high number of split and uniquely mapped spanning reads (or a negative score otherwise).

Artefact list. Fusions identified in multiple tumor types are mostly considered to be of high false positive rate or of low biological interest (i.e. read-through fusions). In total, 171 samples from 15 different entities were used to generate an artefact list including fusions identified in no less than three different entities (Figure 2.3). To increase the detection accuracy, previously verified fusions were manually extracted from the blacklist. Some fusions in the blacklist, however, could still be true and play an important role in tumor formation in different tumor types (false negative fusions). ConfFuse assigns a negative score to fusions in the artefact list.

Occurrence of fusion genes. Fusion genes with different fusion transcripts (i.e. splice variants) in the same samples may be of high true positive rate, especially those fusion transcripts of high count of split reads and spanning reads. ConfFuse gives a positive score to these candidates.

Read through. Two adjacent genes in the same orientation may give rise to an apparent fusion due to read-through transcription and aberrant splicing rather than genome rearrangement. Although some may acquire novel functions, the vast majority are expected to be false positives. Fusions with read-through or alternative splicing are assigned a negative score.

Open reading frame. True oncogenic fusions typically preserve the open reading frame in order to form a functional fusion protein. Fusions without an open reading frame are therefore given a negative score.

Breakpoint of fusions. Homology of breakpoint shows the number of nucleotides at the fusion splice region that map equally well to first fusion partner or second fusion partner. The location of fusion breakpoint play an critical role in demonstrating evidence supporting true positive fusions. When the locations of fusion splicing are at exon boundaries, those are more likely true positive fusions. It may be of low biological interest when a breakpoint is located downstream of the 3' fusion partner. Fusions with high breakpoint homology were given a negative score by confFuse, as are fusions with breakpoint locations not at exon boundaries or located downstream of the 3' fusion partner.

The initial confidence score is 10 and the final confidence score is the sum of the score weights of different features. The weights of single/combined features are shown in Table 2.1.

Table 2.1: The weights of single and combined features in confFuse scoring algorithm.

Features	Score weight
Single features	
Fusion in artefact list	-6
Fusion with alternative splicing between adjacent genes	-4
Fusion with read through	-4
Fusion occurs in the same gene	-4
Breakpoint locates in 3' fusion partner downstream or UTR3p	-4
Fusion splice not at exon boundaries	-1.5
Breakpoint homology ≥ 10	-1
Without open reading frame	-1
Max of proportion of the spanning reads in 5' gene or 3' gene that span a repeat region >0.9	-1
Fusion from adjacent genes	-0.5
Fusion produced by intrachromosomal rearrangement	-0.5
Max of proportion of the spanning reads in 5' gene or 3' gene that span a repeat region between 0.8 and 0.9	-0.5
Combined features*	
If (5' gene or 3' gene with zero detected reads) and (occurrences ≥ 2) and (span_count - num_multi_map + split_count < 30)	-2
If span_count = num_multi_map	-1.5
If num_multi_map / span_count > 0.8 and span_count > 5	-1
If (span_count - num_multi_map < 5) and (number of split reads < 5)	-1
If span_count - num_multi_map < 5	-0.5
If occurrences ≥ 2 and (max_proportion < 0.5) and non-read-through and non-alternative-splicing and (100 \geq span_count - num_multi_map + split_count > 40) and (num_multi_map / span_count < 0.2)	+0.5

Continued on next page

Table 2.1 – continued from previous page

Features	Score weight
If occurrences ≥ 2 and (max_proportion <0.5) and non-read-through and non-alternative-splicing and ($100 \geq \text{span_count} - \text{num_multi_map} + \text{split_count} > 40$) and ($\text{num_multi_map} / \text{span_count} < 0.2$) and (location of breakpoint in 5' gene in coding region)	+1
If occurrences ≥ 2 and (max_proportion <0.5) and non-read-through and non-alternative-splicing and ($\text{span_count} - \text{num_multi_map} + \text{split_count} > 100$) and ($\text{num_multi_map} / \text{span_count} < 0.9$)	+1.5
If occurrences ≥ 2 and (max_proportion <0.5) and non-read-through and non-alternative-splicing and ($100 \geq \text{span_count} - \text{num_multi_map} + \text{split_count} > 40$) and ($\text{num_multi_map} / \text{span_count} < 0.2$) and (location of breakpoint in 5' gene in coding region) and (location of breakpoint in 3' gene in coding or upstream)	+1.5
If occurrences ≥ 2 and (max_proportion <0.5) and non-read-through and non-alternative-splicing and ($\text{span_count} - \text{num_multi_map} + \text{split_count} > 100$) and ($\text{num_multi_map} / \text{span_count} < 0.9$) and (location of breakpoint in 5' gene in coding region)	+2
If occurrences ≥ 2 and (max_proportion <0.5) and non-read-through and non-alternative-splicing and ($\text{span_count} - \text{num_multi_map} + \text{split_count} > 100$) and ($\text{num_multi_map} / \text{span_count} < 0.9$) and (location of breakpoint in 5' gene in coding region) and (location of breakpoint in 3' gene in coding or upstream)	+2.5

num_multi_map: number of multiple mapped spanning reads

span_count: number of spanning reads supporting the fusion

split_count: number of split reads supporting the fusion prediction

occurrences: occurrences of fusion gene pairs

max_proportion: max of proportion of the spanning reads in 5' gene or 3' gene that span a repeat region

* Noted: combined features are not all independent.

Chapter 3

Results

3.1 CNVs and SNVs/Indels in breast cancer

3.1.1 CNVs in breast cancer

Comparison of 44 primary and 50 refractory breast tumors shows different distributions of copy number variance (Figure 3.1). Refractory tumors harbor much more amplification in chromosome 8, where 8q24 has been reported as a risk locus which showed tissue-specific long-range interaction with MYC in prostate, breast and colon cancer [86].

Cyclin-dependent kinase inhibitor 2A (CDKN2A) is located in the deletion region in chromosome 9, which were identified as focal CNV (deletion) in three breast tumors (3/50, 6%) and one primary tumor. CDKN2A is a tumor suppressor gene and plays an important role in cell cycle, which is critical to cancer development. Deletion of CDKN2A associates with phenotype and genotype in childhood acute lymphoblastic leukemia (ALL) [87]. Loss of CDKN2A could result in oestrogen-independent cell cycle progression [88].

Runt-related transcription factor 3 (RUNX3) is located in the deletion region in chromosome 1, which was identified in two primary (2/44) and four refractory (4/50) breast tumors. It has been reported that RUNX3 was frequently deleted in various tumors, including colon, neuroblastoma and breast cancer [89].

Estrogen-related receptor gamma (ESRRG) located in chromosome 1 is important in control of cellular metabolism in breast cancer [90]. Three refractory (3/50) and one primary (1/44) tumor harbor ESRRG amplification.

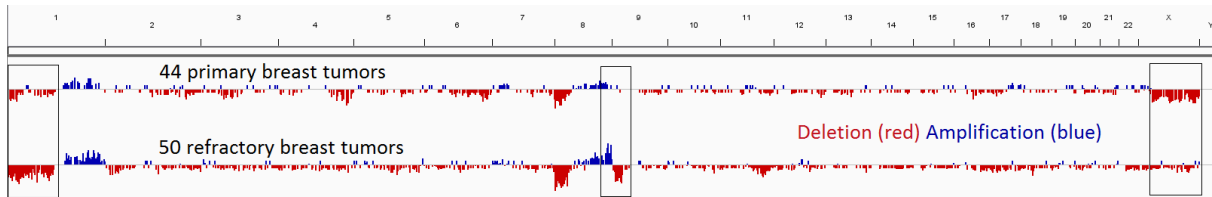


Figure 3.1: Copy number variance in primary and refractory breast tumors. The most obviously different regions (shown in black box) are located on chromosome 1, 8, 9 and X.

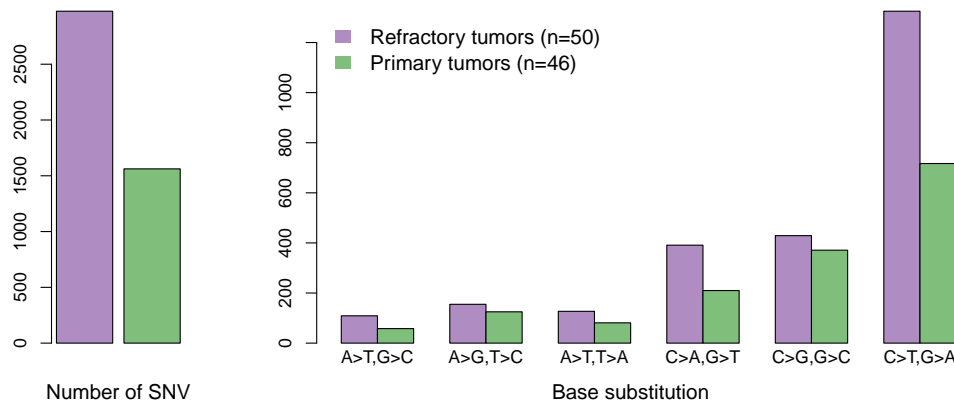


Figure 3.2: Distribution of base substitutions in breast cancer. Comparing with primary tumors, refractory tumors have similar distribution of base substitution but higher number of somatic mutations.

3.1.2 Somatic mutations in breast cancer

In total, 1562 and 2975 somatic SNVs or small Indels were identified in 46 primary breast tumors and 50 refractory breast tumors, respectively (Figure 3.2). These two groups show similar distribution of base substitution. Higher number of somatic mutation, however, is observed in refractory tumors (Figure 3.2).

A gene list with 731 genes was generated based on different KEGG pathways (ErbB, estrogen, MAPK, PI3K-AKT-mTor and Ras signalling pathway), tamoxifen-related genes (KEGG) and 32 significantly mutated genes taken from the literature [14]. There is not much difference between primary and refractory tumors in terms of the number of mutations (Figure 3.3 and Figure 3.4). 145 and 112 somatically mutated genes from the 731 genes were identified in refractory and primary tumors, respectively. PIK3CA and TP53 are the top two frequently mutated genes (15 and 8 in 46 primary tumors, 15 and 13 in 50 refractory tumors). The top ten recurrently mutated genes in both primary and refractory tumors have been previously reported [91].

Calcium channel, voltage-dependent, alpha (CACNA) 14 subunits (CACNA1A-S and CACNA2D1-4) are involved in MAPK signalling pathway. It has been reported that “methylation-dependent transcriptional silencing of CACNA2D3 may contribute to the metastatic phenotype of

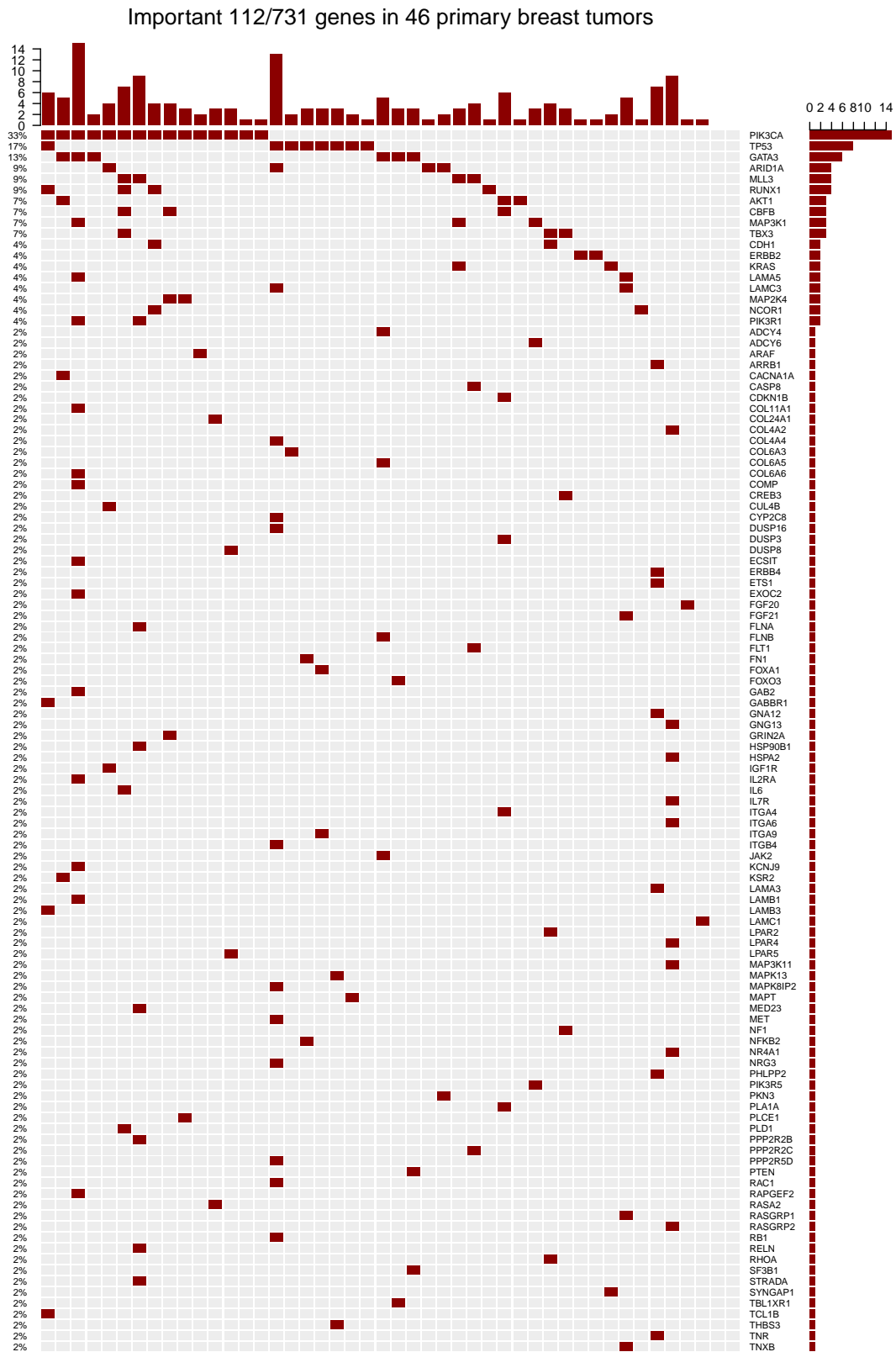


Figure 3.3: SNVs and Indels in primary breast tumors across different pathways, including ErbB, estrogen, MAPK, mTor, Ras, PI3K-AKT, as well as tamoxifen-related genes and 32 reported significantly mutated genes. In total, there are 731 selected genes, 112 of which harbor mutations (SNVs or Indels).

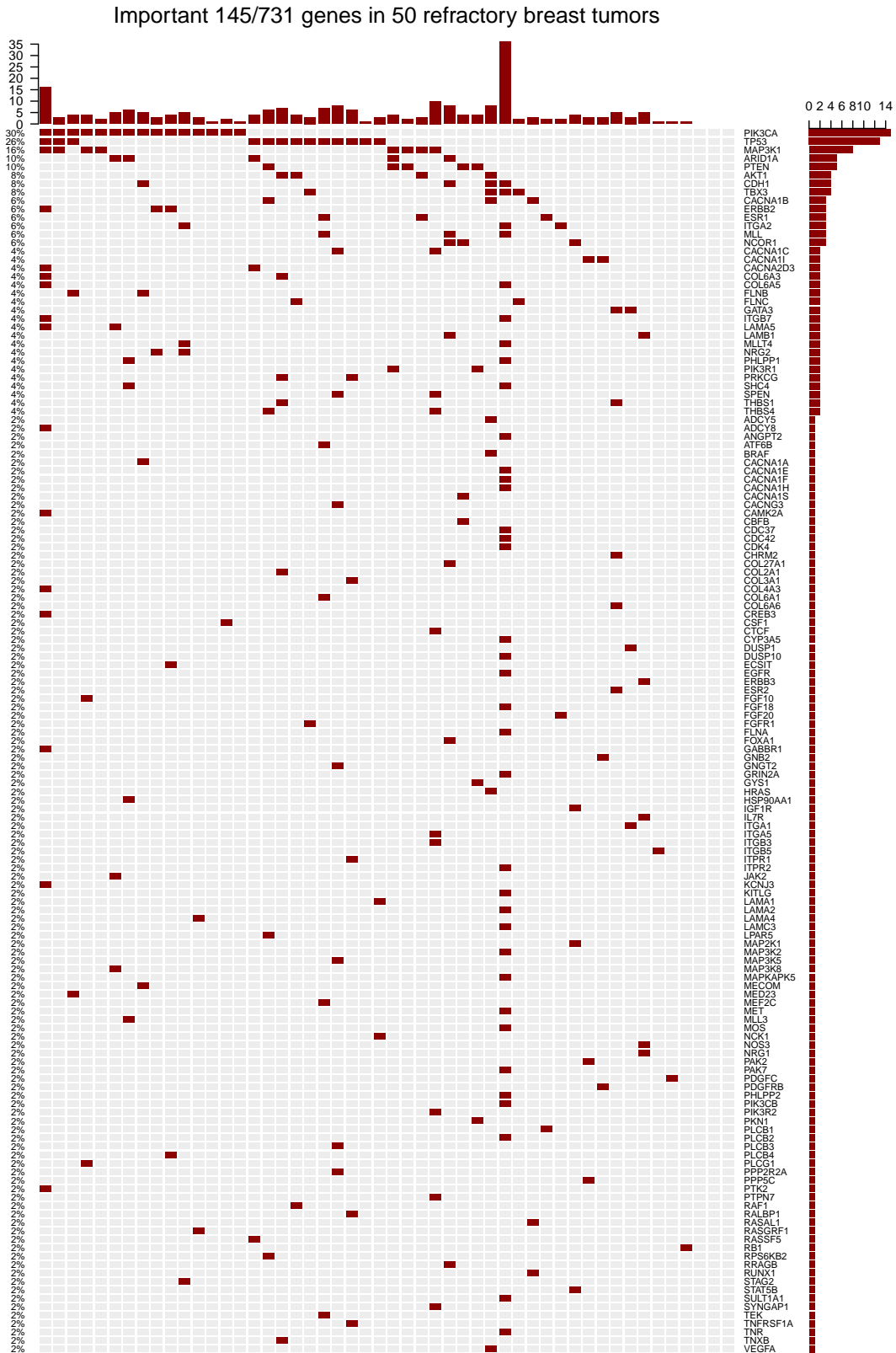


Figure 3.4: SNVs and Indels in refractory breast tumors across different pathways, including ErbB, estrogen, MAPK, mTor, Ras, PI3K-AKT, as well as tamoxifen-related genes and 32 reported significantly mutated genes. In total, there are 731 selected genes, 145 of which harbor mutations (SNVs or Indels).

breast cancer" [92]. One CACNA1A mutation was identified in one primary tumor (~2%, 1/46) (Figure 3.3) and ten different CACNA subunit mutations were detected in 12 refractory tumors (24%, 12/50) (Table 3.1), including CACNA2D3 mutation in two samples (Figure 3.4).

Table 3.1: Mutations of calcium channel, voltage-dependent, alpha subunits (CACNA).

Gene	Sample ID	Chromosome	Position	Reference	Alternative
CACNA1A	615a439	19	13345795	A	C
CACNA1A	IUCQ_T1	19	13563823	T	G
CACNA1B	RZBM_M1	9	140907686	G	A
CACNA1B	T2VO_M1	9	140952667	A	T
CACNA1B	YA4W_M1	9	140807677	G	T
CACNA1C	007M_M1	12	2702384	G	C
CACNA1C	7FNO_M1	12	2760896	A	C
CACNA1E	E65C_M1	1	181721309	C	G
CACNA1F	E65C_M1	X	49068406	C	T
CACNA1F	E65C_M1	X	49081314	C	G
CACNA1H	E65C_M1	16	1265311	G	A
CACNA1I	35XC_M1	22	40082285	G	A
CACNA1I	F7FD_M1	22	40069065	G	A
CACNA1S	NF9D_M1	1	201058422	G	T
CACNA2D3	e64126c	3	54798274	G	A
CACNA2D3	4R5V_M1	3	54798253	A	C

Note: “_T1” indicates primary tumors and the remaining are refractory tumor samples.

Taking 100 genes from estrogen signalling pathway into account, two groups of refractory-specific somatic mutations have been identified, including estrogen receptor (ESR1 and ESR2) and 1-phosphatidylinositol-4,5-bisphosphate phosphodiesterase beta (p.Q244H in PLCB1, p.D981H in PLCB2, p.D32E in PLCB3 and p.D933H in PLCB4) (Figure 3.5). It indicates that patients probably acquired somatic mutations during treatment. ESR1 somatic mutations associate with hormone-resistant breast cancer [7]. A novel somatic mutation¹ S118P, located in ESR1 activation function 1 (AF1) domain, has been identified in the refractory sample WL6X_M1. In addition, H459Q somatic mutation in estrogen-related receptor gamma (ESRRG) was detected.

3.1.3 Expression of mutant allele in breast cancer

Tumor DNA allele frequencies in both primary and refractory tumors are mostly less than 0.5, which may indicate low tumor content in the breast tumor samples. Sequence coverage is approximately 100× and the correlation coefficient between tumor DNA alleles and RNA alleles are 0.58 and 0.51 in primary and refractory tumors, respectively. A little higher disperse distribution is observed in refractory tumors than in primary ones (0.58<0.51) (Figure 3.6).

¹It has been confirmed that ESR1 S118P is a somatic mutation instead of a germline mutation in sample WL6X_M1.

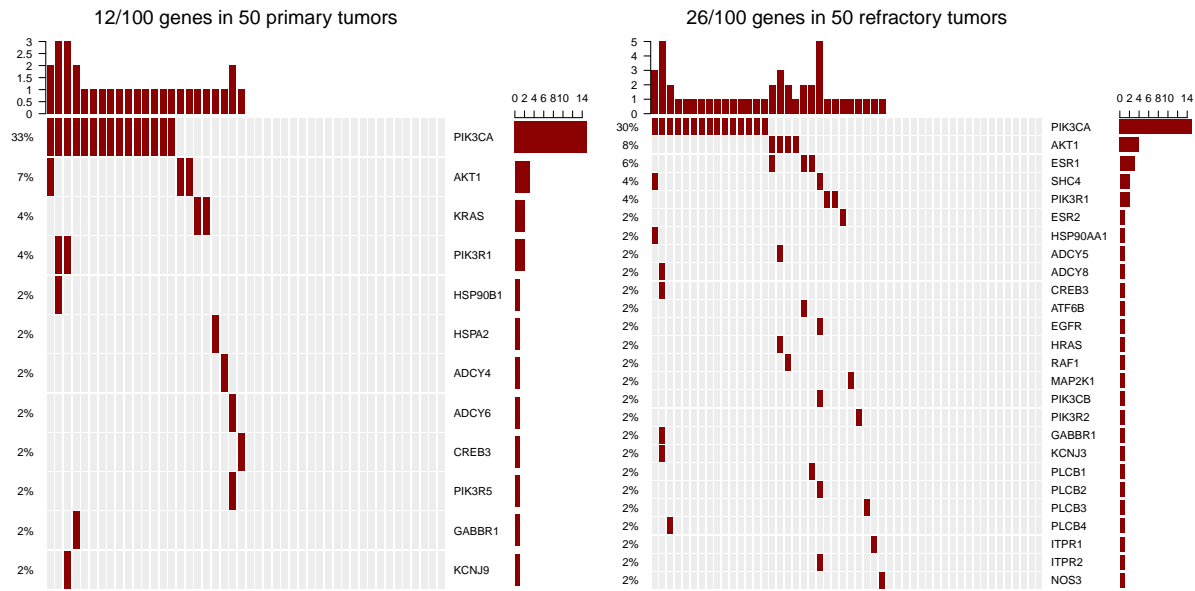


Figure 3.5: SNVs and Indels in the list of genes ($n=100$) from estrogen pathway in breast primary and refractory tumors. Mutations of two gene families ESR and PLCB were only detected in refractory samples, indicating they may be acquired mutations.

3.2 ConfFuse

As mentioned in Chapter 2.3, most fusion gene detection tools generate a large number of false positive fusion transcripts. Therefore, I developed an additional downstream filtering algorithm, confFuse, to address this problem. In this section, the performance of confFuse and the improvement in fusion gene detection are given in detail.

3.2.1 Generation of artefact list

Fusions identified in multiple samples from different tumor types are mostly considered to be of high false positive rate. In total, we used 171 paired-end RNA-seq samples from 15 different entities to generate the artefact list. When considering fusion candidates identified by deFuse-v0.6.1 in no less than three entities (recurrence >3), 2,190 fusions were selected for the artefact list (Figure 3.7). For candidates identified in >4 and >5 entities, there are 1,409 and 995 fusions in the artefact list, respectively. In this study, a threshold of three was chosen for the final artefact list. Of note, a small number of additional putative artefacts are still identified with each increase in the number of different tumor types, suggesting that accuracy could be further improved by increasing the sample size used to generate the artefact list.

In total, 5,881/9,169 (64%) putative fusion transcripts identified in 96 published samples

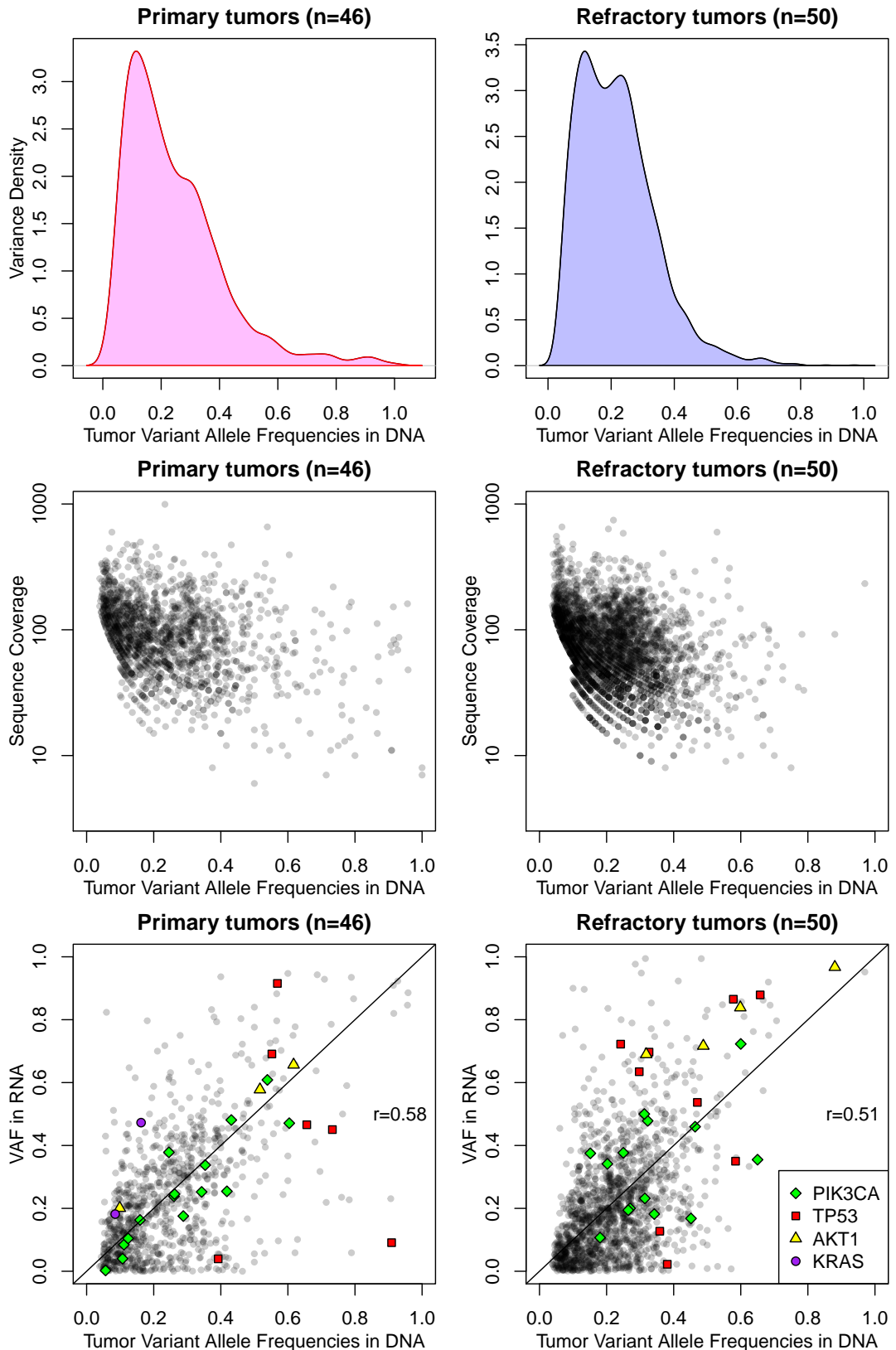


Figure 3.6: Tumor DNA allele variance and tumor allele expression in primary and refractory breast tumors. Read coverage at RNA level is no less than 10. Higher disperse distribution is observed in refractory tumors (bottom).

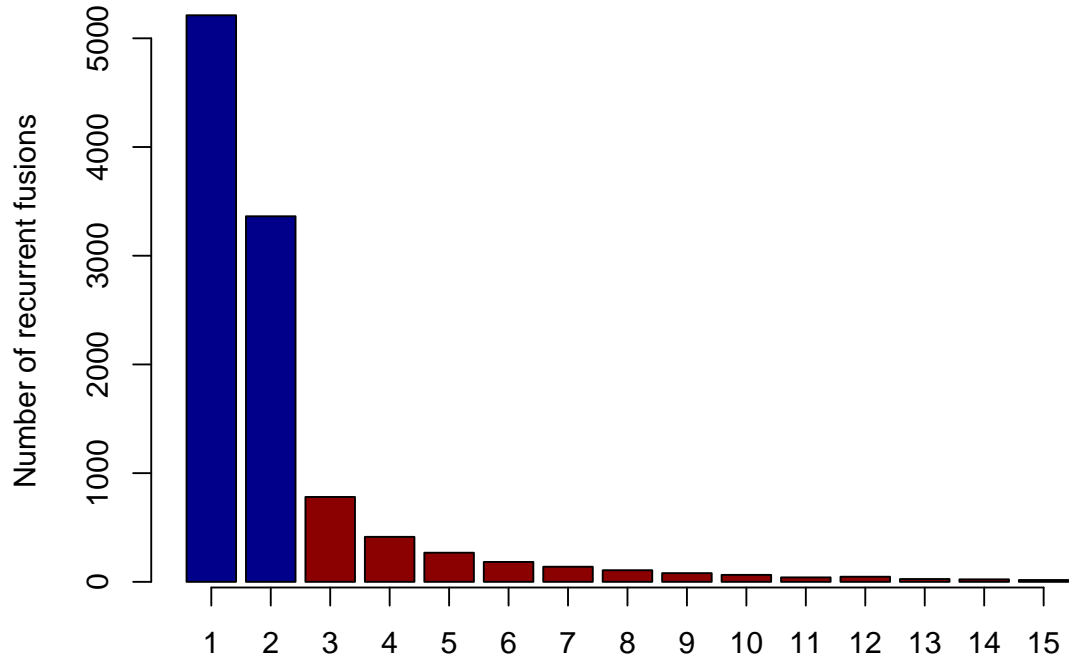


Figure 3.7: The number of recurrent fusions in 15 different entities. Fusions identified in ≥ 3 entities were chosen for the final artefact list, resulting in total of 2,190 artefact fusion genes (red).

were found in the artefact list. 3,666 of 5,881 (62.3%) were fusions from adjacent genes and 5,378/5,881 (91.5%) were identified by deFuse as being a product of alternative splicing.

3.2.2 Recovery rate of validated fusions

In total, 8,083 fusion gene candidates (9,169 putative transcripts) from 96 published samples were identified by deFuse using default settings, 126 of which were previously validated by RT-PCR (Suppl. Table S2). ConfFuse called 301 high-confidence fusion genes (score ≥ 8 , 301/8,083, 3.7%). Among the 301 fusions were 108 of the 126 validated fusions, resulting in a recovery rate of 85.7% (108/126). The remaining previously validated fusions were either scored less than 8 ($n=5$) or were not detected or were already filtered by default deFuse parameters ($n=13$). Two of 126 were scored less than 6.5 (Table 3.2).

3.2.3 Comparison of alternative fusion detection tools

96 paired-end RNA-seq samples from seven published studies were reanalyzed by different fusion detection tools (deFuse, SOAPfuse and FusionMap). Each of the 96 samples harbored at least

Table 3.2: The recovery of validated fusions for deFuse, confFuse-6.5 and confFuse-8.

Published	Number of samples	deFuse fusion transcripts	deFuse fusion genes	confFuse score ≥ 8	Validated fusions	Overlap	confFuse score <8	confFuse score <6.5	Un-detected
Lung cancer liver metastasis [93]	1	237	214	5	1	1	0	0	0
Biphenotypic sinonasal sarcoma [94]	1	315	274	2	1	1	0	0	0
Pilocytic astrocytoma [95]	7	571	514	9	8	8	0	0	0
Thyroid cancer [54]	5	754	651	4	5	4	0	0	1
Ependymoma [96]	7	1165	1019	7	7	6	0	0	1
Lung adenocarcinoma [97]	28	2915	2569	73	39	28	2	1	9
Glioma [55]	47	3212	2842	201	65	60	3	1	2
Total	96	9169	8083	301	126	108	5	2	13

There are 126 previously validated fusions by RT-PCR. 301 high confidence candidates (score >8) were generated by confFuse. The recovery of confFuse and deFuse are 108/126 and 113/126, respectively. Fusion gene pairs with different breakpoints (different fusion transcripts) were counted only once.

one previously validated fusion. These samples were sequenced with different read lengths with a range from 51bp to 101bp (Suppl. Table S1). The number of reads in those samples ranges from ~ 15 million to ~ 206 million (Suppl. Figure S1).

While comparing the recovery rate of 126 previously RT-PCR validated fusions among different fusion gene calling methods (Suppl. Table S2), we used default settings in all tools to avoid parameter bias. DeFuse reports all fusion transcripts with probability ≥ 0.5 by default in the result file (*results.filtered.tsv*). Based on the original deFuse paper [50], deFuse probability 0.81 was additionally chosen as a threshold to examine recovery rate. Fusion genes with different putative fusion transcripts were counted only once and the order of 5' and 3' fusion partners was ignored to simplify the comparison. Score thresholds 6.5 and 8 were used in confFuse for medium to high (medium+high) and high confidence calls, respectively.

Comparing with other tools, fusionMap, deFuse, deFuse-0.81 (deFuse with probability ≥ 0.81), soapFuse, confFuse-6.5 (score ≥ 6.5) and confFuse-8 (high-confidence candidates scored ≥ 8) showed recovery rates of 88.9%, 89.7%, 84.9%, 73.0%, 88.1% and 85.7% respectively for the 126 validated fusions (Figure 3.8; Table 3.3 and Table 3.4), indicating confFuse can dramatically reduce the number of candidates from 8,083 to 301 without compromising detection accuracy related to other available tools. In addition, the correlation between confFuse score and recovery rate in the 96 published samples is given in Figure 3.9.

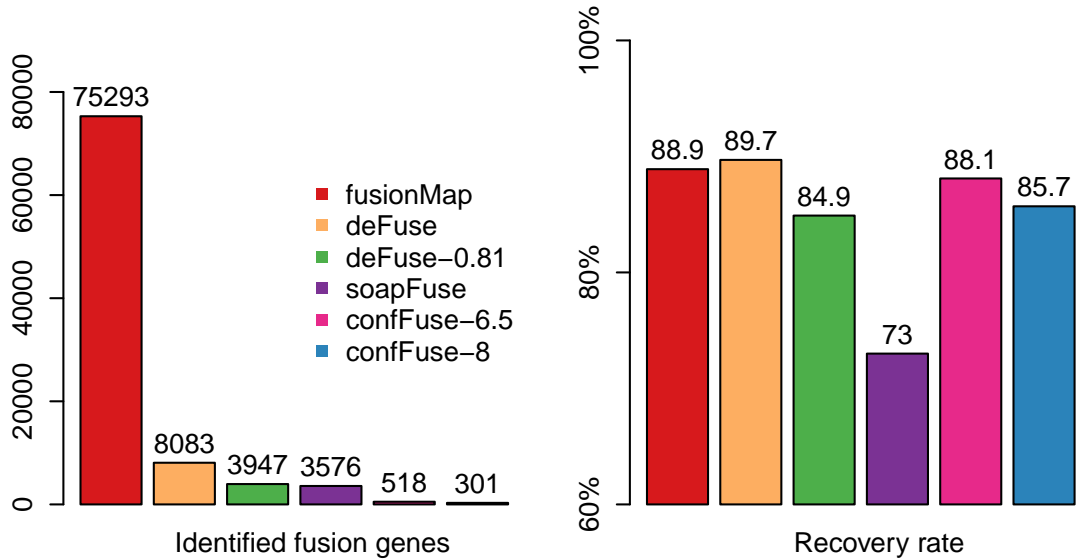


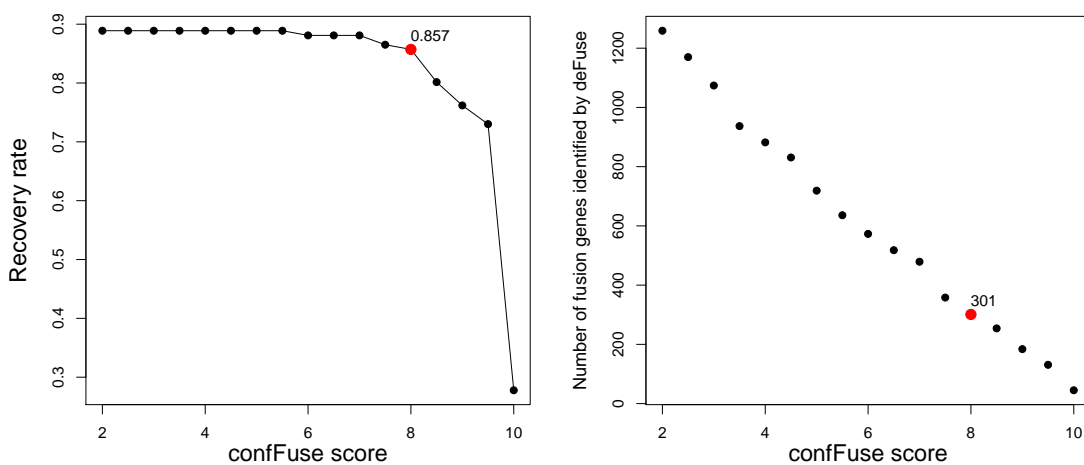
Figure 3.8: Identified fusion genes and recovery rate of validated fusions among different tools. 126 fusions were previously validated by RT-PCR. Five methods (fusionMap, deFuse, deFuse-0.81, confFuse-6.5 and confFuse-8) performed similarly in terms of recovery rate. ConfFuse generated much less fusion candidates than the others while identifying comparable number of validated fusions.

Table 3.3: The recovery of validated fusions in fusionMap.

Published	Number of samples	FusionMap transcripts	FusionMap fusion genes	Validated fusion	Overlap	un-detected
Biphenotypic sinonasal sarcoma	1	224	221	1	1	0
Lung cancer liver metastasis	1	704	676	1	1	0
Thyroid cancer	5	279	272	5	5	0
Pilocytic astrocytoma	7	559	533	7	7	0
Ependymoma	7	2089	2072	8	8	0
Lung adenocarcinoma	28	25384	25176	39	34	5
Glioma	47	46884	46343	65	56	9
Total	96	76123	75293	126	112	14

Table 3.4: The recovery of validated fusions in soapFuse.

Published	Number of samples	soapFuse transcripts	soapFuse fusion genes	Validated fusion	Overlap	undetected
Lung cancer liver metastasis	1	61	56	1	1	0
Biphenotypic sinonasal sarcoma	1	223	183	1	1	0
Thyroid cancer	5	319	291	5	4	1
Ependymoma	7	377	319	8	7	1
Pilocytic astrocytoma	7	477	330	7	6	1
Lung adenocarcinoma	28	1259	1101	39	22	17
Glioma	47	1439	1296	65	51	14
Total	96	4155	3576	126	92	34

**Figure 3.9:** ConfFuse score and recovery rate in 96 published samples. In total, 126 fusion genes were validated, 113 of which were identified by deFuse. ConfFuse detected 108 of 126 known validated fusions with score threshold 8. The right figure shows the correlation between confFuse score and the number fusions identified by deFuse.

3.2.4 Comparison of deFuse probability and confFuse confidence score

The distribution of deFuse probability was compared with confFuse confidence score for all putative fusion transcripts in 96 published samples (Figure 3.10). Notably, there are many putative transcripts with a high deFuse probability that get a low score (~ -8) with confFuse. None of these were in the list of 126 known validated fusions.

3.2.5 Validation of confFuse predicted candidates

To evaluate the accuracy of high-confidence candidate predictions (score ≥ 8), three primary breast tumor samples were sequenced to generate paired-end RNA-seq data. The transcript variant with the highest score was chosen for validation for fusion genes with multiple putative fusion transcripts. In total, deFuse predicted 1,026 fusion genes in the three samples, 18 of which were scored ≥ 8 by confFuse. All 18 high-confidence candidates were validated with RT-PCR followed by Sanger sequencing, resulting in a 100% positive validation rate (Suppl. Table S3). A plot showing the 18 high-confidence validated fusions is given in Figure 3.11.

In addition, some candidates scoring less than eight were randomly chosen for validation in order to get a more comprehensive picture of confFuse confidence scores. Based on the validation results in three primary breast tumor samples ($\sim 69\%$, 9/13 fusions validated, $6.5 \leq \text{score} \leq 7.5$), fusion candidates scored between 6.5 and 7.5 were considered as medium-confidence fusions. Furthermore, 30% low-confidence candidates (3/10, score ≤ 6) were experimentally validated. The validation results are shown in supplementary Table S3 .

To the best of my knowledge, the 18 novel fusion genes haven't been validated before. Interestingly, one of them (QKI:PACRG) was predicted in three of 1,019 breast cancer samples from TCGA [72], indicating that QKI:PACRG may be a novel recurrent fusion in breast cancer. QKI has different isoforms and can suppress cell proliferation, regulate the NUMB gene to prevent inappropriate activation of the Notch signaling pathway in lung cancer [98]. PACRG is an evolutionarily conserved protein and plays an important role in outer-doublet microtubule morphogenesis [99]. The likely biological consequence of this fusion, however, remains unclear.

3.2.6 ConfFuse performance in data sets with verified fusion genes

In the 22 pediatric glioblastoma multiforme from ICGC project, 50 fusions were previously validated by RT-PCR, 46 of which are in the list of 242 high-confidence fusions. Comparing with

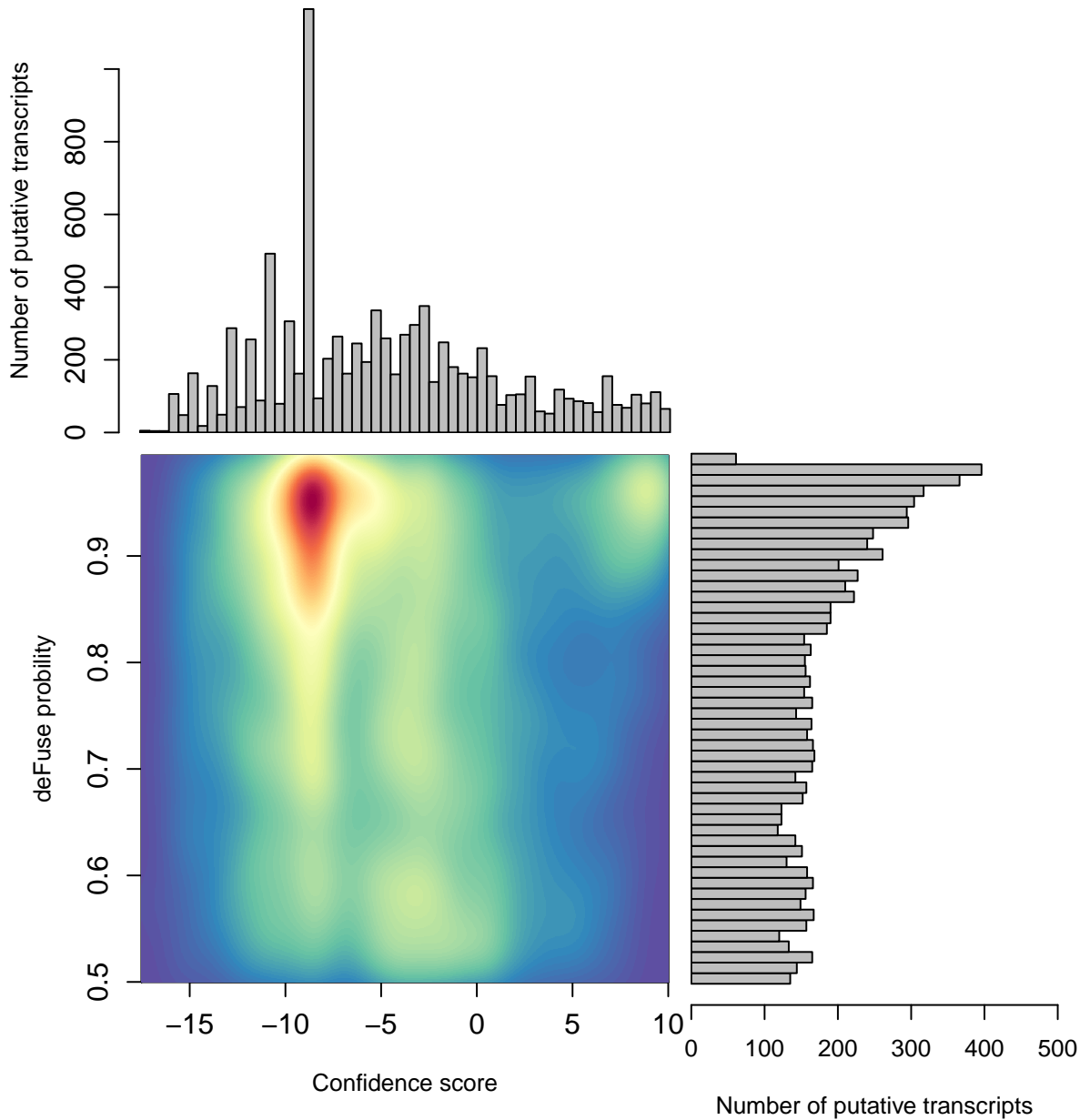


Figure 3.10: Comparison of probability predicted by deFuse and confidence score by confFuse in 96 published RNA-seq samples. High density is of red color and low density is of blue color.

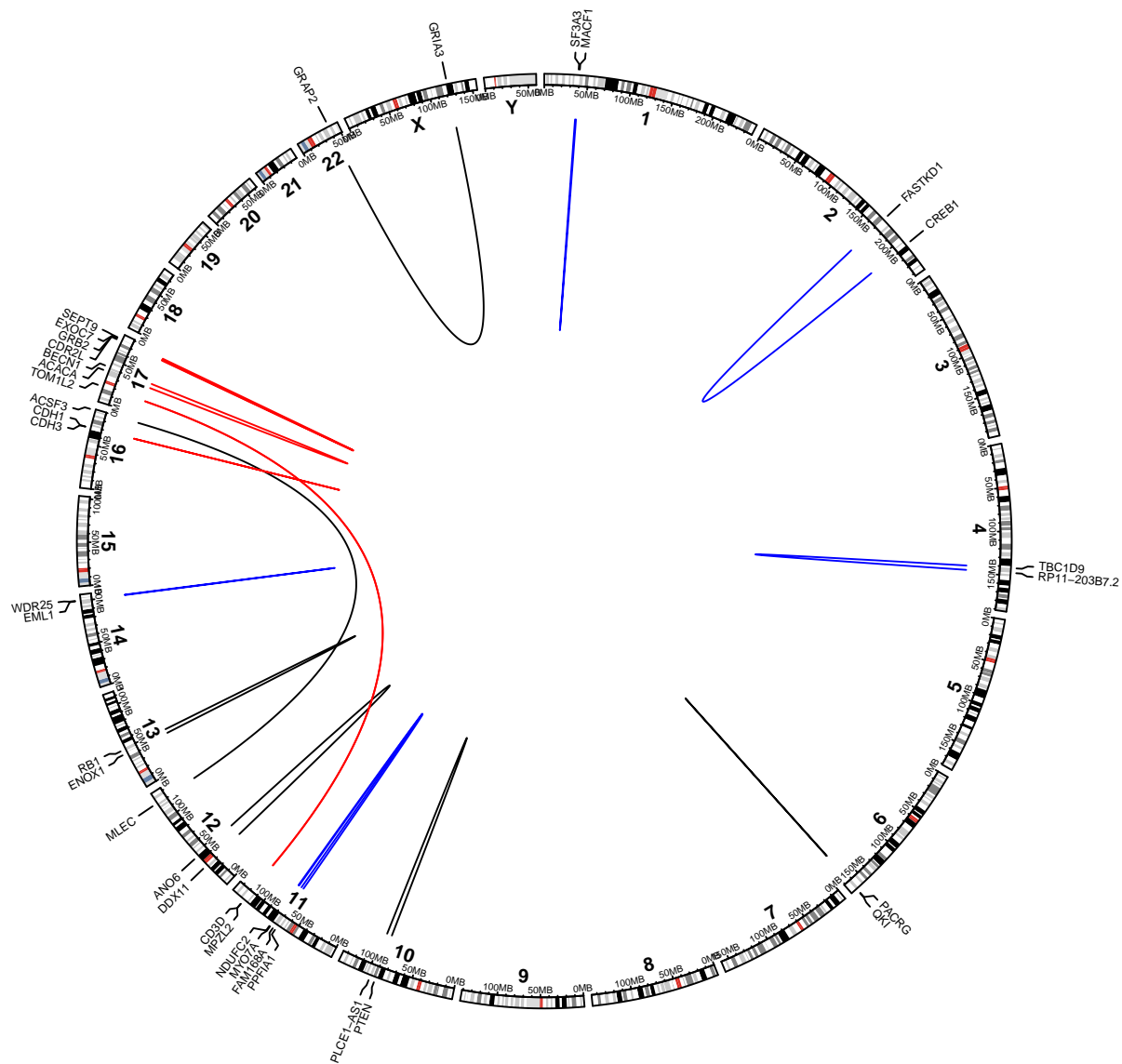


Figure 3.11: 18 high-confidence fusions validated by RT-PCR followed by Sanger sequencing in three primary breast tumor samples (AC72 red, 8HNA black and DR8V blue).

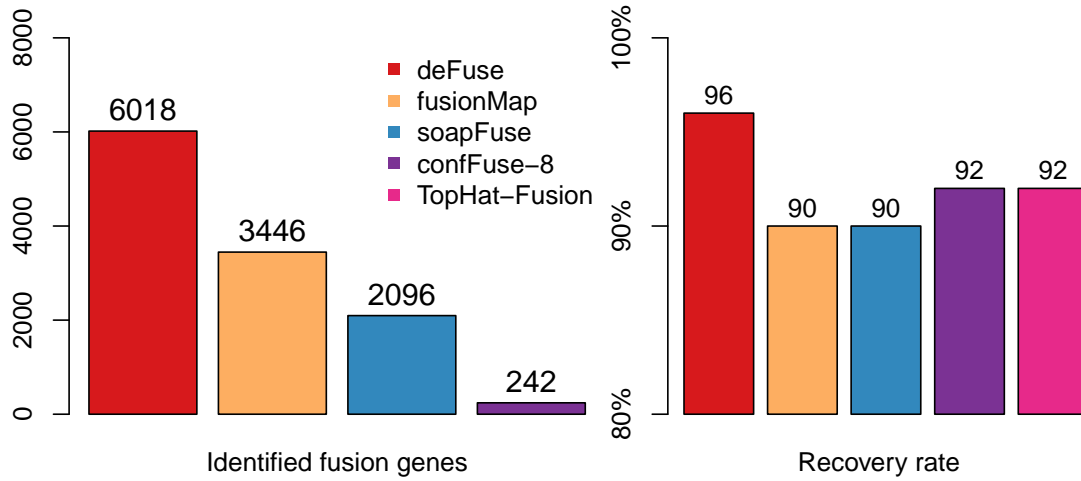


Figure 3.12: Comparison of different fusion detection tools in 22 GBM. All methods perform well with $\geq 90\%$ recovery rate. ConfFuse dramatically reduces the number of fusion candidates from 6,018 to 242. The number of fusions detected by TopHat-Fusion is not available.

other three tools (Tophat-Fusion², soapFuse and fusionMap), confFuse achieved a recovery rate of 92% which is similar to the other tools (Figure 3.12).

242 of 6,018 fusion genes were scored ≥ 8 as being high-confidence by confFuse. Fusion candidates³ based on whole genome sequencing and mate-paired sequencing were identified by structural variance detection tools CREST and DELLY. 150 of 242 high-confidence candidates have evidence either from previously validated fusions or DNA-seq support (whole genome sequencing and mate-paired sequencing), resulting in a *validated rate* of $\sim 62\%$ (150/242) (Figure 3.13).

In the 27 RNA-seq samples from the INFORM project, 94 of 8,549 fusion genes were scored ≥ 8 , 25 of which were previously validated by RT-PCR⁴ (Table 3.5). Another two validated fusions were scored as 5.5 and 7. Recurrent fusions EWSR1:FLI1, EWSR1:ERG and PAX3:FOXO1 were identified by confFuse.

²Fusion genes identified by TopHat-Fusion were provided from David T.W. Jones. The total number of fusions detected by TopHat-Fusion is not available.

³Fusion candidates based on WGS and mate-paired sequencing are from David T.W. Jones.

⁴Independent validation was done by Stefan Pfister's group.

Table 3.5: High-confidence fusion genes in 27 INFORM samples (n=94), 25 of which were previously validated by RT-PCR (boldface).

Gene1	Gene2	Sample ID	Gene1	Gene2	Sample ID
ACTG1	ACTB	I007_002	PAX3	FOXO1	AC_00A
CAMKMT	ALK	TU_00A	PAX3	FOXO1	BE_00B
CARS	ALK	ES_00A	PAX3	FOXO1	ST_00E
DCX	CAPN6	BE_00B	PAX3	FOXO1	HL_00B
DNAH2	C17orf85	HD_00M	PAX3	FOXO1	I019_001
DNAJC21	ARL15	I023_001	PDGFRA	KIT	I027_003
DRAXIN	ATN1	FR_00C	POLR2B	HOPX	I027_003
EWSR1	ERG	FR_00C	PRKAR1A	CNTROB	HD_00M
EWSR1	ERG	ST_00D	PTGES3	MYT1L	HL_00B
FAM131B	BRAF	BE_00F	PTPRZ1	AC006159.3	HD_00M
FAM228B	CD81	ES_00A	PTPRZ1	MET	HD_00M
FKBP1A	FAM71E1	I023_001	PUM1	CEP95	ST_00E
FLI1	EWSR1	MS_00B	QRICH2	MRC2	HD_00M
FLI1	EWSR1	MS_00C	RAB3GAP1	HADHA	ES_00A
FLI1	EWSR1	MS_00G	RFC2	CLIP2	HD_00M
FLI1	EWSR1	GO_00A	RNF213	ABR	HD_00M
FLI1	EWSR1	HD_00P	RP11-3L8.3	C9orf72	I023_001
FLI1	EWSR1	I041_001	RP11-440L14.1	MYO7A	ST_00A
FLI1	EWSR1	I042_001	SLC22A23	BPHL	I023_001
FLI1	EWSR1	LZ_00A	SLC35D2	PGM5	I023_001
GMEB1	EXT2	I015_001	SMC5	RP11-289F5.1	I023_001
GOLGB1	EYA1	I015_001	SMPDL3B	CNBP	ST_00E
GRAMD1B	CELF2	I007_002	SOCS5	KIF1A	I015_001
GUSBP2	GUSBP11	I007_002	SPAG7	FAM117A	HD_00M
HBD	HBB	I074_001	SPATA8	DYRK1A	I023_001
HLA-G	HLA-C	I019_001	SPTBN4	CA8	I023_001
HLA-L	HLA-B	HL_00B	STK35	SAMD4B	I023_001
HLA-L	HLA-B	I027_003	STON2	CD82	I015_001
HLA-L	HLA-B	I074_001	STXBP1	NTMT1	I023_001
INPP5D	ABL1	I074_001	SUGT1	NOL6	ST_00E
IVNS1ABP	IL8	I019_001	SUV420H1	NUMA1	ST_00A
KIAA1211	HEATR7B2	HD_00M	SYNPO2L	FAM177A1	TU_00A
KIF27	CNTNAP3B	I023_001	TANC2	ITGAE	HD_00M
LILRA6	AC008984.2	I019_001	TBC1D15	FAM109A	MS_00C
LNX1	CEP135	I027_003	TCERG1L	GPR123	I023_001
LNX1	KDR	I027_003	TMEM165	KDR	I027_003
MFF	ARIH2	LZ_00A	TSFM	SPRYD4	HL_00B
MLLT10	MLL	I007_002	UNKL	IFT140	ST_00D
NAA10	HAUS7	I019_001	USP46	KCNK17	I023_001
NASP	LUZP1	TU_00A	USP46	NMU	I027_003
NFX1	HMCN1	ST_00D	USP8	MLL	ST_00A
NOTCH2	DIO1	I015_001	VPS35	HSBP1	TU_00A
NOTCH2	LRRC42	I015_001	VSTM1	LSM14A	I023_001
NTRK2	GKAP1	I023_001	WT1	EWSR1	AC_00B
OTOG	ATP2B1	TU_00A	WWC2	PDLIM3	I023_001
OTUB1	NAA40	BE_00B	ZNF202	FCHSD2	I007_002
PAMR1	ABTB2	I023_001	ZNF577	SLC8A2	I023_001

Note: The order of fusion partner 5' and 3' is ignored to simplify comparison. Another two validated fusions CIC:DUX4L7 and RELA:C11orf95 were scored as 5.5 and 7 by confFuse, respectively.

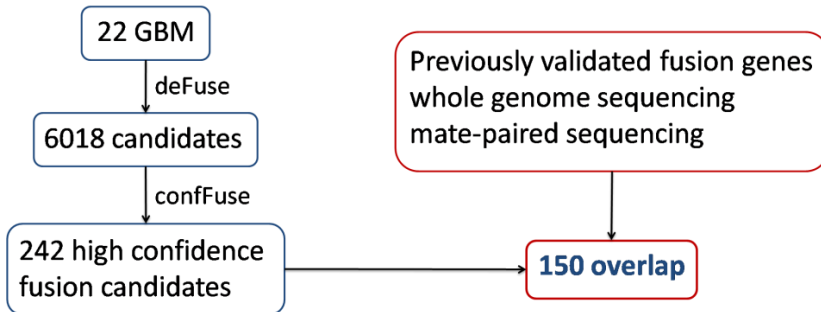


Figure 3.13: Validated fusions in 22 GBM based on known fusions and DNA-seq supporting evidence. 150 of 242 confFuse candidates are reconfirmed, resulting in a *validation rate* of ~62%.

3.3 Fusion genes in different tumor entities

3.3.1 Sarcoma

The HIPO-028 project aims to identify *actionable* genetic alteration in soft-tissue sarcoma based on whole-exome and whole-transcriptome profiling. In total, 83 sarcoma RNA-seq samples were analyzed and confFuse identified 680 high-confidence fusions (1253 fusions scored ≥ 6.5) (Suppl. Table S4), 19 of which were recurrent fusions (Table 3.6), including well-known fusion SS18:SSX1 in synovial sarcoma [100] and fusion FUS:DDIT3 in myxoid liposarcoma [101].

Table 3.6: Recurrent fusion genes identified in HIPO-028 sarcoma samples.

Gene1	Gene2	Recurrence (score ≥ 8)	Gene1	Gene2	Recurrence ($6.5 \leq$ score < 8)
SSX1	SS18	4	LRRC37A2	KANSL1	2
FUS	DDIT3	4	SH3PXD2A	AC021066.1	2
GRIP1	CSAD	2	SLC25A3	RPL6P25	2
MDM2	CPM	2	TMTC2	METTL25	2
RAPGEF3	ESPL1	2	TPH2	TMTC2	2
RP11-547C5.2	ATP2B1	2	TRHDE	SP1	2
STAT6	NAB2	2	ZRANB3	IFI6	2
TMEM106C	GIT2	2			
UBC	NCOR2	2			
UBE2N	CPM	2			
VDR	TSFM	2			
VTI1A	TPH2	2			

Several recurrent fusion partners were identified, including fusion partner fibroblast growth factor receptor substrate 2 (FRS2) in nine samples, E3 Ubiquitin protein ligase MDM2 (proto-oncogene) in nine samples, protein tyrosine phosphatase receptor-type R (PTPRR) in three samples and Ras-related protein Rap-1b (RAP1B) in three samples (Table 3.7). Fusion OSBPL8:PRPRR

was identified in one of 1,019 TCGA breast cancer samples and fusions C12orf28:MDM2 and FRS2:MDM2 were identified in two different TCGA lung adenocarcinoma samples ($n=487$), respectively. In addition, a novel fusion RICTOR (rapamycin-intensive companion of MTOR)::AKT1 (RAC-alpha serine/threonine-protein kinase) was categorized as being high-confidence in one sample.

Table 3.7: Fusions with recurrent partners (score ≥ 8) in 83 sarcoma samples.

Gene1	Gene2	Sample ID	Gene1	Gene2	Sample ID
MDM2	CAND1	91Z1	PTPRR	LGR5	RZA9
MDM2	CENPL	91Z1	PTPRR	OSBPL8	NTAT
MDM2	KCNMB4	91Z1	PTPRR	PPM1H	JSF3
MDM2	AL583842.3	TT6Q	CTDSP2	FRS2	6SSR
MDM2	C12orf28	RW8V	ANO2	FRS2	NTAT
MDM2	CPM	RW8V	EFHC1	FRS2	91Z1
MDM2	CPM	6MN5	DAB1	FRS2	HLDX
MDM2	KATNA1	T56Q	RP11-620J15.3	FRS2	TT6Q
MDM2	FAM5B	NF4Z	LRRC8B	FRS2	W7DB
MDM2	PIP4K2C	JSF3	MARCH9	FRS2	W7DB
MDM2	PTPRD	8UBW	PRTFDC1	FRS2	LL1U
MDM2	SNX9	W7DB	SRXN1	FRS2	LL1U
RAP1B	ELK3	RW8V	METTL25	FRS2	8UBW
RAP1B	LRRC8C	W7DB	PDE4DIP	FRS2	2CJV
RAP1B	RPS6KA3	6SSR	MDM2	FRS2	W7DB

Note: The order of fusion partner 5' and 3' is ignored to simplify comparison.

3.3.2 Prostate cancer

Based on RNA-seq data from 11 published early-onset prostate cancer [53], 849 fusion genes were called by deFuse, 24 of which were identified as high-confidence fusions (score ≥ 8) by confFuse. The well-known E26 transformation-specific (ETS) fusion genes were identified in 10 of 11 samples, which are the same as previously published results [53]. Among the 24 candidates, 17 were confirmed by DNA-seq, FISH validation or known ETS fusions, resulting in a ~70% (17/24) recovery rate (Table 3.8). Furthermore, a novel 3' fusion partner CEP85 of gene TMPRSS2 (TMPRSS2:CEP85) was identified.

The ICGC early-onset prostate cancer project conducts a system genomic analysis to identify hereditary mechanisms and to find optimal treatment regimens based on NGS data such as WGS and RNA-seq. A cohort of 84 unpublished prostate cancer RNA-seq from ICGC project shows 117 high-confidence fusion genes (score ≥ 8) from identified 9,043 candidates (371 fusions scored ≥ 6.5) (Suppl. Table S5). In total, ~48.8% (41/84) of samples harbor rearrangements of TMPRSS2, ERG, ETV1 or ETV4. Several novel fusion genes were identified, including RIOBP:ERG,

Table 3.8: 24 high-confidence fusion genes identified in 11 early-onset prostate cancer by confFuse. The confirmed evidence (DNA-seq support) is from published paper [53].

SampleID	Gene1	Gene2	Support from DNA-seq	Descriptions
EOPC_01	PPAP2A	MICAL2	Y	FISH validated
EOPC_01	RBM47	FBXL14	Y	DNA-seq support
EOPC_01	ZNF37A	BCL2L13	-	-
EOPC_02	SLC45A3	ERG	Y	ETS fusion
EOPC_02	TFG	GPR128		validated in other tumors
EOPC_03	SNRPN/SNURF	ETV1	Y	DNA-seq support
EOPC_04	MIPEP	FOXP1	Y	FISH validated
EOPC_04	TMPRSS2	ERG	-	ETS fusion
EOPC_05	TMPRSS2	ERG	-	ETS fusion
EOPC_05	VPS8	SHISA5	-	-
EOPC_06	PPP2R1A	GPX3	-	-
EOPC_06	SLC45A3	ERG	Y	ETS fusion
EOPC_06	TMEFF2	DTWD2	Y	DNA-seq support
EOPC_06	TMPRSS2	EPB41L1	Y	DNA-seq support
EOPC_07	SETD1A	H6PD	-	-
EOPC_07	TMPRSS2	ERG	-	ETS fusion
EOPC_08	TMPRSS2	ERG	-	ETS fusion
EOPC_09	CEP85	ARHGAP35	-	-
EOPC_09	TMPRSS2	CEP85	-	-
EOPC_09	TMPRSS2	ERG	Y	ETS fusion
EOPC_09	TMPRSS2	ERG	-	ETS fusion
EOPC_011	LINC00365	ABCC4	-	-
EOPC_011	PRPH2	NEDD4L	Y	FISH validated
EOPC_011	TMPRSS2	ERG	-	ETS fusion

TMPRSS2:LNX1, AGR:ETV1 and RAB4A:ETV4. Three recurrent fusion genes were identified as being high-confidence, namely TMPRSS2:ERG (34/84, ~40%), KLK3:KLK2 (17/84, ~20%) and SLC45A3:ERG (2/84, ~2%). A further analysis of kallikrein-related peptidase gene family (prostate-specific antigen is a member), including KLK3 and KLK2, should be followed in order to find out whether there are aberrations.

3.3.3 Glioblastoma multiforme

The HIPO-016 project aims to identify potential molecular markers and therapy-interference points in adult gliomas by integration of clinical data and deep sequencing data such as RNA-seq, DNA-methylation and exom-seq. In the HIPO-016 project, there are 48 adult GBM, 22 low-grade glioma tumors and 5 healthy brain RNA-seq samples. 470 fusion candidates (score ≥ 6.5) were identified, 227 of which were scored ≥ 8 (Suppl. Table S6). Twelve recurrent fusion genes were identified, including a novel fusion ST7:MET which was validated by RT-PCR followed by Sanger sequencing⁵ (Table 3.9). Another MET fusion (JAZF1:MET) was also identified. A plot of the 12 recurrent fusions is given in Figure 3.14.

Four novel rearrangements of glioma-associated oncogene homolog 1 (GLI1), namely

⁵Validation has been done by Yonghe Wu.

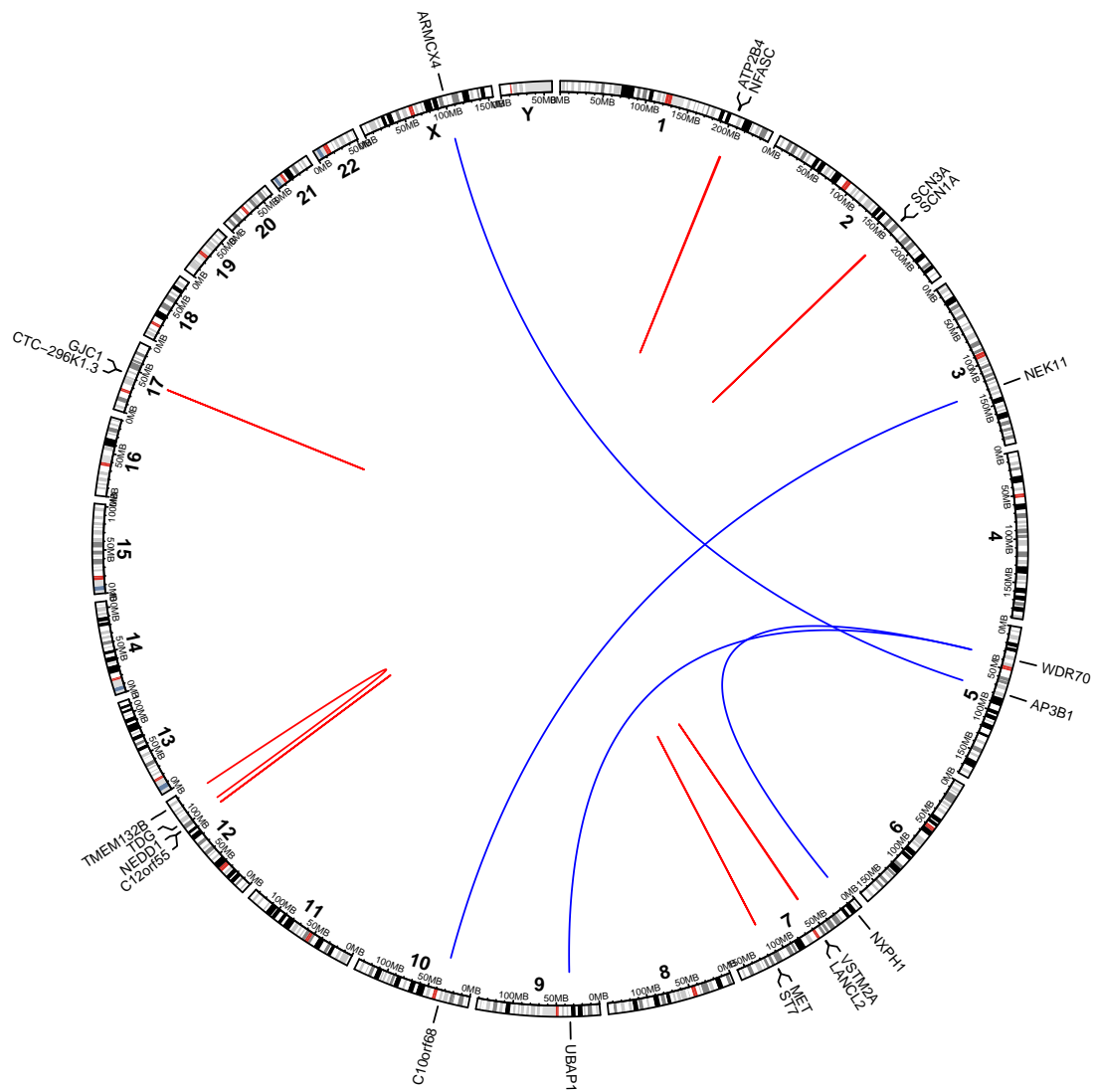


Figure 3.14: Plot of 12 recurrent fusions (score ≥ 6.5) in 48 GBM samples. Blue color shows the inter-chromosome fusions and red color represents the intra-chromosome fusions.

Table 3.9: Recurrent fusions (n=12, score ≥ 6.5) in 48 GBM samples.

Gene1	Gene2	Recurrence	Gene1	Gene2	Recurrence
TRIO	ARHGEF3	3	TMEM132B	TDG	2
SCN3A	SCN1A	3	ST7	MET*	2
NEDD1	C12orf55	3	NFASC	ATP2B4	2
WDR70	UBAP1	2	NEK11	C10orf68	2
WDR70	NXPH1	2	GJC1	CTC-296K1.3	2
VSTM2A	LANCL2	2	ARMCX4	AP3B1	2

Note: The order of fusion partner 5' and 3' is ignored to simplify comparison.

* Fusion ST7:MET in two different samples was experimentally validated.

AATF:GLI1, CPSF6:GLI1, DDIT3:GLI1 and INHBE:GLI1, were identified in four different samples (three fusions scored ≥ 7 and one scored 3.5). Interestingly, expression of GLI1 is much higher in samples with GLI1 rearrangement than in ones without GLI1 fusions (Figure 3.15), indicating that over expression of GLI1 maybe a result of fusion. Validation of GLI1 rearrangements and further analysis should be carried on in the future.

3.3.4 Germinal-center derived B-cell malignant lymphoma

The project ICGC-MMML-Seq (Molecular Mechanisms in Malignant Lymphoma by Sequencing) aims to translate finding based on NGS data to clinics. A cohort of 135 GCB-lymphoma samples from project ICGC-MMML-Seq was analyzed by confFuse. In total, 380 fusions (score ≥ 6.5) were identified by confFuse, 174 of which were scored ≥ 8 (Suppl. Table S7). Among the 135 samples, 118 of them harbored at least one fusion with score ≥ 6.5 (74 samples with at least one fusion scored ≥ 8) (Figure 3.16). Comparison of the median number of fusions identified that one sample (ID 4145528) harbors much more putative fusion candidates than the others (67 fusions scored ≥ 6.5 and 32 fusions scored ≥ 8) (Figure 3.16). Score threshold 6.5 was chosen for further analysis in this cohort because previously reported IGH:BCL2 rearrangement was identified as being scored ≥ 6.5 in several samples (mentioned below).

In total, 50 of 135 samples harbor at least one fusion which has fusion partner immunoglobulin (IG), such as immunoglobulin kappa locus (IGK) and immunoglobulin heavy locus (IGH). Multiple recurrent rearrangements were identified, including previously published ones such as IG:MYC (in six samples), BCL2:IGH in 11 samples, BCL6:IGH in six samples and IG rearrangements (IGKJ5:IGKV5-2 in eight samples) (Table 3.10 and Figure 3.17).

In addition, several novel recurrent fusions were identified, such as HLA-DPB1:HLA-DRB1 (n=7) and RIPK1:SERPINB9 (n=4). Receptor-interacting serine/threonine-protein kinase 1 (RIPK1) plays an important role in caspase-independent cell death [102]. Protease inhibitor 9 (SERPINB9) is a member of the serine protease inhibitor family, which can specifically inhibit

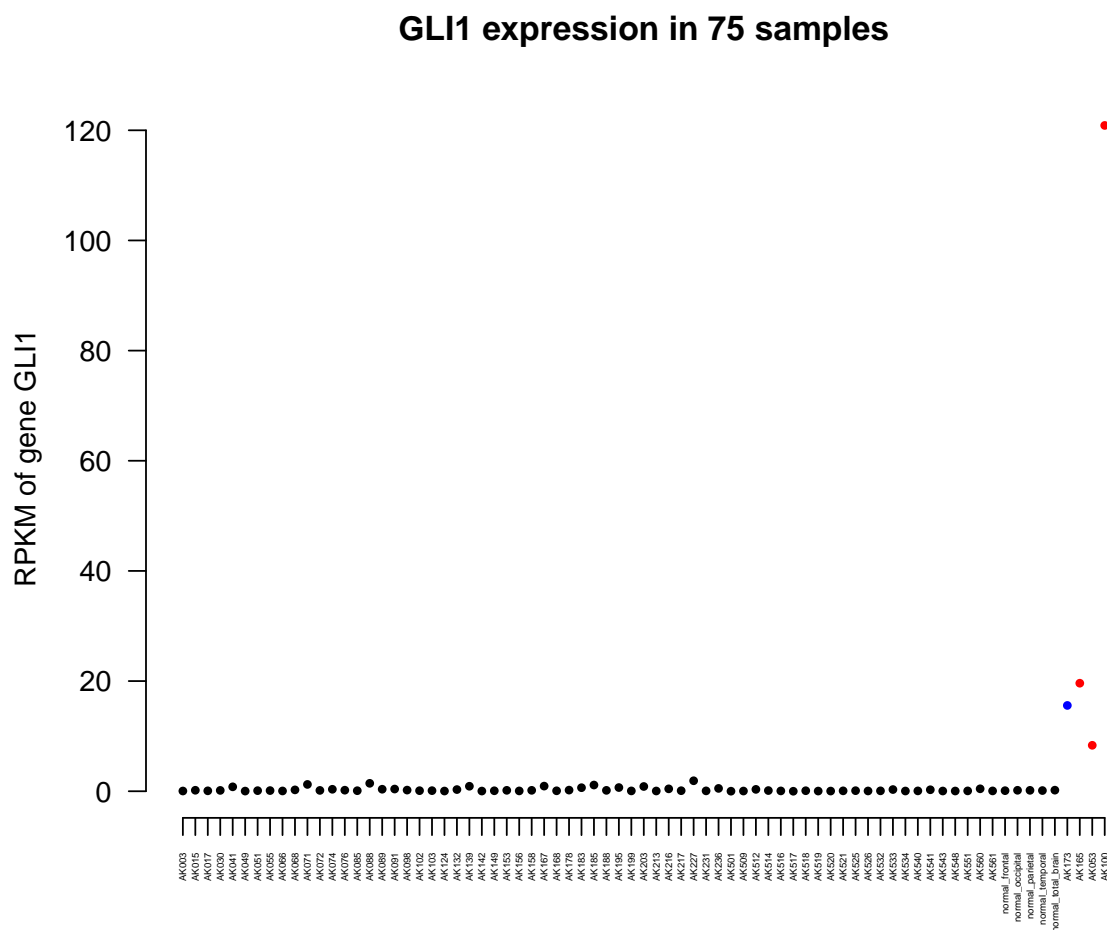


Figure 3.15: Gene expression of GLI1 in 75 samples (48 GBM, 22 low-grade gliomas and five healthy brain samples). Fusions AATF:GLI1 and CPSF6:GLI1 (score ≥ 8) were identified in sample AK100 and AK053, respectively (red). Another fusion DDIT3:GLI1 (score=7) was found in sample AK165 (red) and fusion INHBE:GLI1 was detected as a read-through transcript in sample AK173 (blue).

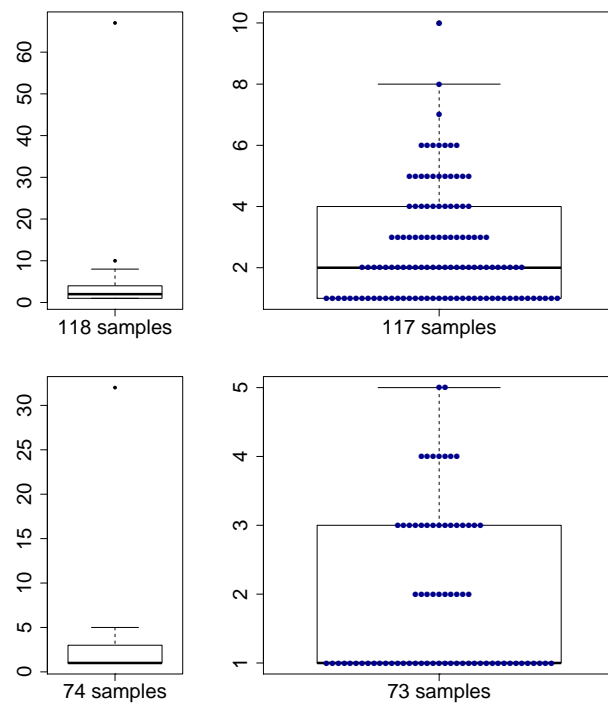


Figure 3.16: Number of fusions scored ≥ 6.5 (top) and ≥ 8 (bottom) in 135 lymphoma samples. One sample has very high number of predicted fusions, indicating higher level of genomic aberration. Most of the remaining samples harbor ≤ 4 fusions. The right box plots show the results after removing one outlier.

Table 3.10: 29 recurrent fusion genes (score ≥ 6.5) in 135 lymphoma samples.

Gene1	Gene2	Recurrence	Gene1	Gene2	Recurrence
IGKJ5	IGKV5-2	8	IGHM	RP11-211G3.2	2
HLA-DPB1	HLA-DRB1	7	LYZ	RP11-186B7.4	2
AC016831.7	SYT9	6	AL122127.3	RP11-1136L8.1	2
HERC2P3	RERE	6	IGHM	MYC	2
ASMT	HLA-DQA1	5	KIAA0922	MND1	2
GPR128	TFG	4	FCRL3	LSAMP	2
RIPK1	SERPINB9	4	CHMP1A	IGLL5	2
AL122127.3	BCL6	4	BCL2	IGHJ6	2
ATAD3A	SH3BP1	3	BCL2	IGHJ3	2
BCL2	IGHJ5	3	BCL6	IGHG3	2
BCL2	IGHJ4	3	HLA-B	HLA-G	2
BCL2	IGHG1	3	HLA-B	HLA-F	2
SLC16A14	TRIP12	2	HLA-DPB1	HLA-DRB5	2
LYN	TGS1	2	ANXA1	CD58	2
KIF20B	SPINK9	2			

Note: The order of fusion partner 5' and 3' is ignored to simplify comparison.

Table 3.11: Nine validated fusions in lymphoma samples.

Sample	Gene1	Gene2	Deletion	Score
B0979	CTSB	C8orf12	Y	2
B0979	RAI1	TOM1L2	Y	-8.5
B0979	ESCO1	GREB1L	Y	-2.5
B2196	ARID5B	SOX5	N	10
B2193	ZNF407	EPSTI1	N	10
B2190	ZC3H11A	ATP2B4	N	7.5
C1635	RCSD1	MPZL1	Y	-1
C1561	CCDC106	U2AF2	Y	0
B0981	TRAF3IP2	CD109	N	9.5

Note: The order of fusion partner 5' and 3' is ignored to simplify comparison.

granzyme B (a cytotoxic serine protease) in the cytosolic granules of cytotoxic T lymphocytes and natural killer cells [103]. A novel fusion HLA-E:HLA-B has been experimentally validated in esophageal squamous cell carcinoma [104]. The biological function of this fusion (HLA-E:HLA-B), however, remains unclear.

An independent validation of nine fusions has been done in this project⁶. All the four non-deletion fusions were identified with score ≥ 7.5 . The rest five deletion fusions have not been identified as medium/high confidence fusions (Table 3.11).

⁶Independent validation was done by Reiner Siebert's group.

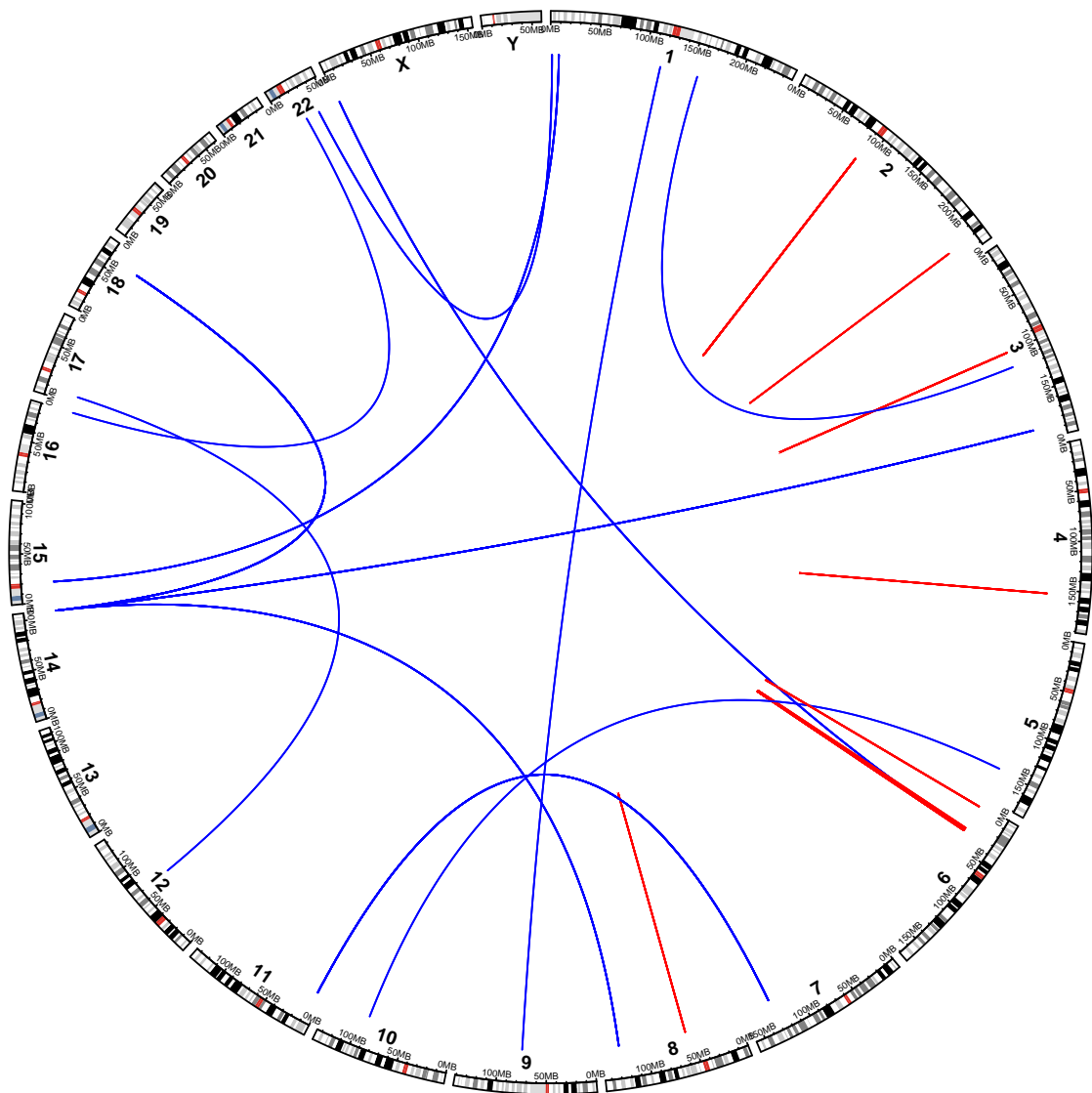


Figure 3.17: Plot of 29 recurrent fusion genes scored ≥ 6.5 in 135 lymphoma samples. Blue shows the inter-chromosome fusions and red color represents the intra-chromosome fusions.

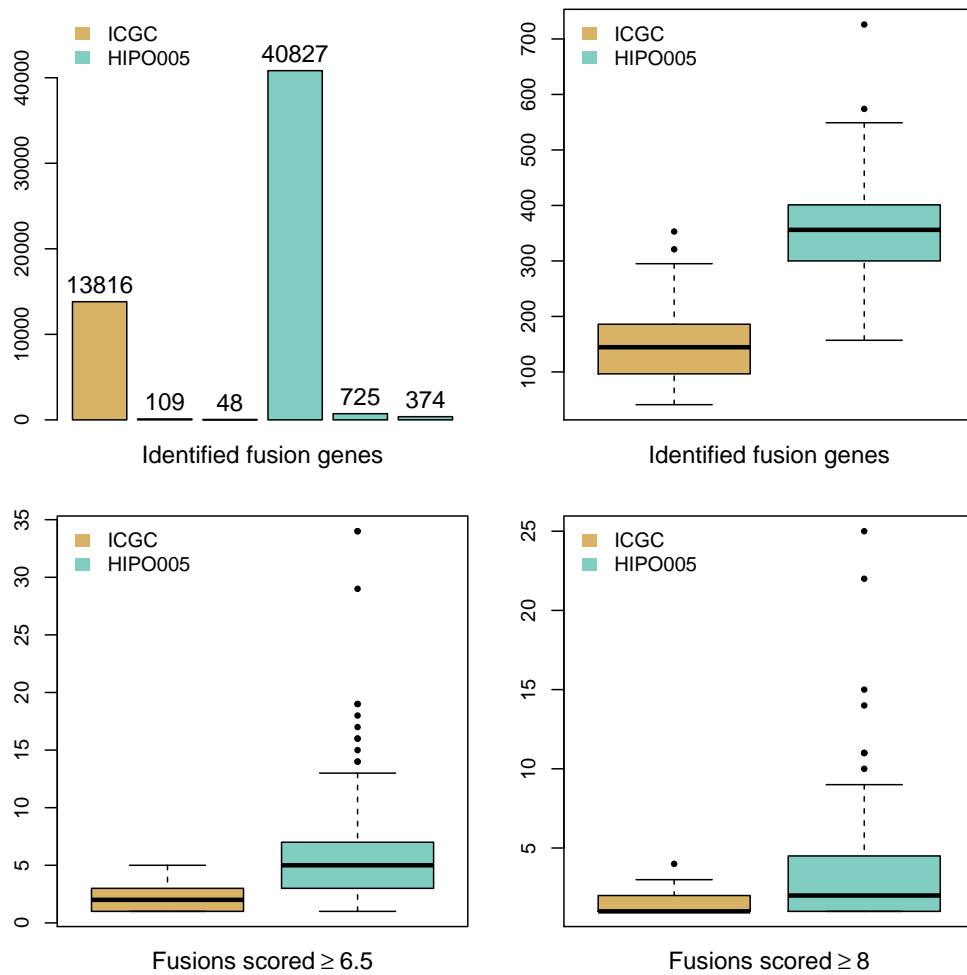


Figure 3.18: Number of fusions identified in CLL samples from ICGC ($n=96$) and HIPO-005 ($n=114$). Numbers of high-confidence fusions identified in projects ICGC and HIPO-005 are 116 and 374, respectively (209 and 725 fusions scored ≥ 6.5).

3.3.5 B-cell chronic lymphocytic leukemia

The HIPO-005 aims to identify the critical gene mutations which may result in therapy resistance or partially sensitive in CLL samples based on exom-seq and RNA-seq data. In total, 374 of 40,827 fusion genes were identified as being high-confidence in 114 CLL RNA-seq samples from the HIPO-005 project (725 fusions scored ≥ 6.5) (Suppl. Table S8). In 96 published CLL samples from the respective ICGC project [105], 48 of 15,501 fusion genes scored ≥ 8 (109 fusions scored ≥ 6.5). The number of fusions identified in HIPO-005 samples was much higher than the one in ICGC samples (Figure 3.18).

Many recurrent fusions were identified in CLL samples from both ICGC and HIPO-005 (Table 3.12). Most of the recurrent fusions identified here are novel and have not been reported before,

including CXCR4:PTMA, CXCR4:CHD2 and CXCR4:GNAS. The gene fusion CXCR4:PTMA was identified in 82 of 114 CLL samples from HIPO-005 (score ≥ 6.5). To make a complementary detection, another fusion detection tool fusionMap was applied on these CLL samples. In total, 96 samples from HIPO-005 harbor CXCR4:PTMA fusion which was detected by either confFuse or fusionMap. Another highly recurrent fusion partner is KLF2 (31 samples scored ≥ 6.5 , 16 samples scored ≥ 8), which plays an important role in development, erythroid differentiation, adipogenesis and T-cell differentiation [106].

Table 3.12: Recurrent fusions in CLL samples from HIPO-005 (n=114) and ICGC (n=96).

Gene1	Gene2	HIPO-005- score ≥ 6.5	HIPO-005- score ≥ 8	ICGC- score ≥ 6.5	ICGC- score ≥ 8
CHD2	B2M	32	32	1	1
CXCR4	CHD2	19	19	NA	NA
GNAS	CXCR4	13	13	2	2
YPEL5	CXCR4	13	13	NA	NA
IGHA2	IGHA1	12	12	8	8
CXCR4	BCL2L11	9	9	1	1
GNAS	B2M	9	9	1	1
TCF3	OAZ1	9	9	1	1
PTMA	CXCR4	82	8	7	NA
OAZ1	CSNK1G2	8	8	NA	NA
RBM38	CXCR4	8	8	NA	NA
KLF2	FOSB	7	7	NA	NA
DDX5	CXCR4	6	6	NA	NA
UBC	NCOR2	6	6	NA	NA
CXCR4	B2M	5	5	NA	NA
CXCR4	CLK1	5	5	NA	NA
USP34	NAV3	6	4	NA	NA
OAZ1	KLF2	4	4	1	1
TFG	GPR128	4	4	4	3
KLF2	AKAP8	4	4	NA	NA
UBB	CXCR4	4	4	NA	NA
TMEM18	PTMA	7	3	NA	NA
RGPD5	BCL2L11	5	3	NA	NA
CXCR4	ATP6V0C	3	3	NA	NA
KLF2	ACTB	3	3	NA	NA
NOC4L	FBRSL1	3	3	NA	NA
PNRC1	BACH2	3	3	NA	NA
PTMA	OAZ1	3	3	NA	NA
SIK1	KLF2	3	3	NA	NA

Continued on next page

Table 3.12 – continued from previous page

Gene1	Gene2	HIPO-005-score \geq 6.5	HIPO-005-score \geq 8	ICGC-score \geq 6.5	ICGC-score \geq 8
UBXN4	CXCR4	3	3	NA	NA
UNKL	UBE2I	3	3	NA	NA
VAV2	PTMA	3	3	NA	NA
RERE	HERC2P3	4	2	3	NA
UBB	DDX5	4	2	NA	NA
HLA-G	HLA-B	3	2	1	1
HLA-DRB1	HLA-DPB1	2	2	1	NA
IGKV5-2	IGKJ5	2	2	4	3
IGHA1	B2M	2	2	NA	NA
KLF2	CXCR4	2	2	NA	NA
KLF2	DDX5	2	2	NA	NA
MAFK	MAD1L1	2	2	NA	NA
PTMA	FOSB	2	2	NA	NA
PTP4A1	PHF3	2	2	NA	NA
RP11-20I23.1	CXCR4	2	2	NA	NA
SFMBT1	PTMA	2	2	NA	NA
TGIF1	CXCR4	2	2	NA	NA
USP11	KLF2	2	2	NA	NA
KLF2	JSRP1	22	1	NA	NA
RGPD5	PTMA	3	1	NA	NA
HLA-DRB5	HLA-DPB1	2	1	NA	NA
RP11-20I23.1	PDPK1	2	1	NA	NA
SIK1	PTMA	2	1	NA	NA
SPINK9	KIF20B	2	1	NA	NA

Note: The order of fusion partners 5' and 3' is ignored. Fusions labeled in boldface were validated in at least one of three samples (details in Table 3.13).

Three samples from HIPO-005 were chosen to validate some of the recurrent fusions. 15 of 18 candidates were successfully verified using RT-PCR followed by Sanger sequencing (Table 3.13). Fusions CXCR4:PTMA and CXCR4:CHD2 were validated in all three samples. Most of validated fusions have CXCR4 as fusion partner. The fusion boundary for CXCR4 locates either at the end of exon 1 or at the beginning of exon 2, and for PTMA, is located at the beginning of exon 2. The structures of ten different validated fusions are shown in Figure 3.19 and Figure 3.20.

High expression regions were observed upstream (within 13 kb) of CXCR4 in CLL samples, whereas low or no expression of these regions was detected in breast cancer, ependymoma

Table 3.13: 15 fusions validated by RT-PCR and Sanger sequencing in three CLL samples.

5' gene	3' gene	5' chr	5' break point	3' chr	3' break point	Sample ID	confFuse score
B2M	CHD2	15	45003811	15	93428745	QGBA	8.5
CXCR4	PTMA	2	136875616	2	232576058	QGBA	6.5
CXCR4	CHD2	2	136875616	15	93428745	QGBA	9
CXCR4	GNAS	2	136875616	20	57470667	OXXE	8.5
B2M	CXCR4	15	45003811	2	136873482	OXXE	9
BCL2L11	CXCR4	2	111878765	2	136873482	OXXE	8.5
CXCR4	DDX5	2	136875616	17	62500960	OXXE	9
CXCR4	PTMA	2	136875616	2	232576058	OXXE	6.5
CXCR4	CHD2	2	136875616	15	93428745	OXXE	optimized
CXCR4	CHD2	2	136875616	15	93428745	A72M	9
YPEL5	CXCR4	2	30369928	2	136873482	A72M	8.5
BCL2L11	PTMA	2	111878765	2	232576058	A72M	6.5
CXCR4	PTMA	2	136875616	2	232576058	A72M	6.5
CXCR4	GNAS	2	136875616	20	57470667	A72M	optimized
B2M	GNAS	15	45003811	20	57470667	A72M	optimized

Recurrent fusion genes were labeled with different colors.

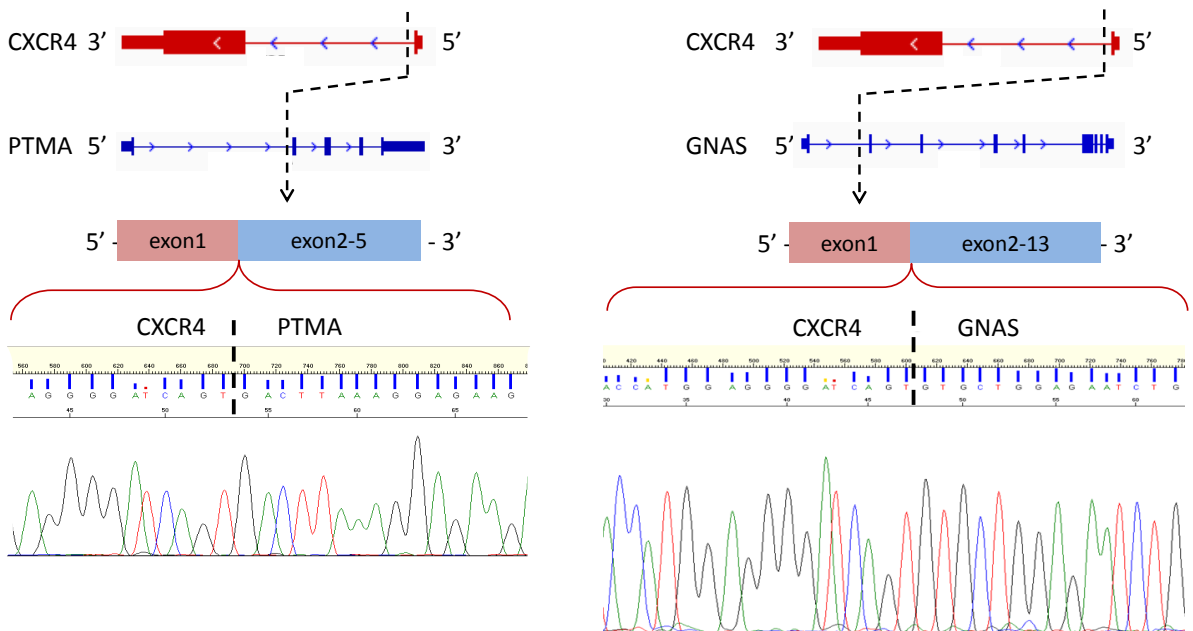


Figure 3.19: Structure of fusions CXCR4:PTMA and CXCR4:GNAS in CLL, and Sanger sequencing of fusion boundaries.

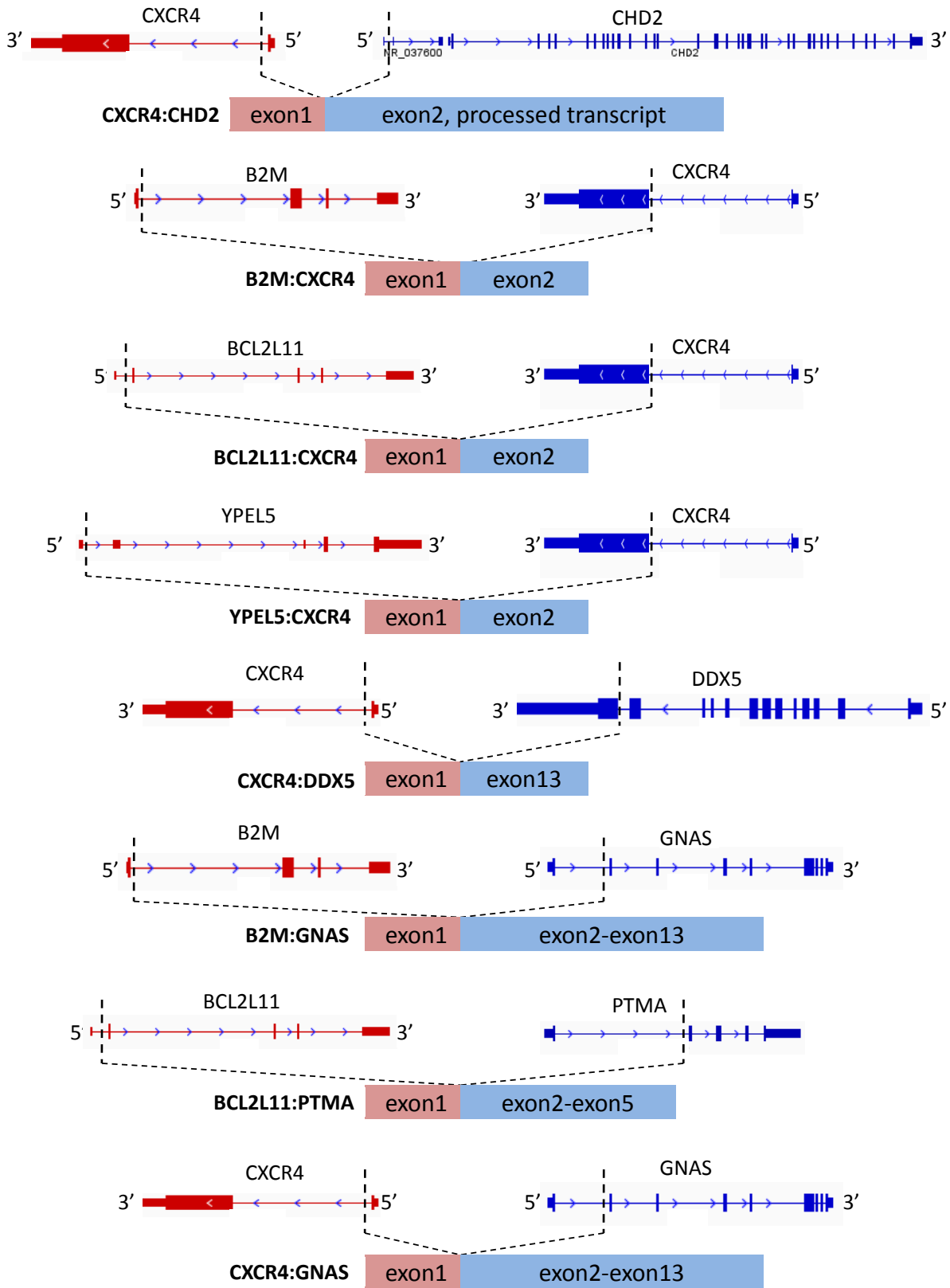


Figure 3.20: Structures of eight validated fusions in CLL.

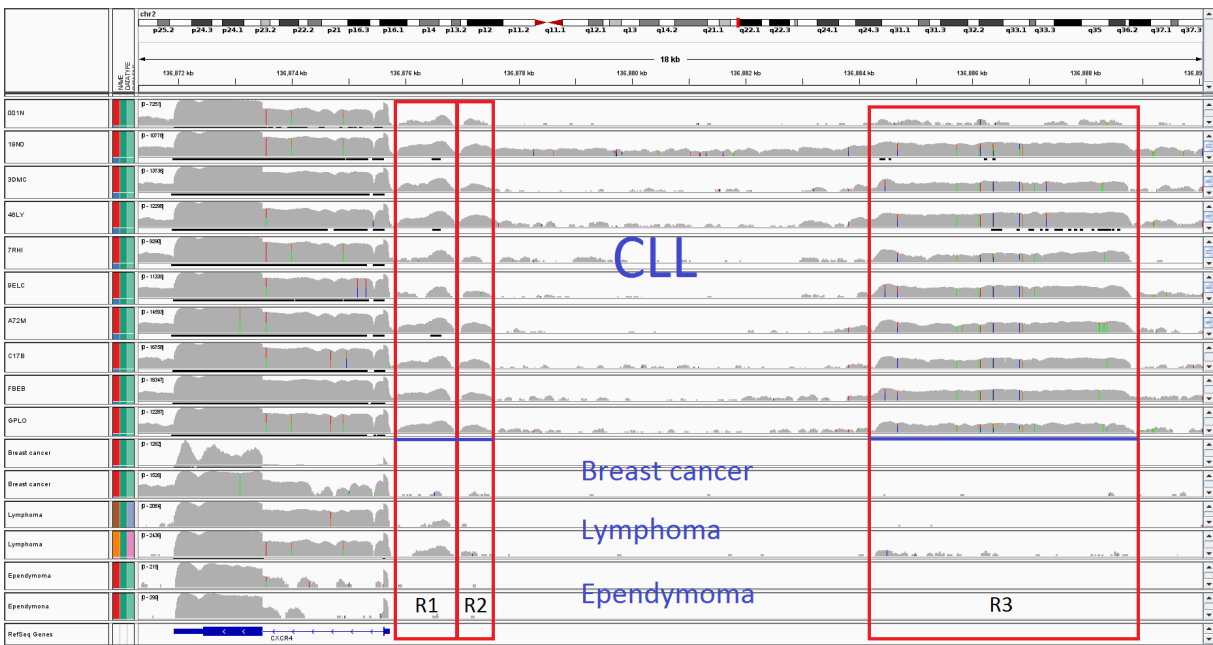


Figure 3.21: Expression of novel regions located CXCR4 upstream. The IGV snapshot shows the log-scale expression. Many reads were mapped on the region 3 (R3) of CXCR4 upstream in CLL samples but not in other entities, which indicates expression in this region may be CLL specific.

or lymphoma samples (Figure 3.21). Interestingly, these three regions were not annotated by Gencode Genes (v18). Comparison of samples with fusion CXCR4:PTMA ($n=96$) and samples without this fusion ($n=18$) shows significantly different expression of gene CXCR4 (t-test, $p=0.00035$) and non-annotated region R1 (t-test, $p=0.036$). There is no significant difference in expression in non-annotated regions R2 and R3 between samples with and without CXCR4:PTMA fusion (Figure 3.22). Furthermore, samples with fusion CXCR4:PTMA shows a lower correlation between R3 and CXCR4 expression ($r=0.143$) than the ones without this fusion (Figure 3.23).

3.3.6 Ependymoma

A epigenomic analysis aims to identify the drivers in ependymoma based different NGS data such as ChiP-seq, RNA-seq and WES. Analysis of 25 strand-specific RNA-seq ependymoma samples (24 tumors, 1 cell line) shows in total 4,709 fusion genes identified by deFuse, 67 of which were scored >6.5 by confFuse (Suppl. Table S9). Six recurrent fusions were identified, including previously reported fusions C11orf95:RELA ($n=5$) [107] and YAP1:MAMLD1 ($n=3$) in our published paper [96]. The other four recurrent fusions are NEDD1:C12orf55 (C12orf55 is also known as CFAP54) ($n=17$), CXorf59:CXorf22 ($n=7$), CXorf59:HMGB1P16 ($n=5$) and LINC00969:SDHAP1 ($n=2$).

Neural precursor cell expressed, developmentally down-regulated 1 (NEDD1), which is

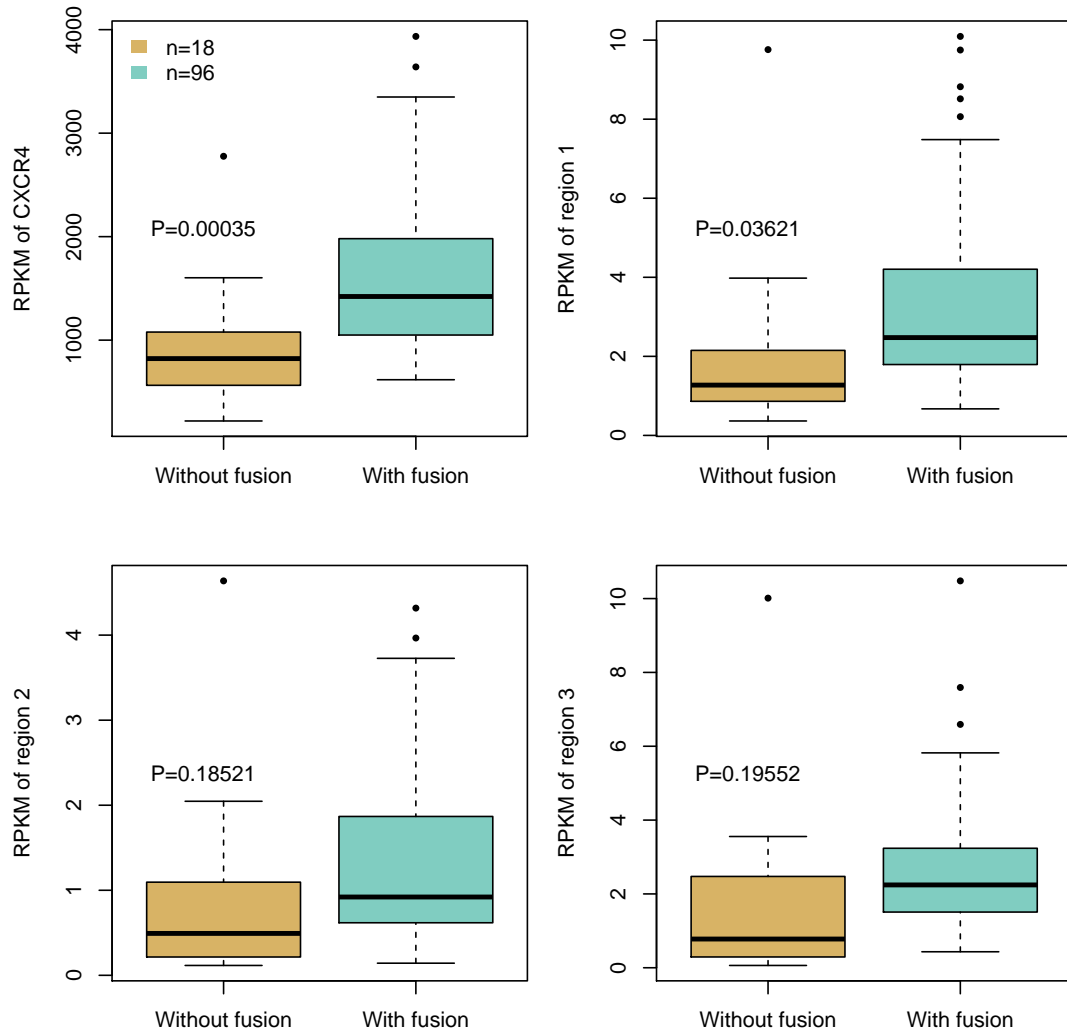


Figure 3.22: Expression of CXCR4 and non-annotated regions in two groups (CLL samples with fusion CXCR4:PTMA and ones without this fusion from the HIPO-005 project).

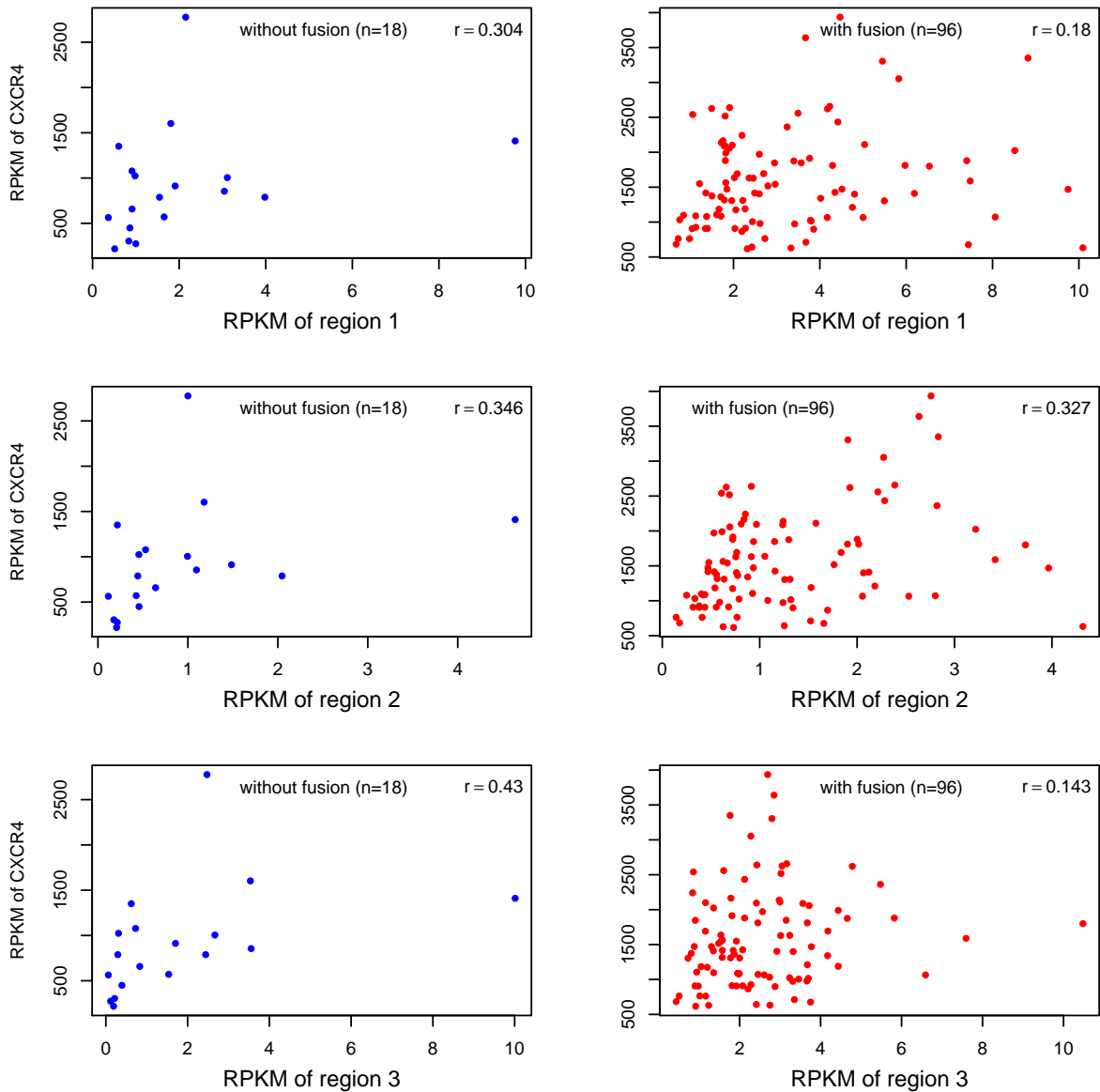


Figure 3.23: Correlation coefficient between CXCR4 and non-annotated regions in two groups (CLL samples with fusion CXCR4:PTMA and ones without this fusion from the HIPO-005 project).

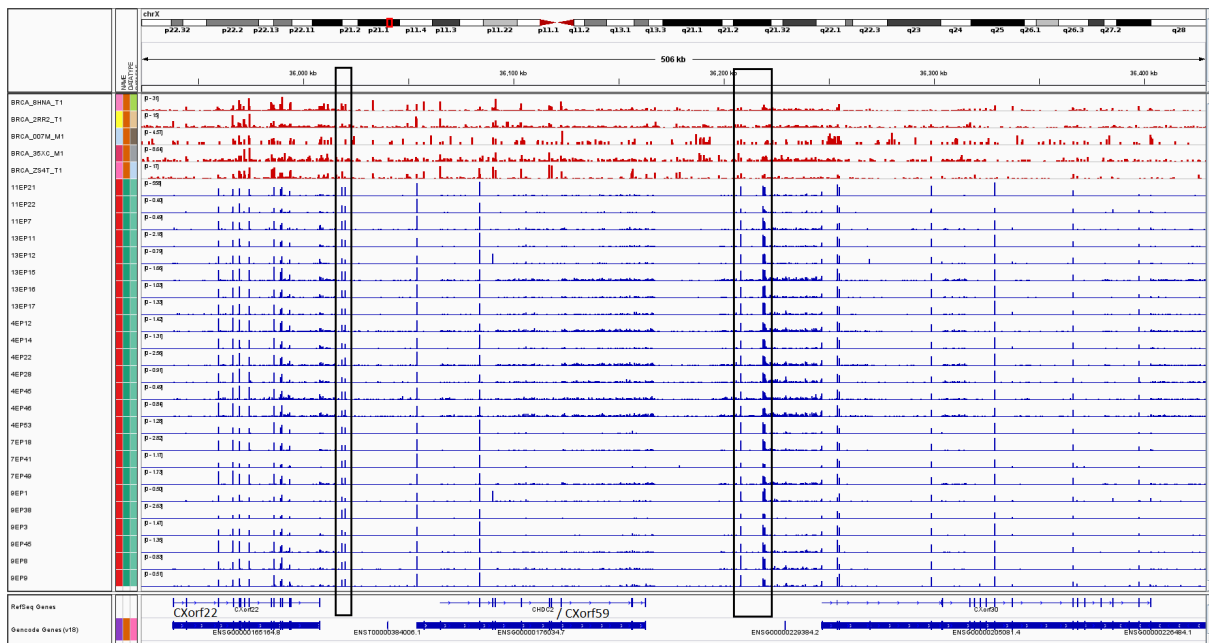


Figure 3.24: Non-annotated expressed regions in ependymoma. Two regions in black box which are not annotated by RefSeq Genes and Gencode Genes (V18), present clear expression peaks. Genes CXorf22 and CHDC2(CXorf59) are involved in recurrent fusions.

localized in the centrosome, plays an important role in meiotic spindle stability and chromosome segregation in mammalian oocytes [108]. Interestingly, two non-annotated regions near CXorf59 and CXorf22 show obviously expression peaks, indicating that novel transcripts may be there (Figure 3.24).

3.3.7 Breast cancer

The HIPO-017 project aims to identify new fusion genes and biomarkers for breast cancer by interrogating whole-exome and whole-transcriptome profiling. The mapping quality control of 98 samples from HIPO-017 project and an overview of multidimensional scaling (MDS) of 106 breast tumor RNA-seq samples are given in supplementary Figure S2 and Figure S3, respectively. The rate of uniquely mapped reads ranges from 80% to 95% with a median of ~90%. Furthermore, high strand-specific rate (median, ~98%) and low ribosome RNA content rate (median, ~3%) were achieved.

In total, 53 primary and 65 refractory breast tumor RNA-seq samples were included in the thesis. 40,021 fusion transcripts (33,035 fusion genes) have been predicted, 895 of which were identified as being high-confident candidates (score ≥ 8) and 1,768 were scored ≥ 6.5 (Suppl. Table S10). The median numbers of fusions scored ≥ 8 and ≥ 6.5 are ~5 and ~10, respectively

Table 3.14: Distribution of fusion genes identified in 118 breast tumors across 13 different functional categories (fusions scored ≥ 6.5).

Category	Number of genes	Involved gene in fusions	Number of fusions	Number of samples
Notch signalling pathway	48	8	10	9
Ras superfamily	154	13	14	14
p53 signalling pathway	68	14	26	21
Estrogen signalling pathway	100	17	28	22
HIF1 signalling pathway	106	17	30	18
Tumor suppressor	258	23	34	24
Solute carrier family	321	31	34	26
ErbB signalling pathway	87	26	50	34
Ras signalling pathway	227	36	62	33
MAPK signalling pathway	257	43	69	42
Pi3k-Akt-mTOR pathway	368	49	87	50
Proto oncogene	233	44	96	40
census gene (COSMIC)	571	113	211	71

(Suppl. Figure S4).

To uncover the potentially biological importance of fusion genes, 13 different functional categories of fusion genes were analyzed (score ≥ 6.5), including different key cancer signalling pathways, gene families and biologically important genes (Table 3.14). The number of fusion genes in each category ranges from 10 to 211 with corresponding 9 to 71 different tumor samples. Details of fusion genes (score ≥ 6.5) in the 13 categories are given in supplementary Table S11. Some fusion genes are involved in different categories. For example, PAK1 participates in ErbB pathway, MAPK pathway and Ras pathway. It should be noted that not all of the high-confidence fusion genes were exemplified in each category.

3.3.7.1 Ras superfamily

Fourteen different fusions were detected in seven primary and seven refractory samples, including recurrent rearrangements of ADP-ribosylation factor-like protein (ARL) gene family ($n=2$, e.g. ANO1:ARL2) and Ras-related protein Rab (RAB) gene family ($n=8$, e.g. RAB25:SRGAP2B).

ADP-ribosylation factor-like protein 2 (ARL2) plays an important role in microtubule dynamics and cell cycle in breast tumor cells [109]. Furthermore, ARL2 is associated with p53 localization and chemosensitivity in a breast cancer cell line [110]. High level expression of Ras-related protein 25 (RAB25) is correlated with lymphatic metastasis in ER⁺ and PR⁺ breast cancer [111].

3.3.7.2 Solute carrier family

34 different rearrangements of solute carrier (SLC) gene family were detected in 10 primary and 16 refractory samples. The function of solute carrier genes in cancer cells shows significant impact on cancer therapy by directly bringing anticancer drugs into cancer cells and by uptaking of nutrients for tumor growth and survival [112]. Recently, a study published in *Nature* shows that SLC38A9 as a lysosomal membrane-resident protein plays an important role in amino acid transport by controlling the amino-acid-induced mTORC1 activation [113].

3.3.7.3 HIF1 pathway

30 different fusions were detected in eight primary and ten refractory breast tumor samples, including recurrent rearrangements of phosphofructokinase (PFK) gene family ($n=2$) and protein kinase C (PRKC) gene family ($n=4$).

3.3.7.4 Notch pathway

Ten different fusions were identified in three primary and six refractory samples. Functionally recurrent rearrangements of Notch gene families have been reported in breast cancer [39]. Three Notch gene fusions were identified in one primary and two refractory samples, of which fusion SEC22B:NOTCH2 was previously reported in a breast cell line [39]. In addition, recurrent rearrangements of corepressor interacting with RBPJ 1 (CIR1) have been identified in one primary sample (OSBPL6:CIR1) and one refractory samples (CERS6:CIR1).

3.3.7.5 TP53 pathway

26 different fusions were identified in twelve primary and nine refractory samples. Six recurrent rearrangements of PPM1D ($n=5$), THBS1 ($n=3$), PTEN ($n=2$), SESN1 ($n=2$), CCND1 ($n=2$) and CCNE1 ($n=2$) were detected.

Protein phosphatase, Mg²⁺/Mn²⁺ dependent, 1D (PPM1D) dependent signalling has been reported as being “*a novel target to improve the efficacy of chemotherapeutic agents in resistant breast cancer cells*” [114]. The cycling genes, including CCND1 and CCNE1, play an important role in cell cycle by activating cyclin-dependent kinase (CDK) [115].

3.3.7.6 Estrogen pathway

28 different fusions were identified in ten primary and twelve refractory samples. Fusion ESR1:CCDC170 has been reported as recurrent rearrangements in endocrine-resistant luminal

B tumors [40] and it was identified in three refractory and one primary sample. In addition, a novel fusion CDH8:ESR1 was detected in one refractory sample. The other recurrent fusion partners include ADCY8 (n=2), GNAI3 (n=2), ITPR2 (n=2) as well as SOS gene family (n=3), CREB gene family (n=3) and PLCB gene family (n=3).

Guanine nucleotide-binding protein G(k) subunit alpha (GNAI3) can inhibit hepatocellular carcinoma cell migration and invasion [116]. Activation of cAMP response element-binding protein (CREB) is required to enhance aromatase expression in tamoxifen-resistant human breast cancer cells compared with control MCF-7 cells [117]. Phospholipase C (PLC) has six structure isotypes such as 1-Phosphatidylinositol-4,5-bisphosphate phosphodiesterase beta (PLCB). Interestingly, fusions of PLCB members were only detected in three refractory tumor samples.

3.3.7.7 Ras pathway

62 different fusions were detected in 33 samples, including recurrent rearrangements of fibroblast growth factor (FGF) gene family (n=5), Protein kinase (PRK) gene family (n=5), Phospholipases A2 (PLA2) gene family (n=3), RAPGEF5 (n=2), GNB1 (n=2), GNG12 (n=2), KITLG (n=2) and NF1 (n=4).

Fibroblast growth factor 14 (FGF14), a member of fibroblast growth factor (FGF) gene family, is “*an intracellular modulator of voltage-gated sodium channels*” in central nervous system [118]. Rearrangements of FGF14 were only identified in three refractory tumors. In addition, rearrangements of FGF3, FGFR2 and FDF19 were detected in one refractory and two primary tumors, respectively.

Guanine nucleotide binding protein (G Protein), beta polypeptide 1 (GNB1) can be regulated by phytoestrogens through estrogen receptor pathway in breast MCF-7 cells [119]. Guanine nucleotide binding protein (G Protein), gamma 12 (GNG12) can negatively regulate the inflammatory response in the microglial cell line [120].

KIT-ligand (KITLG), also known as stem cell factor, can activate its receptor tyrosine kinase c-Kit, resulting in c-Kit’s autophosphorylation and initiation of signal transduction [121]. Fusions of KITLG were found in one primary and one refractory tumor (SH2D4A:KITLG).

Neurofibromatosis type 1 (NF1) is associated with high risk of breast cancer development in women, especially at younger ages (< 50) [122]. Recurrent rearrangements of NF1 were identified in two primary and two refractory tumors.

3.3.7.8 ErbB pathway

50 different fusions were detected in 34 samples, including recurrent rearrangements of ERBB gene family (n=3), NRG gene family (n=4), PAK gene family (n=5), PTK2 (n=4) and GRB2

(n=3).

Human epidermal growth factor receptor 2 (HER2) encoded by ERBB2 show overexpression in ~20%-30% of breast cancer tumors [123]. It has been a drug target for HER2 positive breast cancer patients using Trastuzumab which is a HER2 receptor blocker [123]. Fusion ERBB2:ALG6 was found in one refractory tumor. Rearrangements of ERBB4 were detected in two primary tumors.

Neuregulin 1 (NRG1), a ligand of HER3 receptor, may induce cancer stem cell like characteristics in breast cancer cell lines [124]. Lapatinib is a drug acting as an inhibitor of EGFR and HER2 [125]. A combination treatment using lapatinib and pertuzumab can induce tumor growth regression, which may overcome lapatinib-resistance due to NRG1-mediated signalling in HER2-amplified breast cancer [125]. Fusions ATP8A1:NRG1 and NRG1:MAK16 were identified in two primary samples. In addition, MLL5:NRG3 and SIN3A:NRG4 were found in two refractory samples.

Growth factor receptor-bound protein 2 (GRB2) is one of the most significantly downregulated genes in HER2 mutated breast cancer based on transcriptional analysis [126]. Fusion GRB2:TSEN54 was found in one refractory tumor; fusions GRB2:SEPT9 and GRB2:RNFT1 were identified in two primary tumors.

Protein kinase C alpha (PRKCA) downregulates estrogen receptor expression by suppressing c-JUN phosphorylation in ER⁺ breast cancer cells and may be a potential target to treat ER⁺ and tamoxifen-resistant breast cancer [127]. Fusions TMRM104:PRKCA and PRKCA:BEND5 were detected in two primary tumors and PRKCA:USP32 was in one refractory tumor. In addition, fusion PRKCB:ARFGEF2 was identified in one refractory tumor.

PAK1 encodes serine/threonine protein kinase PAK1 and high level expression of PAK1 is associated with poor clinical outcomes in luminal breast cancer [128]. Rearrangements of PAK1 have been identified in one refractory and three primary samples. In addition, fusion JAG1:PAK7 was detected in one primary sample.

Protein tyrosine kinase 2 (PTK2) is a focal adhesion-associated protein kinase (FAK) which plays an important role in regulation of cellular responses such as cell adhesion, migration and survival [129]. Interestingly, different fusions of PTK2 have been only detected in four primary tumors.

A Her2 breast cancer pathway analysis based on INGENUITY is given in Figure 3.25.

3.3.7.9 PI3K-AKT-mTOR pathway

87 different fusions were detected in 50 samples, including recurrent rearrangements of collagen (COL) gene family (n=7), integrin (ITG) gene family (n=9), MAMA4 (n=2), RPTOR (n=2) and

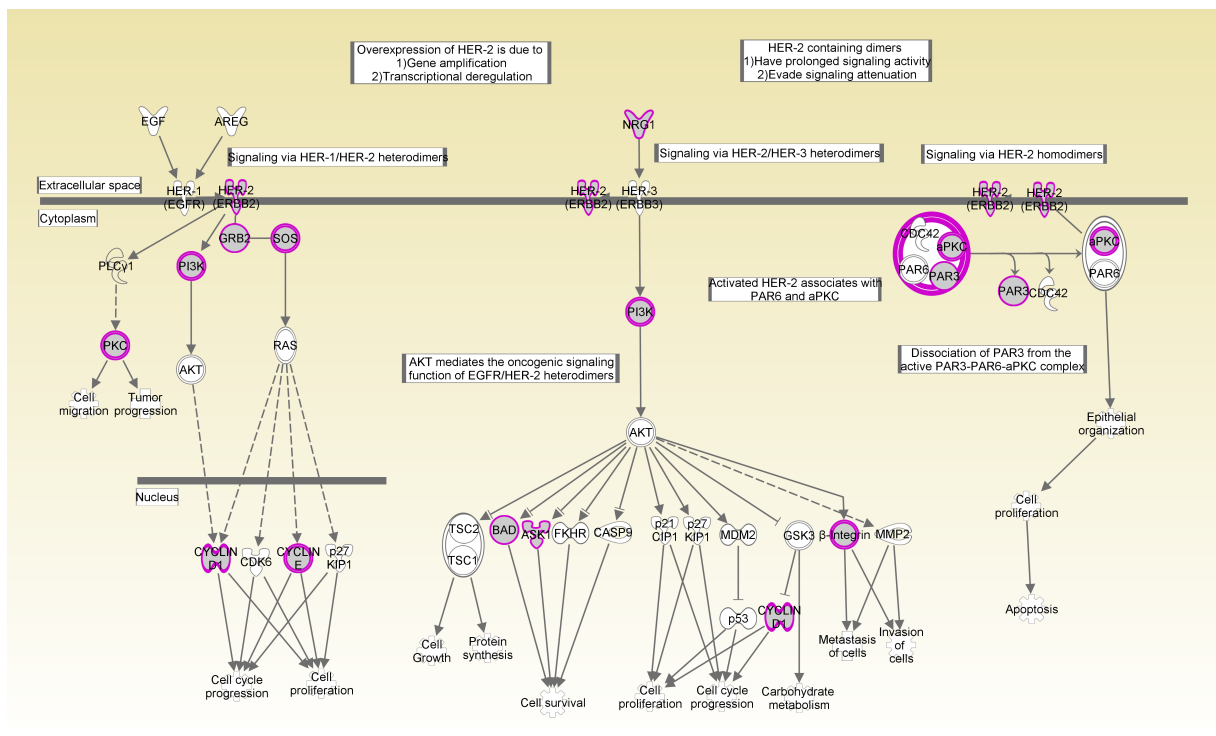


Figure 3.25: Fusion-involved genes in Her2 breast cancer pathway based on INGENUITY (labeled with red color).

RPS6KB1 (n=5).

Ribosomal protein S6 kinase beta-1 (RPS6KB1), encoding the 70kDa ribosomal protein S6 kinase (p70S6K), is involved in various human diseases and it performs as “*a biomarker for response to immunosuppressant as well as anticancer effects of inhibitors of the mTOR*” [130]. RPS6KB1 activates ESR1 by phosphorylating ESR1 on serine 167, which is a key position, leading to ESR1 mediated cell proliferation in breast cancer [131]. Interaction between tamoxifen and RPS6KB1 has been identified and phosphorylated RPS6KB1 significantly associated with tamoxifen resistance [132]. Rearrangements of RPS6KB1 were identified in two primary and three refractory tumors. In addition, fusion of RPS6KA1 was found in one primary tumor.

3.3.7.10 MAPK pathway

69 different fusions were detected in 42 samples, including recurrent rearrangements of calcium-channels voltage-dependent (CACN) gene family (n=5), dual specificity protein phosphatase (DUSP) gene family (n=2), mitogen-activated protein kinase (MAPK) related genes (n=10) and serine/threonine-protein kinase TAO (TAOK) gene family (n=5).

Mitogen-activated protein kinases (MAPKs) consist of different protein-serine/threonine kinases, which play important roles in signal transduction pathways that regulate cell functions such as proliferation and apoptosis [133]. Rearrangements of MAPK related genes were identified in one refractory and nine primary tumors.

The MAPK pathway analysis based on INGENUITY is shown in Figure 3.26.

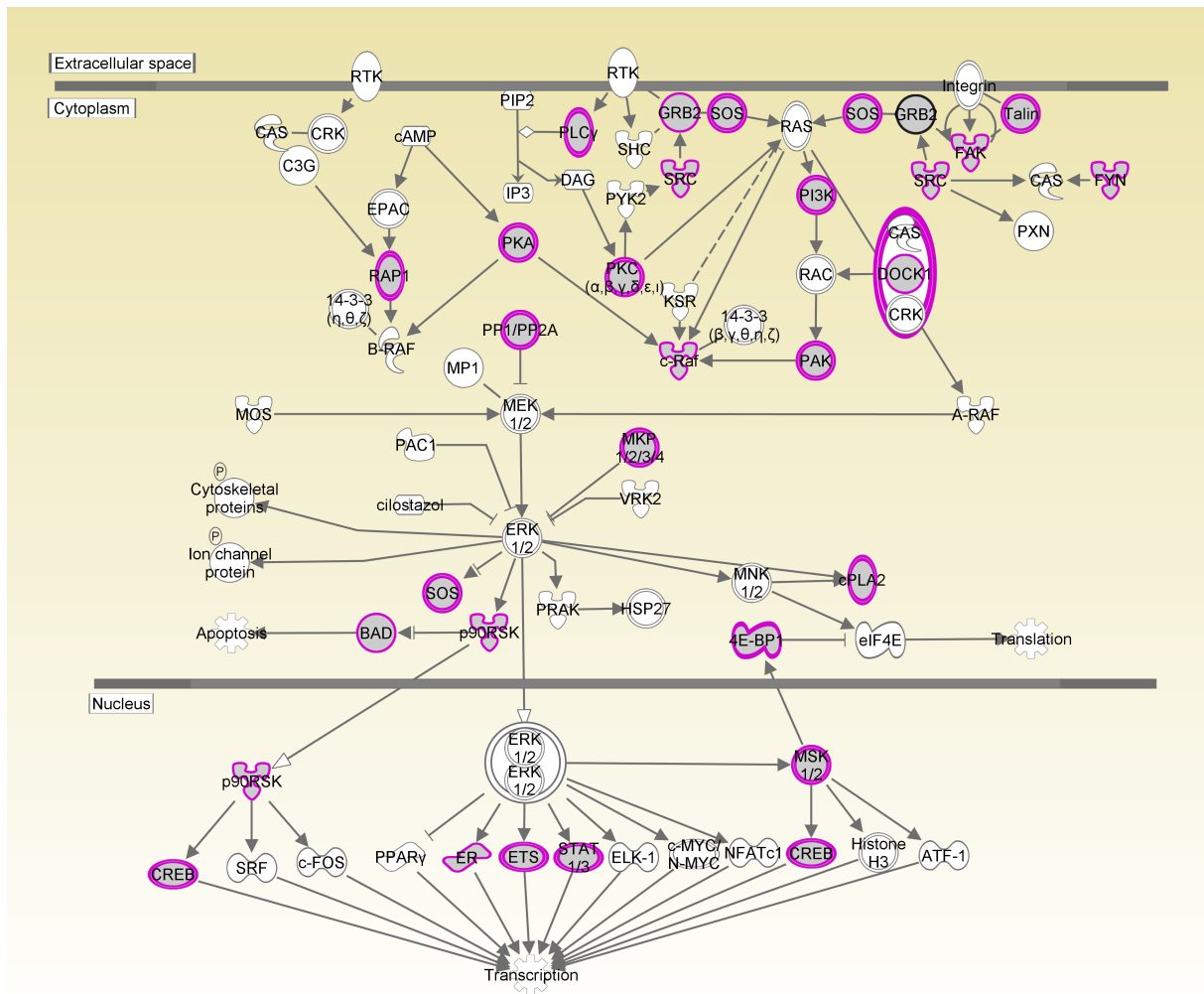
3.3.7.11 Tumor suppressor gene

34 different fusions were detected in 24 samples, including recurrent rearrangements of BUB1B (n=2), CDC73 (n=2), MTUS1 (n=2), PTEN (n=2) and neurofibromin (NF) gene family (n=5).

Mitotic checkpoint serine/threonine-protein kinase BUB1 beta (BUB1B) can interact with BRCA2 [134] and can correct mitotic checkpoint impairment and microtubule-kinetochore attachment defects [135]. Rearrangements of BUB1B were identified in one primary and one refractory tumor.

3.3.7.12 Oncogene

96 different fusions were detected in 40 samples, including recurrent rearrangements of ETV6 (n=2), HLF (n=2), MECOM (n=2), MKL1 (n=2), USP6 (n=2), RARA (n=3), RB1 (n=2), MYEOV (n=4), RNF213 (n=5), RUNX1 (n=5), TRIM37 (n=6) and BCAS3 (n=7).



© 2000-2015 QIAGEN. All rights reserved.

Figure 3.26: Fusion-involved genes in the MAPK signalling pathway based on INGENUITY (labeled with red color).

Table 3.15: Recurrent rearrangements of fusion partner genes found in the list of census genes (COSMIC).

Gene	Number*	Gene	Number*	gene	Number	Gene	Number*
CDK12	8	PTPRC	3	PTEN	2	HLF	2
RUNX1	5	PRDM1	3	PSIP1	2	ETV6	2
RNF213	5	USP6	2	NUMA1	2	DNM2	2
ESR1	5	SND1	2	NRG1	2	CLTC	2
PDE4DIP	4	SMARCA4	2	NOTCH2	2	CDC73	2
NF1	4	SEPT9	2	MKL1	2	CCNE1	2
MSI2	4	RB1	2	MECOM	2	CCND1	2
BRIP1	4	RANBP17	2	LPP	2	BUB1B	2
TFG	3	RAD51B	2	LASP1	2	BRD4	2
SPOP	3	PTPRK	2	KAT6B	2	AKAP9	2
RARA	3	PTPRB	2	HOOK3	2	AFF3	2

* Number of samples with rearrangement event of corresponding fusion partner gene.

Breast carcinoma amplified sequence 3 (BCAS3) may be correlated with tamoxifen responses [136]. Furthermore, BCAS3 was identified as a chromatin target of metastasis-associated protein 1 (MTA1), a presumed corepressor of estrogen receptor ($ER\alpha$) [137]. Rearrangements of BCAS3 were detected in four primary and three refractory tumors.

3.3.7.13 Census gene (COSMIC)

211 different fusions were detected in 71 samples, including recurrent rearrangements of lysine acetyltransferase (KAT) gene family ($n=4$), protein tyrosine phosphatase, receptor type (PTPR) gene family ($n=6$) and other genes (Table 3.15).

BRCA1 interacting protein C-terminal helicase 1 (BRIP1) has interaction with BRCA1 during the process of DNA repair [138]. Rearrangement of BRIP1 has been identified in one primary and 3 refractory samples.

3.3.7.14 Recurrent fusions

56 recurrent fusions (score ≥ 6.5) were identified in 118 breast tumor samples (Table 3.16), including previously reported fusion ESR1:CCDC170.

Ankyrin repeat domain 30A (ANKRD30A) encodes breast cancer antigen NY-BR-1, which expresses only in normal or malignant breast tissue but not in other types of tissue [139].

Probable E3 ubiquitin-protein ligase HERC2 (HERC2) has opposite function of BRCA1-associated RING domain protein 1 (BARD1) that is essential for BRCA1 stability, and can interact with BRCA1 for degradation during S Phase of cell cycle [140].

Table 3.16: Recurrent fusions in 118 breast tumor samples (n=56, score ≥ 6.5).

Gene1	Gene2	Recurrence	Gene1	Gene2	Recurrence
ATP8A2P1	ATP8A2	28	TRMT2A	OR2J3	2
ATP8A2P1	ANKRD30A	17	TPTE2P5	RP11-64P12.8	2
HERC2	C11orf72	8	TMC2	PRCP	2
ZNF761	TMEM8B	7	SYN3	ACOT13	2
ZNF761	GULP1	7	STXBP4	ACOX1	2
WDR70	NXPH1	7	SSBP2	DHFR	2
RP11-20F24.4	ANKRD30A	7	SRSF1	CHN2	2
MCFD2	HSD17B4	7	SOX5	ELF1	2
RP11-20F24.4	ATP8A2	6	SKAP1	CA10	2
NAV3	ANKRD30A	6	SEPT7P2	KAT7	2
ITGB5	GOLM1	5	SECISBP2L	MTR	2
TTC6	MIPOL1	4	RP11-182J1.12	GOLGA6A	2
IKZF2	AC079610.1	4	RP11-167N24.6	ACSS3	2
IBTK	CERS5	4	RP11-159D12.5	CHN2	2
ESR1	CCDC170	4	RIMS2	C6orf203	2
WDPCP	PDZD9	3	PTPN20B	BMS1P2	2
UBXN2A	TARBP1	3	PSIP1	MIR5007	2
TPTE2P5	TPTE2	3	NPLOC4	HLF	2
THSD4	CYP27C1	3	NADSYN1	C20orf94	2
THBS1	RP11-624L4.1	3	MTMR4	CDR2L	2
TFG	GPR128	3	LUZP2	ELP4	2
SH3D19	LRBA	3	HERPUD2	ASTN2	2
LGMN	CDC14A	3	HERPUD2	AC007349.7	2
ZPLD1	NFKBIZ	2	EXOC7	CDR2L	2
ZNF512B	PDE1C	2	DISP1	C10orf68	2
WHAMM	RP11-752G15.9	2	CHODL	ASTN2	2
USP32	BCAS3	2	CCDC74A	AC093838.7	2
UBC	UBB	2	ATP8A2	ANKRD30A	2

Note: The order of fusion partner 5' and 3' is ignored to simplify comparison. Fusions labeled with green color are from paired B2HF_T1 & B2HF_M1, with labeled blue color are from paired 0E5B_T1 & T2VO_M1 and labeled with red color are from paired DMG3_T1 & DMG3_M1.

Fusion MCFD2:HSD17B4 was not verified by Sanger sequencing in one primary tumor (AC72). It, however, turns out that a novel/non-annotated transcribed region locates upstream of HSD17B4 (Suppl. Figure S5). Interestingly, the novel expressed region directly connects to the second exon of HSD17B4 instead of the first exon, indicating that this combination may result in a new isoform of HSD17B4 in sample AC72. The other six refractory tumors with predicted rearrangement of HSD17B4 also express in the novel region.

3.3.7.15 Fusions related to tamoxifen and estrogen metabolism

Tamoxifen can be metabolized by cytochrome P450 (CYP) and flavin-containing monooxygenase (FMO), and the inactivation of tamoxifen and its metabolites are via various UDP-

glucuronosyltransferase (UGT) and sulfotransferase (SULT) (Suppl. Figure S8) [141]. Rearrangements of CYP genes were identified in two primary and four refractory tumors. Fusions FMO5:PRPF3 and ADAMTS12:UGT3A2 were found in one primary and one refractory tumor, respectively. In addition, fusion EIF2AK2:SULT6B1 was detected in one refractory tumor.

In estrogen metabolism, CYP, SULT and UGT are involved (Suppl. Figure S7) [142]. Furthermore, hydroxysteroid (17-Beta) dehydrogenase 1 (HSD17B1) participates in converting androstenedione to testosterone. A newly expressed region located upstream of HSD17B4 was mentioned before.

3.3.7.16 Potential fusion proteins

Not all fusion transcripts could be translated into proteins due to lack of an open reading frame or an out-of-frame fusion. Among the high-confidence fusion genes, confFuse can further identify a reliable subset (labeled *precious*, inter-chromosome) which are predicted to be able to produce fusion proteins, especially for those with high number of supporting reads and abnormal exon expression before and after fusion boundary. In some ideal cases, dramatically different exon expression before and after fusion boundary can be observed in IGV plot, showing strong evidence supporting a generated fusion protein (Figure 3.27 and Figure 3.28). 20 fusions harboring >40 split reads and >30 spanning reads are given in Table 3.17. Recurrent fusion protein MYB:NFIB has been previously reported in carcinomas of the breast and head and neck [37].

Table 3.17: Potential fusion proteins (inter-chromosome) identified by confFuse in 118 breast tumor samples.

5' gene	3' gene	Sample ID	5' gene	3' gene	Sample ID
ACER3	GOLGA7	ZQC5_T1	MAP2K4	IFT122	SR1R_M1
ACSF3	MLEC	8HNA_T1	MYB	NFIB	Q4W1_T1
ADAM9	PPFIA1	7DTJ_T1	NEMF	LAMA4	EDTK_T1
C16orf72	RALGAPA2	I4ZX_T1	PFKFB2	CEP192	HMXT_T1
CLTC	PDE3B	2RR2_T1	PPP1R12B	KCNMB4	TW0Z_T1
EPB41L5	POLB	I4ZX_T1	PTK2	MMP1	TC6T_T1
ERO1L	PDSS2	EDTK_T1	RPS6KB1	CAMSAP2	Q6FY_T1
FAM135A	SLC35E3	F7FD_M1	SLC25A42	CCT6B	LRU2_M1
FBXL4	RP4-604K5.1	QYXQ_M1	TMEM189	PRKCE	TX2S_T1
FOXJ3	SESN1	2RR2_T1	UBAP2	ELOVL2	DMG3_M1

Fusions of more than 40 split reads and 30 spanning reads are shown (n=20). Fusions labeled with *precious* in confFuse output are inter-chromosome and open reading frame preserved. Fusion protein MYB:NFIB has been reported in carcinomas of the breast and head and neck [37].

Another set of likely fusion proteins were selected by >40 split reads, >30 spanning reads and gene distance >1 mb (intra-chromosome and score=9.5). In total, 43 different potential

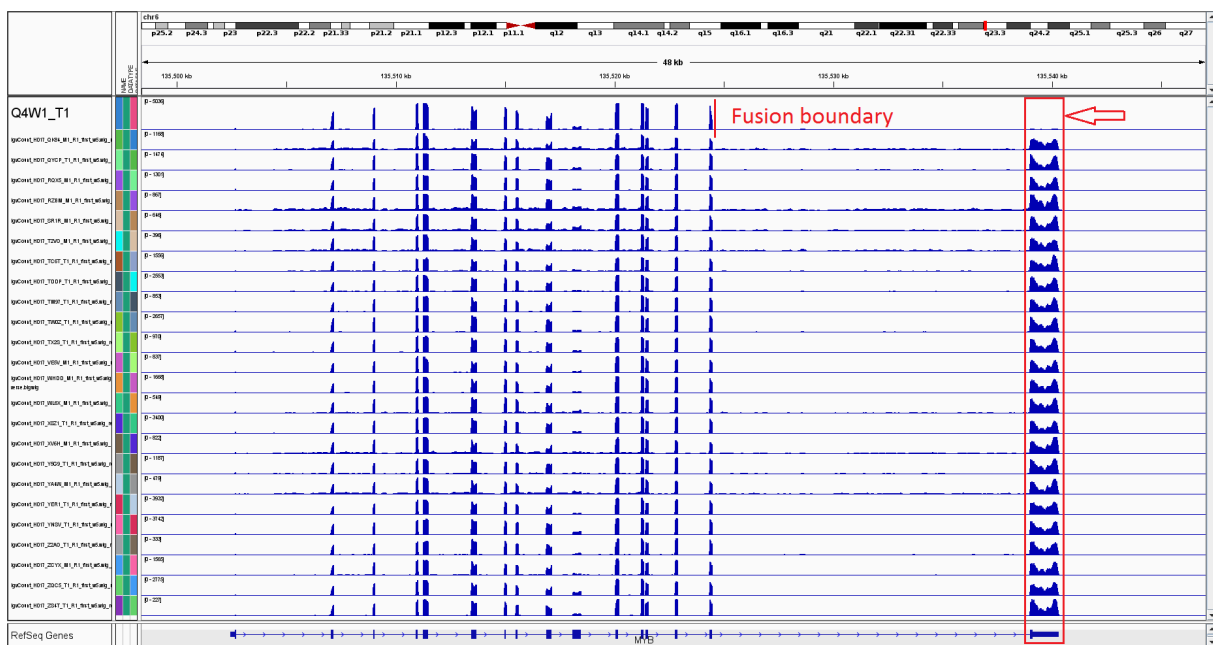


Figure 3.27: Example of fusion MYB:NFIB leading to abnormal exon expression in 5' fusion partner in one triple negative breast tumor (Q4W1_T1). The possible DNA breakpoint may locate between the last two exons of MYB because the last exon expresses much lower than the second last exon. The predicted fusion MYB:NFIB is very likely to produce a fusion protein.

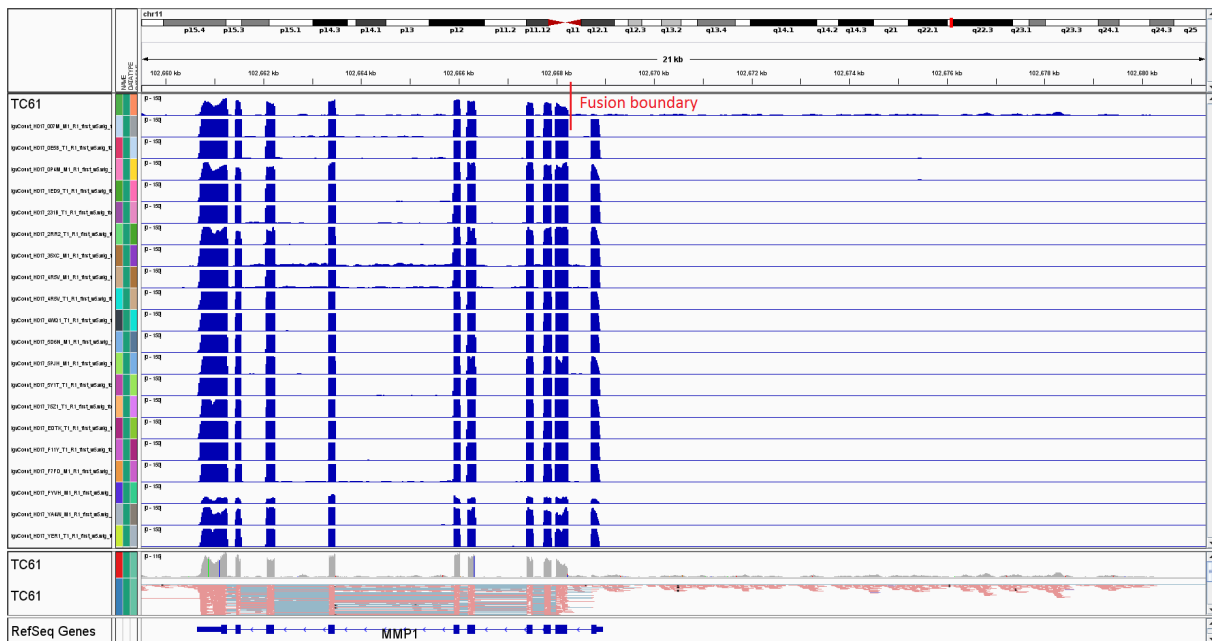


Figure 3.28: Example of fusion (PTK2:MMP1) leading to abnormal exon expression in 3' fusion partner in one breast tumor (TC61_T1). Expression of the first exon is much lower than the second one, indicating that the possible DNA break point may locate between the first and the second exon of MMP1.

fusion proteins under this criteria were identified in 11 refractory and 17 primary tumor samples (Table 3.18). Two potential fusion proteins FMO5:PRPF3 and RNF43:HEATR6 were exemplified in Figure 3.29. Remarkably differential exon expression before and after fusion boundary in both fusion partners can be observed in IGV plot.

3.3.7.17 Fusions in paired primary-refractory breast tumors

In total, five paired primary-refractory breast tumor samples were analyzed. Three pairs harbor recurrent fusions which were mentioned above in Table 3.16. Recurrent fusion genes were not identified in these five refractory tumors. However, six recurrent fusion partners were detected in primary-refractory pairs, including STXBP4, PPM1D, NPLOC4, LRBA, ELOVL2 and BCAS3.

3.3.8 Fusion features across entities

Some tumor entities have specific fusions such as TMPRSS2:ERG in prostate cancer and IG:MYC in lymphoma. Interestingly, different genomic distributions of fusion genes across tumor entities have been identified (Figure 3.30), indicating that fusion genes are not randomly distributed in a specific tumor entity.

Table 3.18: Potential fusion proteins (intra-chromosome) identified by confFuse in 118 breast tumor samples (n=43).

5'gene	3' gene	Sample ID	5'gene	3' gene	Sample ID
ACACA	BECN1	AC72_T1	KIF13B	PTK2	X0Z1_T1
ANO1	ARL2	T6Z1_M1	MED13L	PRKAB1	L50R_T1
ARHGAP23	MSI2	cf2f24	MYO1D	ADORA2B	EDTK_T1
BRD4	NFIX	Y5G9_T1	NDUFC2	PPFIA1	DR8V_T1
CDC42BPA	ASTN1	Q6FY_T1	NUP133	CDC42BPA	Q6FY_T1
CDC42BPA	TDRD5	Q6FY_T1	PCBD1	KCNMA1	L50R_T1
CIR1	OSBPL6	TX2S_T1	RAB22A	ACOT8	2S2Q_T1
CTPS2	SCML2	HMXT_T1	RB1	ENOX1	8HNA_T1
DDB1	ORAOV1	L50R_T1	RNF43	HEATR6	2RR2_T1
DOCK5	ADAM32	WHDD_M1	RPRD2	ACP6	TW0Z_T1
EIF3H	CSMD3	2RR2_T1	RPRD2	GJA5	TW0Z_T1
ERO1L	MYH6	EDTK_T1	SHANK2	LRP5	ZQC5_T1
FAM3B	TRAPPC10	X0Z1_T1	SND1	CASD1	46DP_M1
FMO5	PRPF3	HY35_T1	TADA2A	MSI2	b9b21b9
FREM2	RB1	TX2S_T1	TAOK1	C17orf79	8MNH_T1
GLS	HAT1	HMXT_T1	TBCD	USP36	cf2f24
HELZ	ACSF2	cf2f24	TMEM104	PRKCA	F11Y_T1
HELZ	GDPD1	2RR2_T1	UQCRC1	RBM6	RQX5_M1
HSPD1	NCKAP1	cf2f24	UTP18	PIP4K2B	QYXQ_M1
INPP5A	RASGEF1A	46DP_M1	WWP1	CSMD3	35XC_M1
ITGB5	PDIA5	SR1R_M1	YIPF1	ROR1	f1ae704
KDM2A	MS4A14	JVRW_M1			

Fusions were chosen by >40 split reads, >30 spanning reads, gene distance >1 mb (intra-chromosome) and score=9.5 (n=43).

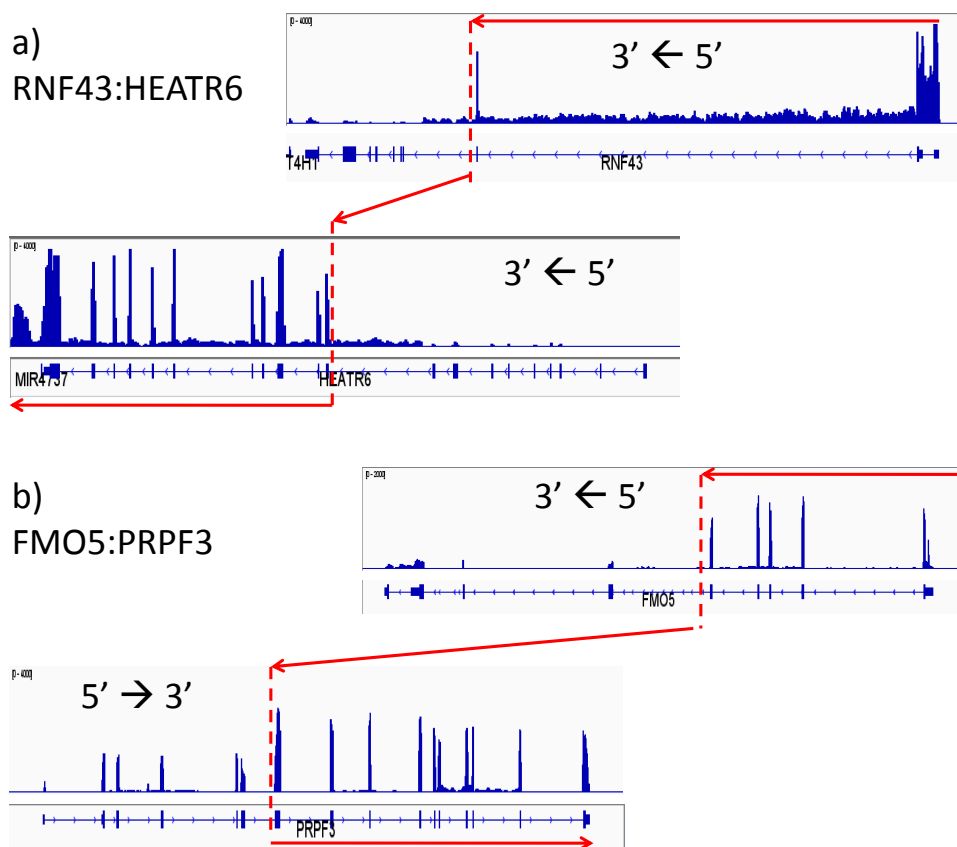


Figure 3.29: Examples of potential fusion proteins (intra-chromosome) in two primary breast tumors. Fusion boundaries were labeled with red dash line.

Chromosome 2 and chromosome 17 are the hot spots of fusion genes for CLL and breast cancer, respectively. Chromosome 12 is hot spot for both GBM and sarcoma. In addition, chromosome 2 and 6 are hot spots of fusions in lymphomas, and chromosome 19 and 21 in prostate cancer.

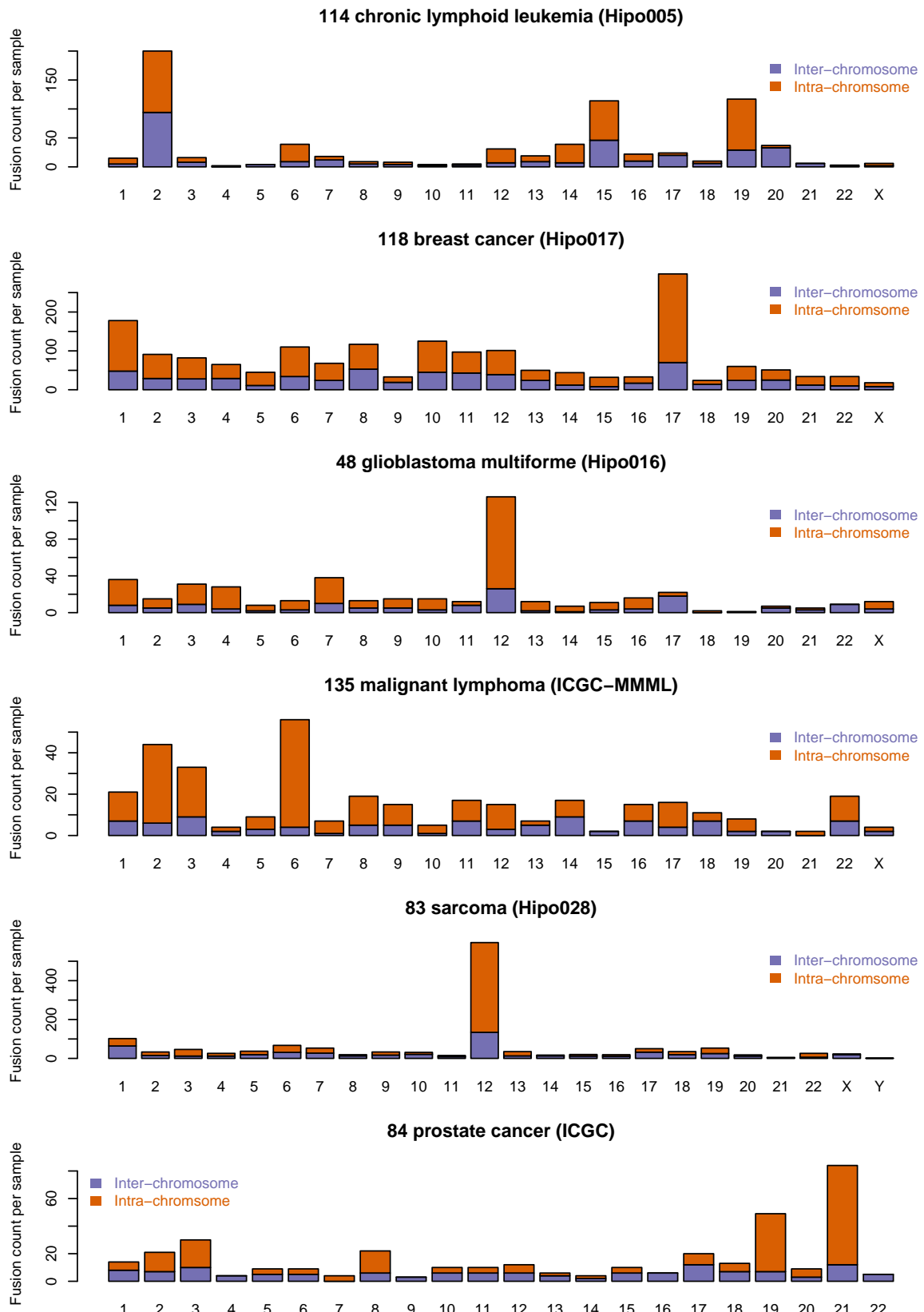


Figure 3.30: Genomic distributions of high confidence fusions across tumor entities, including inter-chromosome and intra-chromosome fusions.

Chapter 4

Discussion and outlook

4.1 Fusion gene detection

4.1.1 ConfFuse performance

A great number of fusion detection tools have been recently published. All the tools claim that they have better performance compared to alternative tools based on their individual data set. These tools may have bias towards individual synthetic data, specific cell line or tumor data (e.g. limited number of different tumor entities or different cell lines). Furthermore, even after filtering step using their methods, these tools still generate a large number of predicted fusion transcripts, most of which may be false positives or of low biological interest (e.g. precursor read-through transcripts). Therefore, I developed confFuse, a new scoring algorithm, which can be applied on paired-end RNA-seq across tumor entities with both high true positive rate and high detection accuracy.

Based on the previous experience and common usage in the scientific literature such as number of citations (Chapter 1.1), deFuse was chosen as basis for developing additional filtering algorithm for downstream analysis. The scoring algorithm confFuse assigns each putative fusion transcript a confidence score based on deFuse reports. Compared with alternative tools (soapFuse, fusionMap and deFuse) based on 96 published RNA-seq samples from different tumor entities, confFuse can significantly reduce the number of fusion candidates (301 high-confidence candidates from 8083 predicted fusion genes) and retain high detection accuracy (recovery rate 85.7%) (Figure 3.8).

Furthermore, a screen of 22 GBM tumors identified 242 high-confidence fusions from 6,018 unfiltered deFuse candidates. Approximately 62% (150/242) were either experimentally validated or confirmed by DNA-seq. In addition, approximately 72% of high-confidence fusions

(17/24 from 849 unfiltered deFuse predictions in 11 published prostate tumors) were confirmed by FISH validation, DNA-seq or by the occurrence of the well known ETS fusions in prostate cancer. Another analysis of 27 INFORM tumors with 27 previously validated fusions identifies 94 high-confidence fusions, 25 of which are previously verified, resulting in a recovery rate of approximately 93% (25/27).

In three breast tumor samples, 100% true positive rate for high-confidence fusion candidates ($\text{score} \geq 8$) was achieved. Furthermore, 69% of medium-confidence candidates ($6.5 \leq \text{score} \leq 7.5$) and 30% of low-confidence candidates ($0.5 \leq \text{score} \leq 6$) were experimentally verified. While applying confFuse on three CLL samples, 15 of 18 candidates were successfully validated.

In summary, confFuse can reliably select high-confidence fusion genes that are more likely to be biologically relevant, achieving both high validation rate and high detection accuracy, while reducing the number of candidates to a restricted number for validation.

4.1.2 Problems with deFuse

DeFuse generates several unique features which are not available in some tools, such as fusion transcripts which are very useful in designing primers for experimental validation. It has the highest fusion detection accuracy in terms of recovery rate based on different tumor RNA-seq data (Figure 3.8 and Figure 3.12). However, deFuse is not perfect and still has some problems/disadvantages.

- **Failed runs**

For some unknown reasons, deFuse could not be applied on some samples. Currently, several hundreds of RNA-seq samples were successfully processed by deFuse but some samples failed to run, including two GBM and four breast cancer samples. Additional efforts would be necessary to solve this problem in the future.

- **Computational resource**

DeFuse demands high computer power. For example, it requires approximately two to three days for processing 200 million RNA-seq paired-end reads. In some unusual cases, deFuse took several hundreds hours (walltime) and used several hundreds GB memory running in a ten-core computer (Suppl. Figure S6). Furthermore, deFuse requires large disk storage (typically more than 250GB) for running a sample of 200 million paired-end reads. Due to the high computational resource requirement, deFuse may have disadvantages in practice such as clinical application.

- **Order of fusion gene partners**

For the same fusion gene pair, deFuse reports different 5' fusion partners. For example, deFuse may predict fusion transcripts 5'-A-B-3' and 5'-B-A-3' for gene A and B. In order to identify the right order of fusion partners, further *in silico* validation using complimentary tools such as BLAT

is necessary.

- **Visualization of fusion gene**

DeFuse does not provide SAM/BAM files as output, making it impossible to visualize reads mapped to fusion genes in IGV and making it unable for further downstream analysis.

4.1.3 Possible improvement

Currently, 23 features were used in confFuse (Chapter 2.1). The weightings of features are mostly based on biological importance of fusion structures and partially based on supervised learning by observation. Further systematic analysis of these features and other new features may be useful in improving the scoring algorithm. The artefact list should also be improved to reduce the number of false negative candidates. Additional annotation of predicted fusion transcripts such as structure simulation and functional domain should be considered too.

Published paired-end RNA-seq data with validated fusions are a very good reference resource for improving fusion detection methods. More than one hundred validated fusion genes were included in this thesis. Adding more samples with experimentally validated fusions may help in systematic optimization of the confFuse scoring scheme.

DeFuse performs better than other tools in terms of fusion accuracy detection. It, however, still could not detect all potential fusion genes. There may be a way to improve the fusion detection sensitivity by combining confFuse with other different tools such as fusionMap.

4.2 Fusion genes in different tumor entities

ConfFuse was applied on several unpublished data set from HIPO projects and ICGC projects. Several well-known fusion genes have been identified such as SS18:SSX1 in synovial sarcoma, FUS:DDIT3 in myxoid liposarcoma, IGH:MYC in lymphoma, C11orf95:RELA and YAP1:MAML1 in ependymoma as well as SEC22B:NOTCH2 and ESR1:CCDC170 in breast cancer, which provide much more evidence supporting that confFuse method performs well across different tumor entities.

Furthermore, a large number of novel fusion candidates has been detected. Biological functions of these novel identified fusion genes could be further studied after successful experimental validation. Based on previous studies, some fusion genes were observed in specific tumor entities, such as SS18:SSX1 in sarcoma and TMPRSS2:ERG in most of prostate cancer, C11orf95:RELA and YAP1:MAML1 in ependymoma, indicating that these fusions may be driver mutations and have clinical relevance. Fusion genes are not randomly distributed across chromosomes and hot

spots of fusion genes in six tumor entities have been identified (Chapter 3.30), proposing that there are specific fusion-driven diseases.

In HIPO-005 CLL samples, several recurrent fusion genes have been identified and validated such as CXCR4:PTMA. Interestingly, expression of CXCR4 significantly associates with fusion CXCR4:PTMA. Higher expression of CXCR4 was observed at RNA level in CLL samples with fusion CXCR4:PTMA. Another interesting finding is a non-annotated expressed region located upstream of CXCR4. It has been demonstrated that CXCR4 plays an important role in heterotypic adherence to bone marrow stromal cells [143]. Several receptor antagonist have been used to inhibit CXCR4 [144]. Those new finding may lead to more comprehensive understanding of CXCR4 at genetic level. Although 15 fusion candidates have been experimentally verified, the biological functions of them are still unclear. To uncover whether those fusions are CLL specific, healthy blood RNA-seq samples will be analyzed for comparison in the future.

After understanding the biological functions of fusion genes, it may go further to clinical application. Currently, several drugs have been applied on targeting gene fusions in malignant disorders, such as ALK fusion in non-small-cell lung carcinoma as well as BCR:ABL1 in chronic myelogenous leukemia and acute lymphoblastic leukemia [4].

4.3 Biomarker discovery in breast cancer

4.3.1 CNV

Comparison of copy number variance in primary and refractory breast tumors shows difference in some regions including several important genes such as CDKN2A and ESRRG (Figure 3.1). Further biological interpretation of the different CNVs between primary and refractory tumors are necessary to address the question of treatment resistance. As mentioned in the introduction (Chapter 1.4), more than ~80% fusion transcripts associated with CNV based on nine tumor entities from TCGA data. Integration of CNV and fusion genes based on breast cancer from HIPO-017 will be analyzed in the future.

4.3.2 SNV/Indel

Interestingly, three MAST mutations (p.E1544K in MAST2, p.S900C in MAST3 and p.G2043V in MAST4) were identified only in three refractory tumors but MAST rearrangement were not detected, while functional rearrangements of MAST kinase have been reported in breast cancer [39].

Mutations of CACNA family genes, which are involved in MAPK signalling pathway, are highly

prevalent in refractory tumors (24%, 12/50) compared to primary tumor (~2%, 1/46) (Table 3.1). In 11 published ER-positive metastatic breast cancer cases, three patients harbored CACN mutations (~27%, 3/11), including CACNA1A, CACNA1F and CACNA1E in one case, as well as CACNA1E and CACNB1 in two other cases [7]. Interestingly, CACNA2D3 associates with steroid receptor co-activator-3 (SRC-3) and ESR1 in a chromatin immunoprecipitation-based study [145]. Furthermore, rearrangements of CACNA were identified in one primary and two refractory tumors.

In addition, mutations of PLCB family genes involved in estrogen signalling pathway, were only identified in refractory tumors (8%, 4/50). Receptor-mediated activation of PLC, including PLCB1-4, results in phosphatidylinositol 4,5-bisphosphate (PIP2) hydrolysis, leading to inactivation of the TRPM7 channel [146]. TRPM7 is required for metastasis formation in a mouse xenograft model and highly expressed TRPM7 can predict poor outcomes in breast cancer patients [147]. Mutations of TRPM1 and TRPM6 were detected in two refractory tumors. Beside single point mutations in PLCB family genes, rearrangements of them have been only identified in three refractory samples. The fusions TRPM7:LEO1 and TRPM7:MAPK6 were identified in a refractory tumor. Higher number of mutations in estrogen signalling pathway were observed in refractory tumor samples (Figure 3.5), which may indicate that patients acquired those mutations during endocrine treatment. Based on these findings, I came up with the hypothesis that mutations of CACNA and PLCB family genes may be a novel acquired resistance mechanism in addition to ESR1 mutation.

4.3.3 Fusion-related genes

- **ESR1 and GRB2**

Several ESR1 rearrangements have been reported, including ESR1:YAP1, ESR1:POLH, ESR1:AKAP12 and ESR1:CCDC170 in breast cancer [88]. Among 118 breast cancer samples, three refractory tumors and one primary tumor harbor ESR1:CCDC17. Additionally, one novel fusion CDH8:ESR1 was identified in a refractory tumor. Fusion ESR1:CCDC170 may engage GRB2-associated-binding protein 1 (GAB1) to enhance cell motility and downstream growth factor signalling and to reduce endocrine sensitivity [40]. Three fusions (GRB2:TSEN54, GRB2:RNFT1 and validated GRB2:SEPT9) were identified in one refractory and two primary tumors. Another fusion GRB7:KLHL11 was detected in a refractory sample. Both GRB2 and GRB7 contain SRC homology 2 (SH2) domain which can interact with estrogen receptor [148].

- **RPS6KB1**

As mentioned above (Chapter 3.3.7.9), RPS6KB1 is involved in various diseases and has interaction with ESR1 and tamoxifen in breast cancer. Furthermore, it has been reported that

mTORC1 regulates transcription and translation through interaction with eukaryotic translation initiation factor 4E-binding protein 1 (EIF4EBP1) or RPS6KB1 [149]. Fusion SGCZ:EIF4EBP1 was found in one refractory tumor and rearrangements of RPS6KB1 have been identified in two primary and three refractory tumors, including RPS6KB1:VMP1 and potential fusion protein RPS6KB1:CAMSAP2. In addition, fusion of RPS6KA1 was found in one primary tumor and point mutation of RPS6KB2 was detected in a refractory tumor. Furthermore, another mutation of RPS6KB2 was reported in 1 of 11 hormone resistant metastatic breast tumors [7] and recurrent fusion RPS6KB1:VMP1 was identified in TCGA database (4 of 1019 primary tumors) [72]. Distance between VMP1 and RPS6KB1 on chromosome 17 is approximately 60 kb. These novel findings together with previous reports as mentioned in Chapter 3.3.7.9 may suggest that aberrations of RPS6KB1 may play a role in breast cancer.

- **STXBP4**

Five refractory tumors and one primary tumor harbor different rearrangements of syntaxin binding protein (STXBP4), including fusion ACOX1:STXBP4 identified in paired tumors (B2HF_T1 and B2HF_M1). STXBP4, also known as synip, can be phosphorylated by AKT2 to regulate docking/fusion of glucose transporter 4 (GLUT4)-containing vesicles on the plasma membrane [150]. It has been reported that 17β -estradiol enhances estrogen receptor dependent rapid signalling, leading to increased glucose uptake, which may provide energy demands for high proliferation in MCF-7 breast cancer cells [151]. This suggests that aberration of STXBP4 may affect the glucose uptake which is an essential step for cell proliferation.

- **Metabolism-related genes**

HSD17B1, one of 17β -hydroxysteroid dehydrogenase (HSD17B), is involved in estrogen metabolism by converting estrone to estradiol [152]. Single point mutations of HSD17B11 (p.T252A) and HSD3B1 (p.G141A) were detected in one primary and one refractory tumor, respectively. Recurrent HSD17B12 mutations (p.S251F and p.G121V) were found in two refractory tumors.

Several gene families participate in metabolism of tamoxifen and estrogen, including CYP, SULT, FMO, UGT (Suppl. Figure S7 and Figure S8). Five CYP mutations were detected in five primary tumors (5/46) and six different CYP mutations were detected in five different refractory tumors (5/50). SULT and UGT mutations were identified in two primary and three refractory tumors (Suppl. Table S12). In addition, rearrangements of CYP were identified in six refractory tumors and two primary tumors, and two refractory tumors harbor rearrangements of SULT and UGT. One potential fusion protein FMO5:PRPF3 (Figure 3.29.b) was identified in a primary tumor.

Solute carrier (SLC) transporters play an important role in cancer therapy through uptake of anticancer agents in cancer cells and essential nutrients for tumor growth and survival

[112]. Approximately 32% (21/65) refractory and ~19% (10/53) primary tumors harbor rearrangements of SLC.

Aromatase inhibitor resistance may be agent-selective as tumors can still respond to other endocrine therapies such as a different aromatase inhibitor class, tamoxifen or fulvestrant [88]. Based on the aberration of genes involved in estrogen and tamoxifen metabolism, I propose the hypothesis that abnormality of metabolism is a possible mechanism of endocrine therapy resistance.

4.4 Outlook

The NGS technologies, especially paired-end RNA-seq, provide a platform to uncover fusion genes. Although a great number of fusion detection tools have been developed in the last few years, a perfect tool which can detect all fusion genes in a sample is still not available. DeFuse performs better than several alternative tools but could still be improved in term of fusion detection accuracy. ConfFuse, as a downstream filtering method mainly dependent on deFuse, can dramatically reduce the total number of predicted fusion transcripts with comparable detection accuracy. It may be possible to increase the fusion detection accuracy by ensemble of different tools, while remaining comparable true positive rate in resulted fusion candidates.

Fusion genes have been identified as driver mutations in several tumor entities, indicating that there may be fusion-specific driven tumor. In this thesis, hundreds of novel fusion genes have been identified in different tumor entities, including more than 60 highly reliable predicted fusion proteins in breast cancer. Further functional characterization of fusion genes should be carried out to understand how they regulate or interfere cellular processes and which targets they interact with. Understanding fusion gene function and their importance in cancer will provide important insights to discover novel biomarkers for cancer treatment or patient stratification.

Supplementary

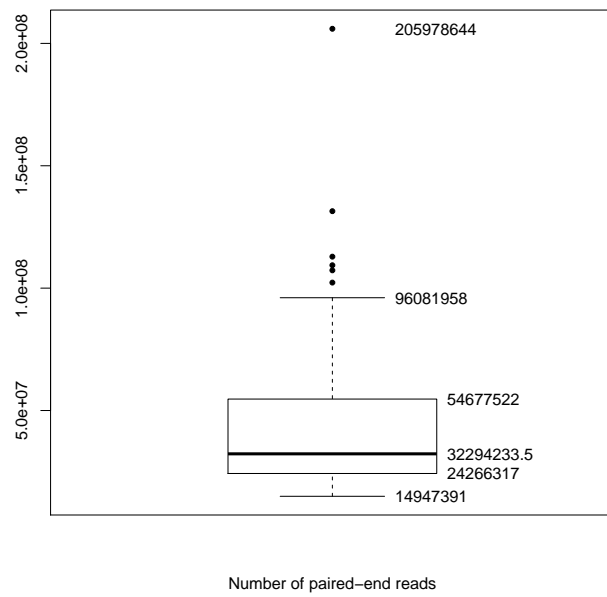


Figure S1: The number of read pairs in 96 published paired-end RNA-seq samples from seven different studies.

Table S1: Sequenced-read length of seven published studies.

Entities	RNA-seq paired-end read length (bp)
Lung cancer liver metastasis	2 × 101
Biphenotypic sinonasal sarcoma	2 × 50
Pilocytic astrocytoma	2 × 51
Thyroid cancer	2 × 75
Ependymoma	2 × 101
Lung adenocarcinoma	2 × 101
Glioma	2 × 101

Table S2: Validated fusions from 96 paired-end RNA-seq samples in seven published studies.

Sample ID	Gene1	Gene2	deFuse	confFuse score ≥ 8	fusion- Map	SOAP- Fuse	confFuse score<8
CGGA_1024	PLA2G6	CRYBB1	Y	Y	Y	Y	
CGGA_1026	MLL3	CHGB	Y	Y	N	N	
CGGA_1026	VHL	BRK1	Y	Y	Y	Y	
CGGA_1034	SBF2	AP2A2	Y	Y	Y	Y	
CGGA_1034	SCUBE2	RASSF7	Y	Y	Y	Y	
CGGA_1034	SPAG6	CD81	Y	Y	Y	N	
CGGA_1046-1	TPT1	AADAT	Y	Y	Y	Y	
CGGA_1046-1	ZNF197	CHMP2B	Y	Y	Y	Y	
CGGA_1049	OGDH	CCM2	Y	Y	Y	N	
CGGA_1049	TPM3	ADAR	Y	Y	Y	Y	

Continued on next page

Table S2 – continued from previous page

Sample ID	Gene1	Gene2	defFuse	confFuse score ≥ 8	fusion-Map	SOAP-Fuse	confFuse score<8
CGGA_1059	MYO10	MARCH6	Y	Y	Y	Y	
CGGA_1068	PTPRZ1	MET	Y	Y	Y	Y	
CGGA_1077	LANCL2	DNAH11	Y	Y	Y	Y	
CGGA_1079	CELA1	BIN2	Y	Y	N	Y	
CGGA_1094	GPR162	CCDC39	Y	Y	Y	N	
CGGA_1094	SLC6A8	GABRA3	N	N	Y	Y	
CGGA_1109	TACC3	FGFR3	Y	Y	N	Y	
CGGA_1113	XRCC6BP1	CTDSP2	Y	Y	Y	Y	
CGGA_1118	SNTG1	PVRL2	Y	Y	Y	Y	
CGGA_1119	PLAGL2	HCK	Y	Y	Y	Y	
CGGA_1170	TSFM	CDK4	Y	N	N	Y	7
CGGA_1175	DENND5B	B4GALNT3	Y	Y	Y	Y	
CGGA_1175	MED13L	GRIP1	Y	Y	Y	N	
CGGA_1234	PODXL	BGN	Y	Y	Y	Y	
CGGA_1240	VPS29	GLTP	Y	Y	Y	Y	
CGGA_1251	CLPSL1	BRPF3	Y	Y	Y	Y	
CGGA_1251	FAM155A	COL4A1	Y	Y	Y	Y	
CGGA_1272	SNTG1	PVRL2	Y	Y	Y	N	
CGGA_1272	ST7	CTTNBP2	N	N	N	N	
CGGA_1287	PTN	DGKI	Y	Y	Y	N	
CGGA_1313	TACC3	FGFR3	Y	Y	Y	Y	
CGGA_1324	CBX3	C15orf57	Y	N	Y	Y	1.5
CGGA_1324	KCNC2	CDK17	Y	Y	Y	Y	
CGGA_1329	GPC6	COG3	Y	Y	Y	N	
CGGA_1329	SERP2	LHFP	Y	Y	Y	N	
CGGA_1329	TCF7L1	KIF1B	Y	Y	Y	Y	
CGGA_1329	URI1	SLC6A20	Y	Y	Y	Y	
CGGA_1329	ZMIZ1	MAT1A	Y	Y	Y	Y	
CGGA_245	IL1RAP	FGF12	Y	Y	Y	Y	
CGGA_274	MTAP	C9orf92	Y	Y	N	Y	
CGGA_309	FARP2	DTNB	Y	Y	Y	Y	
CGGA_374	FBXO2	CBL	Y	Y	N	Y	
CGGA_374	MGAT5	KIAA0825	Y	Y	Y	Y	
		/C5orf36					
CGGA_374	TTLL11	FIBCD1	Y	Y	Y	Y	
CGGA_413	SYMPK	CLASRP	Y	Y	Y	Y	
		/SFRS16					
CGGA_413	TMEM178B	AHCYL2	Y	Y	Y	N	
CGGA_491	RIBC1	HUWE1	Y	Y	Y	Y	
CGGA_493	TGFB1	SAE1	Y	Y	Y	Y	
CGGA_564	ZC3H11A	REN	Y	Y	Y	Y	
CGGA_578	MRPS28	ASPH	Y	Y	N	Y	
CGGA_578	PFKP	FRMD4A	Y	Y	Y	Y	
CGGA_603	VEZT	CORO1C	Y	Y	Y	Y	
CGGA_604	SLC26A11	RNF213	Y	Y	Y	Y	
CGGA_616	CPNE5	ANXA6	Y	Y	Y	Y	
CGGA_661	PTPRZ1	MET	Y	Y	Y	Y	
CGGA_704	MLH1	IFT80	Y	Y	N	Y	

Continued on next page

Table S2 – continued from previous page

Sample ID	Gene1	Gene2	defFuse	confFuse score≥8	fusion-Map	SOAP-Fuse	confFuse score<8
CGGA_796	RAD51C	PITPNA	Y	Y	Y	Y	
CGGA_802	RXRA	NEK6	Y	Y	Y	Y	
CGGA_815	SH3GL1	CHAF1A	Y	N	Y	Y	7.5
CGGA_842	TACC3	FGFR3	Y	Y	Y	Y	
CGGA_859	LZTR1	BCR	Y	Y	Y	N	
CGGA_878	NFATC3	CPNE2	Y	Y	Y	Y	
CGGA_D27	SLC26A11	RNF213	Y	Y	Y	N	
CGGA_D36	SHISA5	APEH	Y	Y	Y	N	
CGGA_D64	PTPRZ1	MET	Y	Y	Y	Y	
T22	NTRK3	ETV6	Y	Y	Y	N	
T23	BRAF	AGK	N	N	Y	Y	
T24	NTRK3	ETV6	Y	Y	Y	Y	
T25	PPARG	CREB3L2	Y	Y	Y	Y	
T5	RET	NCOA4	Y	Y	Y	Y	
AK55	KIF5B	RET	Y	Y	Y	Y	
SRR1028024	PAX3	MAML3	Y	Y	Y	Y	
LC_C11	UBR4	ATP13A2	Y	Y	Y	Y	
LC_C12	KRAS	CDH13	N	N	Y	N	
LC_C15	TNFSF11	APLP2	Y	Y	Y	Y	
LC_C16	MAN1A2	IGSF3	Y	Y	Y	Y	
LC_C17	TXNRD1	GPR133	Y	Y	Y	Y	
LC_C24	RAB21	FRS2	N	N	Y	N	
LC_C25	ZFYVE9	CGA	Y	Y	Y	Y	
LC_C25	UBE2E1	ASCC3	N	N	Y	Y	
LC_C26	TCTEX1D4	ARHGEF16	Y	N	Y	Y	7
LC_C36	SLC16A7	MUCL1	Y	Y	Y	Y	
LC_S11	HYOU1	C11orf93	Y	Y	N	N	
LC_S12	NDUFAF6	CMBL	Y	Y	Y	N	
LC_S13	FGFR2	CIT	Y	Y	Y	Y	
LC_S15	XRCC1	MAL	Y	Y	N	Y	
LC_S18	NMRK2	MIER2	Y	Y	Y	N	
LC_S18	RBM14	FGF3	Y	Y	N	N	
LC_S18	ITGB1BP3	DNM2	N	N	N	Y	
LC_S19	MAST4	ERBB2IP	Y	Y	Y	Y	
LC_S2	RET	KIF5B	Y	Y	Y	Y	
LC_S20	MAP3K3	BCAS3	N	N	Y	Y	
LC_S20	SFTPA2	FTL	N	N	Y	N	
LC_S20	PECAM1	MAP3K3	N	N	N	N	
LC_S23	MBIP	AXL	Y	Y	Y	N	
LC_S26	CEP112	BRWD1	Y	Y	Y	N	
LC_S26	EML4	ALK	Y	Y	Y	Y	
LC_S26	PRKCE	MAP4K3	Y	Y	Y	Y	
LC_S29	SRSF4	SNRNP40	Y	Y	Y	N	
LC_S35	TTC19	ATPAF2	Y	Y	Y	Y	
LC_S38	SCAF11	PDGFRA	Y	Y	Y	N	
LC_S38	SPTLC3	MAOA	Y	Y	Y	Y	
LC_S39	ROS1	CD74	Y	Y	Y	N	
LC_S39	SIPA1L3	LSM14A	Y	Y	Y	Y	

Continued on next page

Table S2 – continued from previous page

Sample ID	Gene1	Gene2	defFuse	confFuse score \geq 8	fusion- Map	SOAP- Fuse	confFuse score<8
LC.S42	RET	KIF5B	Y	Y	Y	N	
LC.S42	TRMT11	TPD52L1	Y	N	Y	N	5.5
LC.S42	UTRN	OS9	N	N	Y	N	
LC.S46	MGAT5	HNMT	Y	Y	Y	Y	
LC.S48	SLC34A2	ROS1	Y	Y	Y	N	
LC.S51	MID1	EDA	N	N	Y	Y	
LC.S9	ROS1	CCDC6	Y	Y	Y	Y	
ICGC_PA112	RNF130	BRAF	Y	Y	Y	Y	
ICGC_PA112	RUFY1	TMEM178B	Y	Y	Y	N	
ICGC_PA134	NTRK2	NACC2	Y	Y	Y	Y	
ICGC_PA144	CLCN6	BRAF	Y	Y	Y	Y	
ICGC_PA159	QKI	NTRK2	Y	Y	Y	Y	
ICGC_PA58	MKRN1	BRAF	Y	Y	Y	Y	
ICGC_PA82	QKI	NTRK2	Y	Y	Y	Y	
ICGC_PA96	RNF130	BRAF	Y	Y	Y	Y	
11EP21	YAP1	MAMLD1	Y	Y	Y	Y	
2EP25	YAP1	MAMLD1	Y	Y	Y	Y	
3EP29	YAP1	MAMLD1	Y	Y	Y	Y	
3EP45	YAP1	FAM118B	Y	Y	Y	N	
3EP6	YAP1	MAMLD1	Y	Y	Y	Y	
4EP46	YAP1	MAMLD1	N	N	Y	Y	
9EP45	YAP1	MAMLD1	Y	Y	Y	Y	

Note: The order of fusion partner 5' and 3' is ignored to simplify comparison.

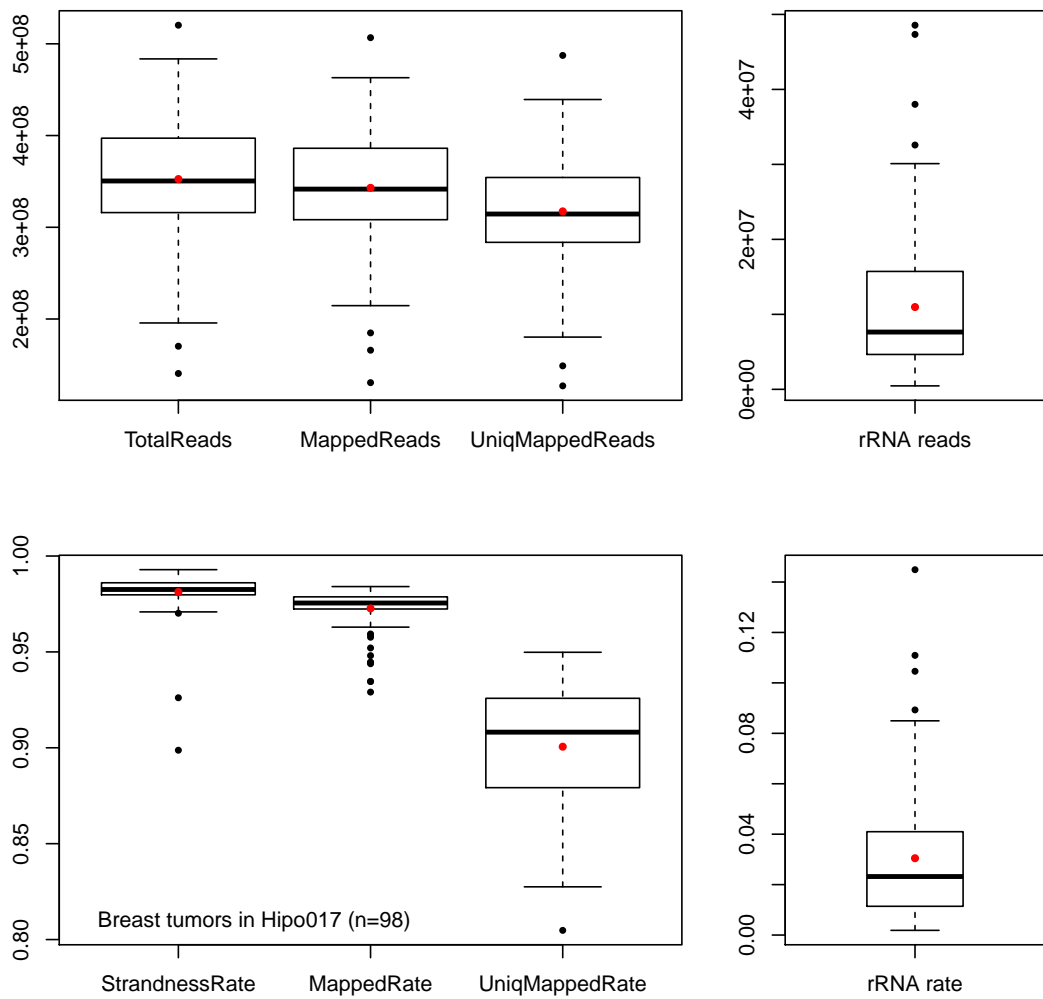


Figure S2: Mapping quality control of 98 breast RNA-seq samples in HIPO-017. It shows total number of sequencing reads, mapped reads, uniquely mapped reads, ribosome RNA reads and their corresponding rates. In addition, strand-specific rates are shown.

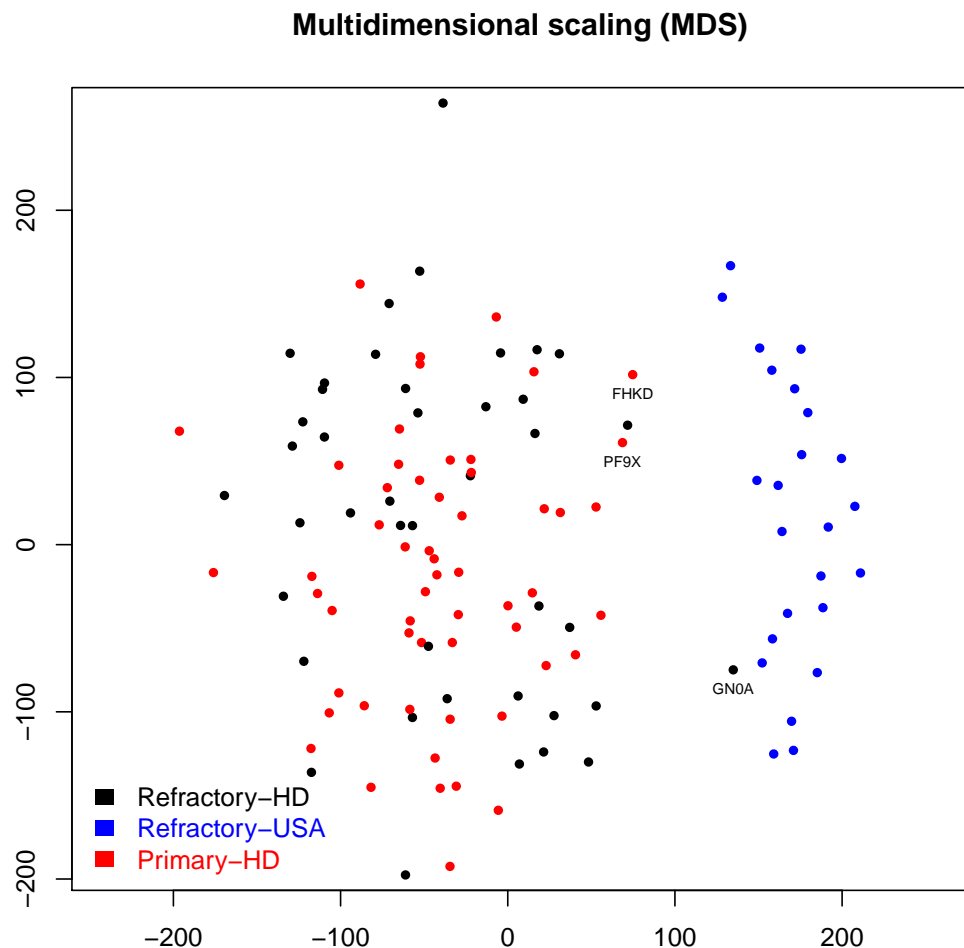


Figure S3: Multidimensional scaling of 122 breast tumor RNA-seq samples, including 24 RNA-seq samples from Ellis's group in USA (blue). The HIPO-017 samples are separated from the Ellis's samples due to using different sequencing protocols, where strand-specific protocol was used in HIPO-017 and polyA+ protocol was applied on Ellis's samples. Two samples (PF9X and FHKD) were prepared with old version of library chemistry. One refractory sample (GN0A) was grouped with Ellis's samples. Normalization was based on DESeq [153].

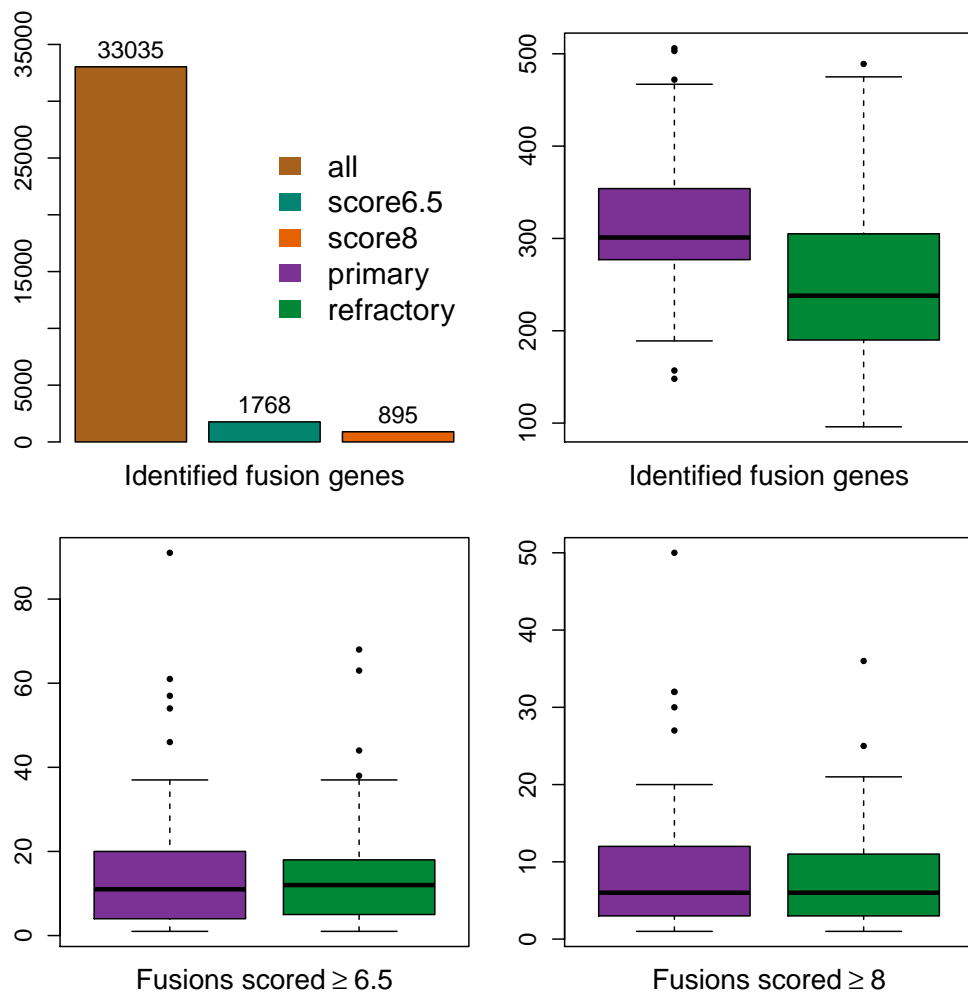


Figure S4: Number of fusions in 118 breast tumors (53 primary and 65 refractory). 895 fusion genes were identified as being high-confidence fusions. The median of fusions scored ≥ 6.5 is ~ 10 in both primary and refractory samples.

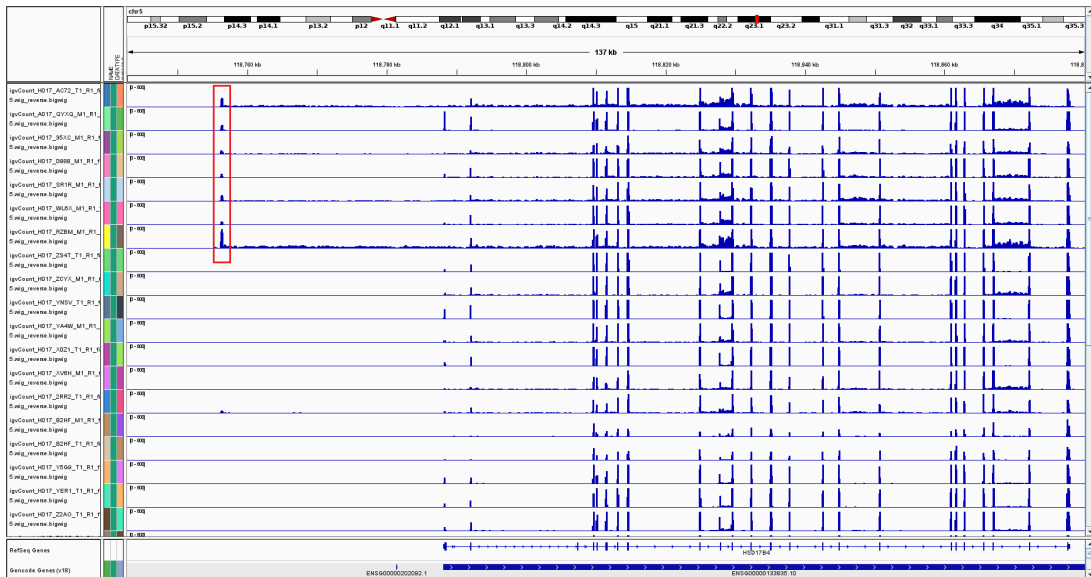


Figure S5: Novel non-annotated region shown in red box in upstream of gene HSD17B4.

Tbi-cluster	
Logged in : Zhiqin Huang Log out	
Active jobs Completed jobs Nodes Job categories Projects Preferences Server About	
Showing details for job : 4191382	
Use as MinJobId Use as MaxJobId	
Requested and used resources	
Attribute	Value
Owner	huangz
Name	A017_WQL2_M1_R1_defuse
Submit arguments	-o /icgc/dkf2isdf/analysis/hipo/hipo_017/cluster_messages/all_encode15 -N A017_WQL2_M1_R1_defuse -v LeftReads=/icgc/dkf2isdf/analysis/hipo/hipo_017/A017_WQL2_M1_R1_defuse/A017-WQL2-M1_R1_NoIndex_L004_R1_complete_filtered.fastq.gz,RightReads=/icgc/dkf2isdf/analysis/hipo_017/A017_WQL2_M1_R1_defuse/A017-WQL2-M1-R1_NoIndex_L004_R2_complete_filtered.fastq.gz,smID_path=/icgc/dkf2isdf/analysis/hipo/hipo_017/results_2014/transcriptome_analysis/results_per_pid/A017_WQL2_M1_R1/home/huangz/scripts/defuse/run_defuse_highMem.sh
Queue	highmem
Job Type	BATCH
Status	COMPLETED
Queued	Tue Sep 29 13:22:33 2015
Started	Tue Sep 29 15:58:35 2015
Ended	Mon Oct 19 13:07:54 2015
Exit Code	0
Start count	1
Exec Host	tbi-hm02
Requested walltime	1000:00:00
Elapsed walltime	477:09:19
CPU time	4454:20:21
CPU time / cores	445:26:02
CPUs avg. utilized	9.34
Cores	10
Memory Requested	360.0 GB
Maximum Memory Used	408.7 GB
Memory Efficiency	1.14

Figure S6: Example of required computer resource in running deFuse. Typically, deFuse needs two to three days for processing 200 million RNA-seq paired-end reads.

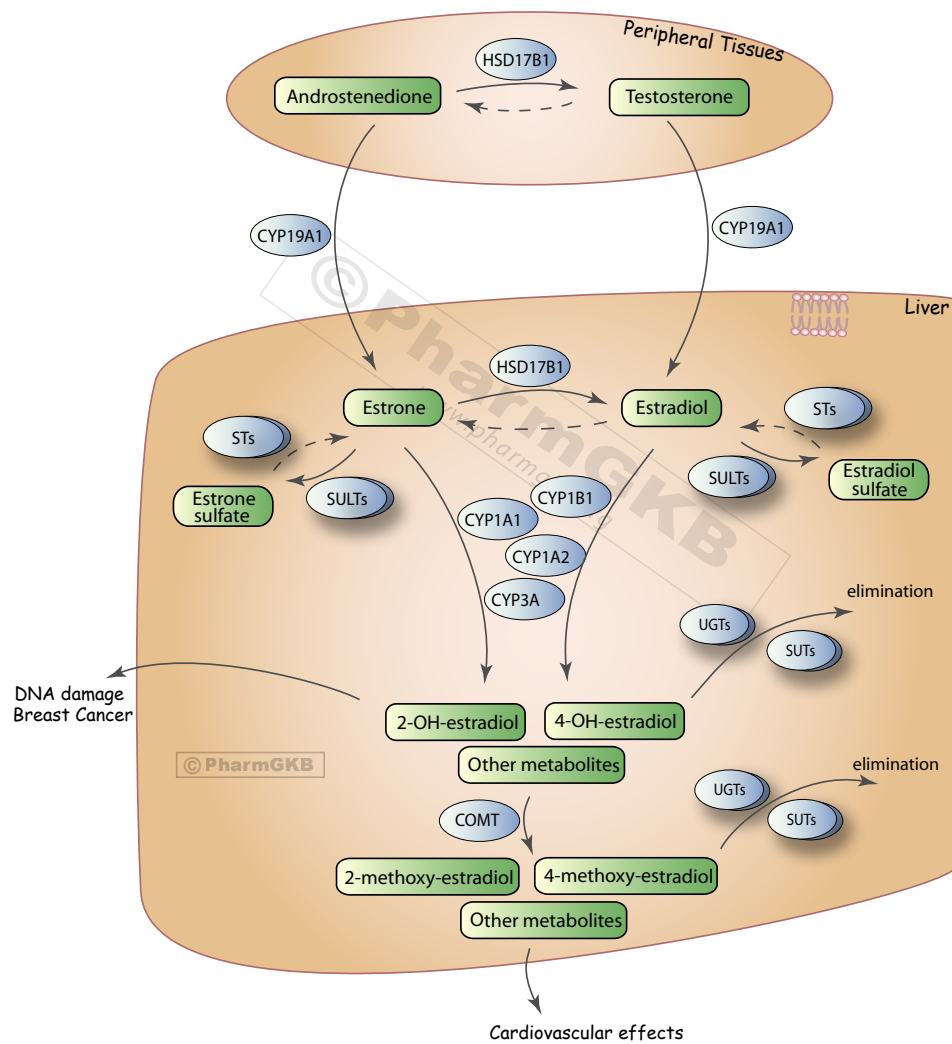


Figure S7: Estrogen metabolism in the liver. There are at least three different gene sets, including cytochrome P450 (CYP), UDP-glucuronosyltransferase (UGT) and sulfotransferase (SULT). HSD17B1 plays an important role in estrogen metabolism. Image source:[142].

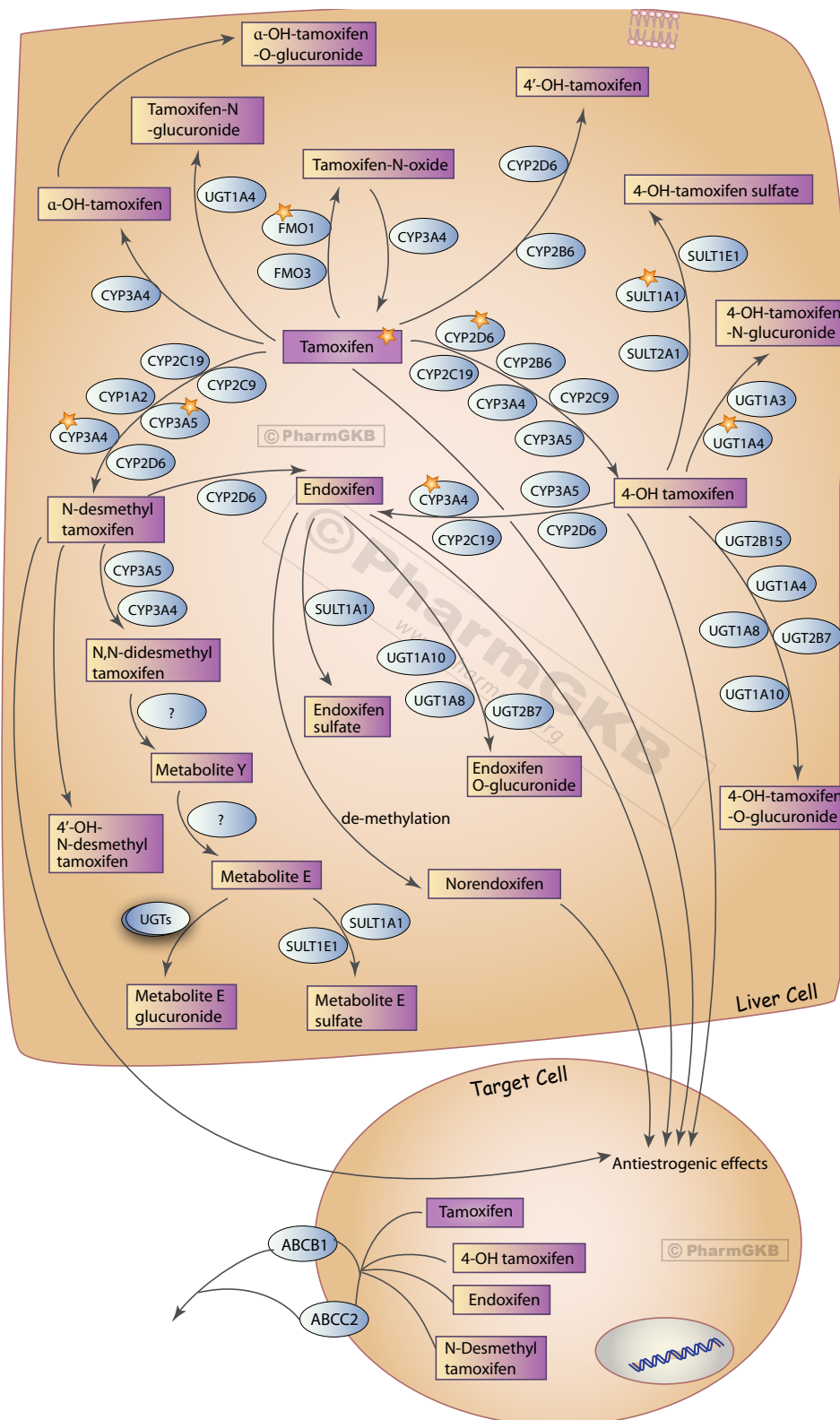


Figure S8: Tamoxifen metabolism in the liver. There are at least four different gene sets involved in the tamoxifen metabolism, including cytochrome P450 (CYP), flavin-containing monooxygenase(FMO), uridine 5'-diphospho-glucuronosyltransferase (UDP-glucuronosyltransferase, UGT) and sulfotransferase (SULT). Image source:[141].

Table S3: Validation results of three breast tumor samples using RT-PCR followed by Sanger sequencing.

SampleID	FusionID	Gene1	Gene2	Validated	Score	defFuse probability	defFuse	fusionMap	soapFuse
AC72	301018	ACACA	BECN1	Y	9.5	0.96	Y	Y	Y
AC72	300242	EXOC7	CDR2L	Y	9.5	0.96	Y	Y	Y
AC72	27755	CD3D	TOM1L2	Y	9	0.89	Y	Y	N
AC72	27745	MPZL2	TOM1L2	Y	8.5	0.68	Y	Y	Y
AC72	302014	GRB2	SEPT9	Y	8.5	0.72	Y	Y	Y
AC72	871500	CDH1	CDH3	Y	8	0.95	Y	Y	N
AC72	1617622	NXPH1	WDR70	N	7.5	0.81	Y	N	N
AC72	297858	TADA2A	SLC25A19	Y	7	0.5	Y	N	N
AC72	300268	TOM1L2	B9D1	Y	7	0.85	Y	N	N
AC72	275228	MCFD2	HSD17B4	N	6.5	0.5	Y	N	N
AC72	1081289	LRRK63	RP1-71H24.1	Y	5.5	0.91	Y	N	N
AC72	512447	DNM3	METTL13	N	4.5	0.75	Y	Y	Y
AC72	302444	KANSL1	ARL17A	Y	1.5	0.58	Y	N	N
8HNA	421007	ACSF3	MLEC	Y	10	0.9	Y	Y	N
8HNA	304034	RB1	ENOX1	Y	9.5	0.96	Y	Y	Y
8HNA	353134	QKI	PACRG	Y	9.5	0.9	Y	Y	Y
8HNA	585858	PTEN	RP11-76P2.3	Y	9	0.88	Y	Y	N
			/PTEN-AS						
8HNA	144217	GRAP2	GRIA3	Y	9	0.98	Y	Y	N
8HNA	438945	ANO6	DDX11	Y	8	0.8	Y	Y	Y
8HNA	585857	PTEN	PLCE1	Y	6.5	0.62	Y	N	N
8HNA	604375	TMEM8B	ZNF761	N	6.5	0.9	Y	N	N
8HNA	326878	RP11-	CRISPLD2	Y	6.5	0.98	Y	Y	N
8HNA	47226	680G10.1							
8HNA	47226	ASTN2	CHODL	N	6.5	0.58	Y	N	N

Continued on next page

Table S3 - continued from previous page

SampleID	FusionID	Gene1	Gene2	Validated	Score	defFuse	defFuse	fusionMap	soapFuse
8HNA	522585	LINS	AP3B1	N	6	0.9	Y	N	N
8HNA	350788	BTN3A2	BTN3A3	N	4.5	0.91	Y	N	N
8HNA	55371	DTX2P1-	PMS2P3	N	2.5	0.64	Y	N	N
		UPK3BP1-							
		PMS2P11							
DR8V	398749	TBC1D9	RP11-203B7.2	Y	9.5	0.91	Y	Y	N
DR8V	354132	WDR25	EML1	Y	9.5	0.98	Y	Y	N
DR8V	687	NDUFC2	PPFIA1	Y	9.5	0.87	Y	Y	N
DR8V	141456	MACF1	SF3A3	Y	9	0.91	Y	Y	Y
DR8V	68889	CREB1	FASTKD1	Y	8.5	0.98	Y	N	Y
DR8V	1254	FAM168A	MYO7A	Y	8.5	0.96	Y	Y	Y
DR8V	512	RAB6A	FCHSD2	Y	7	0.7	Y	N	N
DR8V	337	PPFA1	RP11-800A3.3	Y	7	0.94	Y	N	N
DR8V	398750	TBC1D9	RP11-203B7.2	N	7	0.99	Y	Y	N
DR8V	923	MYEOV	UCP2	Y	7	0.87	Y	N	N
DR8V	203	LRP5	RP11-800A3.3	Y	7	0.92	Y	N	N
DR8V	676	P2RY6	UCP2	Y	7	0.82	Y	N	N
DR8V	277099	GOLM1	ITGB5	N	6	0.74	Y	N	N
DR8V	3351	SCGB2A2	AC011293.1	N	6	0.61	Y	N	N
DR8V	254250	EFHC1	EXOC2	N	3.5	0.87	Y	N	N
DR8V	233980	BANP	CTD-2547E10.3	Y	0.5	0.91	Y	N	N

Note: The order of fusion partner 5' and 3' is ignored to simplify comparison.

Table S4: Fusions identified in 83 sarcoma samples.

Gene1	Gene2	Sample	Score	Gene1	Gene2	Sample	Score
AAR2	PREX1	UGJA	≥8	Metazoa_SRPP	CHAMP1	91Z1	≥6.5
ABHD15	TOP3A	QX1T	≥8	Metazoa_SRPP	DNMT1	Q0QG	≥6.5
ABHD3	PRR4	PC8Y	≥8	METTL21A	C1orf186	EZNS	≥6.5
ABHD3	TAS2R14	PC8Y	≥8	METTL21B	STAB2	TT6Q	≥8
ABR	RP5-936J12.1	60AP	≥8	METTL25	TMTC2	6SSR	≥8
ABR	NLGN4Y	UYD8	≥8	METTL25	RP11-	T56Q	≥8
					793H13.10		
AC006465.3	PI15	6Z0N	≥8	MGP	FBLN1	A7M2	≥6.5
AC013461.1	SPAG16	JSF3	≥8	MIER2	TMTC2	RZA9	≥8
AC016629.2	VBP1	ZDBB	≥8	MIOS	PHF14	VEJN	≥8
AC018865.8	AC140481.1	V7AX	≥8	MIP	PPFIA2	6MN5	≥8
AC021066.1	CERS5	HLDX	≥8	MKL1	MYH9	LXSA	≥8
AC021066.1	PPHLN1	HLDX	≥8	MLL3	PLXNA4	W1PS	≥8
AC090044.1	AC062020.2	91Z1	≥6.5	MLL5	E2F7	JSF3	≥6.5
AC091517.1	ARID2	5TGD	≥8	MLL5	ZDHHC17	JSF3	≥8
AC104794.4	HNRPLL	M428	≥8	MMS22L	UTRN	LL1U	≥8
AC131097.4	ZCCHC17	48LU	≥8	MOB3B	GPNMB	2SQ0	≥6.5
AC131213.1	SARNP	FGYL	≥8	MON2	SARNP	LFKM	≥8
ACACB	PTPRB	NF4Z	≥8	MRPL48	PC	82DG	≥8
ACACB	RP13-653N12.1	NF4Z	≥8	MSMP	MB	EU4K	≥6.5
ACACB	WDR66	NF4Z	≥8	MSNP1	DYRK2	JSF3	≥6.5
ACACB	PIP4K2C	TT6Q	≥8	MSRB3	C5orf58	8UBW	≥6.5
ACAD10	MAPKAPK5	NF4Z	≥8	MSRB3	CHPT1	TT6Q	≥6.5
ACAT2	ARHGAP9	LL1U	≥8	MSRB3	NCKAP1L	LFKM	≥8
ACP1	AC068491.1	91Z1	≥6.5	MSRB3	MYBPC1	TT6Q	≥8
ACSS3	PPP1R12A	6MN5	≥8	MSRB3	SYT9	TT6Q	≥8
ACSS3	RASSF9	8UBW	≥8	MTCH1	AC092170.1	91Z1	≥6.5
ACSS3	R3HDM2	LL1U	≥8	MTUS2	RB1	EC1C	≥8
ACSS3	CNKS2R2	RZA9	≥8	MUCL1	RP1-34H18.1	JSF3	≥8
ACTA2	ACTB	60AP	≥8	MUCL1	TPH2	JSF3	≥8
ACTA2	ACTG2	KWB3	≥8	MUCL1	TMTC3	RW8V	≥8
ACTB	ACTG1	KWB3	≥8	MXI1	PRKG1	0UB7	≥8
ADAM18	FNDC3A	LVPU	≥8	MYBPC1	PARPBP	TT6Q	≥8
ADAMTS2	AHRR	91Z1	≥8	MYBPC1	RP11-58A17.4	TT6Q	≥8
ADAMTS1	PDCD2L	QX1T	≥8	MYH7	MSMP	EU4K	≥6.5
ADCY10	KAT2B	PC8Y	≥8	MYH9	C18orf1	LXSA	≥6.5
ADGB	STXBP5	8UBW	≥8	MYH9	RP11-1L12.3	LXSA	≥8
AEBP2	USF2	8UBW	≥8	MYO18B	XKR3	G9EG	≥8
AGAP1	GIMAP4	2SQ0	≥8	MYO9B	ZNF431	RZA9	≥8
AGAP2	DTX3	TT6Q	≥8	MYSM1	RAB3IP	HLDX	≥8
AHI1	GLMN	W7DB	≥8	NAA50	MRAS	GLXU	≥6.5
AHR	AC004540.5	2SQ0	≥6.5	NAB2	STAT6	A7M2	≥8
AHR	P2RX5	2SQ0	≥8	NAB2	STAT6	XMEQ	≥8
AICDA	FBXO17	8UBW	≥8	NADK	FILIP1	OWEN	≥6.5
AIFM1	SERPINA7	EZNS	≥8	NAE1	RP11-543E8.1	VEJN	≥8
AIMP1	SEC31A	EZNS	≥8	NALCN	RB1	CZN2	≥8
AKAP6	NUBPL	Q0QG	≥8	NAP1L1	OS9	6SSR	≥8
AKT1	RICTOR	GLXU	≥8	NAP1L1	RP1-34H18.1	6SSR	≥8

Continued on next page

Table S4 – continued from previous page

Gene1	Gene2	Sample	Score	Gene1	Gene2	Sample	Score
AL583842.3	MDM2	TT6Q	≥8	NAP1L1	PAWR	LFKM	≥8
ALG14	CTDSP2	W7DB	≥8	NAP1L1	SLC16A7	LFKM	≥8
ALKBH5	HMGB3P23	EZNS	≥8	NAP1L4P3	ASTN2	5KJM	≥6.5
ANGPT4	MMS22L	LL1U	≥8	NAV2	GAS2	6Z0N	≥6.5
ANKLE2	AGAP2	TT6Q	≥6.5	NAV3	CAND1	LFKM	≥6.5
ANKLE2	RP11-571M6.6	TT6Q	≥8	NBPF11	TRHDE	W7DB	≥8
ANKRD13A	RAB3IP	TT6Q	≥8	NCOA3	TCP10L2	91Z1	≥8
ANKRD32	RP11-133F8.2	91Z1	≥8	NCOR1	CTC-297N7.9	JSF3	≥6.5
ANKRD52	SLC16A7	LFKM	≥8	NCOR2	UBC	5KJM	≥8
ANKRD6	SNX9	8UBW	≥8	NCOR2	UBC	UMND	≥8
ANKS1B	TMEM117	6MN5	≥8	NDUFAF4	SPICE1	QX1T	≥8
ANO10	ERC2	PC8Y	≥8	NDUFAF5	MDM2	LL1U	≥6.5
ANO2	URM1	2SQ0	≥8	NEDD4	ABR	60AP	≥6.5
ANO2	FRS2	NTAT	≥8	NEK10	RNF126	48LU	≥8
ANO4	RP1-34H18.1	LL1U	≥8	NELL2	ANO6	JSF3	≥6.5
ANO6	CRADD	5TGD	≥8	NFATC1	NPC1	NTAT	≥8
ANO6	LUM	5TGD	≥8	NFATC2	CABLES1	VEJN	≥6.5
ANO6	C12orf28	JSF3	≥8	NFKBIB	NUP155	8UBW	≥8
ANO6	TPH2	JSF3	≥8	NHSL1	NOS1AP	S81X	≥8
ANP32B	SNX30	91Z1	≥8	NLGN1	MFN1	GLXU	≥6.5
ANTXR2	UBA6	OWEN	≥8	NLGN4X	STS	RZA9	≥8
AP2A2	RPLP2	ZDBB	≥8	NLRP7	ZNF461	Q0QG	≥8
AP5Z1	NUDT1	T56Q	≥8	NMMAT3	NAA50	GLXU	≥6.5
ARF3	ATP10A	63LW	≥8	NOL9	LARP1	JSF3	≥6.5
ARHGEF25	ZDHHC17	6SSR	≥8	NOS1AP	CPM	5TGD	≥6.5
ARHGEF7	DNAH2	QX1T	≥8	NOSTRIN	EPC2	JSF3	≥6.5
ARID2	DCN	5TGD	≥8	NPHP3	MRPS22	GLXU	≥6.5
ARID2	TMEM5	HLDX	≥8	NPLOC4	CSNK1D	Q0QG	≥6.5
ARIH2	VPS8	9C3U	≥8	NR1H4	MSRB3	TT6Q	≥6.5
ARMC8	RBP1	GLXU	≥8	NR1H4	RP11-175P13.3	TT6Q	≥8
ASB9	LRIG3	RW8V	≥8	NR2C1	LTA4H	FGYL	≥6.5
ASF1B	SPC24	ERAH	≥8	NR3C1	URGCP	WHGE	≥8
ASH1L	ATF6	W7DB	≥8	NREP	CCND1	VK9K	≥6.5
ASPH	EPB41L4A	GLXU	≥8	NRF1	AC107021.1	9C3U	≥6.5
ASPSCR1	TFE3	N61A	≥8	NRXN3	WIF1	8UBW	≥8
ASTN1	ANO6	5TGD	≥6.5	NTSE	EFHC1	91Z1	≥6.5
ASXL3	CS	PC8Y	≥8	NTN4	SH3BGR	RW8V	≥8
ATF1	EWSR1	UGJA	≥8	NTN4	TENC1	RW8V	≥8
ATF1	TBC1D15	UGJA	≥8	NTRK3	RFX7	PC8Y	≥8
ATF7	METTL25	T56Q	≥8	NTS	UHRF1BP1L	T56Q	≥8
ATG7	SGOL1	ZDBB	≥8	NUBPL	DTX3	JSF3	≥6.5
ATIC	SFPQ	YHM7	≥8	NUMB	RP11-362K2.2	63LW	≥8
ATP12A	SKA3	ZDBB	≥8	NUMB	TPH2	63LW	≥8
ATP2B1	RP11-547C5.2	6MN5	≥8	NUP107	TMEM87A	63LW	≥8
ATP2B1	RP11-547C5.2	RW8V	≥8	NUP107	RABGAP1L	91Z1	≥8
ATP6VOA4	CADPS2	2SQ0	≥8	NUP107	SERINC5	91Z1	≥8
ATP6VOA4	SND1	2SQ0	≥8	NUP107	STX6	91Z1	≥8
ATP6V1A	NMMAT3	GLXU	≥8	NUP210L	RAD9B	2CJV	≥8
ATP6V1A	ZMAT3	GLXU	≥8	NUP37	ELK3	TT6Q	≥6.5

Continued on next page

Table S4 – continued from previous page

Gene1	Gene2	Sample	Score	Gene1	Gene2	Sample	Score
ATP6V1H	CDKN2A	91Z1	≥8	OR6C1	CTDSP2	6SSR	≥6.5
ATP7A	PREX2	GLXU	≥8	OR6C66P	ACSS3	6MN5	≥6.5
ATP8A2	RB1	QX1T	≥8	OR6K5P	FGGY	HLDX	≥6.5
ATP9B	RP11-433A23.1	ZDBB	≥8	OS9	RP11-754N21.1	63LW	≥8
ATXN10	TMT2C	8UBW	≥8	OS9	PPFIA2	TT6Q	≥8
AVIL	BX004987.4	HLDX	≥8	OSBPL8	TRHDE	8UBW	≥8
AVIL	DNM3	W7DB	≥8	OSBPL8	RP11-571M6.6	JSF3	≥8
AVIL	NBPF20	W7DB	≥8	OSBPL8	TSPAN31	JSF3	≥8
B4GALNT1	GLS2	PC8Y	≥8	OSBPL8	PTPRR	NTAT	≥8
B4GALT3	CCDC53	5TGD	≥8	OSBPL8	SYNE1	NTAT	≥8
BASP1	SLC15A2	Q0QG	≥8	OTOA	PPFIBP2	Q0QG	≥8
BAZ2A	KCNMB4	JSF3	≥8	OTOG	CPSF6	LFKM	≥6.5
BAZ2A	PTPRQ	LFKM	≥8	OTUD1	GPNPAT1	Q0QG	≥6.5
BBS9	PTPRD	EU4K	≥8	PAK2	COL6A6	9C3U	≥6.5
BCAT2	TFPT	2SQ0	≥8	PAK7	BCKDHB	RW8V	≥6.5
BCKDHB	SMAP1	NTAT	≥8	PAPOLA	ATP2B1	T56Q	≥6.5
BCL2L13	SLC25A18	RZA9	≥8	PAPPA2	ATG5	91Z1	≥6.5
BCOR	ZC3H7B	PC8Y	≥8	PAPPA2	PTPRR	91Z1	≥8
BEST3	ADPRHL1	91Z1	≥6.5	PARD3B	ANKRD44	JSF3	≥6.5
BEST3	NUP107	TT6Q	≥8	PARD3B	EPC2	JSF3	≥6.5
BICD1	ROCK1	PC8Y	≥8	PAWR	RP11-320P7.2	63LW	≥8
BIRC6	MDM1	JSF3	≥8	PCDH7	CDH7	ZDBB	≥6.5
BIRC6	LINC00265	WHGE	≥8	PCP4L1	SDHC	ZDBB	≥8
BOC	RAB7A	9C3U	≥8	PDE4DIP	BIRC6	WHGE	≥6.5
BRWD1	RP11-230G5.2	RW8V	≥8	PDK3	DDX3X	5KJM	≥6.5
BTG3	HHAT	9C3U	≥8	PDSS2	EYS	91Z1	≥6.5
BTLA	SLC35A5	GLXU	≥8	PDZD9	GALNTL2	VEJN	≥6.5
C12orf28	SH3BP2	8UBW	≥8	PIEZ02	UVRAG	2SQ0	≥8
C12orf28	DNM3	91Z1	≥8	PIGC	RP11-956E11.1	W7DB	≥8
C12orf28	GRIA3	91Z1	≥8	PIGL	NCOR1	60AP	≥6.5
C12orf28	MDM2	RW8V	≥8	PIP4K2C	RP11-443D10.3	TT6Q	≥8
C12orf50	CPM	2CJV	≥8	PKD1L2	INSIG2	ERAH	≥6.5
C12orf55	CUX2	2CJV	≥8	PLAUR	ETHE1	8UBW	≥6.5
C12orf56	RP11-611E13.2	6SSR	≥8	PLAUR	ZNF404	W6TV	≥8
C12orf56	RP1-34H18.1	6SSR	≥8	PLCB1	ZFR2	8UBW	≥8
C12orf56	NACA	LFKM	≥8	PLEKHA8P1	RP11-81H14.2	JSF3	≥8
C12orf66	SP1	6SSR	≥8	PLIN2	CEBD	GLXU	≥6.5
C16orf96	XYLT1	6SSR	≥8	PLXNC1	METTL7A	RW8V	≥6.5
C17orf103	C11orf30	0UB7	≥6.5	PLXNC1	TENC1	RW8V	≥8
C17orf75	YWHAE	VEJN	≥8	PMCH	TSFM	TT6Q	≥8
C17orf79	TMEM184A	72GV	≥8	PMP22	RDH12	UYD8	≥8
C18orf1	LGR4	LXSA	≥8	POC1B	TMT2C	NF4Z	≥8
C19orf47	GAPVD1	2SQ0	≥8	POLR2KP2	FTSJ2	M428	≥6.5
C19orf47	SLC25A25	2SQ0	≥8	POU2F2	ZNF568	8UBW	≥8
C1orf105	KIAA0825	91Z1	≥8	PPAP2C	USE1	RZA9	≥8
C22orf13	LGALS2	G9EG	≥8	PPFIA2	ESPL1	6MN5	≥6.5
C6orf170	AL357515.1	91Z1	≥6.5	PPFIA2	CNOT2	NTAT	≥6.5
CABIN1	SEC14L3	G9EG	≥8	PPFIA2	COPE	TT6Q	≥6.5
CALCRL	CCDC150	JSF3	≥8	PPM1H	ANO6	JSF3	≥6.5

Continued on next page

Table S4 – continued from previous page

Gene1	Gene2	Sample	Score	Gene1	Gene2	Sample	Score
CALD1	PPP1R1A	LL1U	≥8	PPM1H	MYL6	JSF3	≥6.5
CALU	SRI	NTAT	≥8	PPM1H	PTPRR	JSF3	≥8
CAMK2G	VCL	LXSA	≥8	PPOX	BEST3	HLDX	≥6.5
CAND1	ASCC3	LL1U	≥6.5	PPOX	RP11-588G21.2	HLDX	≥8
CAND1	DNM3	91Z1	≥8	PPP1R10	AL137003.1	9C3U	≥6.5
CAND1	MDM2	91Z1	≥8	PPP1R12A	NFIA	63LW	≥6.5
CAND1	E2F7	LFKM	≥8	PPP2R4	AC005621.1	12C6	≥6.5
CAND1	LRIG3	LFKM	≥8	PPP6R2	DAP	2SQ0	≥6.5
CAND1	ELK3	TT6Q	≥8	PQLC1	ADNP2	G9EG	≥6.5
CANX	AC073128.10	WHGE	≥6.5	PQLC1	TXNL4A	Q0QG	≥8
CAPNS1	A1BG	8UBW	≥6.5	PRIM1	CAPS2	LFKM	≥6.5
CAPRIN2	LGR5	JSF3	≥8	PRIMA1	LRP11	NTAT	≥6.5
CAPS2	RP11-244J10.1	5TGD	≥8	PRLR	PPP1R12A	5TGD	≥6.5
CAPZA2	ST7-OT4	WHGE	≥8	PRPF4	RP11-360A18.2	TT6Q	≥8
CASP8	AP2S1	6SSR	≥6.5	PRR14L	KIAA1671	T56Q	≥6.5
CAV1	ATP6V0A4	2SQ0	≥6.5	PRRC2C	CPSF6	2CJV	≥6.5
CBX3	GRAMD3	12G6	≥8	PRRC2C	CNOT2	HLDX	≥6.5
CBX5	E2F7	LFKM	≥8	PRRC2C	CPM	HLDX	≥6.5
CBX5	PPP1R12A	LFKM	≥8	PRRC2C	FASLG	PC8Y	≥6.5
CBX5	USP15	LFKM	≥8	PRRC2C	SCYL3	7GAB	≥8
CC2D1A	EMR2	RZA9	≥8	PRTFDC1	PTCHD3	LL1U	≥8
CCDC132	CALD1	12G6	≥6.5	PSEN1	RP11-	63LW	≥8
					1008C21.1		
CCDC28A	NT5E	91Z1	≥8	PSMC2	DLGAP1-AS3	2SQ0	≥6.5
CCDC38	VDR	6MN5	≥8	PSMD1	COL3A1	2SQ0	≥6.5
CCDC59	GIT2	6MN5	≥8	PSMD8	RP11-20J1.1	TT6Q	≥8
CCDC59	DAD1	8UBW	≥8	PSMF1	ZNF800	LL1U	≥8
CCDC93	NCKAP5	2SQ0	≥8	PSTPIP2	TSPAN9	PC8Y	≥8
CCER1	TMPRSS12	RW8V	≥8	PTGES3	MSRB3	LFKM	≥6.5
CCNT1	RAP1B	JSF3	≥8	PTGIS	ZFP64	VEJN	≥8
CCNT2	SYNE1	48LU	≥8	PTPRB	OSBPL8	NTAT	≥6.5
CCR3	CTNNB1	PC8Y	≥8	PTPRM	SPIRE1	ERAH	≥8
CCT2	RP11-120I21.2	LL1U	≥8	PTPRN2	SP140	48LU	≥8
CCT5	RAI14	8UBW	≥8	PTPRQ	ZFC3H1	JSF3	≥8
CD2AP	CDC5L	0UB7	≥8	PTPRR	HOXC5	LFKM	≥6.5
CD320	ZNF560	7GAB	≥8	PTPRR	RP11-611E13.2	91Z1	≥8
CD63	HMGA2	LFKM	≥8	PTPRR	TBC1D15	JSF3	≥8
CD63	RAB3IP	LFKM	≥8	PUS7	AP000567.27	2SF3	≥6.5
CD63	RPSAP52	LFKM	≥8	PUS7L	GRIP1	JSF3	≥6.5
CDC16	DNM3	91Z1	≥8	QARS	CADPS	GLXU	≥6.5
CDH18	KDM5A	8UBW	≥8	R3HDM2	CCNT1	JSF3	≥6.5
CDH19	PCGF3	ZDBB	≥8	RAB21	SLC38A1	63LW	≥8
CDH2	TSPAN8	PC8Y	≥8	RAB21	TSPAN8	63LW	≥8
CDK17	SARNP	RZA9	≥8	RAB21	TMEM5	LFKM	≥8
CDK17	CPSF6	TT6Q	≥8	RAB27B	RP11-114H23.1	PC8Y	≥8
CDK17	RP11-620J15.2	TT6Q	≥8	RAB27B	RP11-114H23.2	PC8Y	≥8
CDK17	SSH1	TT6Q	≥8	RAB3IP	TBC1D15	LFKM	≥8
CDK17	XRCC6BP1	TT6Q	≥8	RAB7A	ARID4B	9C3U	≥6.5
CDK4	CPM	91Z1	≥8	RABGAP1L	MDM2	91Z1	≥6.5

Continued on next page

Table S4 – continued from previous page

Gene1	Gene2	Sample	Score	Gene1	Gene2	Sample	Score
CDK4	MR1	91Z1	≥8	RABGAP1L	MTCH1	91Z1	≥6.5
CDK4	STX6	91Z1	≥8	RABGAP1L	PDSS2	91Z1	≥6.5
CDK4	ELK3	TT6Q	≥8	RAP1B	RPS6KA3	6SSR	≥8
CDK8	DGKH	M428	≥8	RASA3	PDSS2	91Z1	≥6.5
CDKAL1	DNM3	91Z1	≥8	RASIP1	ZNF542	8UBW	≥8
CDKAL1	NUP107	91Z1	≥8	RASSF3	AC005307.3	LFKM	≥6.5
CDKAL1	SNX14	91Z1	≥8	RASSF3	RP11-620J15.3	LFKM	≥8
CEACAM7	ZNF566	8UBW	≥8	RASSF9	MYF6	NTAT	≥6.5
CECR1	CRKL	T56Q	≥8	RB1	GPR110	GQPU	≥6.5
CENPL	MDM2	91Z1	≥8	RB1	LINC00358	YHM7	≥6.5
CEP290	RP11-150C16.1	RW8V	≥8	RB1CC1	AC016113.1	QX1T	≥6.5
CEP78	SEC61B	12C6	≥8	RBFOX3	ROR2	OWEN	≥8
CERS4	RAB11B	QX1T	≥8	RBMS1	RNF10	JSF3	≥8
CERS6	TSPAN31	6SSR	≥8	RBMS2	FRS2	LFKM	≥6.5
CHAMP1	RP11-360A9.2	91Z1	≥8	RBMS2	IFNG-AS1	LFKM	≥6.5
CHD2	TNRC6C	63LW	≥8	RBMS2	PTPRR	LFKM	≥6.5
CHD9	NUP93	Q0QG	≥8	RCBTB1	DLEU1	WHGE	≥6.5
CHN1	SEMA3E	2SQ0	≥8	REV3L	CPM	91Z1	≥6.5
CHPT1	YWHAQ	TT6Q	≥8	REV3L	RP11-222A5.1	91Z1	≥8
CHRD	RCBTB2	9C3U	≥8	RFTN2	SLC40A1	JSF3	≥8
CHRNA6	PLAT	8UBW	≥8	RFX1	IL27RA	A7M2	≥6.5
CHST11	RNF111	63LW	≥8	RGL1	MYO5C	PC8Y	≥6.5
CIB2	TBC1D2B	91Z1	≥8	RGPD5	PID1	91Z1	≥6.5
CIT	NAA25	NF4Z	≥8	RGS8	HERC2P2	PC8Y	≥6.5
CLU	RPS24	9C3U	≥8	RNA5SP299	RBM20	48LU	≥6.5
CMKLR1	NTNG1	GJQ0	≥8	RNASEL	SCYL3	W7DB	≥8
CNOT2	SRGAP1	JSF3	≥8	RND3	AC009313.1	JSF3	≥6.5
CNOT2	ZDHHC17	JSF3	≥8	RNF114	MYO18A	VEJN	≥6.5
CNOT2	PTPRR	LL1U	≥8	RNF182	SNRNP48	LL1U	≥8
CNOT2	HMGAA2	NTAT	≥8	RNU7-14P	RBBP8	VEJN	≥6.5
CNTLN	PTPRD	EU4K	≥8	RP11-1022B3.1	FGGY	HLDX	≥6.5
COL11A1	USP6	60AP	≥8	RP11-	BTG1	5TGD	≥6.5
			1041F24.1				
COL14A1	SLC7A5P1	W1PS	≥8	RP11-114H23.1	OS9	5TGD	≥6.5
COL1A1	ACTA2	9C3U	≥6.5	RP11-	CDK4	TT6Q	≥6.5
			123M21.1				
COL1A1	CHRDL2	9C3U	≥6.5	RP11-	CDK4	TT6Q	≥6.5
			123M21.2				
COL1A1	COL1A2	HLDX	≥8	RP11-125O18.1	RAD54L2	PC8Y	≥6.5
COL1A1	COL3A1	HLDX	≥8	RP11-13A1.3	CPSF6	2CJV	≥6.5
COL4A2	CHRDL2	9C3U	≥6.5	RP11-14I4.3	DCBLD1	8UBW	≥6.5
COL4A3	SP100	GLXU	≥8	RP11-168J19.2	PPP1R1A	LFKM	≥6.5
COL6A2	DSCAM	PC8Y	≥8	RP11-171L9.1	FRS2	63LW	≥6.5
COL6A3	B2M	QIEE	≥6.5	RP11-171L9.1	ZDHHC17	JSF3	≥8
COLEC12	SENP2	Q0QG	≥8	RP11-181K3.4	GRM1	W7DB	≥6.5
COPZ1	OSBPL8	LFKM	≥8	RP11-202H2.1	RP1-34H18.1	6SSR	≥6.5
COPZ1	TSPAN8	RW8V	≥8	RP11-203B7.2	TCEAL3	JSF3	≥8
COX10-AS1	NME1	Q0QG	≥8	RP11-21J18.1	SPIRE1	ERAH	≥8
COX11	NEBL	LL1U	≥8	RP11-21J7.1	CSNK1D	Q0QG	≥6.5

Continued on next page

Table S4 – continued from previous page

Gene1	Gene2	Sample	Score	Gene1	Gene2	Sample	Score
COX16	DCTN2	63LW	≥8	RP11-230G5.2	HMGA2	TT6Q	≥6.5
CPM	GRB2	63LW	≥8	RP11-254B13.1	TMTC1	PC8Y	≥8
CPM	NFIA	63LW	≥8	RP11-265P11.1	NUP107	6SSR	≥6.5
CPM	TMOD3	63LW	≥8	RP11-267N12.3	YEATS4	5TGD	≥8
CPM	GIT2	6MN5	≥8	RP11-	GDF11	LFKM	≥6.5
				274M17.1			
CPM	MDM2	6MN5	≥8	RP11-280O1.2	HMGA2	S81X	≥6.5
CPM	UBE2N	6MN5	≥8	RP11-290L1.5	TSFM	NTAT	≥8
CPM	RP11-222A5.1	91Z1	≥8	RP11-297H3.3	NME7	7GAB	≥6.5
CPM	STX6	91Z1	≥8	RP11-314D7.1	LRRK2	LL1U	≥6.5
CPM	TRAF3IP2-AS1	91Z1	≥8	RP11-314D7.1	ZDHHC17	LL1U	≥8
CPM	MCL1	HLDX	≥8	RP11-314D7.4	TMTC3	RW8V	≥8
CPM	OSBPL8	JSF3	≥8	RP11-319G6.1	ARMC8	GLXU	≥6.5
CPM	MDM2	RW8V	≥8	RP11-320P7.1	LRIG3	RW8V	≥6.5
CPM	NUP107	RW8V	≥8	RP11-325F22.2	ANO7	JSF3	≥6.5
CPM	UBE2N	RW8V	≥8	RP11-328N19.1	MAN2B2	ZDBB	≥6.5
CPM	SMARCA4	TT6Q	≥8	RP11-335O4.1	LGR5	RZA9	≥6.5
CPM	LRRC8C	W7DB	≥8	RP11-	DCTN2	63LW	≥6.5
				340M11.1			
CPNE5	DLEU2	QX1T	≥8	RP11-341G23.4	CCT2	TT6Q	≥6.5
CPNE8	SRGAP1	JSF3	≥8	RP11-362K2.2	MON2	LFKM	≥6.5
CPSF6	CCDC59	6MN5	≥6.5	RP11-362K2.2	SLC38A2	63LW	≥8
CPSF6	DPY19L2	LFKM	≥8	RP11-375F2.2	PLXNC1	HLDX	≥6.5
CPSF6	MUCL1	LFKM	≥8	RP11-389K14.3	FANCC	12C6	≥6.5
CPSF6	LRRK2	LL1U	≥8	RP11-394D2.1	ERP44	2SQ0	≥6.5
CR1L	EEA1	2CJV	≥8	RP11-399D2.1	DDX6	2SQ0	≥6.5
CR1L	RABGAP1L	2CJV	≥8	RP11-438P9.2	IARS	91Z1	≥6.5
CREB3L1	ZNF254	48LU	≥8	RP11-43N5.1	PLXNC1	HLDX	≥6.5
CSAD	GRIP1	6MN5	≥8	RP11-43N5.1	METTL21B	LL1U	≥6.5
CSAD	GRIP1	RW8V	≥8	RP11-43N5.1	SPRYD4	LFKM	≥8
CSF1	LSAMP	23V2	≥8	RP11-480I12.7	RPS6KC1	EZNS	≥8
CSRP2BP	SEC23B	GQPU	≥8	RP11-483I13.4	LRRC8C	W7DB	≥6.5
CTA-714B7.5	DNM2	ERAH	≥8	RP11-506B6.6	LAMA4	CZN2	≥6.5
CTB-114C7.4	CPSF6	LL1U	≥6.5	RP11-508M1.5	SIRT7	48LU	≥8
CTC-400I9.2	CELF2	2SQ0	≥6.5	RP11-511B23.1	EPHA7	LL1U	≥6.5
CTC-454M9.1	ANKRD32	91Z1	≥6.5	RP1-152L7.1	TMEM14A	91Z1	≥8
CTD-2066L21.3	DROSHA	2SQ0	≥8	RP11-541G9.1	SVOP	TT6Q	≥8
CTD-2201E18.3	CTB-157D17.1	8UBW	≥6.5	RP11-541G9.1	TSFM	TT6Q	≥8
CTD-2218K11.2	ATG5	91Z1	≥6.5	RP11-54A9.1	KCNC2	LFKM	≥6.5
CTD-2337A12.1	MLL3	LL1U	≥8	RP1-154K9.2	KDM6A	VEJN	≥6.5
CTD-3239E11.2	CHMP4C	M428	≥6.5	RP11-565A3.2	MECP2	JSF3	≥6.5
CTDSP2	BEST3	W7DB	≥6.5	RP11-565P22.2	CPM	5TGD	≥6.5
CTDSP2	SGPL1	2CJV	≥8	RP11-571M6.7	PPP1R12A	63LW	≥6.5
CTDSP2	FRS2	6SSR	≥8	RP11-57H12.3	GINM1	W7DB	≥6.5
CTDSP2	RP11-110A12.2	6SSR	≥8	RP11-57P19.1	NEO1	PC8Y	≥6.5
CTDSP2	FGD4	7GAB	≥8	RP11-57P19.1	NTRK3	PC8Y	≥6.5
CTDSP2	SLC38A4	7GAB	≥8	RP11-58A17.4	CAND1	TT6Q	≥6.5
CTDSP2	EYS	8UBW	≥8	RP11-58A17.4	MDM2	TT6Q	≥6.5
CTDSP2	SPRYD4	LFKM	≥8	RP11-58A17.4	RP11-123O10.4	TT6Q	≥6.5

Continued on next page

Table S4 – continued from previous page

Gene1	Gene2	Sample	Score	Gene1	Gene2	Sample	Score
CTDSP2	SLC31A1	TT6Q	≥8	RP11-596D21.1	HECTD1	N61A	≥6.5
CTDSPL	ARHGEF3	9C3U	≥6.5	RP1-15D23.2	FBXL17	91Z1	≥6.5
CTNNAL1	NEK6	RW8V	≥8	RP1-15D23.2	NUP107	91Z1	≥6.5
CTNNAL1	RP11-202G18.1	RW8V	≥8	RP11-611E13.2	GRIA3	91Z1	≥6.5
CTSB	ERI1	KWB3	≥8	RP11-611E13.2	LRIG3	RW8V	≥6.5
CTTN	SUCLG2	0UB7	≥8	RP11-611E13.2	RP11-571M6.8	RW8V	≥6.5
CUBN	EPC1	JSF3	≥8	RP11-611E13.2	SYT1	LL1U	≥8
CUBN	RP11-799O21.1	JSF3	≥8	RP11-611O2.3	FGGY	63LW	≥6.5
CUX1	DLG1	9C3U	≥8	RP11-620J15.2	COPZ1	LFKM	≥6.5
CUZD1	FOXO1	6MN5	≥8	RP11-620J15.2	HMGA2	LFKM	≥6.5
CYP39A1	CD2AP	GJQ0	≥6.5	RP11-620J15.3	RP11-32B5.7	PC8Y	≥6.5
CYP7B1	TMEM200A	LL1U	≥8	RP11-690D19.1	MMP13	W6TV	≥6.5
DAB1	FGGY	HLDX	≥8	RP11-6F2.7	GRM7	9C3U	≥6.5
DAB1	FRS2	HLDX	≥8	RP11-6N13.1	EPB41L4A	6MN5	≥6.5
DAB1	PRKACB	HLDX	≥8	RP11-706O15.5	MIER2	RZA9	≥6.5
DAOA	AVIL	2CJV	≥6.5	RP11-718O11.1	IFLTD1	PC8Y	≥6.5
DBC1	UBE3B	TT6Q	≥8	RP11-718O11.1	RYR3	63LW	≥8
DBX2	RAB21	JSF3	≥8	RP11-753H16.3	PRKACB	HLDX	≥6.5
DCTN2	AC139931.1	NTAT	≥6.5	RP11-753H16.3	MYH9	LXSA	≥6.5
DCTN2	RP11-362K2.2	63LW	≥8	RP11-754N21.1	RNA5P360	5TGD	≥6.5
DCTN2	RP11-624L4.1	63LW	≥8	RP11-754N21.1	ZDHHC17	JSF3	≥8
DCTN2	TRHDE	63LW	≥8	RP11-762I7.5	FRS2	LFKM	≥6.5
DCTN2	SYNE1	NTAT	≥8	RP11-766N7.3	TMEM19	LFKM	≥8
DDIT3	FUS	2SF3	≥8	RP11-768F21.1	KDM2B	ZDBB	≥6.5
DDIT3	FUS	CHZ6	≥8	RP11-788H18.1	ZDHHC17	LL1U	≥8
DDIT3	UST	NTAT	≥8	RP11-78C3.1	FYN	91Z1	≥6.5
DDIT3	FUS	S1JM	≥8	RP11-793H13.8	RP11-314D7.4	LFKM	≥6.5
DDIT3	FUS	Y20T	≥8	RP11-804L24.2	NWD1	VEJN	≥6.5
DDR2	METTL13	S81X	≥8	RP11-81H14.2	HMGA2	8UBW	≥6.5
DEF6	FRS3	8UBW	≥8	RP11-81H14.2	LRFN5	8UBW	≥6.5
DEPDC4	NR1H4	TT6Q	≥8	RP11-834C11.5	CERS5	RW8V	≥6.5
DHPS	CA10	2SF3	≥6.5	RP11-85G21.2	PEX1B	2CJV	≥6.5
DHRS7B	RP5-1112F19.2	VEJN	≥8	RP11-85G21.2	RNF115	2CJV	≥6.5
DHX15	UBE2K	EZNS	≥8	RP11-86H7.1	RAPGEF2	CZN2	≥6.5
DHX16	GNL1	8UBW	≥8	RP11-8L2.1	NUP54	EZNS	≥6.5
DKK2	PDE7A	GLXU	≥8	RP11-90C1.1	ZDHHC17	JSF3	≥8
DLEU1	TSPAN9	W6TV	≥8	RP11-90K18.1	AARS	OWEN	≥6.5
DMD	ARHGAP6	2SQ0	≥6.5	RP11-93L9.1	GRID2	WHGE	≥6.5
DNAJB1	ELK3	TT6Q	≥8	RP11-93O17.1	CDC16	91Z1	≥6.5
DNAJC1	LRRK2	LL1U	≥8	RP11-96H19.1	ADAMTS20	5TGD	≥6.5
DNAJC3	RB1	5KJM	≥8	RP11-96H19.1	RP11-118A3.1	5TGD	≥6.5
DNER	TNS1	91Z1	≥8	RP11-96H19.1	RP11-297H3.4	LFKM	≥6.5
DNM2	DTX3	TT6Q	≥8	RP11-977G19.11	7SK	LFKM	≥6.5
DNM3	CTDSP2	7GAB	≥6.5	RP1-34H18.1	GLIPR1L1	LFKM	≥6.5
DNM3	CTD-2021H9.1	91Z1	≥6.5	RP1-34H18.1	TBC1D15	LFKM	≥8
DNM3	CTDSP1	W7DB	≥6.5	RP1-35C21.2	KCNMB4	91Z1	≥6.5
DNM3	EXOC2	91Z1	≥8	RP1-81F6.1	PDE7B	7GAB	≥6.5
DNM3	GRIP1	91Z1	≥8	RP3-340B19.2	CUL9	8UBW	≥6.5

Continued on next page

Table S4 – continued from previous page

Gene1	Gene2	Sample	Score	Gene1	Gene2	Sample	Score
DNM3	RAB3IP	91Z1	≥8	RP4-794H19.2	DAB1	HLDX	≥6.5
DNM3	VAMP4	91Z1	≥8	RP4-800F24.1	PTPRB	HLDX	≥6.5
DNM3	RP11-14O19.2	W7DB	≥8	RP5-1030M6.2	CBFA2T2	ZDBB	≥6.5
DNM3	TSFM	W7DB	≥8	RP5-1063M23.2	KIAA1109	GLXU	≥6.5
DNMT1	RP11-105C19.1	Q0QG	≥8	RPH3A	DCN	NF4Z	≥6.5
DOCK2	ZNF101	8UBW	≥8	RPH3A	RP11-123O10.2	NF4Z	≥6.5
DPM1	PHF12	VEJN	≥8	RPH3A	TMEM132C	NF4Z	≥8
DPP10	ARID5A	VEJN	≥6.5	RPH3A	UBE3B	NF4Z	≥8
DPP8	AKAP8L	12C6	≥6.5	RPH3AL	TP53	VEJN	≥8
DPY19L3	SND1	2SQ0	≥8	RPL21P103	MYBPC1	TT6Q	≥6.5
DRAM1	FGD6	TT6Q	≥8	RPL30	HMGA2	1T2G	≥6.5
DSC2	HRH4	Q0QG	≥8	RPL6P25	SLC25A3	RW8V	≥8
DTX3	TSPAN8	JSF3	≥8	RPL7P45	ARID4A	91Z1	≥6.5
DUSP27	POU2F1	ZDBB	≥8	RPRD1A	C18orf34	VEJN	≥6.5
DUX4L8	CIC	MAVY	≥6.5	RPS10P3	KAT6A	YHM7	≥6.5
DYRK2	RP11-620J15.2	6SSR	≥8	RPS3	IGFBP5	9C3U	≥6.5
DYRK2	RPS6KA3	6SSR	≥8	RPSAP52	CS	LFKM	≥6.5
DYRK2	SP1	6SSR	≥8	RPSAP52	SARNP	RZA9	≥8
E2F7	AC124890.1	LFKM	≥6.5	SAP130	DNM3	91Z1	≥6.5
EARS2	RIOK3	0UB7	≥8	SARNP	TMEM19	LFKM	≥8
EBPL	LRCH1	WHGE	≥8	SASH1	EFHC1	91Z1	≥6.5
EEA1	LRRIQ1	2CJV	≥8	SASH1	RABGAP1L	91Z1	≥6.5
EEA1	RP11-13A1.3	2CJV	≥8	SBF1	KIRREL3	2SQ0	≥6.5
EEA1	TBK1	2CJV	≥8	SBNO2	ANKS1B	RZA9	≥6.5
EEA1	VWC2	T56Q	≥8	SCAF8	TMEM181	7GAB	≥8
EEF1A1P11	IGF2R	W7DB	≥8	SCFD1	KCNMB4	91Z1	≥6.5
EEF2	DAPK3	QIEE	≥6.5	SCN10A	UQCRC1	PC8Y	≥8
EEFSEC	KPNA1	WHGE	≥8	SCN8A	FRS2	LL1U	≥6.5
EFHC1	DNM3	91Z1	≥6.5	SCN8A	TPH2	LL1U	≥8
EFHC1	FRS2	91Z1	≥8	SCYL3	NME7	7GAB	≥6.5
EFNA5	SERINC5	91Z1	≥8	SDK1	USP42	VEJN	≥8
EGFR	OGDH	VEJN	≥8	SEC16B	TOR1AIP1	PC8Y	≥8
EIF3D	TXN2	2SF3	≥8	SERINC3	AP001607.1	48LU	≥6.5
EIF3E	PAG1	8UBW	≥8	SERINC5	C12orf28	91Z1	≥6.5
ELF2	SLC24A3	GLXU	≥8	SERINC5	CDK4	91Z1	≥6.5
ELK3	C12orf55	TT6Q	≥6.5	SERINC5	NEDD1	KWB3	≥6.5
ELK3	R3HDM2	NTAT	≥8	SERINC5	FBXL12	YRZB	≥6.5
ELK3	HOXC5	RW8V	≥8	SERINC5	STX6	91Z1	≥8
ELK3	HOXC6	RW8V	≥8	SETD1B	RAD9B	2CJV	≥6.5
ELK3	RAP1B	RW8V	≥8	SGK3	COL4A3	GLXU	≥6.5
EN1	FAM153C	GLXU	≥8	SGSM1	TNRC6B	G9EG	≥8
ENSA	BAZ2A	JSF3	≥6.5	SH3BP1	ATAD3A	QIEE	≥6.5
EPB41L5	MAPKAPK2	JSF3	≥8	SH3PXD2A	AC021066.1	6MN5	≥6.5
EPC2	LRP2	JSF3	≥8	SH3PXD2A	AC021066.1	RW8V	≥6.5
EPHX1	ENAH	QX1T	≥6.5	SHFM1	SRPK2	G9EG	≥8
EPM2A	RPAP2	W7DB	≥8	SLC16A7	PTPRQ	5TGD	≥6.5
EPYC	METAP2	RW8V	≥8	SLC22A20	PROCR	12C6	≥6.5
EPYC	RP11-394J1.2	RW8V	≥8	SLC25A27	CD2AP	GJQ0	≥6.5

Continued on next page

Table S4 – continued from previous page

Gene1	Gene2	Sample	Score	Gene1	Gene2	Sample	Score
ERC2	SNRK	PC8Y	≥8	SLC25A3	RPL6P25	6MN5	≥6.5
ESPL1	RAPGEF3	6MN5	≥8	SLC26A10	DPF3	63LW	≥6.5
ESPL1	RAPGEF3	RW8V	≥8	SLC2A13	GRIP1	PC8Y	≥6.5
ETHE1	MACROD2	8UBW	≥8	SLC2A13	RPL29P32	PC8Y	≥6.5
EVC2	FRAS1	EZNS	≥8	SLC35E3	NELL2	7GAB	≥6.5
EVX1	PDE1C	EU4K	≥8	SLC35E3	HS3ST5	T56Q	≥6.5
EXOC2	FYN	91Z1	≥8	SLC35F1	EFHC1	91Z1	≥6.5
EXOC2	GTF3C6	91Z1	≥8	SLC35F1	METTL13	91Z1	≥6.5
EYA4	PREP	LL1U	≥8	SLC38A2	LRIG3	63LW	≥6.5
FAM105B	CLPTM1L	2SQ0	≥6.5	SLC38A4	FAM19A2	7GAB	≥6.5
FAM182A	TPH2	JSF3	≥8	SLC52A1	SSH1	TT6Q	≥8
FAM182B	TPH2	JSF3	≥8	SLC9A8	ANKFY1	VEJN	≥6.5
FAM189A1	BLOC1S6	12C6	≥6.5	SLCO1B1	NFIB	GLXU	≥6.5
FAM193A	AC019118.3	2SQ0	≥6.5	SMARCA2	DAB1	QX1T	≥6.5
FAM19A2	DDX23	LL1U	≥6.5	SMARCA4	PCDH19	TT6Q	≥6.5
FAM204A	NR3C1	48LU	≥8	SMARCC2	PPM1H	JSF3	≥6.5
FAM210B	EYA2	ZDBB	≥6.5	SMG6	ALKBH5	EZNS	≥6.5
FAM214A	RYR3	63LW	≥8	SMG6	HMGB3P23	EZNS	≥6.5
FAM214A	SLC38A1	63LW	≥8	SMG9	IFT20	0UB7	≥6.5
FAM22B	YWHAE	VK9K	≥8	SMPDL3A	SND1	LL1U	≥8
FAM24B	snoU13	6MN5	≥8	SND1	AKAP7	LL1U	≥6.5
FAM5B	MDM2	NF4Z	≥8	snoU13	C12orf60	Q0QG	≥6.5
FBXL18	ARSB	12C6	≥6.5	snoU13	CUZD1	RW8V	≥6.5
FBXL3	TOP3A	QX1T	≥8	SNRK	RP5-1027O15.1	TT6Q	≥6.5
FBXL7	METTL25	8UBW	≥8	SNRNP48	GPR126	LL1U	≥6.5
FER	KIAA1109	GLXU	≥8	SNRNP3	PES1	G9EG	≥6.5
FGD6	MYO1H	TT6Q	≥8	SNRNP3	PRNP	T56Q	≥6.5
FGFR1OP2P1	PAN3	ZDBB	≥8	SNX13	SOSTDC1	IVPU	≥8
FIGN	EVPL	GLXU	≥6.5	SNX24	RGS13	2CJV	≥6.5
FIS1	BCR	G9EG	≥6.5	SOX2-OT	COL4A2	12C6	≥6.5
FMO1	GOLPH3L	2CJV	≥8	SOX2-OT	LRRK1	SSYE	≥6.5
FMO3	TRHDE	S81X	≥8	SOX3	PAK1	0UB7	≥6.5
FN1	AC114499.1	23V2	≥6.5	SP1	RPS6KA3	6SSR	≥6.5
FOXN3	TELO2	GLXU	≥8	SPAG6	FRS2	LL1U	≥6.5
FRAS1	IGJ	EZNS	≥8	SPARC	H19	91Z1	≥6.5
FRMD6	FAM120A	2SQ0	≥6.5	SPARC	COL1A2	EZNS	≥6.5
FRS2	AC139931.1	8UBW	≥6.5	SPARC	MMP9	YHM7	≥6.5
FRS2	CDK18	8UBW	≥6.5	SPSB4	TM9SF2	WHGE	≥8
FRS2	CPM	8UBW	≥6.5	SRGAP1	HMGAA2	6SSR	≥6.5
FRS2	CDK2	LL1U	≥6.5	SRGAP1	TAC3	LFKM	≥8
FRS2	FAM19A2	LL1U	≥6.5	SRGAP2B	LRAT	ERAH	≥6.5
FRS2	AC131213.1	RZA9	≥6.5	SRPK2	TCF4	12C6	≥8
FRS2	DPYD	W7DB	≥6.5	SS18	SSX1	BV4N	≥8
FRS2	PDE4DIP	2CJV	≥8	SS18	SSX1	L2JM	≥8
FRS2	METTL25	8UBW	≥8	SS18	VPS4B	PC8Y	≥8
FRS2	PRTFDC1	LL1U	≥8	SS18	SSX1	S4JF	≥8
FRS2	SRXN1	LL1U	≥8	SS18	SSX1	V7AX	≥8
FRS2	RP11-620J15.3	TT6Q	≥8	SSH1	LRRC10	TT6Q	≥6.5
FRS2	LRRC8B	W7DB	≥8	SSR1	RP11-127H5.1	T56Q	≥6.5

Continued on next page

Table S4 – continued from previous page

Gene1	Gene2	Sample	Score	Gene1	Gene2	Sample	Score
FRS2	MARCH9	W7DB	≥8	ST8SIA1	KLHDC5	60AP	≥6.5
FRS2	MDM2	W7DB	≥8	ST8SIA1	MBP	PC8Y	≥6.5
GABBR2	PDGFRA	2SQ0	≥8	STAB2	DNM2	TT6Q	≥6.5
GAS2	TSFM	7GAB	≥8	STAT5B	DEAF1	6Z0N	≥6.5
GBP1	NEGR1	EZNS	≥8	STAT6	RAP1B	RW8V	≥6.5
GDAP2	ST7L	VEJN	≥8	STAU1	HS3ST3A1	VEJN	≥6.5
GFM1	SOX2-OT	GLXU	≥8	STK24	DNAJC3	5KJM	≥6.5
GFPT2	TRIO	GLXU	≥8	STK24	DZIP1	5KJM	≥6.5
GINM1	RWDD3	W7DB	≥8	STX6	MARCH9	91Z1	≥6.5
GIT2	TMEM106C	6MN5	≥8	STXBP5	GOPC	T56Q	≥6.5
GIT2	TMEM106C	RW8V	≥8	SVEP1	PPFIA2	TT6Q	≥6.5
GLDC	METTL16	VEJN	≥8	SVEP1	WDR31	TT6Q	≥8
GLG1	MT1F	QX1T	≥8	SVOP	LRRC10	TT6Q	≥6.5
GLG1	MT1X	QX1T	≥8	SVOP	SSH1	TT6Q	≥6.5
GLI1	FANCC	YRZB	≥6.5	SYN3	KLF16	ERAH	≥6.5
GLI1	PTPRQ	JSF3	≥8	SYNE1	DCBLD1	T56Q	≥6.5
GLI1	MKL1	LXSA	≥8	SYT1	CS	LFKM	≥6.5
GLI1	ZFAND5	YRZB	≥8	SYT1	RASSF3	LFKM	≥6.5
GLT25D2	ACACB	NF4Z	≥6.5	SYT1	USP15	7GAB	≥8
GM2AP2	C1orf112	91Z1	≥6.5	SYT1	TMEM19	LFKM	≥8
GNA12	RNASEH2B	M428	≥8	TAMM41	PRICKLE2	GLXU	≥6.5
GNB5	PTPRB	63LW	≥8	TARSL2	FAM169B	PC8Y	≥6.5
GNG12	COL22A1	5KJM	≥6.5	TAX1BP3	RP11-536P6.3	2SQ0	≥6.5
GNS	KRR1	LFKM	≥8	TBC1D15	LGR5	8UBW	≥6.5
GNS	TMEM5	LFKM	≥8	TBC1D15	HOXC5	LFKM	≥6.5
GPC5	DNAJC3	12G6	≥6.5	TBC1D28	KDM2A	0UB7	≥6.5
GRB2	KCNMB4	63LW	≥8	TBC1D5	C1orf81	9C3U	≥6.5
GRIA3	PPFIA2	TT6Q	≥8	TBC1D9	ASTN2	2SQ0	≥6.5
GRIA3	ZNP618	TT6Q	≥8	TBCK	SEC31A	EZNS	≥6.5
GRIP1	ADAM17	TT6Q	≥6.5	TBP	DUSP6	2CJV	≥6.5
GRIP1	MSRB3	8UBW	≥8	TCEA1	SOX17	91Z1	≥6.5
GRIP1	PLCZ1	8UBW	≥8	TCF7L1	ATG2B	2CJV	≥6.5
GRIP1	TMTC2	8UBW	≥8	TDRD12	CSPP1	GLXU	≥6.5
GRIP1	ZDHHC17	8UBW	≥8	TDRD12	PDZRN4	GLXU	≥6.5
GRIP1	PPP1R12A	JSF3	≥8	TENC1	ELK3	RW8V	≥6.5
GRIP1	LRIG3	LFKM	≥8	TERT	TRIO	8UBW	≥8
GRM1	CPSF6	7GAB	≥6.5	TFB1M	MDM2	7GAB	≥6.5
GRM7	LEKR1	9C3U	≥8	TFDP1	RP11-568A7.2	91Z1	≥6.5
GRN	ACTG1	N61A	≥6.5	TFDP1	TMEM217	91Z1	≥8
GS1-410F4.4	ANKHD1	8UBW	≥6.5	TGFB2	TKTL1	GLXU	≥8
GSK3B	MITF	9C3U	≥8	TIMELESS	RBMS2	LFKM	≥6.5
GSK3B	RP11-319G6.1	9C3U	≥8	TK1	RASL11A	9C3U	≥6.5
GSTA1	DNM3	91Z1	≥6.5	TKTL1	RP13-884E18.2	GLXU	≥6.5
GTF2A1	KPNA3	GLXU	≥8	TMEFF2	ANKRD44	JSF3	≥6.5
GTF2I	MPP7	OWEN	≥8	TMEM117	CNOT2	JSF3	≥6.5
GTSF1	AGAP2	HLDX	≥6.5	TMEM117	NELL2	JSF3	≥6.5
GTSF1	TTLL7	HLDX	≥8	TMEM117	DIP2B	LL1U	≥6.5
GXYLT2	RP11-735B13.1	PC8Y	≥8	TMEM19	RPSAP52	FGYL	≥6.5
GYPC	BIN1	91Z1	≥6.5	TMEM194A	GPR182	91Z1	≥6.5

Continued on next page

Table S4 – continued from previous page

Gene1	Gene2	Sample	Score	Gene1	Gene2	Sample	Score
HELB	SCFD1	8UBW	≥8	TMEM194A	ATXN7L3B	LFKM	≥6.5
HLA-DRB6	HLA-DPB1	SSYE	≥6.5	TMEM198B	BEST3	LL1U	≥6.5
HMGA2	SETD1B	2CJV	≥8	TMEM5	RP11-305O6.3	LFKM	≥6.5
HMGA2	IL22	JSF3	≥8	TMEM56	RP11-620J15.1	W7DB	≥6.5
HMGA2	TRHDE	JSF3	≥8	TMEM80	STAT5B	6Z0N	≥6.5
HMGA2	ZDHHC17	LFKM	≥8	TMEM87A	HOXC5	63LW	≥6.5
HMGA2	KERA	LL1U	≥8	TMLHE	MED12	CZN2	≥6.5
HMGA2	RP11-13A1.3	NF4Z	≥8	TMOD3	ZNF808	63LW	≥8
HMGA2	RP1-34H18.1	RW8V	≥8	TMTC2	RP11-268G12.1	6SSR	≥6.5
HMGB1P36	FOXP1	PC8Y	≥6.5	TMTC2	LRFN5	8UBW	≥6.5
HNRNPU	AL592494.5	YHM7	≥6.5	TMTC2	PDE4DIP	JSF3	≥6.5
HOXC4	C12orf54	RW8V	≥6.5	TMTC2	METTL25	NTAT	≥6.5
HOXC5	C12orf54	RW8V	≥6.5	TMTC2	ELMO1	T56Q	≥6.5
HOXC5	NABP2	LFKM	≥8	TNFSF12	RBFOX3	OWEN	≥6.5
HOXC5	NACA	LFKM	≥8	TNMD	UBE3B	TT6Q	≥8
HSPB8	RPH3A	NF4Z	≥8	TNNT1	SRRM2	EU4K	≥6.5
HYDIN	NTNG1	W7DB	≥8	TNR	MDM2	91Z1	≥6.5
ICT1	KCTD2	LL1U	≥8	TNRC18	MICALL2	M428	≥6.5
IDS	ODZ3	JSF3	≥8	TNRC6C	RP11-136F16.1	63LW	≥6.5
IFI16	RP11-335O4.1	HLDX	≥8	TNS1	CXCR2	KWB3	≥6.5
IFNG-AS1	C12orf28	NTAT	≥6.5	TOR1AIP2	UNC13C	PC8Y	≥8
IFNG-AS1	RP11-620J15.3	LFKM	≥8	TPH2	TMTC2	6MN5	≥6.5
IFNGR1	SLC35E3	91Z1	≥8	TPH2	CR381670.1	JSF3	≥6.5
IGF2	COL1A2	6MN5	≥6.5	TPH2	ERBB4	JSF3	≥6.5
IGF2R	OS9	W7DB	≥8	TPH2	OSBPL8	JSF3	≥6.5
IGLL5	IGLV4-69	CHZ6	≥8	TPH2	PPP1R12A	JSF3	≥6.5
IKZF2	IFNG-AS1	JSF3	≥6.5	TPH2	RP11-54A9.1	JSF3	≥6.5
IL26	ITGB1	JSF3	≥8	TPH2	TMTC2	JSF3	≥6.5
ILF3	ZNF560	Q0QG	≥8	TPH2	FRS2	LL1U	≥6.5
IRAK3	DNM3	S81X	≥6.5	TPH2	SCAF11	LL1U	≥6.5
IRAK3	METTL21B	FGYL	≥8	TPH2	HMGA2	NTAT	≥6.5
IRAK4	PPHLN1	6MN5	≥8	TPH2	NBPF11	W7DB	≥6.5
IRAK4	RP11-230G5.2	JSF3	≥8	TPH2	NBPF12	W7DB	≥6.5
ISM1	ZEB1	YHM7	≥8	TPH2	VTI1A	6MN5	≥8
ITGA5	PRKACB	HLDX	≥8	TPH2	VTI1A	RW8V	≥8
ITGA5	TRHDE	LFKM	≥8	TPM1	CHRDL2	9C3U	≥6.5
ITGAE	NCOR1	60AP	≥8	TPM1	MGP	9C3U	≥6.5
ITPR2	CAPRIN2	Q0QG	≥6.5	TPM2	MYL2	EU4K	≥6.5
JAKMIP2	TNIP1	WHGE	≥8	TPM2	TPM1	KWB3	≥6.5
JAZF1	SUZ12	72GV	≥8	TPM2	KRT17	LXSA	≥6.5
KATNA1	MDM2	T56Q	≥8	TPM2	TPM4	KWB3	≥8
KCNC2	LGR5	T56Q	≥8	TRAPPC12	ELK3	TT6Q	≥6.5
KCNH1	CDK18	8UBW	≥6.5	TRAPPC8	RP11-386P4.1	PC8Y	≥6.5
KCNIP4	ALB	6Z0N	≥6.5	TRAPPC9	KNTC1	12C6	≥6.5
KCNIP4	FAM13A	EZNS	≥6.5	TRAPPC9	COL22A1	6MN5	≥6.5
KCNIP4	SCARB2	EZNS	≥8	TRAV41	NCKAP1	8UBW	≥6.5
KCNJ12	DPM1	VEJN	≥6.5	TRHDE	FRS2	63LW	≥6.5
KCNMA1	RAD9B	2CJV	≥8	TRHDE	RP11-171L9.1	63LW	≥6.5
KCNMA1	YWHAE	VK9K	≥8	TRHDE	SP1	6MN5	≥6.5

Continued on next page

Table S4 – continued from previous page

Gene1	Gene2	Sample	Score	Gene1	Gene2	Sample	Score
KCNMB4	COCH	8UBW	≥6.5	TRHDE	CPM	HLDX	≥6.5
KCNMB4	MDM2	91Z1	≥8	TRHDE	RP11-	JSF3	≥6.5
					498M15.1		
KCNMB4	MSRB3	JSF3	≥8	TRHDE	RP11-956E11.1	JSF3	≥6.5
KCNMB4	ZDHHC17	JSF3	≥8	TRHDE	SP1	RW8V	≥6.5
KCTD1	AKAP10	VEJN	≥6.5	TRHDE	RP11-366L20.4	W7DB	≥6.5
KDM1B	EYS	WHGE	≥6.5	TRHDE	YEATS4	S81X	≥8
KDM4C	RP11-536O18.1	EU4K	≥8	TRIM65	WBP2	W6TV	≥8
KIAA0146	RPL39L	GLXU	≥8	TRPC4	TSC22D1	0UB7	≥8
KIAA0355	CCDC59	8UBW	≥6.5	TRPM3	FAM122A	T56Q	≥6.5
KIAA0895	IFI6	RZA9	≥6.5	TSFM	NELL2	7GAB	≥6.5
KIAA0947	CTDSP2	5TGD	≥6.5	TSFM	NUP210L	PC8Y	≥6.5
KIAA1109	SMPD4	GLXU	≥8	TSFM	VDR	6MN5	≥8
KIAA1191	NEURL1B	M428	≥8	TSFM	VDR	RW8V	≥8
KIAA1199	C20orf196	Q0QG	≥6.5	TSPAN31	BBS10	6SSR	≥6.5
KIAA1211	CLOCK	EZNS	≥6.5	TSPAN31	SNORA40	91Z1	≥6.5
KIAA1324L	DNAJC2	2SQ0	≥6.5	TSPAN8	OR10AD1	JSF3	≥6.5
KIAA1586	PRIM2	8UBW	≥8	TSPAN8	PTPRQ	LFKM	≥6.5
KIAA1715	BAZ2B	V7AX	≥6.5	TSPAN8	RP11-81H14.2	NTAT	≥6.5
KIAA1919	SASH1	91Z1	≥8	TTC39B	CREB5	EU4K	≥6.5
KIAA2026	UBBP4	VEJN	≥8	TUFT1	C12orf55	FGYL	≥6.5
KIF13A	MFSD12	UYD8	≥8	TULP4	PTN	LL1U	≥6.5
KIF5A	RP1-34H18.1	RW8V	≥8	TXND11	RP11-77K12.1	NTAT	≥6.5
KIF5A	TMRSS12	RW8V	≥8	U6	SEC23IP	0UB7	≥6.5
KIFAP3	NEDD1	FGYL	≥8	U6	PDE7B	7GAB	≥6.5
KITLG	FRS2	2CJV	≥6.5	U6	IQSEC3	8UBW	≥6.5
KLF11	CHPT1	TT6Q	≥6.5	U6	TMEM194A	91Z1	≥6.5
KLHL22	FBLN1	S81X	≥6.5	U6	GJB6	9C3U	≥6.5
KNDC1	MYB	W7DB	≥8	UAP1	DDR2	S81X	≥6.5
KPNA1	GTPBP8	WHGE	≥6.5	UBB	UBC	60AP	≥8
KRR1	RP11-101K23.1	6MN5	≥8	UBE2G1	DOK5	VEJN	≥6.5
KRT86	PPHLN1	HLDX	≥8	UBN2	SNORA48	2SQ0	≥6.5
LAMA4	TRAF3IP2	91Z1	≥8	UBXN7	RNA5SP231	9C3U	≥6.5
LCORL	SLC2A9	ZDBB	≥8	UNC5D	SNTG1	BV4N	≥6.5
LCT	GYPC	91Z1	≥6.5	URI1	BSPRY	TT6Q	≥6.5
LDHAL6CP	KRR1	LFKM	≥6.5	USP42	AC006465.3	BV4N	≥6.5
LDLR	RP11-110A12.2	RZA9	≥8	USP44	EPYC	RW8V	≥6.5
LGALS3BP	PUS7	2SF3	≥8	USP45	ANKRD32	91Z1	≥6.5
LGR4	MDK	LXSA	≥8	USP6	AIG1	5KJM	≥6.5
LGR5	ACSS3	8UBW	≥6.5	UST	R3HDM2	NTAT	≥6.5
LGR5	PTPRR	RZA9	≥8	UTP20	NUP107	TT6Q	≥6.5
LIFR	PRSS12	GLXU	≥8	UTP6	ZNF521	VEJN	≥8
LIN52	M6PR	63LW	≥8	VAV3	GBP1P1	W7DB	≥6.5
LIN7A	ARID2	5TGD	≥6.5	VCP	TMEM206	2SQ0	≥6.5
LINC00478	AP000470.2	EZNS	≥6.5	VDR	RP11-221N13.4	6MN5	≥6.5
LINC00478	AP000477.3	EZNS	≥6.5	VPS35	KPNA7	UMND	≥6.5
LINC00670	STX8	GQPU	≥8	VPS41	DPP10	JSF3	≥6.5
LL22NC03-80A10.6	CABIN1	G9EG	≥6.5	VPS8	TCF20	12C6	≥6.5

Continued on next page

Table S4 – continued from previous page

Gene1	Gene2	Sample	Score	Gene1	Gene2	Sample	Score
LL22NC03-80A10.6	MICALL1	G9EG	≥8	VPS8	GM2AP1	9C3U	≥6.5
LMTK2	PUS7	G9EG	≥8	VWC2	KCNMB4	JSF3	≥6.5
LPAR6	NALCN	CZN2	≥8	WASH3P	TPT1-AS1	LXSA	≥6.5
LPHN1	FXR2	QX1T	≥6.5	WIF1	FRS2	8UBW	≥6.5
LRBA	DLEU2	QX1T	≥6.5	WNT10B	ATP10A	63LW	≥6.5
LRCH1	KIAA1704	EC1C	≥6.5	WRAP53	GTF2A1	GLXU	≥6.5
LRFN5	FRS2	8UBW	≥6.5	WSB1	RP11-131K5.1	QX1T	≥6.5
LRFN5	HMGA2	8UBW	≥6.5	XIRP2	NAP1L1	6SSR	≥6.5
LRIG3	BCL11B	NTAT	≥6.5	XRCC5	FTX	GLXU	≥6.5
LRP1	CCDC59	JSF3	≥6.5	XRCC6BP1	PPHLN1	HLDX	≥6.5
LRP1	SLC16A7	LFKM	≥8	XRCC6BP1	RASSF3	LFKM	≥6.5
LRP1	SLC11A2	RW8V	≥8	XRCC6BP1	FRS2	TT6Q	≥6.5
LRP1	RAB3IP	RZA9	≥8	XRN1	RP11-167H9.4	T56Q	≥6.5
LRP4	CKAP5	WHGE	≥6.5	Y_RNA	MARCH6	12C6	≥6.5
LRP8	MAGOH	CHZ6	≥8	Y_RNA	RAB21	W7DB	≥6.5
LRRC37A2	KANSL1	1T2G	≥6.5	YEATS2	IL17RD	9C3U	≥6.5
LRRC37A2	KANSL1	S4JF	≥6.5	YEATS4	RP11-654D12.2	LL1U	≥6.5
LRRC48	NCOR1	60AP	≥8	YLPM1	ZFYVE26	JSF3	≥8
LRRC48	RP5-947P14.1	60AP	≥8	YWHAE	CRK	LXSA	≥6.5
LRRC8C	RAP1B	W7DB	≥8	YWHAH	YEATS4	LL1U	≥6.5
LRRC8C	RP11-362K2.2	W7DB	≥8	YWHAZP2	HHAT	JSF3	≥6.5
LRRC8D	SUCO	W7DB	≥8	ZBBX	SDHAP2	G9EG	≥6.5
LTBP4	SAE1	Q0QG	≥8	ZBTB24	ZBTB49	LL1U	≥8
IVRN	KDM2B	2CJV	≥6.5	ZCCHC11	AC092661.1	BV4N	≥6.5
IVRN	RP11-324P9.1	2CJV	≥8	ZCWPW2	BSDC1	PC8Y	≥6.5
LYZ	TMTC2	6SSR	≥8	ZFC3H1	TSPAN8	JSF3	≥6.5
LYZ	OTOGL	LFKM	≥8	ZFC3H1	RP11-1038A11.3	PC8Y	≥6.5
LYZ	NSUN6	LL1U	≥8	ZFP64	RP11-372K20.1	9C3U	≥6.5
MACF1	PLA2G2A	VK9K	≥8	ZFP64	NF1	VEJN	≥6.5
MACROD2	GABARAPL1	Q0QG	≥6.5	ZFP64	SUZ12	VEJN	≥6.5
MAFIPL	ESCO1	PC8Y	≥6.5	ZFX	SMS	6SSR	≥6.5
MAGT1	AC093901.1	GLXU	≥6.5	ZHX3	TOP1	ZDBB	≥6.5
MAGT1	CPA6	GLXU	≥6.5	ZMAT5	IGLV3-21	G9EG	≥6.5
MAPKBP1	SLC25A13	48LU	≥8	ZMYND11	SOX5	YHM7	≥6.5
MARCH11	SCARA3	NTAT	≥8	ZNF146	MYBPC1	TT6Q	≥6.5
MARS	CELSR2	JSF3	≥6.5	ZNF18	ZNF333	TT6Q	≥8
MARS	CTD-2526M8.2	PC8Y	≥6.5	ZNF277	EGFR	12C6	≥6.5
MARS	PMEL	LFKM	≥8	ZNF280D	NTRK3	PC8Y	≥6.5
MATN2	HMGA2	1T2G	≥6.5	ZNF333	RPL21P122	TT6Q	≥6.5
MBIP	RP11-149A7.2	2SQ0	≥8	ZNF345	RAI14	8UBW	≥6.5
MBTD1	AL845154.2	VEJN	≥6.5	ZNF407	ZNF516	PC8Y	≥8
MCPH1	VWA8	LVPU	≥8	ZNF430	YEATS4	RZA9	≥6.5
MDM1	MSRB3	8UBW	≥8	ZNF44	BET1L	Q0QG	≥6.5
MDM1	MED21	JSF3	≥8	ZNF551	RP11-492M23.2	JSF3	≥6.5
MDM2	CDK17	NTAT	≥6.5	ZNF585A	SMARCA4	QIEE	≥6.5
MDM2	PTPRD	8UBW	≥8	ZNF736	VKORC1L1	12C6	≥6.5

Continued on next page

Table S4 – continued from previous page

Gene1	Gene2	Sample	Score	Gene1	Gene2	Sample	Score
MDM2	PIP4K2C	JSF3	≥8	ZNF775	SCAF11	LL1U	≥6.5
MDM2	SNX9	W7DB	≥8	ZNF800	FAM19A2	LL1U	≥6.5
MERTK	KIFAP3	JSF3	≥6.5	ZNF800	FRS2	LL1U	≥6.5
METAP2	RP11-1105G2.3	RW8V	≥8	ZRANB3	IFI6	GQPU	≥6.5
				ZRANB3	IFI6	S4JF	≥6.5

Note: The order of fusion partner 5' and 3' is ignored to simplify comparison.

Table S5: Fusions identified in 84 prostate cancer samples (n=371, score ≥ 6.5).

Gene1	Gene2	Sample	Score	Gene1	Gene2	Sample	Score
AC018816.4	AC018816.3	PCA035	≥ 6.5	RP4-673D20.3	MYH9	PCA062	≥ 6.5
AKT3	ADSS	PCA030	≥ 8	RPL11	DOCK7	PCA069	≥ 6.5
ATP8A2P1	ATP8A2	PCA190	≥ 6.5	RPL13P5	POLR3B	PCA138	≥ 6.5
AXL	ACPP	PCA198	≥ 8	RPL14	EP400	PCA037	≥ 6.5
BCHE	ADAMTS9	PCA158	≥ 8	RPL14	EP400	PCA069	≥ 6.5
C7orf63	AC002127.4	PCA188	≥ 8	RPL14	ATN1	PCA070	≥ 6.5
CALR	AFF1	PCA034	≥ 6.5	RPL14	EP400	PCA090	≥ 6.5
CCDC141	AC009478.1	PCA035	≥ 6.5	RPL14	ATN1	PCA094	≥ 6.5
CDC27	ATRN1L	PCA127	≥ 6.5	RPL14	EP400	PCA106	≥ 6.5
COPA	CCDC19	PCA099	≥ 6.5	RPL14	MED15	PCA106	≥ 6.5
CRTAP	AC008069.1	PCA027	≥ 6.5	RPL14	MIR205HG	PCA106	≥ 6.5
CTD-	CCAR1	PCA062	≥ 6.5	RPL14	EP400	PCA111	≥ 6.5
2545G14.2							
DHRS7	ALOX15B	PCA071	≥ 6.5	RPN2	BPI	PCA025	≥ 8
DIS3L2	AC073263.1	PCA192	≥ 6.5	RPS24	PPIB	PCA030	≥ 6.5
DKK2	AC079949.1	PCA125	≥ 6.5	RRBP1	PTPN2	PCA112	≥ 6.5
DLG2	CAPRIN1	PCA158	≥ 8	RYBP	DTNBP1	PCA116	≥ 6.5
DNAJC11	AC017080.1	PCA021	≥ 6.5	SCG2	CTNNB1	PCA084	≥ 6.5
EEF1DP3	ATF7IP	PCA025	≥ 6.5	SEH1L	RRBP1	PCA112	≥ 8
EMC10	ABCC10	PCA021	≥ 6.5	SEMA6D	AP000487.5	PCA030	≥ 6.5
EML5	AP000525.8	PCA043	≥ 8	SERPINI1	NAT10	PCA158	≥ 8
ENO2	DHRS13	PCA138	≥ 8	SETD5	RAD18	PCA116	≥ 6.5
EPC2	DNAJC11	PCA021	≥ 6.5	SFPQ	RP5-965F6.2	PCA059	≥ 6.5
ERG	AC125238.3	PCA014	≥ 6.5	SGMS1	RPAIN	PCA062	≥ 8
ERG	CHD2	PCA061	≥ 6.5	SHANK2	SEMA6D	PCA030	≥ 8
ERLIN2	ADAM5	PCA196	≥ 8	SHQ1	FOXP1	PCA015	≥ 8
ETV1	AGR2	PCA112	≥ 8	SHROOM3	NOX5	PCA184	≥ 6.5
ETV4	C1orf116	PCA168	≥ 8	SKIL	SDCCAG8	PCA030	≥ 8
EXOSC9	DOCK9	PCA044	≥ 6.5	SKIL	ACPP	PCA100	≥ 8
FAM105A	CDH18	PCA044	≥ 6.5	SLC12A2	KIAA0040	PCA035	≥ 6.5
FAM135A	DDX43	PCA041	≥ 8	SLC22A23	EIF3J	PCA148	≥ 8
FAM160A1	DAGLB	PCA198	≥ 6.5	SLC25A6	FLJ37644	PCA070	≥ 6.5
FAM81A	COPS2	PCA031	≥ 8	SLC25A6	SFN	PCA070	≥ 6.5
FBXO3	AC091493.1	PCA158	≥ 6.5	SLC38A2	NLRP11	PCA016	≥ 6.5
FBXO38	C5orf62	PCA030	≥ 8	SLC45A3	ERG	PCA028	≥ 8
FGD5	EPM2AIP1	PCA158	≥ 6.5	SLC45A3	SKIL	PCA030	≥ 8
FMN2	ADH5	PCA125	≥ 6.5	SLC45A3	ERG	PCA099	≥ 8
FNDC3B	COMMD8	PCA196	≥ 8	SLC8A1-AS1	AC008280.5	PCA192	≥ 8
FOLH1	CUL5	PCA039	≥ 6.5	SLCO5A1	RNA28S5	PCA027	≥ 6.5
FOXJ3	ACPP	PCA198	≥ 8	SLCO5A1	RNA28S5	PCA035	≥ 6.5
FOXN3	AP000525.8	PCA027	≥ 8	SLCO5A1	RNA28S5	PCA057	≥ 6.5
FUT8	DFFA	PCA025	≥ 6.5	SLCO5A1	RYR2	PCA057	≥ 6.5
GOLPH3	C1QTNF3	PCA024	≥ 6.5	SLCO5A1	RNA28S5	PCA058	≥ 6.5
GPM6A	CKAP4	PCA195	≥ 6.5	SLCO5A1	RNA28S5	PCA059	≥ 6.5
GRAMD3	CTC-278L1.1	PCA192	≥ 6.5	SLCO5A1	RNA28S5	PCA060	≥ 6.5
GREB1L	ESCO2	PCA060	≥ 8	SMAD7	EPM2A	PCA035	≥ 8
HFM1	DKK2	PCA058	≥ 6.5	SMAD7	SMAD2	PCA035	≥ 6.5
HIGD1B	ERBB2	PCA192	≥ 8	SMEK1	EML5	PCA043	≥ 8

Continued on next page

Table S5 – continued from previous page

Gene1	Gene2	Sample	Score	Gene1	Gene2	Sample	Score
HIP1R	GDF15	PCA033	≥8	SMG1P1	EMILIN2	PCA158	≥6.5
HLA-K	HLA-A	PCA056	≥6.5	SNRPN	KLF13	PCA045	≥6.5
HNRPLL	ABCC4	PCA116	≥6.5	SOCS5	EIF2AK3	PCA192	≥6.5
hsa-mir-3187	LSM7	PCA057	≥8	SORBS2	MOB1B	PCA184	≥6.5
HTR7	CLK1	PCA030	≥8	SPDEF	ERCC1	PCA031	≥6.5
HTRA4	C8orf42	PCA196	≥8	SPON2	ENOX1	PCA025	≥6.5
IGHGP	IGHG3	PCA099	≥6.5	SPON2	AC027612.3	PCA030	≥6.5
IGHGP	IGHG4	PCA106	≥6.5	SQRDL	ERG	PCA059	≥8
IL6	ARPC4-TTLL3	PCA125	≥6.5	SRBD1	DHX57	PCA192	≥8
IL6ST	ADAMTSL1	PCA041	≥8	SREBF1	ASGR2	PCA198	≥8
ILF2	DYM	PCA057	≥8	SRRM2	CALD1	PCA045	≥6.5
INPP5A	CTC-512J12.6	PCA027	≥6.5	SRRM2	NCL	PCA045	≥6.5
IQSEC1	CLASP2	PCA161	≥6.5	SRRM2	NEFH	PCA059	≥6.5
ITCH	BCAS4	PCA042	≥6.5	SRRM2	PTMS	PCA072	≥6.5
JMJD1C	C10orf107	PCA024	≥6.5	SRRM2	ACIN1	PCA110	≥6.5
JMJD7-	GALK2	PCA031	≥8	STAMBPP	PDE11A	PCA192	≥8
PLA2G4B							
KCNU1	DDHD2	PCA196	≥8	STARD9	MPP5	PCA025	≥6.5
KLK3	KLK2	PCA015	≥8	STAU1	DMGDH	PCA030	≥8
KLK3	KLK2	PCA027	≥8	STX10	AC139099.4	PCA037	≥6.5
KLK3	KLK2	PCA030	≥6.5	STX17	APBA2	PCA041	≥6.5
KLK3	KLK2	PCA035	≥8	SUFU	MINPP1	PCA035	≥8
KLK3	KLK2	PCA037	≥6.5	SUGP1	FAM124A	PCA037	≥8
KLK3	KLK2	PCA038	≥6.5	SUSD1	RPL26	PCA084	≥6.5
KLK3	KLK2	PCA044	≥8	SUZ12	CALR	PCA116	≥6.5
KLK3	KLK2	PCA045	≥8	TACC1	FRY	PCA043	≥8
KLK3	KLK2	PCA056	≥8	TAGAP	SNX9	PCA072	≥8
KLK3	KLK2	PCA059	≥8	TBC1D14	BCAS3	PCA033	≥6.5
KLK3	KLK2	PCA061	≥6.5	TERF2IP	PSMD11	PCA049	≥8
KLK3	KLK2	PCA064	≥6.5	TFAP2A	CPNE4	PCA037	≥8
KLK3	KLK2	PCA069	≥6.5	TFG	GPR128	PCA049	≥8
KLK3	KLK2	PCA070	≥8	TGS1	LYN	PCA026	≥8
KLK3	KLK2	PCA071	≥8	THADA	POLR1A	PCA192	≥8
KLK3	KLK2	PCA090	≥8	THADA	SRBD1	PCA192	≥8
KLK3	KLK2	PCA091	≥8	THNSL2	FBLN1	PCA116	≥6.5
KLK3	KLK2	PCA092	≥6.5	TIMP3	EXOC6B	PCA188	≥6.5
KLK3	KLK2	PCA094	≥8	TLK2	PRKCA	PCA041	≥6.5
KLK3	KLK2	PCA096	≥8	TMBIM6	MSMB	PCA059	≥6.5
KLK3	KLK2	PCA106	≥6.5	TMC6	RELA	PCA026	≥8
KLK3	KLK2	PCA110	≥8	TMEFF2	TMC1	PCA043	≥8
KLK3	KLK2	PCA111	≥8	TMEM181	PLEKHS1	PCA161	≥8
KLK3	KLK2	PCA144	≥8	TMEM232	NDST1	PCA146	≥8
KLK3	KLK2	PCA146	≥6.5	TMEM241	DOK6	PCA190	≥8
KLK3	KLK2	PCA168	≥8	TMEM59	TCF12	PCA184	≥6.5
KLK4	KLK3	PCA031	≥6.5	TMEM91	ATP5SL	PCA198	≥8
KLK4	KLK3	PCA062	≥6.5	TMPO	C10orf11	PCA021	≥8
KLK4	KLK3	PCA098	≥6.5	TMPRSS2	ERG	PCA015	≥8
LCP1	ERG	PCA144	≥6.5	TMPRSS2	ERG	PCA016	≥6.5
LDLR	CLPTM1	PCA168	≥6.5	TMPRSS2	ERG	PCA024	≥8

Continued on next page

Table S5 – continued from previous page

Gene1	Gene2	Sample	Score	Gene1	Gene2	Sample	Score
LPP	KNG1	PCA057	≥8	TMPRSS2	ERG	PCA025	≥8
LRRK2	KIF21A	PCA192	≥8	TMPRSS2	ERG	PCA026	≥8
LSM1	ERICH1-AS1	PCA196	≥8	TMPRSS2	ERG	PCA027	≥8
LYRM5	CCDC91	PCA148	≥8	TMPRSS2	ERG	PCA028	≥8
MAGI1	KIRREL3	PCA037	≥8	TMPRSS2	ERG	PCA031	≥8
MAGI1	FHIT	PCA041	≥8	TMPRSS2	ERG	PCA035	≥8
MAST2	IPP	PCA109	≥8	TMPRSS2	ERG	PCA037	≥8
MBOAT7	CWH43	PCA031	≥8	TMPRSS2	ERG	PCA038	≥8
MBOAT7	ITPR2	PCA031	≥8	TMPRSS2	NEDD4L	PCA038	≥6.5
Metazoa_SRP	FAM54B	PCA198	≥6.5	TMPRSS2	ERG	PCA039	≥8
MLLT4	ERG	PCA015	≥6.5	TMPRSS2	ERG	PCA043	≥8
MOB3B	CAAP1	PCA158	≥6.5	TMPRSS2	ERG	PCA049	≥8
MOBP	HMGN2P46	PCA196	≥6.5	TMPRSS2	ERG	PCA056	≥8
MSLN	DNAH9	PCA192	≥6.5	TMPRSS2	TMEM87B	PCA056	≥8
MSMB	KIAA1324	PCA059	≥6.5	TMPRSS2	IFNGR2	PCA057	≥8
MT-ND5	MT-CO3	PCA043	≥6.5	TMPRSS2	ERG	PCA059	≥8
MYH9	FOXRED2	PCA159	≥6.5	TMPRSS2	ERG	PCA061	≥8
MYO18A	CAMKK1	PCA198	≥8	TMPRSS2	ERG	PCA062	≥8
NCOA2	LACTB2	PCA198	≥8	TMPRSS2	ERG	PCA069	≥8
NCOA3	JPH2	PCA042	≥8	TMPRSS2	ERG	PCA070	≥8
NDC80	C2orf74	PCA034	≥6.5	TMPRSS2	ERG	PCA084	≥8
NDC80	C2orf74	PCA156	≥6.5	TMPRSS2	ERG	PCA093	≥8
NDRG1	ERG	PCA057	≥8	TMPRSS2	ERG	PCA096	≥8
NDUFAF6	CTB-89H12.4	PCA043	≥6.5	TMPRSS2	ERG	PCA098	≥8
NEK11	IPO8	PCA035	≥6.5	TMPRSS2	ERG	PCA106	≥8
NEK11	MBNL1	PCA035	≥8	TMPRSS2	ERG	PCA111	≥8
NF1	AF127577.11	PCA049	≥6.5	TMPRSS2	ERG	PCA116	≥8
NKX3-1	ATE1	PCA021	≥6.5	TMPRSS2	ERG	PCA124	≥8
NME5	NCKAP1	PCA198	≥8	TMPRSS2	ERG	PCA138	≥8
NPC1L1	LIMCH1	PCA042	≥6.5	TMPRSS2	SLC37A1	PCA138	≥8
NPEPPS	NBR1	PCA098	≥8	TMPRSS2	ERG	PCA155	≥8
NPM1	DBN1	PCA037	≥6.5	TMPRSS2	ERG	PCA156	≥8
NR2F6	FCER2	PCA190	≥6.5	TMPRSS2	ERG	PCA159	≥8
NRAS	CNN3	PCA072	≥6.5	TMPRSS2	ERG	PCA161	≥8
NRIP1	NF1	PCA049	≥8	TMPRSS2	ERG	PCA187	≥8
NTM	EIF3M	PCA158	≥8	TMPRSS2	ERG	PCA190	≥8
OMG	NRIP1	PCA049	≥8	TMPRSS2	CLN6	PCA196	≥8
OR4B1	NUP98	PCA113	≥6.5	TMPRSS2	LNX1	PCA196	≥8
PAPOLG	MTA3	PCA192	≥8	TP53	LCN15	PCA113	≥8
PARD3	KIAA1704	PCA027	≥8	TPD52	RP11-48B3.2	PCA198	≥8
PAXIP1	KIAA1549	PCA162	≥6.5	TRAPP10	MYO18B	PCA188	≥8
PDE11A	LRPPRC	PCA192	≥6.5	TRIOBP	ERG	PCA170	≥8
PDIA4	MATN2	PCA034	≥6.5	TXNL1	STARD6	PCA146	≥8
PDZD9	DGKD	PCA043	≥6.5	U6	RBM47	PCA030	≥6.5
PIK3C3	LIPG	PCA021	≥6.5	UBA52	CDKN2B-AS1	PCA039	≥6.5
PLA2G2A	KLK3	PCA045	≥6.5	UBA52	CDKN2B-AS1	PCA109	≥6.5
POLR3B	ING4	PCA138	≥8	UBE2E2	FOXP1	PCA155	≥6.5
POU2F1	DPYD	PCA041	≥8	UBE2E3	PAPOLG	PCA192	≥6.5
POU2F2	ATAD2B	PCA041	≥8	UBP1	STAG1	PCA037	≥8

Continued on next page

Table S5 – continued from previous page

Gene1	Gene2	Sample	Score	Gene1	Gene2	Sample	Score
PPAP2A	MIPEP	PCA064	≥6.5	UGDH	KIF21A	PCA158	≥8
PPAP2A	PDS5B	PCA161	≥6.5	UNC45B	HFM1	PCA043	≥6.5
PPAP2A	FLI1	PCA196	≥8	UNC45B	RPL37A	PCA057	≥6.5
PRIM2	EFHC1	PCA090	≥6.5	UNC45B	HFM1	PCA058	≥6.5
PRIM2	EFHC1	PCA100	≥6.5	UNC45B	ATP4A	PCA084	≥6.5
PRIM2	EFHC1	PCA109	≥6.5	UNC5CL	AFF3	PCA111	≥8
PRIM2	EFHC1	PCA134	≥6.5	USH2A	ETV1	PCA192	≥6.5
PRIM2	EFHC1	PCA139	≥6.5	USP34	COMMD1	PCA159	≥8
PRIM2	EFHC1	PCA144	≥6.5	USP43	SS18	PCA190	≥8
PRKCA	DDX42	PCA084	≥6.5	VDAC3	B3GALTL	PCA138	≥8
PRKCE	NUP205	PCA155	≥6.5	VDAC3	NBN	PCA195	≥8
PRKCH	ERG	PCA070	≥6.5	VEZF1	RPL14	PCA098	≥6.5
PSD3	DAB1	PCA037	≥6.5	WDR90	TMCO7	PCA196	≥6.5
PSD3	ABHD2	PCA161	≥8	WIZ	VPS8	PCA025	≥6.5
PSMB3	GAS7	PCA037	≥6.5	WRAP53	HGS	PCA061	≥6.5
PTEN	MINPP1	PCA035	≥8	WSCD1	TRUB1	PCA015	≥8
PTN	MTHFD1L	PCA030	≥6.5	WWOX	USP34	PCA059	≥8
PTRH2	GATA6	PCA037	≥8	XBP1	TAGLN	PCA060	≥6.5
R3HCC1	PDZRN3	PCA134	≥6.5	XPO7	M6PR	PCA030	≥8
RAB27B	FAM105B	PCA188	≥6.5	YPEL1	RHBDL1	PCA192	≥8
RAB4A	ETV4	PCA110	≥8	Y_RNA	ROGDI	PCA158	≥6.5
RAF1	FHIT	PCA184	≥8	Y_RNA	HMGN2P46	PCA188	≥6.5
RALGAPA2	NKX2-2	PCA031	≥6.5	ZC3H13	FAM48A	PCA144	≥8
RALGAPA2	FHIT	PCA041	≥8	ZDHHC20P1	NPLOC4	PCA112	≥6.5
RAPGEF4	DIS3L2	PCA192	≥6.5	ZDHHC7	ADAMTS18	PCA015	≥6.5
RBL1	C20orf132	PCA138	≥8	ZFHX3	TMPRSS2	PCA138	≥8
RBM27	APBA2	PCA041	≥8	ZFP36	IGKJ5	PCA106	≥6.5
RNA5SP347	IFI6	PCA196	≥6.5	ZFP64	SFXN1	PCA112	≥6.5
RNF13	COLQ	PCA158	≥8	ZMIZ1	CCDC28A	PCA118	≥6.5
RNF170	PARD3	PCA098	≥6.5	ZMIZ1	CCDC28A	PCA196	≥6.5
RNF43	MTMR4	PCA098	≥6.5	ZNF24	CD226	PCA112	≥8
RP11-174O3.1	PTOV1	PCA038	≥8	ZNF292	RP1-263J7.2	PCA192	≥6.5
RP11-174O3.1	PTOV1	PCA069	≥6.5	ZNF292	RP11-532N4.2	PCA198	≥6.5
RP11-19O2.4	GPATCH8	PCA044	≥6.5	ZNF473	TBX3	PCA030	≥6.5
RP11-20I23.3	RAE1	PCA031	≥6.5	ZNF503	ADK	PCA025	≥6.5
RP11-416L21.1	EML4	PCA196	≥6.5	ZNF652	RBM3	PCA111	≥6.5
RP11-417J1.1	ODC1	PCA146	≥6.5	ZNF677	NLRP4	PCA190	≥8
RP11-480D4.3	ODC1	PCA146	≥6.5	ZNF717	GSK3B	PCA158	≥6.5
RP11-505K9.4	ACAA2	PCA138	≥8	ZNF737	RP11-508M1.3	PCA127	≥6.5
RP11-505K9.4	CEP164	PCA138	≥8	ZNF737	DACT3	PCA190	≥8
RP11-617D20.1	PANK1	PCA112	≥6.5	ZP3	HSPA1B	PCA170	≥6.5
RP11-902B17.1	LIFR	PCA158	≥6.5				

Note: The order of fusion partner 5' and 3' is ignored to simplify comparison.

Table S6: Fusions identified in 48 GBM samples (n=470, score ≥ 6.5).

Gene1	Gene2	Sample	Score	Gene1	Gene2	Sample	Score
AF146191.4	ADCY8	AK053r	≥ 6.5	RP11-141O11.2	CTC-340D7.1	AK203r	≥ 6.5
AGAP2	ACACA	AK100r	≥ 6.5	RP11-152F13.8	GOLGA6B	AK051r	≥ 6.5
APP	ABCC4	XEMY	≥ 8	RP11-159D12.5	EFCAB13	U676	≥ 6.5
ARMCX4	AP3B1	7EN2	≥ 6.5	RP11-166D19.1	FGF3	AK173r	≥ 6.5
ARMCX4	AP3B1	AK100r	≥ 6.5	RP11-204C23.1	RAF1	AK124r	≥ 6.5
AUTS2	AC011288.2	JGR2	≥ 8	RP11-22B23.2	CHD4	AK199r	≥ 6.5
C9orf11	APTX	LEZR	≥ 8	RP11-272B17.2	LRIG3	AK053r	≥ 6.5
CBFA2T3	ANKRD11	AK142r	≥ 6.5	RP11-272B17.2	AP3B1	AK173r	≥ 6.5
CBWD1	AL583842.3	AK213r	≥ 6.5	RP11-272B17.2	R3HDM2	AK173r	≥ 8
CCDC171	AP3B1	K82Q	≥ 6.5	RP11-345F18.1	CHIC2	L5XL	≥ 6.5
CDC27	ACTN4	AK227r	≥ 6.5	RP11-347I19.3	NOS1	XEMY	≥ 8
CDC42EP3	BMP2K	DD22	≥ 6.5	RP11-362K2.2	CPSF6	AK053r	≥ 6.5
CDK14	AKAP9	JGR2	≥ 8	RP11-364L4.3	HSPA4L	AK199r	≥ 6.5
CDKAL1	ARHGAP12	XEMY	≥ 8	RP11-366L20.2	BIRC6	XEMY	≥ 8
CDKN2B	BNC2	L5XL	≥ 6.5	RP11-372K20.1	GTF3C4	AK153r	≥ 8
CHD9	AMFR	GA6F	≥ 8	RP11-384J4.2	NOVA1	AK199r	≥ 8
CHIC2	AC111194.1	L5XL	≥ 6.5	RP11-386C23.1	JMJD1C	YKZ5	≥ 8
CLEC16A	ACSM1	AK217r	≥ 8	RP11-39E4.1	PLCH1	AK055r	≥ 6.5
CLEC16A	C16orf62	AK217r	≥ 8	RP11-41O4.1	PCDH15	D3VY	≥ 6.5
CNOT2	CCDC126	AK003r	≥ 6.5	RP11-420N3.2	CLCN7	AK124r	≥ 6.5
CNOT2	AC007682.1	AK213r	≥ 6.5	RP11-436F9.1	LANCL2	AK100r	≥ 6.5
CPSF6	CNOT2	AK003r	≥ 8	RP11-463H12.2	CLOCK	L5XL	≥ 8
CTA-292E10.6	CCDC53	AK199r	≥ 8	RP11-467L24.1	CHD9	GA6F	≥ 6.5
CYC1	BAIAP2	AK139r	≥ 6.5	RP11-489P6.1	DTX3	AK053r	≥ 6.5
DARS	ANP32B	761V	≥ 6.5	RP11-149C7.1	PHLPP2	STUK	≥ 8
DCTN2	AVIL	59ND	≥ 8	RP11-4F22.2	KIF3B	AZH7	≥ 6.5
DCTN2	CTDSP2	59ND	≥ 6.5	RP11-519M16.1	GAB1	AK199r	≥ 6.5
DCTN2	ACACA	AK100r	≥ 8	RP11-571M6.6	LIMA1	AK142r	≥ 6.5
DGKA	ARHGEF25	AK142r	≥ 6.5	RP11-571M6.7	ACACA	AK100r	≥ 6.5
DGKZ	CADPS2	AK173r	≥ 8	RP11-571M6.8	MBD6	AK100r	≥ 6.5
DPY19L1	ADCY7	AK227r	≥ 6.5	RP11-589P10.7	EFCAB13	U676	≥ 6.5
DYRK1A	AP000946.2	XEMY	≥ 6.5	RP11-58A17.4	AATF	AK100r	≥ 8
EFCAB2	CAPN8	AK178r	≥ 8	RP11-58A17.4	GLI1	AK100r	≥ 8
EFCAB6	AC073610.1	AK199r	≥ 6.5	RP11-58A17.4	GRIP1	XEMY	≥ 8
EFCAB6	ARF3	AK199r	≥ 8	RP11-608B3.1	KLF3	AK199r	≥ 6.5
EIF2AK4	CHURC1	AK100r	≥ 8	RP11-611E13.2	PTPRR	AK003r	≥ 6.5
EPHB2	CD164	AK139r	≥ 6.5	RP11-614O9.3	KIAA0284	59ND	≥ 6.5
EPM2A	DLG1	AK053r	≥ 6.5	RP11-620J15.2	ACACA	AK100r	≥ 8
ERGIC2	A2MP1	AK199r	≥ 8	RP11-620J15.3	CTDSP2	AK053r	≥ 8
ERP27	CCDC117	AK199r	≥ 8	RP11-620J15.3	ACACA	AK100r	≥ 8
EXOC1	CLOCK	L5XL	≥ 8	RP11-620J15.3	PPM1H	AK199r	≥ 6.5
FAF1	AGBL4	K48U	≥ 8	RP11-655H13.2	EPC1	XEMY	≥ 8
FAM133B	AC006374.2	JGR2	≥ 6.5	RP11-657O9.1	RAB6B	JGR2	≥ 6.5
FHDC1	DGKG	K48U	≥ 6.5	RP11-690J15.1	NCOR2	AK217r	≥ 8
FNDC3A	ABCC4	AK199r	≥ 8	RP11-707P17.1	MGA	K48U	≥ 6.5

Continued on next page

Table S6 – continued from previous page

Gene1	Gene2	Sample	Score	Gene1	Gene2	Sample	Score
FRMD4B	FBXL2	AK213r	≥8	RP11-729M20.1	GAB1	AK199r	≥6.5
FSD1L	FKTN	DUHE	≥8	RP11-739N20.2	LANCL2	DUHE	≥6.5
FSTL5	CLCN3	VNDF	≥8	RP11-849H4.2	OTOG	AK173r	≥6.5
GDF10	GCLC	XEMY	≥6.5	RP11-94P11.4	DHCR24	AK185r	≥6.5
GJC1	CTC-296K1.3	23H0	≥6.5	RP11-974F13.6	RP11-1023L17.1	AK199r	≥6.5
GJC1	CTC-296K1.3	AK003r	≥6.5	RP1-230L10.1	QKI	AK003r	≥6.5
GLI1	DDIT3	59ND	≥6.5	RP3-410C9.1	MIR3687	AK213r	≥6.5
GLI1	CPSF6	AK053r	≥8	RP3-453D15.1	NR2E1	AK203r	≥6.5
GLI1	AATF	AK100r	≥8	RP5-1024C24.1	DNAJC24	AK124r	≥8
GLI1	ACACA	AK100r	≥6.5	RPGRIP1L	FTO	GA6F	≥6.5
GNB1	CAMTA1	D3H7	≥6.5	RPH3A	HECTD4	K48U	≥6.5
GNPDA2	C4orf52	AK199r	≥8	RPS4X	COL6A4P1	AK124r	≥8
GRIP2	GPD1L	AK213r	≥8	RPTOR	CBX2	YKZ5	≥8
GRM7	COL6A4P1	AK124r	≥6.5	RTF1	MGA	K48U	≥8
GTF2IRD1	GTF2I	K48U	≥8	SACS	LINC00543	7EN2	≥6.5
HMGA2	BIRC6	XEMY	≥6.5	SAMD12	MTSS1	JGR2	≥8
HNRNPH1	AGAP1	AK178r	≥8	SARDH	COL5A1	AK178r	≥8
HOOK1	DARS	AK051r	≥6.5	SCD5	RP11-302F12.3	AK199r	≥8
HPSE2	FRMD4A	XEMY	≥8	SCD5	PCBD2	JGR2	≥6.5
HSCB	CDK17	AK199r	≥8	SCFD2	POLR2B	AK003r	≥8
HSPA4L	GAB1	AK199r	≥8	SCLT1	METTL21B	AK199r	≥8
ICAM2	ASXL1	AZH7	≥8	SCN3A	SCN1A	59ND	≥8
IL1RAPL2	EMC3	AK124r	≥8	SCN3A	SCN1A	9JGR	≥6.5
ISPD	AGMO	AK178r	≥8	SCN3A	SCN1A	AK217r	≥6.5
ITPR1	FANCD2	AK124r	≥6.5	SDC2	CPQ	STUK	≥8
JAK2	GLIS3	D3VY	≥8	SDR42E2	DCTN5	AK217r	≥6.5
JMJD1C	CDH23	XEMY	≥6.5	SEC22B	RP11-277L2.2	DUHE	≥6.5
KAT2B	ITPR1	AK124r	≥8	SEC61G	EGFR	AK071r	≥6.5
KCNH8	IQCJ-SCHIP1	AK124r	≥6.5	SEMA3C	RALA	AK217r	≥6.5
KDR	CHIC2	L5XL	≥8	SERINC5	NEDD1	LEZR	≥6.5
KIAA0556	FOPNL	AK003r	≥8	SERPINA5	DAAM1	AK199r	≥6.5
KIAA1328	GLI1	AK100r	≥6.5	SETBP1	CHST9	D3H7	≥8
KIAA2026	INTS9	9JGR	≥8	SFMBT2	FAM171A1	23H0	≥8
KIAA2026	FARP1	AK124r	≥6.5	SHISA5	GBE1	AK213r	≥8
KIAA2026	ERMP1	AK217r	≥6.5	SHISA5	PFKFB4	AK213r	≥6.5
KIF17	CAMTA1	D3H7	≥8	SHISA5	PTPN23	AK213r	≥8
KIF5A	AVIL	AK053r	≥8	SLBP	FGFR3	K48U	≥6.5
KITLG	ANKS1B	AK199r	≥6.5	SLC12A3	FTO	GA6F	≥6.5
KLF3	CTDSP2	AK199r	≥8	SLC13A3	PRKCA	AZH7	≥6.5
KRR1	AGAP2	59ND	≥6.5	SLC14A1	NOL4	D3H7	≥6.5
LAMP2	FAM70A	K48U	≥8	SLC16A7	MDM2	AK053r	≥6.5
LANCL2	EGFR	AK053r	≥6.5	SLC16A7	R3HDM2	AK173r	≥8
LAP3	FAM114A1	AK199r	≥6.5	SLC16A7	GRIP1	XEMY	≥8
LATS2	FRY	AK217r	≥8	SLC25A18	CECR2	JGR2	≥6.5
LCTL	ARNT2	AK003r	≥8	SLC35E3	SLC16A7	AK053r	≥8
LGI1	HAPLN2	AK142r	≥6.5	SLC38A4	GRIN2B	AK003r	≥8
LIMA1	FAM19A2	AK142r	≥6.5	SLC7A6	NFATC3	K48U	≥8

Continued on next page

Table S6 – continued from previous page

Gene1	Gene2	Sample	Score	Gene1	Gene2	Sample	Score
LIN52	ACOT2	AK074r	≥8	SLFN11	FOXK2	U676	≥8
LINC00478	FOLH1	XEMY	≥6.5	SLIT1	CERS5	K48U	≥8
LINS	AP3B1	AK203r	≥6.5	SMARCA2	GLIS3	77FF	≥6.5
LIPJ	AP3B1	STUK	≥6.5	SMARCB1	CHST8	VNDF	≥6.5
LMBR1	ATXN2	77FF	≥8	SMG1	SH3BGR	AK051r	≥8
LNX2	CDK8	AK124r	≥8	snoU13	SNAPC3	D3VY	≥6.5
LRIG3	CPM	AK053r	≥8	snoZ247	EML6	XEMY	≥8
LRIG3	CPSF6	AK053r	≥8	snoZ247	TTC27	XEMY	≥8
LRRC37A2	KANSL1	AK203r	≥6.5	SNTG2	IL1R2	XEMY	≥6.5
MAP4	C20orf194	AK199r	≥8	SPAST	ARHGAP12	XEMY	≥8
MARCH9	ATXN7L3B	AK003r	≥6.5	SPATA6	LINS	AK098r	≥6.5
MARS	DCTN2	3LK6	≥6.5	SPDYA	KCNS3	D3VY	≥6.5
MARS	CTDSP2	AK053r	≥8	SPG21	FANCI	AK185r	≥8
MARS	ACACA	AK100r	≥8	SPHKAP	PPP3CC	AK124r	≥8
MBNL1	ATP2B2	AK124r	≥8	SRGAP3	IQCJ-SCHIP1	AK124r	≥6.5
MDM2	ARHGEF25	59ND	≥8	SRPK2	AC011288.2	LEZR	≥6.5
MDM2	ATXN7L3B	AK003r	≥6.5	ST7	MET	AK173r	≥8
MDM2	FRMD5	AK003r	≥8	ST7	MET	AK199r	≥8
MDM2	IFNG-AS1	AK003r	≥8	ST7-AS1	MET	AK199r	≥8
MDM2	MDM1	AK003r	≥6.5	ST7-OT4	MET	AK199r	≥8
MDM4	EGFR	AK185r	≥8	STAG1	RP11-731C17.1	GA6F	≥6.5
MET	JAZF1	JGR2	≥8	STAG2	SMARCA1	AK153r	≥8
MET	JAZF1-AS1	JGR2	≥8	STIM2	GUF1	AK199r	≥8
METTL1	ACACA	AK100r	≥8	STOX2	ING2	AK199r	≥8
METTL1	FGF3	AK173r	≥8	STPG1	PPP1R12B	AK074r	≥8
METTL21B	ACACA	AK100r	≥6.5	STXBP3	GPSM2	K48U	≥6.5
METTL21B	MBD6	AK100r	≥8	STYXL1	POR	JGR2	≥8
MFN2	FBXO44	K82Q	≥8	SUMF1	SNX12	AK124r	≥6.5
MGA	DMXL2	K48U	≥8	SUMO2P2	SNAPC3	D3VY	≥6.5
MKLN1	CCDC57	AK074r	≥8	SUZ12P	EXOC7	AZH7	≥6.5
MON2	KDM2B	XEMY	≥6.5	SUZ12P	RP11-260O18.1	K82Q	≥6.5
MORN3	KDM2B	STUK	≥8	SYNE2	CHURC1-FNTB	AK178r	≥8
MOV10	CSDE1	D3VY	≥8	SYNRG	INHBE	AK100r	≥8
MP RIP	HNRNPK	AK139r	≥6.5	TADA2A	B4GALNT1	AK100r	≥8
MRPS9	AC013402.2	XEMY	≥8	TAF3	RP11-325P15.3	AK217r	≥6.5
MRPS9	AC068535.4	XEMY	≥8	TBC1D15	KCNC2	AK003r	≥8
MSH2	CALM2	K48U	≥6.5	TBC1D15	CPM	AK142r	≥8
MTAP	ADAM28	L5XL	≥8	TBC1D15	MDM2	AK142r	≥6.5
MTMR8	BRWD3	AK124r	≥8	TBC1D15	OR6C68	AK142r	≥6.5
MYT1L	AC013402.2	XEMY	≥6.5	TBC1D22A	DNAH10	AK199r	≥6.5
MYT1L	AC068535.4	XEMY	≥6.5	TBC1D22A	PTMS	AK199r	≥8
MZT1	LCP1	AK142r	≥8	TBC1D5	GRM7	AK124r	≥6.5
NBPF20	NBPF15	AK213r	≥6.5	TCEB3	ID3	AK139r	≥6.5
NCAM1	LAPTM4B	K48U	≥8	TCEB3	MDS2	AK139r	≥8
NCOR2	CDH20	761V	≥6.5	TCF20	SRGAP1	AK199r	≥8
NCS1	HNRNPUL2	K48U	≥8	TDRD12	PAK7	AK066r	≥6.5
NDEL1	AC005772.2	77FF	≥6.5	TERT	CCDC127	YKZ5	≥8
NDRG1	AF146191.4	AK053r	≥8	TIAM1	NBEA	XEMY	≥8
NDRG1	EFR3A	VNDF	≥8	TIAM2	PCDH10	AK217r	≥6.5

Continued on next page

Table S6 – continued from previous page

Gene1	Gene2	Sample	Score	Gene1	Gene2	Sample	Score
NDUFA4L2	MARS	59ND	≥8	TLE4	NTRK2	JGR2	≥8
NEDD1	C12orf55	AK074r	≥6.5	TLN2	RP11-38G5.1	AK003r	≥6.5
NEDD1	C12orf55	LEZR	≥6.5	TM4SF19	PCYT1A	YKZ5	≥6.5
NEDD1	C12orf55	WFRL	≥6.5	TMC1	SHC3	AK053r	≥6.5
NEK11	C10orf68	AK074r	≥6.5	TMEM132B	TDG	59ND	≥6.5
NEK11	C10orf68	WFRL	≥6.5	TMEM132B	TDG	AK168r	≥6.5
NFASC	MAP4	AK074r	≥8	TMEM164	GMPS	AK124r	≥8
NFASC	ATP2B4	AK185r	≥8	TMEM35	MTMR8	AK124r	≥8
NFASC	GS1-18A18.2	DUHE	≥8	TMEM50B	IFNAR2	761V	≥8
NFASC	ATP2B4	YKZ5	≥6.5	TMEM74	SYBU	K82Q	≥8
NFASC	LAX1	YKZ5	≥8	TMTC1	CTDSP2	AK199r	≥8
NFIB	KIAA2026	7EN2	≥6.5	TMTC1	FAR2	AK199r	≥6.5
NOS1	AC084018.1	XEMY	≥6.5	TMTC1	NCAPD2	AK199r	≥6.5
NOS1AP	IRF6	AK217r	≥8	TMTC1	SEL1L3	AK199r	≥6.5
NOX4	FOLH1	XEMY	≥6.5	TNR	RFWD2	AK199r	≥8
NR5A2	KLHL29	761V	≥6.5	TP63	SOX6	AK217r	≥8
NRXN2	CADPS2	AK173r	≥8	TPH2	LARP4	AK199r	≥8
NTM	EXOC4	AK124r	≥6.5	TPTE2P5	TPTE2	AK203r	≥8
NVL	CAPN8	AK178r	≥6.5	TRIM2	TBCCD1	K48U	≥8
OPTC	CNTN2	AK185r	≥6.5	TRIM36	CCDC112	761V	≥8
OR6C72P	LIMA1	AK142r	≥8	TRIM36	CTB-161J7.2	761V	≥6.5
OR6C74	CYP27B1	AK142r	≥6.5	TRIO	ARHGEF3	AK003r	≥6.5
OS9	KRR1	59ND	≥6.5	TRIO	ARHGEF3	AK066r	≥6.5
OS9	MDM1	AK003r	≥8	TRIO	ARHGEF3	AK100r	≥6.5
OS9	LRIG3	AK053r	≥6.5	TRPC1	FAM159A	3LK6	≥6.5
OSBPL8	OS9	59ND	≥8	TSFM	MDM2	59ND	≥8
OSBPL9	BMP8B	AK139r	≥6.5	TSFM	NAV3	59ND	≥8
OSBPL9	MACF1	AK139r	≥8	TSFM	RP11-611O2.2	59ND	≥8
PACRG	DLG1	AK053r	≥8	TSFM	ACACA	AK100r	≥8
PARP11	L3MBTL2	AK199r	≥8	TSFM	RAB21	AK142r	≥8
PBX3	AC107057.2	AZH7	≥6.5	TSPAN31	SLC35E3	AK003r	≥6.5
PCDHB7	DOT1L	YKZ5	≥6.5	TSPAN9	C12orf5	YKZ5	≥8
PCSK5	C1orf100	AK217r	≥6.5	TTC28	RP11-541G9.1	AK199r	≥6.5
PDGFRA	NMU	L5XL	≥8	TTLL1	C12orf28	AK199r	≥6.5
PEAK1	ADAMTSL3	D3VY	≥6.5	TTLL1	RP11-611E13.2	AK199r	≥8
PFKFB4	FAM198A	AK213r	≥6.5	TULP4	SNX9	AK139r	≥8
PFKFB4	GBE1	AK213r	≥8	U6	ITGB3BP	AK139r	≥6.5
PHF20	CTNNBL1	AK199r	≥8	U6	NFASC	DUHE	≥8
PHIP	APBB1IP	XEMY	≥6.5	UBE2E1	BRWD3	AK124r	≥8
PHYHIPL	AP3B1	3LK6	≥6.5	UBE2E1	RP3-455H14.1	AK124r	≥6.5
PIK3C2B	LANCL2	DUHE	≥8	UBE2E2	CRBN	AK124r	≥8
PIP4K2C	OS9	AK053r	≥8	UBE3B	APOLD1	AK199r	≥6.5
PKNOX2	GRAMD1B	D3VY	≥8	UBR2	FAM65B	AK203r	≥8
PLEKHA6	LANCL2	DUHE	≥8	UBXN2A	TARBP1	AK213r	≥8
PMM1	BTBD2	K48U	≥8	UNC119B	PITPNM2	AK199r	≥6.5
POC1B	CTDSP2	AK199r	≥8	USHBP1	CNOT2	AK098r	≥6.5
POLR1D	CDK8	AK124r	≥6.5	USP12	UBAC2	XEMY	≥6.5
POU6F2	GATAD2A	AK217r	≥6.5	USP32	TBCD	U676	≥6.5
PPFIBP1	NUAK1	AK199r	≥6.5	USP8	RP11-162I7.1	DD22	≥6.5

Continued on next page

Table S6 – continued from previous page

Gene1	Gene2	Sample	Score	Gene1	Gene2	Sample	Score
PPP1R15B	LANCL2	DUHE	≥6.5	UTP18	C1orf86	AK142r	≥6.5
PPP2R3A	MSL2	AK217r	≥8	VCL	PRR12	K48U	≥6.5
PPT1	FOXO6	AK139r	≥8	VOPP1	SEC61G	AK074r	≥8
PREX1	ARFGEF2	K48U	≥6.5	VOPP1	RASEF	AK100r	≥6.5
PRKCA	NCOA6	AZH7	≥8	VPS33A	CLIP1	AK213r	≥6.5
PRR4	ETV6	AK199r	≥8	VSTM2A	LANCL2	AK098r	≥8
PRUNE2	OSBPL2	AK153r	≥8	VSTM2A	LANCL2	AK178r	≥8
PTN	HSPE1	9JGR	≥6.5	WDFY3	GPM6B	AK213r	≥6.5
PTPRD	KDM4C	7EN2	≥6.5	WDR70	NXPH1	AK100r	≥6.5
PTPRR	ATXN7L3B	AK003r	≥6.5	WDR70	UBAP1	AK124r	≥6.5
PTPRR	CPM	AK003r	≥6.5	WDR70	UBAP1	AK199r	≥6.5
PTPRR	CTDSP2	AK003r	≥8	WDR70	NXPH1	AK213r	≥6.5
PTPRR	MDM1	AK003r	≥6.5	XRCC6BP1	CTDSP2	AK053r	≥6.5
PWP1	CAND1	AK199r	≥8	XRCC6BP1	LRIG3	AK053r	≥8
PZP	AGAP2	AK199r	≥8	XRCC6BP1	AATF	AK100r	≥8
QKI	CTAGE13P	AK098r	≥6.5	XRCC6BP1	GRIP1	XEMY	≥8
QKI	DACT2	AK098r	≥8	XYLB	GBE1	AK213r	≥6.5
QKI	OSTM1	AK203r	≥8	XYLB	PTPN23	AK213r	≥6.5
R3HDM2	AVIL	AK173r	≥8	XYLT1	EGFR	AK217r	≥8
RAB21	METTL1	AK142r	≥8	XYLT1	UQCRC2	AK217r	≥8
RAB21	METTL21B	AK142r	≥8	XYLT1	MAML2	K48U	≥8
RAB21	OR6C72P	AK142r	≥6.5	YIPF7	STIM2	AK199r	≥8
RAB6B	EPHB1	JGR2	≥8	Y_RNA	SETD2	AK074r	≥6.5
RABGEF1	CHMP4C	DD22	≥6.5	ZBTB20	SLC12A8	AK053r	≥6.5
RAD51	PIGL	AK100r	≥8	ZCCHC14	JPH3	K48U	≥6.5
RAD51AP1	ATP2A2	AK199r	≥8	ZCCHC8	RSRC2	59ND	≥6.5
RAP1B	OSBPL8	AK003r	≥6.5	ZEB1	ARHGAP12	AK217r	≥8
RAPGEF3	DNAH10	AK199r	≥8	ZEB1	PSAP	K48U	≥8
RASSF2	HAPLN2	AK142r	≥8	ZFR	GOLPH3	K48U	≥8
RB1	GNG5P5	7EN2	≥6.5	ZHX3	CHD6	K48U	≥6.5
RB1	OTUD7A	D3VY	≥6.5	ZNF202	AP000866.1	D3VY	≥6.5
RBMS3	HAACL1	AK213r	≥8	ZNF236	CLPB	AK173r	≥6.5
RCOR3	ACP6	AK217r	≥8	ZNF236	CYB5R4	AK203r	≥6.5
REV3L	FYN	AK071r	≥8	ZNF302	RPS6	AK203r	≥6.5
RMND5A	PLGLA	AK074r	≥6.5	ZNF317	DMWD	AK066r	≥6.5
RNF220	HSPB11	AK139r	≥6.5	ZNF317	ZNF253	AK066r	≥6.5
RNU6-67	NDFIP2	7EN2	≥6.5	ZNF343	RP11-20J15.2	AK203r	≥6.5
ROBO3	CSNK1G1	D3VY	≥6.5	ZNF407	NFIC	K48U	≥6.5
RP11-1055B8.2	C11orf49	AK074r	≥8	ZNF532	FAM60CP	D3VY	≥6.5
RP11-1055B8.6	MCC	AK139r	≥8	ZNF713	SEPT7P2	AK053r	≥6.5
RP11-107C16.2	C10orf137	7EN2	≥6.5	ZNF713	VSTM2A	STUK	≥6.5
RP11-114H23.1	OS9	59ND	≥8	ZNF761	GULP1	AK068r	≥6.5
RP11-116O18.3	NOL4	D3H7	≥6.5	ZNF761	TMEM8B	AK199r	≥6.5
RP11-123O10.4	CNTN1	XEMY	≥6.5	ZNF799	ZNF709	AK071r	≥6.5
RP11-136F16.1	MDM2	59ND	≥8	ZNF92	ZNF85	AK199r	≥6.5

Note: The order of fusion partner 5' and 3' is ignored to simplify comparison.

Table S7: Fusions identified in 135 lymphomas samples (n=380, score \geq 6.5).

Gene1	Gene2	Sample	Score	Gene1	Gene2	Sample	Score
ACOT7	AC007283.5	C1640	\geq 6.5	RAB7L1	IGHD	D0236	\geq 6.5
ALKBH1	ADCK1	D2119	\geq 8	RAD54L2	ANKLE2	D0230	\geq 8
ASH1L	ARHGEF11	D0242	\geq 8	RALGAPB	DNAJC5B	D0228	\geq 6.5
ATP2A3	ANKFY1	D0242	\geq 8	RASA4	BCL2L11	D0230	\geq 6.5
ATP5S	AL122127.3	D2146	\geq 8	RBM6	BCL6	B2195	\geq 8
BCL2	AL122127.25	C0417	\geq 8	REEP1	POLR1A	A1106	\geq 8
BCL6	AL122127.3	B0979	\geq 8	REL	AC010733.4	C1738	\geq 6.5
BCL6	AL122127.3	C3566	\geq 6.5	RENBP	ARHGAP4	D0242	\geq 8
BCL6	AL122127.3	D0228	\geq 6.5	RERE	HERC2P3	B2197	\geq 8
BCL6	AL122127.3	D2137	\geq 6.5	RERE	PEX10	C1565	\geq 8
BZRAP1	ABI3	C1745	\geq 8	RERE	HERC2P3	B0976	\geq 6.5
C11orf53	BTG4	D0242	\geq 8	RERE	HERC2P3	B0981	\geq 6.5
C8orf12	AP3B1	D2136	\geq 6.5	RERE	HERC2P3	C1742	\geq 6.5
CAPZA2	CADPS2	C1739	\geq 8	RERE	HERC2P3	C3568	\geq 6.5
CCDC126	AP3B1	C1739	\geq 6.5	RERE	HERC2P3	D2126	\geq 6.5
CD58	ANXA1	C3567	\geq 6.5	RFWD3	FA2H	D0230	\geq 8
CD58	ANXA1	C3568	\geq 6.5	RFX3	DCAF12	C1636	\geq 6.5
CEP85L	BIRC6	C1565	\geq 6.5	RHBDL3	AL122127.3	D2129	\geq 6.5
CFLAR	ARL6IP6	C0423	\geq 8	RHOH	BCL6	D0251	\geq 8
CHD2	CD80	C3567	\geq 6.5	RNF38	PDCD1LG2	C1636	\geq 8
CIR1	AC004507.1	D2125	\geq 6.5	RP11-10N16.3	IL28RA	B2190	\geq 6.5
CORO1A	CALR	C2874	\geq 6.5	RP11-1101K5.1	EXT1	C2874	\geq 6.5
CSMD3	AC023590.1	C1739	\geq 6.5	RP11-1101K5.1	PKHD1L1	C2874	\geq 6.5
DDX10	ARID5B	D0234	\geq 6.5	RP11-1136L8.1	IGHG1	A1106	\geq 6.5
DIP2B	ASH1L	D2139	\geq 6.5	RP11-1136L8.1	AL122127.3	A1164	\geq 6.5
DLG2	CIITA	C1744	\geq 8	RP11-1136L8.1	IGHD1-26	A1164	\geq 6.5
DNAJC3	CLDN10	B0980	\geq 8	RP11-1136L8.1	AL122127.3	B2188	\geq 6.5
EEF2	C5orf17	C1738	\geq 6.5	RP11-120C12.3	ARID5B	D0242	\geq 6.5
FAM157B	AFG3L1P	D0242	\geq 6.5	RP11-152F13.8	GOLGA6D	B0976	\geq 6.5
FBXO36	AC009950.1	C1731	\geq 6.5	RP11-186B7.4	LYZ	B0980	\geq 6.5
FHIT	CADPS	B2190	\geq 8	RP11-186B7.4	LYZ	C0419	\geq 6.5
FLI1	ETS1	D2122	\geq 6.5	RP11-211G3.2	IGHM	D0254	\geq 6.5
FNBP1	C20orf196	C1561	\geq 8	RP11-211G3.2	IGHG1	D2137	\geq 6.5
GAP43	ABCD3	C1729	\geq 8	RP11-211G3.2	IGHM	D2138	\geq 6.5
GCLC	BTBD9	C1728	\geq 8	RP11-211G3.3	CBLB	D0243	\geq 6.5
GGA3	GABRP	C1635	\geq 8	RP11-30O15.1	LPP	D0242	\geq 6.5
GIT2	ANAPC7	D0242	\geq 8	RP11-3B12.3	CBLB	B2192	\geq 6.5
GNA13	ALPK2	D0241	\geq 8	RP11-427E4.1	LATS1	D0248	\geq 6.5
GNPTAB	DRAM1	D0242	\geq 6.5	RP11-440L16.1	DOCK10	D2130	\geq 8
GUK1	ARF1	B2192	\geq 8	RP11-557C18.4	COG5	A1107	\geq 6.5
HDHD1	ANXA11	C1738	\geq 6.5	RP11-705C15.2	AC103588.1	D2138	\geq 6.5
HEPACAM	DGKH	D0236	\geq 8	RP11-731F5.1	BCL6	C1733	\geq 8
HERC2P8	COTL1	D0254	\geq 6.5	RP11-731F5.1	RP11-211G3.2	C1733	\geq 6.5
HLA-DMA	ABHD16A	D0242	\geq 8	RP11-731F5.2	LAPTM5	D0239	\geq 6.5
HLA-DQA1	ASMT	C1731	\geq 8	RP11-731F5.2	HS2ST1	D0912	\geq 6.5
HLA-DQA1	ASMT	D2126	\geq 8	RP11-73O6.4	PFKFB4	D2120	\geq 6.5
HLA-DQA1	ASMT	B2195	\geq 6.5	RP11-807H22.7	NUMA1	D0242	\geq 6.5
HLA-DQA1	ASMT	C0419	\geq 6.5	RP11-87G24.5	CIITA	B2195	\geq 6.5

Continued on next page

Table S7 – continued from previous page

Gene1	Gene2	Sample	Score	Gene1	Gene2	Sample	Score
HLA-DQA1	ASMT	D0239	≥6.5	RP11-882G5.1	GCNT2	D0242	≥6.5
HLA-DQB2	HLA-DPB1	B2195	≥6.5	RP3-399J4.2	C6orf106	D0242	≥6.5
HLA-DRB1	HLA-DPB1	A1170	≥8	RP4-655J12.5	GON4L	C0420	≥6.5
HLA-DRB1	HLA-DPB1	C1635	≥8	RP5-972B16.2	CASK	A1170	≥6.5
HLA-DRB1	HLA-DPB1	C3560	≥8	RPL14	AC006465.3	D0257	≥8
HLA-DRB1	HLA-DPB1	D2137	≥8	RPL14	E2F4	D0257	≥8
HLA-DRB1	HLA-DPB1	D2139	≥8	RPL24	CEP97	D0242	≥6.5
HLA-DRB1	HLA-DPB1	C0422	≥6.5	RPL28	PCED1B	C1743	≥6.5
HLA-DRB1	HLA-DPB1	D0241	≥6.5	RRM1	NUP98	D0242	≥8
HLA-DRB5	HLA-DPB1	C1744	≥8	RYR2	HSPE1	C1732	≥8
HLA-DRB5	HLA-DPB1	C3566	≥8	SAFB2	INSR	D0242	≥8
HLA-E	HLA-B	B2196	≥6.5	SCO2	PPP6R2	B2192	≥8
HLA-F	HLA-B	B2195	≥8	SCO2	PIM3	C3555	≥8
HLA-F	HLA-C	D2121	≥8	SCO2	PLXNB2	C3555	≥8
HLA-F	HLA-B	D2127	≥8	SDK1	CARD11	D0242	≥6.5
HLA-G	HLA-B	B2197	≥8	SERINC5	NEDD1	D2119	≥6.5
HLA-G	HLA-B	C3556	≥6.5	SERPINB6	SERPINB1	D0242	≥8
HLA-L	HLA-B	D2126	≥8	SERPINB9	RIPK1	B2188	≥8
IGHD4-4	BCL6	D0228	≥6.5	SERPINB9	RIPK1	C1729	≥8
IGHE	BCL6	C1635	≥6.5	SERPINB9	RIPK1	C1741	≥8
IGHE	C15orf37	C3566	≥6.5	SERPINB9	RIPK1	C2876	≥8
IGHG1	CIITA	C1562	≥8	SETD2	RP4-655J12.5	B0980	≥6.5
IGHG1	BCL2L13	B0974	≥6.5	SF3B3	CDH1	D0242	≥8
IGHG1	BCL2	B2193	≥6.5	SFI1	RNF185	A1167	≥8
IGHG1	BCL2	C1737	≥6.5	SFI1	POU2AF1	D0912	≥6.5
IGHG1	IGHE	C1738	≥6.5	SH2B2	CUX1	D0242	≥6.5
IGHG1	BCL2	D0243	≥6.5	SH3BP1	ATAD3A	B2187	≥6.5
IGHG1	BTG1	D2130	≥6.5	SH3BP1	ATAD3A	B2196	≥6.5
IGHG2	CIITA	C1562	≥6.5	SH3BP1	ATAD3A	D2137	≥6.5
IGHG3	CIITA	C1562	≥8	SIPA1L3	FCHSD2	D2137	≥8
IGHG3	BCL6	D0236	≥8	SKAP1	PITPNC1	C3564	≥8
IGHG3	CD86	C1736	≥6.5	SLAMF7	COPA	D0242	≥6.5
IGHG3	BCL6	D0225	≥6.5	SLC38A1	KIF21A	C0416	≥8
IGHG4	BCL2L13	B0974	≥6.5	SLC41A3	AC106722.1	C1736	≥8
IGHG4	IGHG3	B2190	≥6.5	SLC41A3	MBNL1	C1736	≥8
IGHG4	CD86	C1736	≥6.5	SLC43A2	RPA1	D0242	≥6.5
IGHG4	BCL6	C3557	≥6.5	SLC9C1	ATP6V1A	D0242	≥6.5
IGHJ3	BCL2	C3561	≥6.5	SLMAP	PBRM1	D0230	≥6.5
IGHJ3	BCL2	D0243	≥6.5	SLU7	ATP10B	D0242	≥8
IGHJ4	BCL2	C1637	≥6.5	SMAD2	PARD6G	C1731	≥8
IGHJ4	BCL2	C1740	≥6.5	SMARCA4	C3P1	D0242	≥6.5
IGHJ4	BCL2	C1743	≥6.5	SMC6	CHL1	D2126	≥6.5
IGHJ5	BCL2	C1743	≥8	SMCHD1	NDC80	D0242	≥8
IGHJ5	BCL2	B0977	≥6.5	SMU1	MTAP	C1636	≥8
IGHJ5	BCL2	D0238	≥6.5	SMYD3	EFCAB2	B0979	≥8
IGHJ6	BCL2	B2194	≥6.5	SNAP23	CHD7	D0233	≥8
IGHJ6	BCL2	D0253	≥6.5	SNHG3	BCL6	A1170	≥6.5
IGHM	BCL6	C1562	≥6.5	SNX14	FAM165A	D0242	≥6.5
IGKJ5	AC233263.1	B2185	≥6.5	SOS2	POLE2	D0242	≥8

Continued on next page

Table S7 – continued from previous page

Gene1	Gene2	Sample	Score	Gene1	Gene2	Sample	Score
IGKV1-9	IGKJ5	C3561	≥6.5	SOX5	ARID5B	B2196	≥8
IGKV3D-7	IGKJ5	D0241	≥6.5	SP110	FBXO36	C1731	≥8
IGKV4-1	AC096579.13	D2146	≥6.5	SPATA16	NCEH1	D0242	≥8
IGKV5-2	IGKJ5	B0975	≥8	SPG11	ARID4A	C1732	≥6.5
IGKV5-2	IGKJ5	C1639	≥8	SPIB	CD209	C1730	≥8
IGKV5-2	IGKJ2	C3558	≥8	SPINK9	KIF20B	B2188	≥6.5
IGKV5-2	IGKJ5	D0231	≥8	SPINK9	KIF20B	B2189	≥6.5
IGKV5-2	IGKJ5	D0237	≥8	SPPL3	GTF2H3	D0242	≥6.5
IGKV5-2	IGKJ5	D0255	≥8	SRPK2	MLL5	B2197	≥8
IGKV5-2	IGKJ5	D2119	≥8	STAMBPL1	CHUK	D0250	≥8
IGKV5-2	IGKJ5	D2122	≥8	STEAP1B	RAPGEF5	D0242	≥6.5
IGKV5-2	IGKJ5	D2138	≥8	STK24	SLC15A1	D0242	≥6.5
IGKV5-2	AC096579.13	C3559	≥6.5	STK33	IPO7	D0242	≥6.5
IGLC2	FCRLA	D2146	≥8	STYK1	KLRAP1	D0242	≥6.5
IGLC3	FCRLA	D2146	≥8	SYT9	AC016831.7	B2190	≥6.5
IGLL5	CHMP1A	C2876	≥8	SYT9	AC016831.7	B2195	≥6.5
IGLL5	CHMP1A	D2126	≥8	SYT9	AC016831.7	C1728	≥6.5
IRF2BPL	BTBD7	C1640	≥6.5	SYT9	AC016831.7	C1736	≥6.5
IRF4	IGKJ5	C3568	≥8	SYT9	AC016831.7	C1738	≥6.5
ITPR2	FGFR1OP2	D0242	≥6.5	SYT9	AC016831.7	D0226	≥6.5
JARID2	CD83	C1742	≥8	TAF2	SAMD12	C1739	≥8
JMJD1C	FAM188A	D0231	≥6.5	TAF4B	NSG1	C1635	≥8
KIAA1468	CCBE1	D0242	≥6.5	TAOK1	NLK	D0242	≥8
KIF9	CCDC12	D0242	≥8	TBC1D17	AP2A1	D0242	≥6.5
KXD1	DDX39A	B2196	≥8	TEP1	HAUS4	D0242	≥8
LHFPL2	ARSB	D0242	≥6.5	TFB2M	CNST	D0257	≥6.5
LINC00265	CDK13	B2190	≥6.5	TFG	GPR128	C0416	≥8
LNPEP	CTD-2333K2.1	D0228	≥6.5	TFG	GPR128	C1562	≥8
LPAR6	IRF1	C1736	≥8	TFG	GPR128	D0231	≥8
LRRC37A3	BPTF	D0255	≥6.5	TFG	GPR128	D0241	≥8
LSAMP	FCRL3	C0418	≥6.5	TGS1	LYN	C0416	≥8
LSAMP	FCRL3	D0242	≥6.5	TGS1	LYN	D0230	≥6.5
LSM12	ESCO1	D0231	≥6.5	THNSL2	LRWD1	D0230	≥6.5
MAEA	CTBP1	B2192	≥6.5	TIPRL	DCAF6	D0242	≥8
MAN2B1	CHERP	A1170	≥6.5	TMC8	RFX2	C2876	≥8
MAP3K14	HLA-B	D0251	≥6.5	TMC07	COG4	D0242	≥6.5
MAPK1	CDKN1A	D0243	≥8	TMEM159	SLC7A5P1	D0242	≥8
MAPK4	AP1S3	C1731	≥8	TMEM241	RBBP8	D2126	≥6.5
MAPKAPK5	ACAD10	C1728	≥8	TMEM56	ACADM	C1729	≥8
MCFD2	HSD17B4	B2183	≥6.5	TNFRSF10D	MAN1B1	B0979	≥8
MCM3AP	LSS	D0242	≥8	TNFRSF14	CEP104	C0417	≥8
METTL21A	C1orf186	D0256	≥6.5	TNIP1	LIX1	D2138	≥8
MND1	KIAA0922	C3567	≥6.5	TNIP1	RIOK2	D2138	≥8
MND1	KIAA0922	C3568	≥6.5	TOX	EYA1	C1635	≥8
MNDA	CANX	B0979	≥6.5	TOX	NSMAF	D0242	≥8
MORN3	KDM2B	D0242	≥6.5	TRAF3IP2	CD109	B0981	≥8
MTMR12	GOLPH3	D0242	≥6.5	TRAF3IP2	FYN	D0242	≥8
MTMR6	MTAP	C1732	≥8	TRAK1	TEX264	D2122	≥8
MYC	IGHM	A1107	≥8	TRAPPCL11	MT4	D0235	≥6.5

Continued on next page

Table S7 – continued from previous page

Gene1	Gene2	Sample	Score	Gene1	Gene2	Sample	Score
MYC	IGKJ5	B2186	≥8	TRIP12	SLC16A14	B2193	≥8
MYC	AL122127.2	A1107	≥6.5	TRIP12	SLC16A14	B2196	≥8
MYC	KIAA0125	A1107	≥6.5	TRIP12	DIRC3	C1736	≥8
MYC	IGHD	B2187	≥6.5	TRIP12	AC093642.5	C1731	≥6.5
MYC	IGHM	B2187	≥6.5	TTF2	CD101	D0242	≥6.5
MYC	IGHG4	C1739	≥6.5	TTF2	CTB-12O2.1	D0243	≥6.5
MYC	IGHEP1	C2876	≥6.5	U6	RABGAP1L	C3569	≥6.5
MYC	IGHG1	D2136	≥6.5	U7	STAT3	D0242	≥6.5
NEURL	FAM190B	D2139	≥8	UBA3	TMF1	D0232	≥6.5
NGEF	ATAD2B	C1636	≥8	UBA6	PARM1	C1736	≥8
NOC4L	FBRSL1	B2192	≥8	UBAP2	DCAF12	D0242	≥8
NOTCH1	LCN15	D0242	≥8	UBBP5	CASD1	B0978	≥6.5
NUCB2	DOCK8	D2135	≥8	UBC	UBB	D2129	≥8
NUDT9	MUTYH	B2193	≥6.5	UBE2R2	APTX	D0242	≥6.5
NUMB	HEATR4	C1734	≥6.5	UBR2	RP11-190J1.3	D2119	≥6.5
NUP50	FAM118A	B0979	≥8	UNC13B	TATDN2	D0234	≥8
NXPH4	COPZ1	D2139	≥8	USP12	MYCBP2	D2125	≥6.5
OSBPL10	FOXP1	C1728	≥6.5	UVRAG	MAP6	D0242	≥8
OVCH2	NCOA3	D0242	≥8	VPS13B	OXR1	C1739	≥8
PAPOLG	AC007131.2	D0230	≥8	VRK2	RP11-373L24.1	D2120	≥6.5
PARP8	NUSAP1	D2133	≥6.5	VWC2	IKZF1	D0242	≥8
PDCD1LG2	LINGO2	C1636	≥8	WIPF1	CHN1	D0242	≥8
PDE7A	C8orf46	C0424	≥8	WWOX	VAT1L	B2186	≥8
PDGFC	KCTD10	D2130	≥6.5	ZBTB11	SENP7	D0242	≥8
PFDN1	ANKHD1	D0242	≥6.5	ZBTB16	ANKRD30BL	D0230	≥6.5
PGS1	AFMID	D0242	≥8	ZBTB5	RP11-30O15.1	D2129	≥6.5
PIM3	CRELD2	A1167	≥8	ZC3H11A	ATP2B4	B2190	≥6.5
POLDIP3	CAT	B0977	≥8	ZC3H3	EEF1D	C3555	≥8
POU2AF1	EIF4ENIF1	D0912	≥8	ZFP36L1	SAMD15	D0227	≥6.5
PPIAP23	CIITA	D0255	≥6.5	ZNF143	SWAP70	C1635	≥8
PPIL4	GINM1	C3569	≥8	ZNF143	CCDC64	D0232	≥6.5
PPP1R2P9	MYC	D0253	≥6.5	ZNF215	AP3B1	C1745	≥6.5
PRKD1	PPP2R2D	D0242	≥6.5	ZNF217	RCC1	D0245	≥6.5
PSMB6	DRG2	C1739	≥8	ZNF217	SNHG3	D0245	≥6.5
PTPLB	MYLK	D0242	≥6.5	ZNF292	TIAM2	C1562	≥8
PTPRJ	C11orf49	D0230	≥8	ZNF407	EPSTI1	B2193	≥8
PUM1	HYDIN	C1728	≥8	ZNF608	SLC7A1	B2193	≥8
PUS1	GALNT9	B2186	≥8	ZNF610	DYNC1LI2	C1728	≥6.5
PVT1	IGKJ5	D2139	≥8	ZNF66P	HLF	D0230	≥6.5
PVT1	IGHD	C0421	≥6.5	ZNF804A	PDE1A	D2122	≥8
PXDN	ERI1	C1734	≥6.5	ZNF804A	DNAJC10	D2122	≥6.5
R3HCC1L	AP3B1	B2191	≥6.5	ZNRD1	ABCF1	D0242	≥8
RAB3IP	KAT2B	C1732	≥6.5	ZNRD1-AS1	ABCF1	D0242	≥8
RAB7L1	IGHG3	D0236	≥8	ZZZ3	FAM73A	D0242	≥6.5

Note: The order of fusion partner 5' and 3' is ignored to simplify comparison.

Table S8: Fusions identified in 114 CLL samples from HIPO-005.

Gene1	Gene2	Sample	Score	Gene1	Gene2	Sample	Score
IGHA2	IGHA1	001N	≥8	CHD2	B2M	K49C	≥8
JSRP1	CSNK1G2	0TRN	≥6.5	KIF20B	ARHGAP24	K49C	≥6.5
LUC7L2	FCRL2	0TRN	≥6.5	PTMA	CXCR4	K49C	≥6.5
MRPS18A	B4GALT1	0TRN	≥6.5	TAF8	EML2	K49C	≥6.5
PTMA	CXCR4	0TRN	≥6.5	TMEM18	PTMA	K49C	≥6.5
RTP2	NOL10	0TRN	≥6.5	PTMA	CXCR4	KATI	≥6.5
SCAMP4	FGD2	0TRN	≥8	RNY4P27	ABCC4	KATI	≥6.5
TOMM7	EAF2	0TRN	≥8	CXCR4	CHD2	KGAR	≥8
TSC1	EHMT1	0TRN	≥8	GNAS	CXCR4	KGAR	≥8
CXCR4	B2M	0XXE	≥8	IGHA2	IGHA1	KGAR	≥8
CXCR4	BCL2L11	0XXE	≥8	KLF2	AKAP8	KGAR	≥8
DDX5	CXCR4	0XXE	≥8	KLF2	B2M	KGAR	≥8
GNAS	CXCR4	0XXE	≥8	KLF2	CXCR4	KGAR	≥8
MRPS18A	B4GALT1	0XXE	≥6.5	KLF2	FOSB	KGAR	≥8
NOC4L	FBRSL1	0XXE	≥8	KLF2	JSRP1	KGAR	≥6.5
PTMA	CXCR4	0XXE	≥8	PTMA	CXCR4	KGAR	≥6.5
PTMA	CXCR4	0Z63	≥6.5	RERE	HERC2P3	KGAR	≥6.5
TXLNB	MBNL1	0Z63	≥6.5	RGPD5	PTMA	KGAR	≥6.5
CHD2	B2M	15W9	≥8	SIK1	KLF2	KGAR	≥8
CXCR4	CHD2	15W9	≥8	STK3	ARHGAP24	KGAR	≥6.5
FAM60A	DENND5B	15W9	≥8	TFG	GPR128	KGAR	≥8
JSRP1	CSNK1G2	15W9	≥6.5	CHD2	B2M	LAGT	≥8
PTMA	CXCR4	15W9	≥6.5	CXCR4	CHD2	LAGT	≥8
RGPD5	PTMA	15W9	≥8	GNAS	B2M	LAGT	≥8
RNF126	JSRP1	15W9	≥6.5	HMGFB1	CXCR4	LAGT	≥6.5
RNF126	OAZ1	15W9	≥8	KLF2	FOSB	LAGT	≥8
UBC	NCOR2	15W9	≥8	PNRC1	BACH2	LAGT	≥8
CHD2	B2M	19N0	≥8	PTMA	ACTB	LAGT	≥6.5
IGHG4	IGHG3	19N0	≥6.5	PTMA	CXCR4	LAGT	≥6.5
MRPS18A	B4GALT1	19N0	≥6.5	PTMA	FOSB	LAGT	≥8
NUDC	EYA3	19N0	≥8	RP11-20I23.1	CXCR4	LAGT	≥8
PTMA	CXCR4	19N0	≥6.5	RP11-20I23.3	B2M	LAGT	≥6.5
SAMD3	MTHFD1L	19N0	≥6.5	SAMHD1	RP5-977B1.10	LAGT	≥8
SAMD3	PLEKHG1	19N0	≥6.5	TGFBRAP1	MED4	LAGT	≥8
SETBP1	MYO5B	19N0	≥8	TGIF2	SAMHD1	LAGT	≥8
SPINK9	KIF20B	19N0	≥8	UBC	NCOR2	LAGT	≥8
TCF3	OAZ1	19N0	≥8	UBC	PPP1CC	LAGT	≥8
TMEM110	PSMD12	19N0	≥6.5	VAV2	PTMA	LAGT	≥8
TXLNB	MBNL1	19N0	≥6.5	YPEL5	CXCR4	LAGT	≥8
UHRF1	PLIN3	19N0	≥6.5	IGHG4	IGHG3	LBKM	≥6.5
CHD2	B2M	1A5K	≥8	MRPS18A	B4GALT1	LBKM	≥6.5
CXCR4	CHD2	1A5K	≥8	CXCR4	ATP6VOC	LSLK	≥8
IGHG1	AL122127.3	1A5K	≥6.5	PTMA	CXCR4	LSLK	≥8
IGHG1	AL122127.4	1A5K	≥6.5	RGPD6	BCL2L11	LSLK	≥6.5
KLF2	JSRP1	1A5K	≥6.5	RGPD8	PTMA	LSLK	≥6.5
PTMA	CXCR4	1A5K	≥6.5	YPEL5	CXCR4	LSLK	≥8
RBM38	CXCR4	1A5K	≥8	FNDC3A	ATP7B	M76U	≥6.5
SNED1	PTMA	1A5K	≥6.5	MAFK	MAD1L1	M76U	≥8

Continued on next page

Table S8 – continued from previous page

Gene1	Gene2	Sample	Score	Gene1	Gene2	Sample	Score
KIF20B	ARHGAP24	1SP7	≥6.5	MRPS18A	B4GALT1	M76U	≥6.5
STK3	ARHGAP24	1SP7	≥6.5	PTP4A1	PHF3	M76U	≥8
TBRG1	FRG1B	1SP7	≥6.5	SMAP2	NEFLP1	M76U	≥6.5
TFG	GPR128	1SP7	≥8	STK3	ARHGAP24	M76U	≥6.5
IGHA2	IGHA1	2LSW	≥8	CXCR4	B2M	M7OV	≥8
PTMA	CXCR4	2LSW	≥6.5	GNAS	CXCR4	M7OV	≥8
PNPLA7	LIMD2	33WM	≥6.5	HMGB1	CXCR4	M7OV	≥6.5
CHD2	B2M	3DMC	≥8	IGHA2	IGHA1	M7OV	≥8
DDX5	CXCR4	3DMC	≥8	KIF20B	ARHGAP24	M7OV	≥6.5
PTMA	CXCR4	3DMC	≥8	OAZ1	CSNK1G2	M7OV	≥8
RABGAP1L	NEFLP1	3DMC	≥6.5	OAZ1	KLF2	M7OV	≥8
RBM38	CXCR4	3DMC	≥8	PTMA	CXCR4	M7OV	≥6.5
TCF3	OAZ1	3DMC	≥8	PTMA	KLF2	M7OV	≥8
TGIF1	CXCR4	3DMC	≥8	PTMA	OAZ1	M7OV	≥8
ZNF92	ZNF675	3DMC	≥6.5	STK3	ARHGAP24	M7OV	≥6.5
CXCR4	B2M	3IBZ	≥8	KLF2	JSRP1	MA8Z	≥6.5
DDX5	CXCR4	3IBZ	≥8	NBPF12	ANKRD22	MA8Z	≥6.5
EEF1D	CXCR4	3IBZ	≥8	OAZ1	CSNK1G2	MA8Z	≥8
GNAS	CXCR4	3IBZ	≥8	PTMA	CXCR4	MA8Z	≥6.5
GNAS	FAM60A	3IBZ	≥8	TMEM63A	BRCA2	MA8Z	≥8
IGHA1	CXCR4	3IBZ	≥6.5	TOM1L2	FNDC3A	MA8Z	≥8
KLF16	JSRP1	3IBZ	≥6.5	USP34	NAV3	MA8Z	≥8
KLF2	ACTB	3IBZ	≥8	CDC27	ATP2B1	MOWV	≥6.5
KLF2	CXCR4	3IBZ	≥8	CHD2	B2M	MOWV	≥8
KLF2	DDX5	3IBZ	≥8	CXCR4	CHD2	MOWV	≥8
KLF2	EEF2	3IBZ	≥8	OAZ1	CIC	MOWV	≥8
KLF2	FAM65A	3IBZ	≥8	SH3BP1	ATAD3A	MOWV	≥6.5
KLF2	FOSB	3IBZ	≥8	CXCR4	CHD2	MZFG	≥8
KLF2	JSRP1	3IBZ	≥8	IGHA2	IGHA1	MZFG	≥8
LENG8	ATP6VOC	3IBZ	≥8	PTMA	CXCR4	MZFG	≥6.5
PNPLA7	KLF2	3IBZ	≥6.5	RERE	HERC2P3	MZFG	≥6.5
PTBP1	KLF2	3IBZ	≥8	RNASEH2B	MTCH1	MZFG	≥8
PTMA	CXCR4	3IBZ	≥6.5	SPRYD7	MAPK14	MZFG	≥8
PTMA	FAM65A	3IBZ	≥6.5	IGKV5-2	IGKJ5	N4RV	≥8
PTMA	FOSB	3IBZ	≥8	KLF2	JSRP1	N4RV	≥6.5
PTMA	NFE2L2	3IBZ	≥8	PTMA	CXCR4	N4RV	≥6.5
RBM38	CXCR4	3IBZ	≥8	RBM38	CXCR4	N4RV	≥8
RGPD5	BCL2L11	3IBZ	≥6.5	RNASEH2B	ALG8	N4RV	≥6.5
RP11-20I23.1	CXCR4	3IBZ	≥8	TRIM13	FCN3	N4RV	≥8
SIK1	KLF2	3IBZ	≥8	PTMA	CXCR4	N95U	≥6.5
STK3	ARHGAP24	3IBZ	≥6.5	PTMA	HMGN2	N95U	≥6.5
TCF3	OAZ1	3IBZ	≥8	SERINC5	FBXL12	N95U	≥6.5
UBB	ACTB	3IBZ	≥6.5	TMEM110	PSMD12	N95U	≥6.5
UBB	CXCR4	3IBZ	≥8	DDX5	CXCR4	NCP7	≥8
UBB	FAM65A	3IBZ	≥6.5	FCRL5	FCRL3	NCP7	≥6.5
UBB	KLF2	3IBZ	≥8	KLF2	JSRP1	NCP7	≥6.5
UBC	NCOR2	3IBZ	≥8	HLA-DQA1	ASMT	NIA5	≥6.5
USP11	KLF2	3IBZ	≥8	IGHD	AL122127.25	NIA5	≥8
YWHAZ	TGIF1	3IBZ	≥8	IGHM	AL122127.25	NIA5	≥8

Continued on next page

Table S8 – continued from previous page

Gene1	Gene2	Sample	Score	Gene1	Gene2	Sample	Score
PTMA	CXCR4	3JVV	≥6.5	TMEM110	PSMD12	NIA5	≥6.5
IGHA1	CXCR4	46LY	≥6.5	HLA-F	HLA-B	NVTX	≥8
PTMA	CXCR4	46LY	≥6.5	PTMA	CXCR4	NVTX	≥6.5
RNASEH2B	MIPEP	46LY	≥8	CXCR4	ATP6V0C	NYTS	≥8
UBB	CXCR4	46LY	≥8	PTMA	CXCR4	NYTS	≥6.5
UBB	DDX5	46LY	≥6.5	RBM38	CXCR4	NYTS	≥8
UBC	CXCR4	46LY	≥8	RFX1	IL27RA	NYTS	≥6.5
CHD2	B2M	5FFX	≥8	PTMA	CXCR4	O1OE	≥6.5
GNAS	B2M	5FFX	≥8	RBM38	EXTL3	O1OE	≥6.5
IGHA1	B2M	5FFX	≥8	SPSB4	KIAA0586	O1OE	≥8
IGHA1	CXCR4	5FFX	≥6.5	UBC	NCOR2	O1OE	≥8
IGHA2	IGHA1	5FFX	≥8	KLF16	JSRP1	OVF5	≥6.5
KIF20B	ARHGAP24	5FFX	≥6.5	PTMA	CXCR4	OVF5	≥6.5
LRP5L	ADRBK2	5FFX	≥8	TFG	GPR128	OVF5	≥8
OAZ1	CSNK1G2	5FFX	≥8	TMEM18	PTMA	OVF5	≥8
PTMA	CXCR4	5FFX	≥6.5	CYB5R4	C2CD3	P3S9	≥6.5
PTMA	DDX5	5FFX	≥8	PTMA	CXCR4	P3S9	≥6.5
PTP4A1	ELOVL5	5FFX	≥8	ZNF197	RAB6A	P3S9	≥8
STK17B	HSPD1	5FFX	≥6.5	DISP1	C10orf68	PFDT	≥6.5
STK3	ARHGAP24	5FFX	≥6.5	MIR155HG	IGHG3	PFDT	≥6.5
TCF3	JSRP1	5FFX	≥6.5	PTMA	CXCR4	PFDT	≥6.5
UBC	FKBP4	5FFX	≥8	ZFP36L1	MIR155HG	PFDT	≥8
UBC	NCOR2	5FFX	≥8	RERE	HERC2P3	PKOF	≥8
ZNF706	YWHAZ	5FFX	≥6.5	CXCR4	CLK1	PQR8	≥8
IGHG4	IGHG3	5HOD	≥6.5	FNDC3A	DLEU1	PQR8	≥8
JSRP1	CSNK1G2	5HOD	≥6.5	HLA-G	HLA-B	PQR8	≥8
MRPS18A	B4GALT1	5HOD	≥6.5	KDM4A	DAB1	PQR8	≥6.5
PHF21A	PAM16	5HOD	≥6.5	KLF2	FOSB	PQR8	≥8
PTMA	CXCR4	5HOD	≥6.5	KLF2	JSRP1	PQR8	≥6.5
TCF3	OAZ1	5HOD	≥8	PTMA	CXCR4	PQR8	≥6.5
CHD2	AKAP13	5S0Z	≥8	UBB	CXCR4	PQR8	≥8
CHD2	B2M	5S0Z	≥8	WDTC1	FABP3	PQR8	≥8
CXCR4	CHD2	5S0Z	≥8	YPEL5	CXCR4	PQR8	≥8
GNAS	CXCR4	5S0Z	≥8	GNAS	B2M	PWD6	≥8
KLF2	ACTB	5S0Z	≥8	GNAS	CXCR4	PWD6	≥8
KLF2	AKAP8	5S0Z	≥8	IGHG4	IGHG3	PWD6	≥6.5
KLF2	CALR3	5S0Z	≥6.5	JSRP1	CSNK1G2	PWD6	≥6.5
KLF2	DDX5	5S0Z	≥8	KLF2	FOSB	PWD6	≥8
KLF2	FOSB	5S0Z	≥8	KLF2	JSRP1	PWD6	≥6.5
KLF2	JSRP1	5S0Z	≥6.5	PABPC1	EIF1B	PWD6	≥6.5
PNPLA7	KLF2	5S0Z	≥6.5	PTMA	ACTB	PWD6	≥6.5
PTMA	CXCR4	5S0Z	≥6.5	PTMA	CXCR4	PWD6	≥6.5
RASGRP2	KLF2	5S0Z	≥8	SERINC5	FBXL12	PWD6	≥6.5
RNASEH2B-AS1	RB1	5S0Z	≥6.5	SERTAD3	NFATC1	PWD6	≥8
RNASEH2B	RB1	5S0Z	≥8	SPINK9	KIF20B	PWD6	≥6.5
SIK1	KLF2	5S0Z	≥8	SRRM2	HMGB2	PWD6	≥6.5
SRRM2	HMGB2	5S0Z	≥6.5	TCF3	OAZ1	PWD6	≥8
TGFBR2	AC069513.3	5S0Z	≥6.5	TFCP2	EZR	PWD6	≥8

Continued on next page

Table S8 – continued from previous page

Gene1	Gene2	Sample	Score	Gene1	Gene2	Sample	Score
TMEM110	PSMD12	5S0Z	≥6.5	UBB	DDX5	PWD6	≥8
CHD2	B2M	6RZW	≥8	ARMCX4	AP3B1	Q0K9	≥6.5
KIF20B	ARHGAP24	6RZW	≥6.5	CHD2	B2M	Q0K9	≥8
RGPD5	BCL2L11	6RZW	≥8	IGHA1	BCL3	Q0K9	≥8
RP1-276E15.1	HIPK3	6RZW	≥8	KLF2	ACTB	Q145	≥8
STK3	ARHGAP24	6RZW	≥6.5	KLF2	JSRP1	Q145	≥6.5
IGHA2	IGHA1	7RHI	≥8	PTMA	CXCR4	Q145	≥6.5
IGKJ5	BCL2	7RHI	≥8	UBAP1	PTPRC	Q145	≥6.5
PTMA	CXCR4	7RHI	≥6.5	R3HCC1L	BLOC1S6	Q9PA	≥8
SERPINB9	RIPK1	7RHI	≥8	IGHA2	IGHA1	Q9ZM	≥8
TMEM18	PTMA	7RHI	≥8	IGHG4	IGHG3	Q9ZM	≥6.5
CXCR4	CALM1	7YNU	≥8	PTMA	CXCR4	Q9ZM	≥6.5
CXCR4	CHD2	7YNU	≥8	ZNF444	PIK3AP1	Q9ZM	≥6.5
GNAS	B2M	7YNU	≥8	IGHG2	GMDS	QAG4	≥8
GNAS	CXCR4	7YNU	≥8	RAB26	GMDS	QAG4	≥6.5
IGHA1	B2M	7YNU	≥8	RP11-731F5.2	RAB26	QAG4	≥6.5
IGHG4	IGHG3	7YNU	≥6.5	TTYH2	RPL38	QAG4	≥6.5
KLF2	AKAP8	7YNU	≥8	CHD2	B2M	QGBA	≥8
LIMD2	JSRP1	7YNU	≥6.5	CXCR4	CHD2	QGBA	≥8
OAZ1	C19orf24	7YNU	≥8	DDX5	CXCR4	QGBA	≥8
OAZ1	KLF2	7YNU	≥8	GNAS	B2M	QGBA	≥8
PABPC1	EIF1B	7YNU	≥6.5	KIF20B	ARHGAP24	QGBA	≥6.5
PDPK1	ATP6VOC	7YNU	≥6.5	PTMA	CXCR4	QGBA	≥6.5
PTMA	ACTB	7YNU	≥6.5	STK3	ARHGAP24	QGBA	≥6.5
PTMA	C7orf50	7YNU	≥8	GNAS	B2M	QO15	≥8
PTMA	CXCR4	7YNU	≥8	DDX5	CXCR4	RMU2	≥8
PTMA	HMGN2	7YNU	≥6.5	KLF2	CALR3	RMU2	≥6.5
PTMA	KDM4B	7YNU	≥8	PTMA	CXCR4	RMU2	≥8
PTMA	OGFR	7YNU	≥8	PVT1	IGLC3	RMU2	≥6.5
PTMA	PLEKHG1	7YNU	≥8	PVT1	IGLC4	RMU2	≥6.5
PTP4A1	CXCR4	7YNU	≥8	SH3BP1	ATAD3A	RMU2	≥6.5
RPS15	OAZ1	7YNU	≥6.5	TCF3	JSRP1	RMU2	≥6.5
SGTA	JSRP1	7YNU	≥6.5	NUBPL	ADD1	RXC4	≥6.5
SIK1	PTMA	7YNU	≥6.5	OAZ1	CSNK1G2	RXC4	≥8
SSU72	MRPL20	7YNU	≥8	PTMA	CXCR4	RXC4	≥6.5
SUN1	C7orf50	7YNU	≥6.5	RAB33B	JMY	RXC4	≥6.5
TCF3	OAZ1	7YNU	≥8	SERINC5	FBXL12	RXC4	≥6.5
TGIF1	CXCR4	7YNU	≥8	USP34	NAV3	RXC4	≥6.5
TMEM18	PTMA	7YNU	≥6.5	CHD2	B2M	SCQR	≥8
UBE2E3	CXCR4	7YNU	≥6.5	MAP4K5	ECHDC3	SCQR	≥6.5
UBXN4	CXCR4	7YNU	≥8	PRKG2	PLCB1	SCQR	≥6.5
UVSSA	CTBP1	7YNU	≥8	TFG	GPR128	SCQR	≥8
WBP1	CXCR4	7YNU	≥8	NCK2	LRRC16A	SS98	≥6.5
XPO1	CXCR4	7YNU	≥8	PTMA	CXCR4	SS98	≥6.5
YPEL5	CXCR4	7YNU	≥8	SRPK1	KCTD20	SS98	≥8
GNAS	CXCR4	800G	≥8	PTMA	CXCR4	SUEK	≥6.5
METTL21A	C1orf186	800G	≥6.5	YPEL5	CXCR4	SUEK	≥8
OAZ1	CSNK1G2	800G	≥8	CHD2	B2M	TCZE	≥8
PHF21A	PAM16	800G	≥6.5	CXCR4	ATP6VOC	TCZE	≥8

Continued on next page

Table S8 – continued from previous page

Gene1	Gene2	Sample	Score	Gene1	Gene2	Sample	Score
PTMA	CXCR4	800G	≥6.5	CXCR4	BCL2L11	TCZE	≥8
RGPD8	BCL2L11	800G	≥6.5	GNAS	CXCR4	TCZE	≥8
TMEM18	PTMA	800G	≥8	HLA-G	HLA-B	TCZE	≥8
ZC3H4	PCBP1-AS1	800G	≥6.5	KLF2	JSRP1	TCZE	≥6.5
IL10RA	BIRC3	8E7F	≥6.5	PTMA	CXCR4	TCZE	≥6.5
PTMA	CXCR4	8E7F	≥6.5	RBM38	CXCR4	TCZE	≥8
CHD2	B2M	9ELC	≥8	RGPD5	BCL2L11	TCZE	≥8
CXCR4	BCL2L11	9ELC	≥8	RGPD6	PTMA	TCZE	≥6.5
KLF2	DDX39A	9ELC	≥8	SIK1	PTMA	TCZE	≥8
PTMA	BCL2L11	9ELC	≥6.5	TMEM18	PTMA	TCZE	≥6.5
PTMA	CXCR4	9ELC	≥6.5	YPEL5	CXCR4	TCZE	≥8
JSRP1	CSNK1G2	9F34	≥6.5	PTMA	CXCR4	TIW9	≥6.5
KLF2	JSRP1	9F34	≥6.5	CXCR4	CHD2	TMVO	≥8
OAZ1	DAZAP1	9F34	≥8	PTMA	CXCR4	TMVO	≥6.5
PHF21A	PAM16	9F34	≥6.5	YPEL5	CXCR4	TMVO	≥8
PTMA	CXCR4	9F34	≥6.5	ZNF138	NCOR1	TMVO	≥6.5
UBXN4	CXCR4	9F34	≥8	MRPS18A	B4GALT1	TUQ6	≥6.5
USP34	NAV3	9F34	≥6.5	RERE	HERC2P3	TUQ6	≥8
CHD2	B2M	9P4M	≥8	PTMA	CXCR4	TV7J	≥6.5
JSRP1	ATP6V0C	9P4M	≥6.5	UBAP1	PTPRC	TV7J	≥6.5
KLF2	JSRP1	9P4M	≥6.5	CXCR4	BCL2L11	U1QP	≥8
KLF2	KDM4B	9P4M	≥8	CXCR4	CLK1	U1QP	≥8
PNRC1	BACH2	9P4M	≥8	NOC4L	FBRSL1	U1QP	≥8
PTMA	CXCR4	9P4M	≥6.5	PTMA	CXCR4	U1QP	≥6.5
USP34	NAV3	9P4M	≥8	CHD2	B2M	U1TH	≥8
CHD2	B2M	9S37	≥8	CXCR4	CLK1	U1TH	≥8
CXCR4	CHD2	9S37	≥8	IGHA2	IGHA1	U1TH	≥8
IGHG2	IGHG1	9S37	≥6.5	NSRP1	GATAD2A	U1TH	≥6.5
JSRP1	CSNK1G2	9S37	≥6.5	PTMA	CXCR4	U1TH	≥6.5
KSR1	CHD2	9S37	≥8	RBM38	CXCR4	U1TH	≥8
MAFK	MAD1L1	9S37	≥8	SRRM2	IGHD	U1TH	≥6.5
MRPS18A	B4GALT1	9S37	≥6.5	IGHA2	IGHA1	U2VJ	≥8
PTMA	CXCR4	9S37	≥6.5	SH3BP1	ATAD3A	U2VJ	≥6.5
PTMA	JSRP1	9S37	≥6.5	KLF2	JSRP1	U64J	≥6.5
RGPD8	BCL2L11	9S37	≥6.5	PTMA	CXCR4	U64J	≥6.5
RP11-20I23.1	PDPK1	9S37	≥6.5	RBM38	CXCR4	U64J	≥8
TCF3	JSRP1	9S37	≥6.5	YPEL5	CXCR4	U64J	≥8
TCF3	OAZ1	9S37	≥8	CXCR4	BCL2L11	U8HQ	≥8
TESK2	PPIA	9S37	≥6.5	LIMD2	JSRP1	U8HQ	≥6.5
UNKL	UBE2I	9S37	≥8	PTMA	CXCR4	U8HQ	≥6.5
ZFAND6	MORF4L1	9S37	≥6.5	CHD2	B2M	UAYJ	≥8
CHD2	B2M	9VRO	≥8	KLF16	JSRP1	UAYJ	≥6.5
IGHA1	CXCR4	9VRO	≥6.5	LRRC37A2	KANSL1	UAYJ	≥6.5
KLF2	JSRP1	9VRO	≥6.5	OAZ1	KLF2	UAYJ	≥8
PTMA	CXCR4	9VRO	≥6.5	PTMA	CXCR4	UAYJ	≥6.5
TMEM110	PSMD12	9VRO	≥6.5	PTP4A1	PHF3	UAYJ	≥8
YPEL5	CXCR4	9VRO	≥8	RP11-152F13.8	GOLGA6D	UAYJ	≥6.5
CXCR4	B2M	A72M	≥8	SPRYD7	MTMR4	UAYJ	≥8
CXCR4	CHD2	A72M	≥8	SRRM2	ATP6V0C	UAYJ	≥8

Continued on next page

Table S8 – continued from previous page

Gene1	Gene2	Sample	Score	Gene1	Gene2	Sample	Score
HLA-DRB1	HLA-DPB1	A72M	≥8	VAV2	PTMA	UAYJ	≥8
HMGB1	CXCR4	A72M	≥6.5	YPEL5	CXCR4	UAYJ	≥8
PTMA	BCL2L11	A72M	≥6.5	ZNF138	NCOR1	UAYJ	≥6.5
PTMA	CXCR4	A72M	≥6.5	ZNF92	ZNF675	UAYJ	≥6.5
RGPD5	PTMA	A72M	≥6.5	CHD2	B2M	UCF9	≥8
RP3-468B3.2	ITPR3	A72M	≥6.5	CXCR4	CLK1	UCF9	≥8
SH3GLB1	ASCC1	A72M	≥6.5	IGHA1	CXCR4	UCF9	≥6.5
TESK2	PPIA	A72M	≥6.5	NADSYN1	AC005307.3	UCF9	≥6.5
UBC	NCOR2	A72M	≥8	PTMA	CXCR4	UCF9	≥6.5
YPEL5	CXCR4	A72M	≥8	SERINC5	FBXL12	UCF9	≥6.5
CHD2	B2M	A7KR	≥8	NRF1	CLVS1	UJI6	≥6.5
CXCR4	CHD2	A7KR	≥8	STYXL1	C4BPB	UJI6	≥6.5
DDX5	CHD2	A7KR	≥8	TSGA13	CHD7	UJI6	≥8
HMGBl	CXCR4	A7KR	≥6.5	UBAP1	PTPRC	UJI6	≥6.5
HNRNPA2B1	CHD2	A7KR	≥8	GNAS	CXCR4	VFKZ	≥8
JSRP1	CHD2	A7KR	≥6.5	JSRP1	CSNK1G2	VFKZ	≥6.5
N4BP2L1	HMGB1	A7KR	≥8	PTMA	CXCR4	VFKZ	≥6.5
OAZ1	CSNK1G2	A7KR	≥8	CHD2	B2M	VJQU	≥8
PABPC1	EIF1B	A7KR	≥6.5	KLF2	CALR3	VJQU	≥6.5
PDK3	COL28A1	A7KR	≥6.5	OAZ1	KLF2	VJQU	≥8
PTMA	AC131097.3	A7KR	≥6.5	PRAMEL	KDSR	VJQU	≥8
PTMA	CALM2	A7KR	≥8	PTMA	CXCR4	VJQU	≥6.5
PTMA	CXCR4	A7KR	≥8	SERINC5	FBXL12	VJQU	≥6.5
PTMA	HNRNPA2B1	A7KR	≥8	CXCR4	CHD2	VZB0	≥8
PTMA	HNRNPH1	A7KR	≥6.5	FNDC3A	ADAM5	VZB0	≥8
RBM38	PTMA	A7KR	≥8	MACF1	AKIRIN1	VZB0	≥8
REXO1	JSRP1	A7KR	≥6.5	PLCXD1	CNBP	VZB0	≥6.5
RGPD5	BCL2L11	A7KR	≥6.5	RP4-564F22.2	CAMP	VZB0	≥6.5
RGPD6	PTMA	A7KR	≥6.5	TMEM209	ADAM5	VZB0	≥8
RNF126	PTBP1	A7KR	≥8	UQCR10	C1orf194	VZB0	≥6.5
RP11-20I23.1	JSRP1	A7KR	≥6.5	XPO6	CTC-454M9.1	VZB0	≥8
RPS15	OAZ1	A7KR	≥6.5	MRPS18A	B4GALT1	WARE	≥6.5
SF1	HNRNPA2B1	A7KR	≥8	RFX7	AL109763.1	WARE	≥8
TMEM18	PTMA	A7KR	≥6.5	RNF38	FOCAD	WARE	≥8
UBQLN1	HNRNPK	A7KR	≥6.5	RNF38	PARP16	WARE	≥8
UNKL	ATP6VOC	A7KR	≥8	RP1-225E12.2	NUP210	WARE	≥8
UNKL	UBE2I	A7KR	≥8	RP5-1062J16.1	FOCAD	WARE	≥6.5
YPEL5	PTMA	A7KR	≥6.5	TCF3	JSRP1	WARE	≥6.5
ZC3H3	EEF1D	A7KR	≥8	TMPRSS15	RFX7	WARE	≥6.5
CHD2	B2M	AJYE	≥8	UFL1	GIGYF2	WARE	≥6.5
LIMD2	JSRP1	AJYE	≥6.5	KLF2	JSRP1	WHTN	≥6.5
MKRN1	JHDM1D	AJYE	≥8	OAZ1	LIMD2	WHTN	≥8
PTMA	CXCR4	AJYE	≥6.5	PTMA	BCL2L11	WHTN	≥6.5
SH3BP1	ATAD3A	AJYE	≥6.5	CXCR4	BCL2L11	X5Z3	≥8
TMC6	LRCH4	AJYE	≥8	GNAS	B2M	X5Z3	≥8
AKAP8	ACOT7	BO0I	≥6.5	GNAS	CXCR4	X5Z3	≥8
CHD2	B2M	BO0I	≥8	HSPD1	CLK1	X5Z3	≥6.5
CXCR4	B2M	BO0I	≥8	IGHA1	CXCR4	X5Z3	≥6.5
CXCR4	BCL2L11	BO0I	≥8	IGHM	IGHG1	X5Z3	≥8

Continued on next page

Table S8 – continued from previous page

Gene1	Gene2	Sample	Score	Gene1	Gene2	Sample	Score
CXCR4	CHD2	BOOI	≥8	KLF2	JSRP1	X5Z3	≥6.5
GABPB1	B2M	BOOI	≥6.5	OAZ1	CSNK1G2	X5Z3	≥8
KLF2	AKAP8	BOOI	≥8	PDPK2	ATP6VOC	X5Z3	≥6.5
KLF2	JSRP1	BOOI	≥6.5	PTMA	CXCR4	X5Z3	≥6.5
PTMA	BCL2L11	BOOI	≥6.5	PTMA	HMGN2	X5Z3	≥6.5
PTMA	CXCR4	BOOI	≥6.5	RGPD5	BCL2L11	X5Z3	≥8
PTPN12	LHFPL5	BOOI	≥6.5	RP11-20I23.3	CXCR4	X5Z3	≥6.5
RBM38	JSRP1	BOOI	≥6.5	SRSF7	PTMA	X5Z3	≥8
SFMBT1	PTMA	BOOI	≥8	SSU72	SKI	X5Z3	≥8
SRSF7	CXCR4	BOOI	≥8	TCF3	OAZ1	X5Z3	≥8
ZNF407	CNDP1	BOOI	≥6.5	UBB	DDX5	X5Z3	≥6.5
HLA-DRB5	HLA-DPB1	CF04	≥6.5	UBXN4	CXCR4	X5Z3	≥8
NOC4L	FBRSL1	CF04	≥8	UNKL	UBE2I	X5Z3	≥8
YPEL5	CXCR4	CF04	≥8	B2M	ACTB	XMEH	≥8
PTMA	CXCR4	CI7B	≥6.5	CHD2	B2M	XMEH	≥8
CHD2	B2M	CRU4	≥8	IGHM	IGHG4	XMEH	≥6.5
CXCR4	BCL2L11	CRU4	≥8	PPP3CC	PIWIL2	XMEH	≥8
CXCR4	CHD2	CRU4	≥8	PTMA	ACTB	XMEH	≥6.5
GNAS	B2M	CRU4	≥8	PTMA	CXCR4	XMEH	≥6.5
GNAS	CXCR4	CRU4	≥8	PTMA	OAZ1	XMEH	≥8
HMGB1	CXCR4	CRU4	≥6.5	CHD2	B2M	XY05	≥8
IGHA1	CXCR4	CRU4	≥6.5	IGKV5-2	IGKJ5	XY05	≥8
OAZ1	ATP6VOC	CRU4	≥8	MORF4L1	B2M	XY05	≥8
PTMA	CXCR4	CRU4	≥8	OAZ1	CSNK1G2	XY05	≥8
RGPD8	BCL2L11	CRU4	≥6.5	PTMA	CXCR4	XY05	≥6.5
RP11-20I23.1	B2M	CRU4	≥8	PTMA	OAZ1	XY05	≥8
RP11-20I23.1	PDPK1	CRU4	≥8	STK3	ARHGAP24	XY05	≥6.5
SFMBT1	PTMA	CRU4	≥8	UBB	ACTB	XY05	≥6.5
UBB	CXCR4	CRU4	≥8	UBB	DDX5	XY05	≥8
KLF2	JSRP1	CY4B	≥6.5	ZEB1	BMI1	XY05	≥8
UBAC2	PAN3	CY4B	≥8	CXCR4	CHD2	Y67L	≥8
UBC	UBB	CY4B	≥6.5	DLG1	AC090018.1	Y67L	≥6.5
IGHA2	IGHA1	ECD1	≥8	DLG1	APOD	Y67L	≥6.5
IGHG3	AL122127.4	ECD1	≥6.5	FYTTD1	CXCR4	Y67L	≥8
LRRC37A2	KANSL1	ECD1	≥6.5	GNAS	CXCR4	Y67L	≥8
PTMA	CXCR4	ECD1	≥6.5	PTMA	CXCR4	Y67L	≥6.5
SIK3	RP11-680E19.2	ECD1	≥6.5	USP34	NAV3	Y67L	≥8
CHD2	B2M	ES0J	≥8	VAV2	PTMA	Y67L	≥8
SRRM2	IGHD	ES0J	≥6.5	WAC	EPS15L1	Y67L	≥6.5
UHRF1	PLIN3	ES0J	≥6.5	CHD2	B2M	YB12	≥8
LINS	CNOT2	FBE8	≥6.5	CXCR4	CHD2	YB12	≥8
OAZ1	BTBD2	FBE8	≥8	KLF2	JSRP1	YB12	≥6.5
PTMA	CXCR4	FBE8	≥8	PTMA	CXCR4	YB12	≥6.5
MAP4K5	ECHDC3	FHFH	≥6.5	SMEK1	CATSPERB	YB12	≥8
PNRC1	BACH2	FHFH	≥8	HLA-DRB5	HLA-DPB1	YNIY	≥8
PTMA	CXCR4	FHFH	≥6.5	RP4-545L17.7	ANGPT4	YTYV	≥6.5
STK3	ARHGAP24	FHFH	≥6.5	SMCHD1	ATP9B	YTYV	≥8
YPEL5	CXCR4	FHFH	≥8	ALKBH4	AFAP1	YV7I	≥6.5
ZBTB4	EXOC7	FHFH	≥6.5	KLF2	JSRP1	YV7I	≥6.5

Continued on next page

Table S8 – continued from previous page

Gene1	Gene2	Sample	Score	Gene1	Gene2	Sample	Score
MAOA	DDX3X	FK5H	≥8	PNPLA7	LIMD2	YV7I	≥6.5
RP6-113J7.1	DDX3X	FK5H	≥8	PTMA	CXCR4	YV7I	≥6.5
MRPS18A	B4GALT1	FSHB	≥6.5	USP11	KLF2	YV7I	≥8
PTMA	CXCR4	FSHB	≥6.5	VPS18	CHD2	YV7I	≥6.5
USP34	NAV3	FSHB	≥8	CHD2	B2M	Z0HX	≥8
CHD2	B2M	GN55	≥8	CXCR4	CLK1	Z0HX	≥8
CXCR4	CHD2	GN55	≥8	PTMA	CXCR4	Z0HX	≥6.5
HLA-DRB1	HLA-DPB1	GN55	≥8	RP11-309I15.1	NUP88	Z0HX	≥6.5
HLA-G	HLA-B	GN55	≥6.5	STRN4	ARHGAP35	Z0HX	≥8
PTMA	CXCR4	GN55	≥6.5	TMEM110	PSMD12	Z0HX	≥6.5
CXCR4	BCL2L11	GPLO	≥8	ENPP2	BX284650.2	ZCLY	≥6.5
UBAP1	PTPRC	GPLO	≥6.5	GRM7	FCRL1	ZCLY	≥8
USPL1	FLT3	GPLO	≥6.5	IGHA2	IGHA1	ZCLY	≥8
KLF2	FOSB	GTPS	≥8	MRPS18A	B4GALT1	ZCLY	≥6.5
MAN2A1	INTS6	GTPS	≥8	PTMA	CXCR4	ZCLY	≥6.5
PTMA	CXCR4	GTPS	≥6.5	RP11-495P10.1	ENPP2	ZCLY	≥6.5
RANBP9	ATXN1	GTPS	≥8	SUCLA2	DHRS12	ZF32	≥6.5
RANBP9	MAN2A1	GTPS	≥8	ESCO1	EFCAB13	ZRWN	≥6.5
TCF3	OAZ1	GTPS	≥8	GNAS	B2M	ZRWN	≥8
KLF2	JSRP1	JQ6C	≥6.5	RGPD1	KDM3A	ZRWN	≥6.5
PNPLA7	KLF2	JQ6C	≥6.5	PTMA	CXCR4	HNZA	≥6.5
PTMA	CXCR4	JQ6C	≥6.5				

Note: The order of fusion partner 5' and 3' is ignored to simplify comparison.

Table S9: Fusions identified in 25 ependymoma samples (n=67, score \geq 6.5)

Gene1	Gene2	Sample	Score	Gene1	Gene2	Sample	Score
C10orf67	C10orf115	13EP11	\geq 8	NEK11	DISC1	9EP3	\geq 8
CNIH2	AP2A2	9EP38	\geq 8	NRXN2	GALNTL4	9EP38	\geq 6.5
CXorf59	CXorf22	11EP21	\geq 8	NT5DC2	C3orf67	9EP3	\geq 8
CXorf59	CXorf22	13EP15	\geq 8	PPP6R3	DLG2	EP1NS	\geq 8
CXorf59	CXorf22	4EP53	\geq 8	RELA	C11orf95	9EP38	\geq 8
CXorf59	CXorf22	9EP8	\geq 8	RELA	C11orf95	EP1NS	\geq 8
CXorf59	CXorf22	13EP11	\geq 6.5	RELA	C11orf95	11EP22	\geq 6.5
CXorf59	CXorf22	9EP38	\geq 6.5	RELA	C11orf95	4EP45	\geq 6.5
CXorf59	CXorf22	9EP45	\geq 6.5	RELA	C11orf95	7EP41	\geq 6.5
FSIP1	BAZ2A	13EP15	\geq 6.5	RHOD	PACSIN3	EP1NS	\geq 6.5
HIPK3	ABCC8	9EP38	\geq 6.5	RP11-	CDC42BPB	EP1NS	\geq 8
			320M16.2				
HMGB1P16	CXorf59	11EP21	\geq 6.5	RP11-536G4.2	NTN4	13EP11	\geq 6.5
HMGB1P16	CXorf59	13EP11	\geq 6.5	SAA4	FBXO3	9EP38	\geq 6.5
HMGB1P16	CXorf59	4EP22	\geq 6.5	SBF2	RP11-115J23.1	9EP38	\geq 6.5
HMGB1P16	CXorf59	4EP53	\geq 6.5	SDHAP1	AC069513.3	11EP21	\geq 8
HMGB1P16	CXorf59	7EP18	\geq 6.5	SDHAP1	AC069513.3	13EP16	\geq 8
NEDD1	C12orf55	4EP14	\geq 8	SF1	RPS25	9EP38	\geq 6.5
NEDD1	C12orf55	9EP1	\geq 8	SHANK2	MCF2L	11EP22	\geq 6.5
NEDD1	C12orf55	9EP38	\geq 8	SPAG17	MIB2	EP1NS	\geq 8
NEDD1	C12orf55	9EP3	\geq 8	TIMM44	KHDC1	9EP3	\geq 8
NEDD1	C12orf55	11EP21	\geq 6.5	TRAPP4	SWAP70	9EP38	\geq 8
NEDD1	C12orf55	11EP7	\geq 6.5	TSG101	RP11-115J23.1	9EP38	\geq 6.5
NEDD1	C12orf55	13EP11	\geq 6.5	UBXN1	SWAP70	9EP38	\geq 8
NEDD1	C12orf55	13EP15	\geq 6.5	UPF3A	CDC16	7EP18	\geq 8
NEDD1	C12orf55	13EP16	\geq 6.5	UQCR10	C1orf194	4EP12	\geq 6.5
NEDD1	C12orf55	4EP12	\geq 6.5	YAP1	MAMLD1	11EP21	\geq 8
NEDD1	C12orf55	4EP46	\geq 6.5	YAP1	MAMLD1	4EP46	\geq 8
NEDD1	C12orf55	4EP53	\geq 6.5	YAP1	MAMLD1	9EP45	\geq 8
NEDD1	C12orf55	7EP18	\geq 6.5	ZBTB16	KCNQ1	9EP38	\geq 6.5
NEDD1	C12orf55	7EP41	\geq 6.5	ZNF71	INCENP	EP1NS	\geq 6.5
NEDD1	C12orf55	7EP49	\geq 6.5	hsa-mir-4763	LRP5	7EP41	\geq 6.5
NEDD1	C12orf55	9EP45	\geq 6.5	LIMCH1	IRF2BPL	7EP41	\geq 6.5
NEDD1	C12orf55	9EP9	\geq 6.5	LIPJ	AP3B1	13EP11	\geq 6.5
			NEAT1		LTBP3	9EP38	\geq 8

Note: The order of fusion partner 5' and 3' is ignored to simplify comparison.

Table S10: Fusions identified in 118 breast tumor samples (n=1,768, score \geq 6.5).

Gene1	Gene2	Sample	Score	Gene1	Gene2	Sample	Score
AC016629.2	AC009963.6	F7FD_M1	\geq 6.5	RP11-1143G9.4	CAMSAP2	TW0Z_T1	\geq 8
ACSM3	AC092377.1	QYXQ_T1	\geq 6.5	RP11-114M1.1	GFOD1	T6Z1_T1	\geq 6.5
ADAMTS20	ACSS3	F7FD_M1	\geq 8	RP11-11N9.4	NUMA1	615a439	\geq 8
ADK	ADAMTS9-AS2	TDDP_T1	\geq 6.5	RP11-	CA10	JVRW_M1	\geq 8
				120M18.2			
AFF3	AC023672.1	FYVH_M1	\geq 6.5	RP11-1220K2.2	AGK	51CU_M1	\geq 8
AK4	ABCD3	35XC_M1	\geq 6.5	RP11-127H5.1	CSMD3	35XC_M1	\geq 8
AKAP9	ACTR3B	5PJH_M1	\geq 8	RP11-129B22.1	GOLGA4	EDTK_T1	\geq 8
ALDH1A2	ADAM10	OLIZ_T1	\geq 8	RP11-129H15.4	C6orf170	YNSV_T1	\geq 6.5
ANO4	ANKS1B	X0Z1_T1	\geq 6.5	RP11-	BRMS1	3fc2f6	\geq 8
				1407O15.2			
AP000487.6	ADAM9	7DTJ_T1	\geq 6.5	RP11-	FBXO47	LRU2_M1	\geq 6.5
				1407O15.2			
AP3M2	AP000439.3	ZQC5_T1	\geq 8	RP11-141O11.2	CTC-340D7.1	8MNH_T1	\geq 6.5
APP	AC091320.2	SR1R_M1	\geq 8	RP11-146E13.2	AP000525.8	5PJH_M1	\geq 6.5
ARHGAP24	ABCA5	TW0Z_T1	\geq 8	RP11-151E14.1	KDEL1	e64126c	\geq 8
ARHGEF7	AK4P2	4R5V_M1	\geq 6.5	RP11-152F13.8	GOLGA6C	2S2Q_T1	\geq 6.5
ARL2	ANO1	T6Z1_M1	\geq 8	RP11-156P1.3	KANSL1	JVRW_M1	\geq 6.5
ASH2L	ANO1	ZQC5_T1	\geq 8	RP11-159D12.5	CHN2	B2HF_M1	\geq 6.5
ASUN	AKR1D1	4c03c03	\geq 6.5	RP11-159D12.5	CHN2	B2HF_T1	\geq 6.5
ATF7IP	AC027238.1	35XC_M1	\geq 8	RP11-15K3.1	DOCK1	e45fa87	\geq 8
ATG5	ABCA9	b46aa5c	\geq 8	RP11-160O5.1	CDK5RAP3	WHDD_M1	\geq 6.5
ATG5	ASCC3	dd3c42e	\geq 8	RP11-166B2.8	RP11-127I20.4	b46aa5c	\geq 6.5
ATP8A1	ADAM9	L1PK_T1	\geq 8	RP11-167N24.3	NFIA	TW0Z_T1	\geq 6.5
ATP8A2	ANKRD30A	TDDP_T1	\geq 8	RP11-167N24.6	ACSS3	0E5B_T1	\geq 6.5
ATP8A2	ANKRD30A	YER1_T1	\geq 8	RP11-167N24.6	ACSS3	T2VO_M1	\geq 6.5
ATP8A2P1	ANKRD30A	QYXQ_T1	\geq 8	RP11-16F15.2	EHF	WL6X_M1	\geq 8
ATP8A2P1	ATP8A2	QYXQ_T1	\geq 8	RP11-16F15.4	EHF	WL6X_M1	\geq 6.5
ATP8A2P1	ANKRD30A	35XC_M1	\geq 8	RP11-117O3.2	C1orf212	8MNH_T1	\geq 6.5
ATP8A2P1	ANKRD30A	7DTJ_T1	\geq 8	RP11-180P8.1	JARID2	Q6FY_T1	\geq 8
ATP8A2P1	ATP8A2	7DTJ_T1	\geq 8	RP11-182J1.12	GOLGA6A	51CU_M1	\geq 6.5
ATP8A2P1	ATP8A2	9L95_T1	\geq 8	RP11-182J1.12	GOLGA6A	9HTD_T1	\geq 6.5
ATP8A2P1	ATP8A2	KEQ4_T1	\geq 8	RP11-184D12.1	FAM73A	35XC_M1	\geq 6.5
ATP8A2P1	ATP8A2	L1PK_T1	\geq 8	RP11-191G24.1	DNM1L	L50R_T1	\geq 8
ATP8A2P1	ANKRD30A	MA6O_T1	\geq 8	RP11-191L9.4	PPP6R2	b46aa5c	\geq 6.5
ATP8A2P1	ATP8A2	Q6FY_T1	\geq 8	RP11-192H23.4	PYY2	T6Z1_M1	\geq 6.5
ATP8A2P1	ATP8A2	TDDP_T1	\geq 8	RP11-1A16.1	ERO1L	EDTK_T1	\geq 8
ATP8A2P1	ANKRD30A	WL6X_M1	\geq 8	RP11-205K6.2	RALGPS1	PF9X_T1	\geq 6.5
ATP8A2P1	ANKRD30A	YER1_T1	\geq 8	RP11-	LINC00266-1	RZBM_M1	\geq 6.5
				206L10.10			
ATP8A2P1	ATP8A2	YER1_T1	\geq 8	RP11-20F24.4	ANKRD30A	QYXQ_T1	\geq 8
ATP8A2P1	ANKRD30A	ZQC5_T1	\geq 8	RP11-20F24.4	ANKRD30A	0P4M_M1	\geq 8
ATP8A2P1	ATP8A2	ZQC5_T1	\geq 8	RP11-20F24.4	ANKRD30A	6F41_T1	\geq 8
ATP8A2P1	ATP8A2	204ea40	\geq 6.5	RP11-20F24.4	ATP8A2	6F41_T1	\geq 8
ATP8A2P1	ATP8A2	3fc2f6	\geq 6.5	RP11-20F24.4	ATP8A2	7DTJ_T1	\geq 8
ATP8A2P1	ATP8A2	B91A_M1	\geq 6.5	RP11-20F24.4	ATP8A2	AEK9_T1	\geq 8
ATP8A2P1	ATP8A2	DMG3_T1	\geq 6.5	RP11-20F24.4	ATP8A2	IUCQ_T1	\geq 8
ATP8A2P1	ATP8A2	4WQ1_T1	\geq 6.5	RP11-20F24.4	ANKRD30A	WHDD_M1	\geq 8

Continued on next page

Table S10 – continued from previous page

Gene1	Gene2	Sample	Score	Gene1	Gene2	Sample	Score
ATP8A2P1	ATP8A2	5D6N_M1	≥6.5	RP11-20F24.4	ANKRD30A	WL6X_M1	≥8
ATP8A2P1	ATP8A2	5PJH_M1	≥6.5	RP11-20F24.4	ANKRD30A	YA4W_M1	≥8
ATP8A2P1	ANKRD30A	6F41_T1	≥6.5	RP11-20F24.4	ANKRD30A	ZQC5_T1	≥8
ATP8A2P1	ATP8A2	6F41_T1	≥6.5	RP11-20F24.4	ATP8A2	ZQC5_T1	≥8
ATP8A2P1	ATP8A2	75Z1_T1	≥6.5	RP11-20F24.4	ATP8A2	ZCYX_M1	≥6.5
ATP8A2P1	ATP8A2	86DK_M1	≥6.5	RP11-219E7.4	AP000525.8	EDTK_T1	≥8
ATP8A2P1	ANKRD30A	9L95_T1	≥6.5	RP11-219E7.4	EEA1	L50R_T1	≥8
ATP8A2P1	ATP8A2	A0GM_T1	≥6.5	RP11-	KIAA1244	T6Z1_T1	≥6.5
			240M16.1				
ATP8A2P1	ANKRD30A	AEK9_T1	≥6.5	RP11-268G12.1	AGBL5	0XC1_M1	≥8
ATP8A2P1	ATP8A2	AEK9_T1	≥6.5	RP11-281N10.1	NUDCD1	35XC_M1	≥6.5
ATP8A2P1	ANKRD30A	DBBB_M1	≥6.5	RP11-285A15.1	NBAS	b46aa5c	≥8
ATP8A2P1	ATP8A2	DBBB_M1	≥6.5	RP11-285F7.2	CTB-50L17.10	4R5V_M1	≥8
ATP8A2P1	ATP8A2	FHKD_T1	≥6.5	RP11-304C16.3	FUCA2	QYXQ_M1	≥6.5
ATP8A2P1	ATP8A2	PF9X_T1	≥6.5	RP11-30L4.5	DOCK2	D988_M1	≥6.5
ATP8A2P1	ANKRD30A	Q6FY_T1	≥6.5	RP11-310E22.5	C10orf76	D988_M1	≥6.5
ATP8A2P1	ATP8A2	SR1R_M1	≥6.5	RP11-311F12.1	LASP1	Q6FY_T1	≥6.5
ATP8A2P1	ANKRD30A	T2VO_M1	≥6.5	RP11-313P18.1	LOXL1	HY35_T1	≥6.5
ATP8A2P1	ATP8A2	TC6T_T1	≥6.5	RP11-314D7.4	LIMCH1	T6Z1_T1	≥8
ATP8A2P1	ANKRD30A	TDDP_T1	≥6.5	RP11-314D7.4	METTL21B	2S2Q_T1	≥6.5
ATP8A2P1	ANKRD30A	TM97_T1	≥6.5	RP11-314D7.4	ATP5S	8H0R_M1	≥6.5
ATP8A2P1	ANKRD30A	TX2S_T1	≥6.5	RP11-314P15.2	NDST3	ZCYX_M1	≥8
ATP8A2P1	ANKRD30A	WHDD_M1	≥6.5	RP11-330L19.4	BUB1B	YNSV_T1	≥6.5
ATP8A2P1	ATP8A2	WHDD_M1	≥6.5	RP11-356C4.5	ARL17B	8H0R_M1	≥6.5
ATP8A2P1	ATP8A2	WL6X_M1	≥6.5	RP11-357F12.1	NUFIP2	YER1_T1	≥8
BAZ2B	ARID5A	b46aa5c	≥8	RP11-359J23.1	CMIP	SR1R_M1	≥8
BCAS3	ABCA8	Q6FY_T1	≥8	RP11-368P15.1	FERMT2	7FNO_M1	≥8
BCAS3	AC005682.8	B2HF_T1	≥6.5	RP11-393K19.1	CSMD3	35XC_M1	≥6.5
BCL2L14	ASTN2	HMXT_T1	≥6.5	RP11-410A13.3	DHRSX	3b8237c	≥6.5
BECN1	ACACA	AC72_T1	≥8	RP11-420N3.2	DNASE1	b46aa5c	≥6.5
BLMH	ALOX12P1	ZS4T_T1	≥6.5	RP11-420N3.2	GSPT1	b46aa5c	≥6.5
BRIP1	BCAS3	QYXQ_M1	≥6.5	RP11-420N3.2	RP11-166B2.8	b46aa5c	≥6.5
BTBD16	ACSL5	SR1R_M1	≥6.5	RP11-428C19.4	NAV2	4R5V_M1	≥6.5
BTG3	APP	4R5V_M1	≥6.5	RP11-431D12.1	CYP7B1	35XC_M1	≥6.5
C11orf85	ATE1	L50R_T1	≥8	RP11-431D12.1	PKHD1L1	35XC_M1	≥6.5
C12orf66	AFF3	86DK_M1	≥6.5	RP11-431M3.1	KANSL1	JVRW_M1	≥8
C14orf39	ALCAM	WL6X_M1	≥8	RP11-433C9.2	KPNA5	AEK9_T1	≥6.5
C16orf52	BOLA3	SR1R_M1	≥8	RP11-446F3.2	RGMB	WL6X_M1	≥6.5
C5orf22	ATG16L2	4R5V_T1	≥8	RP11-475O6.1	BAIAP2	EDTK_T1	≥8
CAAP1	AC079776.7	699525b	≥6.5	RP11-480O10.2	PPFIA1	FYVH_M1	≥6.5
CALD1	AKR1B10	51CU_M1	≥8	RP11-496I2.3	ATG5	EDTK_T1	≥6.5
CALD1	AKR1B15	51CU_M1	≥6.5	RP11-498D10.4	NKD1	YNSV_T1	≥6.5
CAMK1D	ATE1	L50R_T1	≥6.5	RP11-521I2.3	KIF13B	RQX5_M1	≥6.5
CASP8	AP2S1	B2HF_T1	≥6.5	RP11-522N14.1	BCAS3	2S2Q_T1	≥8
CCDC171	AL589988.1	L50R_T1	≥8	RP11-543E8.2	MGP	bed845b	≥6.5
CCDC74A	AC093838.7	QYXQ_T1	≥6.5	RP11-545L5.1	RP11-	8MNH_T1	≥8
					1407O15.2		
CCDC74A	AC093838.7	I4ZX_T1	≥6.5	RP11-549B18.3	MOCOS	4R5V_M1	≥6.5
CCDC88A	AGFG1	cb6c764	≥6.5	RP11-56B16.5	ATP8B4	HY35_T1	≥6.5

Continued on next page

Table S10 – continued from previous page

Gene1	Gene2	Sample	Score	Gene1	Gene2	Sample	Score
CCND1	ANO1	L50R_T1	≥6.5	RP1-15D23.2	EDARADD	IUCQ_T1	≥6.5
CCNE1	ANKRD27	e64126c	≥8	RP11-5N23.2	FAM188A	4c03c03	≥6.5
CCNI	AC022431.2	5D6N_M1	≥8	RP11-611E13.2	HOOK3	TW0Z_T1	≥6.5
CCR3	ATP7B	RQX5_M1	≥6.5	RP11-624L4.1	PGAP3	35XC_M1	≥6.5
CD5L	ALDH9A1	Q6FY_T1	≥6.5	RP11-626H12.1	NRD1	L50R_T1	≥6.5
CDC42BPA	ASTN1	Q6FY_T1	≥8	RP11-632B21.1	RAB3IP	b9b21b9	≥8
CDC42BPG	7SK	L50R_T1	≥8	RP11-64C1.1	FLNB	cb6c764	≥6.5
CDC42EP3	BMP2K	5D6N_M1	≥6.5	RP11-65J21.3	ABCC1	b9b21b9	≥6.5
CDH20	ATP9B	B2HF_M1	≥8	RP11-662G23.1	PRPF3	TW0Z_T1	≥8
CDH3	CDH1	AC72_T1	≥8	RP11-680G10.1	ACSM3	QYXQ_T1	≥6.5
CDK14	AUTS2	ZCYX_M1	≥6.5	RP11-680G10.1	CRISPLD2	8HNA_T1	≥6.5
CHCHD3	CASD1	46DP_M1	≥8	RP11-702L6.4	HMBOX1	T6Z1_T1	≥6.5
CHN1	AC073465.3	EDTK_T1	≥8	RP11-731N10.1	FABP12	TW0Z_T1	≥6.5
CHODL	ASTN2	51CU_M1	≥6.5	RP11-73H14.1	CCDC138	F7FD_M1	≥6.5
CHODL	ASTN2	8HNA_T1	≥6.5	RP11-73O6.4	CDKL4	b46aa5c	≥6.5
CHSY1	ADAMTS17	8MNH_T1	≥8	RP11-744I24.2	NUP205	TX2S_T1	≥6.5
CIR1	CERS6	5D6N_M1	≥6.5	RP11-744I24.2	OPA1	TX2S_T1	≥6.5
CLASP1	AC064875.2	4R5V_M1	≥6.5	RP11-74C3.1	PPFIA1	L50R_T1	≥8
CMIP	CCNY	SR1R_M1	≥8	RP11-76P2.3	PTEN	8HNA_T1	≥8
CNIH3	C17orf96	Q6FY_T1	≥6.5	RP11-773D16.1	PDS5A	QK84_M1	≥6.5
CNTD1	ACACA	AC72_T1	≥6.5	RP11-783L4.1	KLHL28	F7FD_M1	≥6.5
CNTN4	ANKRD17	699525b	≥8	RP11-800A3.3	LRP5	DR8V_T1	≥6.5
CNTNAP5	CCDC93	Y5G9_T1	≥8	RP11-800A3.3	PPFIA1	DR8V_T1	≥6.5
COG5	ARNT	YNSV_T1	≥8	RP11-805J14.3	RBM14	HY35_T1	≥6.5
COL1A2	COL1A1	af07947	≥8	RP11-805J14.3	RBM14-RBM4	HY35_T1	≥6.5
COL1A2	CASD1	2S2Q_T1	≥8	RP11-805L22.1	ACACA	QYXQ_M1	≥6.5
COL24A1	APBB3	0XC1_M1	≥6.5	RP11-86H7.1	MED13L	F7FD_M1	≥6.5
COL6A5	ACTL6A	NF9D_M1	≥6.5	RP11-89M20.1	NARS2	ZQC5_T1	≥8
CPB1	AP000318.2	ZCYX_M1	≥6.5	RP11-93K22.11	MTUS1	dd3c42e	≥6.5
CRB1	CNIH3	Q6FY_T1	≥6.5	RP11-93L9.1	BRIP1	b46aa5c	≥8
CRHR1	CNTNAP1	b46aa5c	≥6.5	RP11-973H7.2	NR6A1	WHDD_M1	≥8
CRLF3	B4GALNT2	2RR2_T1	≥8	RP11-974F13.6	RP11-1023L17.1	6F41_T1	≥6.5
CRTC3	ARRDC4	HY35_T1	≥6.5	RP11-977P2.1	MTFMT	35XC_M1	≥6.5
CRY2	CD82	F11Y_T1	≥8	RP1-249H1.4	PPIL6	AEK9_T1	≥6.5
CSMD1	AGPAT5	1ED9_T1	≥6.5	RP1-309H15.2	ATXN1	L50R_T1	≥6.5
CTA-392C11.1	AGPAT6	ZQC5_T1	≥8	RP13-16H11.2	NEBL	1ED9_T1	≥6.5
CTA-392C11.1	ACE	cb6c764	≥6.5	RP1-35C21.2	ACBD6	YNSV_T1	≥8
CTB-131B5.5	CDKL3	RZBM_M1	≥6.5	RP1-66C13.4	PPP1R9B	699525b	≥6.5
CTD-2021H9.2	CTD-2021H9.1	QYCP_T1	≥6.5	RP3-406P24.1	B3GNTL1	Q6FY_T1	≥6.5
CTD-	CACNG5	F7FD_M1	≥6.5	RP3-429O6.1	COL14A1	SR1R_M1	≥6.5
2033D24.2							
CTD-2194A8.2	BAD	AEK9_T1	≥8	RP3-453D15.1	FRK	QYXQ_M1	≥6.5
CTD-2542L18.1	AC004381.7	QYXQ_T1	≥8	RP3-486B10.1	MYEOV	L50R_T1	≥8
CTD-2542L18.1	ACSM3	QYXQ_T1	≥8	RP4-562J12.1	GCDH	7FNO_M1	≥6.5
CTNNND2	CENPQ	YNSV_T1	≥6.5	RP4-594L9.2	EHF	F7FD_M1	≥6.5
CTTN	CLNS1A	YNSV_T1	≥6.5	RP4-604K5.1	FBXL4	QYXQ_M1	≥8
CUX1	CPA6	8MNH_T1	≥8	RP4-669L17.4	HELZ	2RR2_T1	≥8
CWC25	CDC27	T6Z1_M1	≥8	RP4-737E23.2	KIAA0556	YNSV_T1	≥6.5

Continued on next page

Table S10 – continued from previous page

Gene1	Gene2	Sample	Score	Gene1	Gene2	Sample	Score
CXADR	APP	4R5V_M1	≥6.5	RP4-810F7.1	ATXN1	T6Z1_T1	≥6.5
CYLD	CNEP1R1	E65C_M1	≥6.5	RP5-1029K10.2	PKN1	WHDD_M1	≥8
CYP4B1	AL136985.1	E65C_M1	≥6.5	RP5-1031J8.1	NCOA6	7DTJ_T1	≥6.5
CYP4F24P	CYP4F12	A0GM_T1	≥6.5	RP5-1112F19.2	DNTTIP1	TX2S_T1	≥6.5
CYTH1	ASPSCR1	cfdf2f24	≥8	RP5-914P20.5	NFATC2	cb6c764	≥6.5
CYTH1	CEP95	cfdf2f24	≥8	RP5-981L23.1	ATP9A	TX2S_T1	≥6.5
DCP2	APC	51CU_M1	≥8	RP5-984P4.1	ARFGEF2	SR1R_M1	≥6.5
DCTN5	COG7	DMG3_M1	≥6.5	RPAP2	NOS1	L50R_T1	≥8
DDHD2	ADAM32	FYVH_M1	≥6.5	RPL18	CDK12	D988_M1	≥6.5
DDX11	ANO6	8HNA_T1	≥8	RPL21P110	PIBF1	8H0R_M1	≥6.5
DDX11L1	AC018816.3	cfdf2f24	≥6.5	RPL31P41	ASPH	2S2Q_T1	≥8
DDX42	ABCA5	Q6FY_T1	≥8	RPL36	GIPC3	SR1R_M1	≥6.5
DDX6	CTD-2216M2.1	HMXT_T1	≥6.5	RPRD2	ACP6	TW0Z_T1	≥8
DENND1B	BRIP1	Q6FY_T1	≥8	RPRD2	GJA5	TW0Z_T1	≥8
DENND4C	ACER2	8H0R_M1	≥8	RPS15AP5	FGFR2	L50R_T1	≥6.5
DGCR2	CECR2	2S2Q_T1	≥8	RPS15AP5	NSMCE4A	L50R_T1	≥6.5
DIRC1	CTDP1	af07947	≥8	RPS24	C10orf11	46DP_M1	≥6.5
DISP1	C10orf68	3b8237c	≥6.5	RPS6KA1	KIAA1522	DMG3_T1	≥6.5
DISP1	C10orf68	4ec8eca	≥6.5	RPS6KA4	KDM2A	JVRW_M1	≥6.5
DMXL2	ARIH1	3fcf2f6	≥6.5	RPS6KB1	BCAS3	B2HF_T1	≥8
DNAJC3	CLDN10	8H0R_M1	≥8	RPS6KB1	CAMSAP2	Q6FY_T1	≥8
DNM2	ADAMTS10	WHDD_M1	≥8	RPS6KB1	BAG4	JVRW_M1	≥6.5
DOCK5	ADAM32	WHDD_M1	≥8	RPTOR	DUS1L	cfdf2f24	≥8
DPP10	C2orf49	Q6FY_T1	≥8	RPTOR	NF1	LRU2_M1	≥6.5
DPP6	AKAP9	ZCYX_M1	≥8	RRAGC	MACF1	2S2Q_T1	≥6.5
DPP6	CNTNAP2	ZCYX_M1	≥8	RSBN1L-AS1	DPP6	5PJH_M1	≥8
DUSP4	CDCA2	WL6X_M1	≥6.5	RUFY1	RAPGEF5	dd3c42e	≥6.5
DYRK1A	ADRM1	X0Z1_T1	≥8	RUNX1	CCDC58	b46aa5c	≥8
DYRK2	CCT2	007M_M1	≥6.5	RUNX1	KPNA1	b46aa5c	≥8
ECT2	C2orf15	35XC_M1	≥6.5	RUNX1	BRE	HMXT_T1	≥8
EFHA2	BLMH	8H0R_M1	≥6.5	RUNX1	FARSB	SR1R_M1	≥8
EFNA1	C1orf167	4c03c03	≥8	RUNX1	PPM1H	2S2Q_T1	≥6.5
EIF2S3	ACOT9	59cb2ad	≥6.5	RUNX1	MOGAT1	SR1R_M1	≥6.5
EIF3H	CSMD3	2RR2_T1	≥8	RUNX1	AGPAT3	X0Z1_T1	≥6.5
ELOVL2	AL137003.1	QYXQ_M1	≥8	RWDD1	RP11-	QYXQ_M1	≥6.5
					126M14.1		
ELOVL2	ATXN1	QYXQ_M1	≥8	RYR1	ACTN4	HMXT_T1	≥8
ELOVL2	ATG5	QYXQ_M1	≥6.5	RYR3	COPS2	35XC_M1	≥6.5
ELP3	DHX30	RQX5_M1	≥8	S100A7A	C1orf43	T6Z1_M1	≥6.5
ELP3	CEBDP	cfdf2f24	≥6.5	S100Z	AGGF1	T2VO_M1	≥8
ENY2	ADCY8	35XC_M1	≥6.5	SAFB	BLNK	5f7b7fb	≥8
EPB42	CWC25	TC6T_T1	≥8	SAP30L	AC114947.1	T6Z1_M1	≥8
EPG5	C18orf25	007M_M1	≥6.5	SARNP	RP11-291B21.2	I4ZX_T1	≥6.5
EPHA7	ATG5	EDTK_T1	≥8	SASH1	PCMT1	T6Z1_T1	≥8
EPS15	ABCA4	L50R_T1	≥8	SBNO1	MPHOSPH9	HMXT_T1	≥8
ERBB2	ACLY	35XC_M1	≥6.5	SBNO2	POLRMT	YNSV_T1	≥6.5
ERBB2	ALG6	35XC_M1	≥6.5	SCAI	ATXN2	H9F4_M1	≥8
ERBB4	CYFIP1	YNSV_T1	≥6.5	SCML2	CTPS2	HMXT_T1	≥8
ERGIC2	CASC1	b9b21b9	≥8	SCML4	RTN4IP1	EDTK_T1	≥6.5

Continued on next page

Table S10 – continued from previous page

Gene1	Gene2	Sample	Score	Gene1	Gene2	Sample	Score
ERGIC3	CEP250	HMXT_T1	≥8	SCN5A	ARPP21	F7FD_M1	≥6.5
ESR1	CDH8	SR1R_M1	≥8	SCRN3	CERS6	5D6N_M1	≥8
ESR1	CCDC170	DMG3_M1	≥6.5	SDC2	CPQ	af07947	≥8
ESR1	CCDC170	OE5B_T1	≥6.5	SDCBP	ADCY8	35XC_M1	≥6.5
ESR1	CCDC170	86DK_M1	≥6.5	SDCBP	CYP7B1	35XC_M1	≥6.5
ESR1	CCDC170	8H0R_M1	≥6.5	SDCBP	KCNB2	35XC_M1	≥6.5
ETV6	ANKS1B	I4ZX_T1	≥8	SDCBP	RP11-1D12.1	35XC_M1	≥6.5
ETV6	BCL2L14	HMXT_T1	≥6.5	SDHAF2	C10orf47	L50R_T1	≥8
EXOC2	EFHC1	4R5V_T1	≥6.5	SDHAP1	AC069513.3	DMG3_T1	≥8
EXOC7	CDR2L	AC72_T1	≥8	SDR42E1	AES	35XC_M1	≥8
EXOC7	CDR2L	B2HF_M1	≥6.5	SEC14L6	LIMK2	L50R_T1	≥8
EYS	ATG5	EDTK_T1	≥8	SEC22B	KDM5B	T6Z1_T1	≥8
EZH2	ESCO1	ZCYX_M1	≥8	SEC22B	NOTCH2	TX2S_T1	≥6.5
FAIM3	C4BPB	cfdf2f24	≥8	SEC63	DDX42	b46aa5c	≥8
FAM107B	C18orf1	cfdf2f24	≥6.5	SEC63	RP11-305B6.3	EDTK_T1	≥6.5
FAM160B1	ABLIM1	HMXT_T1	≥6.5	SECISBP2L	MTR	9L95_T1	≥6.5
FAM172A	ELL2	F7FD_M1	≥8	SECISBP2L	MTR	IUCQ_T1	≥6.5
FAM49B	ADCY8	YNSV_T1	≥8	SEH1L	RIMS3	SR1R_M1	≥8
FAM50B	DUSP22	T6Z1_T1	≥8	SELENBP1	PI4KB	4R5V_M1	≥8
FAM59A	DNAJC1	3b8237c	≥6.5	SEMA3E	SEMA3D	35XC_M1	≥8
FARS2	B3GNTL1	Q6FY_T1	≥6.5	SEMA4B	AKAP13	HY35_T1	≥6.5
FASN	CDK12	cfdf2f24	≥8	SEPT11	EMCN	WL6X_M1	≥6.5
FASTKD1	CREB1	DR8V_T1	≥8	SEPT5	PPIL2	f1ae704	≥8
FBXL20	CTD-2206N4.4	F11Y_T1	≥8	SEPT7	DAB1	35XC_M1	≥6.5
FBXO47	CDC27	LRU2_M1	≥8	SEPT7P2	KAT7	B2HF_M1	≥6.5
FBXW11	DNAH12	HMXT_T1	≥6.5	SEPT7P2	KAT7	B2HF_T1	≥6.5
FBXW8	BTBD11	F11Y_T1	≥6.5	SEPT7P2	LHFPL3	LRU2_M1	≥6.5
FCHSD2	ARAP1	YNSV_T1	≥6.5	SEPT9	CUEDC1	b9b21b9	≥8
FEM1AP2	ANKRD12	ZCYX_M1	≥6.5	SEPT9	GDPD1	b9b21b9	≥8
FGF14	COL4A1	4R5V_M1	≥8	SEPT9	GRB2	AC72_T1	≥8
FGF14	DNM2	4c03c03	≥6.5	SERGEF	ANO3	SR1R_M1	≥8
FGF14	DNAJC3	SR1R_M1	≥6.5	SERPINB9	RIPK1	75Z1_T1	≥8
FGF19	EHD1	L50R_T1	≥6.5	SESN1	CCDC162P	b46aa5c	≥8
FILIP1	ATG5	RQX5_M1	≥8	SESN1	FOXJ3	2RR2_T1	≥8
FLCN	BTC	F7FD_M1	≥8	SETD5	LMCD1	af07947	≥8
FLJ37644	DDX42	Q6FY_T1	≥6.5	SF3A3	MACF1	DR8V_T1	≥8
FMN2	EFCAB7	E65C_M1	≥8	SFI1	RNF185	4R5V_M1	≥6.5
FN1	AC007563.5	TX2S_T1	≥6.5	SFI1	GRAP2	L50R_T1	≥6.5
FOXO3	EYS	EDTK_T1	≥6.5	SFTP4	PDS5A	QK84_M1	≥8
FRG1	CDK5RAP2	PF9X_T1	≥8	SGCE	LRRC6	YNSV_T1	≥8
FRG1B	CDC27	699525b	≥8	SGCZ	RP11-150O12.1	FYVH_M1	≥8
FRMD4A	FAM188A	L50R_T1	≥8	SGCZ	DDHD2	FYVH_M1	≥6.5
FUT8	C14orf39	7FNO_M1	≥6.5	SGCZ	EIF4EBP1	FYVH_M1	≥6.5
FYN	CDK12	cfdf2f24	≥6.5	SGCZ	MRPL13	T2VO_M1	≥6.5
FZD7	AC007966.1	IUCQ_T1	≥6.5	SH2D4A	KITLG	b9b21b9	≥8
G3BP2	CNTN4	699525b	≥6.5	SH3D19	LRBA	OE5B_T1	≥8
G6PC3	FMNL1	TC6T_T1	≥6.5	SH3D19	LRBA	9LEL_M1	≥8
GALNS	DYM	F7FD_M1	≥8	SH3D19	LRBA	B2HF_M1	≥8
GALNT1	DTNA	4R5V_M1	≥6.5	SH3GL1	LRBA	4R5V_M1	≥8

Continued on next page

Table S10 – continued from previous page

Gene1	Gene2	Sample	Score	Gene1	Gene2	Sample	Score
GALNTL6	GALNT7	231B_T1	≥6.5	SHANK2	CTTN	0XC1_M1	≥8
GAN	FAM18B2-	5Y1T_T1	≥6.5	SHANK2	IGF1R	HY35_T1	≥8
	CDRT4						
GDF5	ERGIC3	HMXT_T1	≥6.5	SHANK2	LRP5	ZQC5_T1	≥8
GIPC1	DNM2	WHDD_M1	≥6.5	SHB	KLHL9	LRU2_M1	≥6.5
GLI3	AC005022.1	b46aa5c	≥6.5	SHOC2	PRKG1	4R5V_M1	≥8
GLTSCR2	GLTSCR1	4ec8eca	≥8	SHPRH	ASCC3	QYXQ_M1	≥8
GMDS	GCNT2	F7FD_M1	≥8	SHROOM3	PITX2	ZCYX_M1	≥8
GMEB1	EPB41	YNSV_T1	≥8	SHROOM3	HPRT1	OLIZ_T1	≥6.5
GNA13	C17orf104	cf2f24	≥8	SIAH1	INSR	Y5G9_T1	≥6.5
GNAI3	C1orf101	699525b	≥8	SIM2	IARS	F7FD_M1	≥6.5
GNAI3	FAM102B	0E5B_T1	≥8	SIN3A	NRG4	YA4W_M1	≥8
GNB1	AC004996.1	HMXT_T1	≥8	SIPA1L3	CCNE1	7FNO_M1	≥8
GNB1	AJAP1	SR1R_M1	≥6.5	SIPA1L3	RP11-103B5.2	L50R_T1	≥6.5
GNLY	AC009961.3	b46aa5c	≥8	SKA2	RNF213	cf2f24	≥6.5
GOLGA7	ACER3	ZQC5_T1	≥8	SKAP1	CA10	B2HF_M1	≥8
GON4L	AL513123.1	2RR2_T1	≥6.5	SKAP1	CA10	B2HF_T1	≥8
GOSR1	BLMH	ZS4T_T1	≥6.5	SKI	PRKCZ	231B_T1	≥8
GPD1L	ANO10	TW0Z_T1	≥6.5	SLAIN2	DTHD1	8H0R_M1	≥8
GRHL2	FAM91A1	5f7b7fb	≥8	SLAMF1	CLSPN	JVRW_M1	≥8
GRIA3	GRAP2	8HNA_T1	≥8	SLC13A3	KLF12	FYVH_M1	≥6.5
GSDMA	ACLY	35XC_M1	≥8	SLC15A5	RREB1	SR1R_M1	≥8
GSTM3P1	ARFGEF2	SR1R_M1	≥8	SLC16A12	RNFT2	L50R_T1	≥6.5
H2AFY	FAM13B	2RR2_T1	≥8	SLC16A7	METTL2A	2S2Q_T1	≥6.5
HACE1	COL6A3	5d6b06c	≥6.5	SLC16A9	ANK3	YNSV_T1	≥8
HAS1	AP2A1	75Z1_T1	≥6.5	SLC17A8	GAS2L3	59cb2ad	≥6.5
HAT1	GLS	HMXT_T1	≥8	SLC1A2	C11orf49	0XC1_M1	≥8
HDAC4	ARHGAP21	ZS4T_T1	≥6.5	SLC20A2	NRF1	I4ZX_T1	≥8
HEATR6	BRIP1	QYXQ_M1	≥8	SLC22A20	ACAD11	372fc45	≥6.5
HECTD1	HEATR5A	YNSV_T1	≥8	SLC24A3	AC005220.3	I4ZX_T1	≥6.5
HELZ	ACSF2	cf2f24	≥8	SLC25A17	MKL1	4R5V_M1	≥8
HELZ	GDPD1	2RR2_T1	≥8	SLC25A26	ARHGAP21	WHDD_M1	≥8
HERC2	C11orf72	35XC_M1	≥6.5	SLC25A42	CCT6B	LRU2_M1	≥8
HERC2	C11orf72	5D6N_M1	≥6.5	SLC26A3	CXCL14	HIHE_T1	≥6.5
HERC2	C11orf72	A0GM_T1	≥6.5	SLC26A4	COG5	YNSV_T1	≥8
HERC2	C11orf72	E65C_M1	≥6.5	SLC29A3	ADK	TX2S_T1	≥8
HERC2	C11orf72	JVRW_M1	≥6.5	SLC2A12	PLEKHA7	Y5G9_T1	≥8
HERC2	C11orf72	KEQ4_T1	≥6.5	SLC2A1-AS1	RLF	f1ae704	≥6.5
HERC2	C11orf72	QYCP_T1	≥6.5	SLC30A8	RP11-157E21.1	L50R_T1	≥6.5
HERC2	C11orf72	SR1R_M1	≥6.5	SLC30A9	RP11-162G9.1	H9F4_M1	≥8
HERPUD2	AC007349.7	0E5B_T1	≥8	SLC35B4	PRKG1	46DP_M1	≥8
HERPUD2	ASTN2	0E5B_T1	≥6.5	SLC35E3	FAM135A	F7FD_M1	≥8
HERPUD2	AC007349.7	T2VO_M1	≥6.5	SLC35F4	CLTA	L50R_T1	≥6.5
HERPUD2	ASTN2	T2VO_M1	≥6.5	SLC38A10	RBPMS	cb6c764	≥8
HIST4H4	C12orf69	0E5B_T1	≥8	SLC39A11	BCAS3	Q6FY_T1	≥8
HLA-F	HLA-B	e45fa87	≥8	SLC39A8	DEPDC5	WL6X_M1	≥6.5
HMBOX1	CCDC25	L50R_T1	≥6.5	SLC41A3	PARP9	b46aa5c	≥8
HMGCS1	GZMA	L50R_T1	≥8	SLC45A1	INADL	615a439	≥8
HMGCS1	GZMAP1	L50R_T1	≥6.5	SLC48A1	LIMA1	F7FD_M1	≥8

Continued on next page

Table S10 – continued from previous page

Gene1	Gene2	Sample	Score	Gene1	Gene2	Sample	Score
HNF4G	BMPR2	WHDD_M1	≥6.5	SLC4A10	RBMS1	51CU_M1	≥6.5
HNRNPC	CHD8	cb6c764	≥6.5	SLC4A10	C19orf77	TX2S_T1	≥6.5
HOOK3	C12orf28	TW0Z_T1	≥6.5	SLC6A11	ADAM18	TW0Z_T1	≥8
HOOK3	ADAM5	YA4W_M1	≥6.5	SLC6A6	RPRD2	TW0Z_T1	≥8
HS6ST3	C8orf34	59cb2ad	≥8	SLC8A1-AS1	QRSL1	b46aa5c	≥6.5
hsa-mir-2117	KANSL1	T6Z1_M1	≥8	SLC9A3R1	MYOG	Q6FY_T1	≥8
hsa-mir-4763	RP11-313D6.4	HMXT_T1	≥8	SLCO1A2	NECAP1	5PJH_M1	≥6.5
hsa-mir-4763	PDCD4	HMXT_T1	≥6.5	SLFN12	RP11-686D22.8	T2VO_M1	≥6.5
HTR7	CYP7B1	D988_M1	≥8	SLIRP	CTD-2175M1.4	YNSV_T1	≥6.5
HUWE1	CTPS2	QYXQ_M1	≥8	SLMAP	DNAH12	59cb2ad	≥6.5
HYDIN	BAG4	TW0Z_T1	≥8	SMAD4	MAD2L1	0XC1_M1	≥8
HYDIN	ATG7	TW0Z_T1	≥6.5	SMARCA2	HAUS6	WHDD_M1	≥6.5
IAPP	FOXJ2	5PJH_M1	≥8	SMARCA4	KANK3	Y5G9_T1	≥8
IARS2	ATP1A4	Q6FY_T1	≥8	SMARCA4	PLA2G6	Y5G9_T1	≥8
IBTK	CERS5	GN0A_M1	≥6.5	SMARCAD1	PDLIM5	YNSV_T1	≥8
IBTK	CERS5	DBBB_M1	≥6.5	SMG6	MNT	DMG3_M1	≥8
IBTK	CERS5	F7FD_M1	≥6.5	SMURF2	GTF3C3	75Z1_T1	≥6.5
IBTK	CERS5	TM97_T1	≥6.5	SNAP25-AS1	ESF1	4c03c03	≥6.5
IFT52	CUEDC1	699525b	≥8	SND1	CASD1	46DP_M1	≥8
IFT74	FAM188A	F7FD_M1	≥6.5	SNORA31	EIF3H	B2HF_M1	≥6.5
IGF1R	CCDC33	HY35_T1	≥8	SNORD112	MPI	HY35_T1	≥6.5
IGHGP	IGHG3	4c03c03	≥6.5	snoU13	BEND7	cfd2f24	≥6.5
IGHMBP2	CLPB	372fc45	≥8	SNRNP35	SBNO1	51CU_M1	≥6.5
IKZF2	AC079610.1	0P4M_M1	≥6.5	SNTB1	SAMD12	H9F4_M1	≥8
IKZF2	AC079610.1	2S2Q_T1	≥6.5	SNTG1	CBLB	2RR2_T1	≥8
IKZF2	AC079610.1	5PJH_M1	≥6.5	SNX16	FTO	WL6X_M1	≥8
IKZF2	AC079610.1	MA6O_T1	≥6.5	SNX6	NPAS3	TX2S_T1	≥6.5
IKZF3	ACLY	35XC_M1	≥8	SORBS1	PDLIM1	T2VO_M1	≥6.5
IL12RB2	CDC73	TW0Z_T1	≥6.5	SORL1	RP11-215D10.1	HMXT_T1	≥8
IL1RAPL2	ENOX2	af07947	≥8	SOS1	RP6-65G23.3	b46aa5c	≥8
IL36A	EAF2	DMG3_T1	≥8	SOS1	ARFGEF2	TX2S_T1	≥8
INO80	DNAJC17	HMXT_T1	≥8	SOS2	NGDN	EDTK_T1	≥8
INPP4B	C10orf11	L50R_T1	≥6.5	SOX5	ELF1	0E5B_T1	≥6.5
INPP5K	DPH1	HMXT_T1	≥6.5	SOX5	ELF1	T2VO_M1	≥6.5
INSR	FCER2	Y5G9_T1	≥6.5	SPACA7	LAMP1	4c03c03	≥8
INTS2	AC012065.4	b46aa5c	≥6.5	SPAG9	MMP28	b9b21b9	≥8
INTS2	HSD3B2	F7FD_M1	≥6.5	SPAG9	PSMG4	Q6FY_T1	≥8
INTS8	ERBB4	DMG3_T1	≥6.5	SPAG9	NF1	T6Z1_M1	≥6.5
IQGAP1	DAPK2	35XC_M1	≥8	SPAG9	INPP4B	b46aa5c	≥6.5
IRX1	ALG6	35XC_M1	≥6.5	SPATA13	CTD-2184D3.5	I4ZX_T1	≥6.5
ITGB5	GOLM1	4R5V_T1	≥6.5	SPATA20	PPM1D	B2HF_M1	≥8
ITGB5	GOLM1	6F41_T1	≥6.5	SPATA24	NDST1	HMXT_T1	≥6.5
ITGB5	GOLM1	TDDP_T1	≥6.5	SPATA7	NUFIP2	8H0R_M1	≥6.5
ITGB5	GOLM1	WHDD_M1	≥6.5	SPATS2	FBXO42	51CU_M1	≥8
ITGB5	GOLM1	WL6X_M1	≥6.5	SPEF2	SKP2	IUCQ_T1	≥8
IVD	BUB1B	8H0R_M1	≥8	SPEN	DDI2	51CU_M1	≥8
JAM2	AP001432.14	TX2S_T1	≥8	SPHKAP	MYT1	TX2S_T1	≥8
JARID2	GFOD1	Q6FY_T1	≥6.5	SPINK9	KIF20B	cb6c764	≥6.5
KANK3	CERS4	Y5G9_T1	≥8	SPIRE1	C18orf1	HY35_T1	≥8

Continued on next page

Table S10 – continued from previous page

Gene1	Gene2	Sample	Score	Gene1	Gene2	Sample	Score
KANSL1	DHX8	T6Z1_M1	≥8	SPIRE1	CIDEA	HY35_T1	≥8
KAT6B	AP3M1	L50R_T1	≥8	SPOP	GNA13	2S2Q_T1	≥8
KAT6B	DLG5	QK84_M1	≥6.5	SPOP	HNF1B	T6Z1_M1	≥6.5
KAT7	ARMC2	cfd2f24	≥8	SPOP	MRPL45P2	T6Z1_M1	≥6.5
KAT7	FUT10	8MNH_T1	≥8	SPOP	RP11-192H23.4	T6Z1_M1	≥6.5
KAT8	C16orf93	8H0R_M1	≥6.5	SPOP	RP11-697E22.2	T6Z1_M1	≥6.5
KCNB2	CSMD3	35XC_M1	≥6.5	SPOP	RP11-429O1.1	cfd2f24	≥6.5
KCND2	CDK14	5D6N_M1	≥6.5	SRBD1	ASAP2	FYVH_M1	≥6.5
KCNMA1	C10orf11	L50R_T1	≥8	SRC	METTL2B	46DP_M1	≥6.5
KCNMB4	IRAK3	F7FD_M1	≥8	SRCIN1	DHX40	QYXQ_M1	≥6.5
KDM2A	CCDC88B	JVRW_M1	≥6.5	SRD5A3	AFP	EDTK_T1	≥8
KDM5A	CCDC77	46DP_M1	≥6.5	SRGAP1	GNS	2S2Q_T1	≥8
KHDRBS3	GALNTL2	TWOZ_T1	≥6.5	SRGAP1	OTOGL	RQX5_M1	≥8
KIAA0146	C18orf1	cfd2f24	≥8	SRGAP1	AFF3	86DK_M1	≥6.5
KIAA0368	C9orf84	f1ae704	≥8	SRGAP2	PLEKHA6	4WQ1_T1	≥8
KIAA0907	CCT3	59cb2ad	≥8	SRGAP2B	RAB25	cfd2f24	≥8
KIAA1217	CCNY	1ED9_T1	≥8	SRGAP2B	NUCKS1	4WQ1_T1	≥8
KIAA1217	FAM188A	4c03c03	≥6.5	SRGAP2B	BX284650.1	HWX7_M1	≥6.5
KIAA1522	CEP192	SR1R_M1	≥8	SRGAP2B	LINC00623	QYCP_T1	≥6.5
KIAA1671	CATSPERD	Y5G9_T1	≥6.5	SRP68	RP11-149P24.1	35XC_M1	≥8
KIAA1731	CTTNBP2	0XC1_M1	≥8	SRP72	AC005062.2	35XC_M1	≥6.5
KIF13B	BNIP3L	HIHE_T1	≥8	SRPK2	NRG3	e45fa87	≥8
KIF21A	C12orf40	46DP_M1	≥8	SRSF1	CHN2	B2HF_M1	≥6.5
KIF5B	EPC1	HMXT_T1	≥8	SRSF1	CHN2	B2HF_T1	≥6.5
KITLG	CEP290	b9b21b9	≥6.5	SSBP2	DHFR	OE5B_T1	≥6.5
KITLG	HAUS6	L50R_T1	≥6.5	SSBP2	DHFR	T2VO_M1	≥6.5
KLF3	KDM5B	8H0R_M1	≥8	SSH2	CWC25	WL6X_M1	≥8
KLHL11	GRB7	35XC_M1	≥8	ST3GAL5	PLEKHB1	HMXT_T1	≥6.5
KLHL5	KCNMA1	QK84_M1	≥8	ST8SIA6	GLRA2	cfd2f24	≥6.5
KPNA6	FABP3	8MNH_T1	≥8	ST8SIA6	EXD3	2RR2_T1	≥6.5
KRT18P55	CASC3	T6Z1_M1	≥8	STAM	RP11-750B16.1	af07947	≥6.5
KRT19	CNTNAP1	b46aa5c	≥8	STARD3	DAB1	35XC_M1	≥6.5
KSR2	FBXO21	TWOZ_T1	≥6.5	STAT3	CDK12	T6Z1_M1	≥8
L3MBTL1	CEP95	cfd2f24	≥8	STAT4	AC062020.2	EDTK_T1	≥6.5
L3MBTL1	CDH22	cfd2f24	≥6.5	STAT4	AC098872.3	EDTK_T1	≥6.5
LACE1	BAZ2B	b46aa5c	≥8	STEAP1B	RAPGEF5	8MNH_T1	≥8
LACE1	FIG4	F11Y_T1	≥8	STIP1	PLCB3	DMG3_M1	≥8
LAMTOR1	ARRB1	HWX7_M1	≥8	STK17A	INADL	231B_T1	≥8
LARP4B	HACE1	L50R_T1	≥8	STK17A	N4BP3	L50R_T1	≥6.5
LARP7	AC092661.1	QK84_M1	≥6.5	STK32C	DLG5	e45fa87	≥8
LDLR	ELAVL3	Y5G9_T1	≥8	STK38L	ASAH1	b9b21b9	≥8
LEPROT	FAF1	TWOZ_T1	≥8	STK39	BRIP1	b46aa5c	≥6.5
LEPROT	AGBL4	TWOZ_T1	≥6.5	STOX1	ADK	L50R_T1	≥6.5
LGMM	CDC14A	QYXQ_T1	≥6.5	STRA13	CSNK1D	8MNH_T1	≥8
LGMM	CDC14A	7DTJ_T1	≥6.5	STX16	PHACTR3	8H0R_M1	≥8
LGMM	CDC14A	KEQ4_T1	≥6.5	STX16	RP11-522N14.1	2S2Q_T1	≥6.5
LGR4	GALNTL6	L50R_T1	≥8	STX16-NPEPL1	PHACTR3	8H0R_M1	≥8
LHFPL2	AC013409.1	46DP_M1	≥6.5	STX16-NPEPL1	RP11-522N14.1	2S2Q_T1	≥6.5
LINC00243	CMAHP	5D6N_M1	≥6.5	STX3	RP11-626H12.2	372fc45	≥6.5

Continued on next page

Table S10 – continued from previous page

Gene1	Gene2	Sample	Score	Gene1	Gene2	Sample	Score
LINC00460	CDK12	T6Z1_T1	≥6.5	STXBP4	MARCH10	QYXQ_M1	≥8
LINC00674	C1orf198	Q6FY_T1	≥8	STXBP4	NUP153	QYXQ_M1	≥8
LINS	CNOT2	JVRW_M1	≥6.5	STXBP4	SDF2	cb6c764	≥8
LINS	AP3B1	NL3B_T1	≥6.5	STXBP4	ARHGAP23	cfd2f24	≥8
LIPT1	ECT2	35XC_M1	≥6.5	STXBP4	ACOX1	B2HF_M1	≥8
LOXL1	GABPB1	HY35_T1	≥6.5	STXBP4	ACOX1	B2HF_T1	≥8
LPP	HSD17B4	D988_M1	≥8	STXBP4	C7orf31	B2HF_T1	≥8
LPP	AL133168.3	WL6X_M1	≥8	STXBP4	BRIP1	WHDD_M1	≥8
LRBA	CYB5B	JVRW_M1	≥6.5	SULF1	RHBG	LU50_M1	≥6.5
LRCH2	KIF21A	D988_M1	≥8	SULT6B1	EIF2AK2	59cb2ad	≥8
LRIF1	KCND3	YNSV_T1	≥8	SUMF1	CNTN4	699525b	≥8
LRP2	FASTKD1	59cb2ad	≥8	SUMO1P1	SLC24A3	I4ZX_T1	≥6.5
LRP5	CARNS1	4WQ1_T1	≥8	SUMO3	HSPA13	L50R_T1	≥8
LRP5	CCS	HY35_T1	≥8	SUPT6H	CCR7	T6Z1_M1	≥8
LRRC16A	KDM1B	LU50_M1	≥8	SUV420H1	RP11-619A14.3	4WQ1_T1	≥6.5
LRRC37A11P	CPD	8H0R_M1	≥8	SUZ12P	SDK2	JVRW_M1	≥8
LRRFIP1	AC112715.2	JVRW_M1	≥6.5	SV2C	IQGAP2	E65C_M1	≥6.5
LRRFIP2	GALNTL2	TW0Z_T1	≥8	SVIL	PARD3	4R5V_M1	≥8
LUZP2	ELP4	0E5B_T1	≥6.5	SVIL	RP11-166N17.1	4R5V_M1	≥6.5
LUZP2	ELP4	T2VO_M1	≥6.5	SVIP	RP11-313M3.1	0XC1_M1	≥6.5
IYZ	C1orf106	TW0Z_T1	≥6.5	SYBU	CDCA2	35XC_M1	≥6.5
MACF1	HIVEP3	SR1R_M1	≥6.5	SYCP2L	POU2F1	Q6FY_T1	≥6.5
MACROD2	KIAA1328	4c03c03	≥6.5	SYDE2	RAB3B	L50R_T1	≥6.5
MAD1L1	ERBB2	35XC_M1	≥6.5	SYN2	IGHV1OR21-1	QYXQ_M1	≥6.5
MAK	CDKAL1	T6Z1_T1	≥6.5	SYN3	ACOT13	007M_M1	≥6.5
MAK16	HMBOX1	L50R_T1	≥6.5	SYN3	ACOT13	5PJH_M1	≥6.5
MAOB	EFHC2	59cb2ad	≥8	SYNE2	LINC00478	615a439	≥8
MAP2K4	IFT122	SR1R_M1	≥8	SYNGR2	PGS1	cb6c764	≥8
MAP3K1	ENC1	4R5V_T1	≥8	SYT13	SHANK2	0XC1_M1	≥8
MAP3K5	LRRC16A	OLIZ_T1	≥8	TACC2	C11orf85	L50R_T1	≥6.5
MAPK8	FRMPD2	YN SV_T1	≥6.5	TACC2	GHITM	SR1R_M1	≥6.5
MAPKAPK2	DENND1B	Q6FY_T1	≥8	TACO1	SUMF1	Q6FY_T1	≥6.5
MAPKAPK3	HEMK1	HMXT_T1	≥6.5	TACSTD2	FAM73A	35XC_M1	≥6.5
MARCH10	ARMC2	b46aa5c	≥6.5	TADA2A	MSI2	b9b21b9	≥8
MARCH11	ENPP1	2RR2_T1	≥6.5	TADA2A	SLC25A19	AC72_T1	≥6.5
MBD5	ATL2	4R5V_M1	≥8	TAF13	NUP153	QYXQ_M1	≥8
MBD5	DISP1	35XC_M1	≥6.5	TANC2	PDSS2	b46aa5c	≥8
MCFD2	HSD17B4	QYXQ_M1	≥6.5	TANC2	RPS6KB1	cb6c764	≥8
MCFD2	HSD17B4	e45fa87	≥6.5	TANC2	HEATR6	b46aa5c	≥6.5
MCFD2	HSD17B4	35XC_M1	≥6.5	TANC2	PRDM11	2RR2_T1	≥6.5
MCFD2	HSD17B4	AC72_T1	≥6.5	TANC2	SMARCA4	WHDD_M1	≥6.5
MCFD2	HSD17B4	RZBM_M1	≥6.5	TANK	PSMD14	HMXT_T1	≥8
MCFD2	HSD17B4	SR1R_M1	≥6.5	TAOK1	PCTP	7FNO_M1	≥8
MCFD2	HSD17B4	WL6X_M1	≥6.5	TAOK1	C17orf79	8MNH_T1	≥8
MCRS1	ANKS1B	b9b21b9	≥8	TAOK1	CDK12	IUCQ_T1	≥8
ME1	CD109	DMG3_M1	≥8	TAOK1	KAT6A	HMXT_T1	≥6.5
MECOM	EGFEM1P	SR1R_M1	≥8	TAOK3	RNFT2	TW0Z_T1	≥8
MECOM	GOLIM4	NF9D_M1	≥6.5	TATDN1	FBXO32	YNSV_T1	≥8
MED1	CDK12	8MNH_T1	≥6.5	TATDN2	IDO2	TW0Z_T1	≥8

Continued on next page

Table S10 – continued from previous page

Gene1	Gene2	Sample	Score	Gene1	Gene2	Sample	Score
MED18	EYA3	b9b21b9	≥6.5	TATDN2	RP11-44K6.3	TW0Z_T1	≥6.5
MERTK	C2orf15	Q6FY_T1	≥8	TBC1D16	GGA3	f1ae704	≥8
Metazoa_SR P	ATR	PF9X_T1	≥6.5	TBC1D16	SPECC1	QYXQ_M1	≥6.5
METTL15	CREB3L1	0XC1_M1	≥6.5	TBC1D16	L3MBTL1	cfd2f24	≥6.5
METTL2B	DENND2A	46DP_M1	≥8	TBC1D16	RPL19	cfd2f24	≥6.5
MFHAS1	GPT2	WL6X_M1	≥8	TBC1D23	C3orf26	DMG3_M1	≥8
MFHAS1	CHD9	WL6X_M1	≥6.5	TBC1D3G	NTF4	WL6X_M1	≥6.5
MFSD6	MAPK10	TX2S_T1	≥8	TBC1D3P2	AC008687.1	WL6X_M1	≥6.5
MGAT3	KAT6B	L50R_T1	≥8	TBC1D9	RP11-203B7.2	DR8V_T1	≥8
MGAT4C	CCT2	L50R_T1	≥8	TBC1D9	RP11-362F19.1	4R5V_M1	≥6.5
MICAL1	ITGA11	372fc45	≥6.5	TBCA	BIRC6	YNSV_T1	≥8
MICAL3	CTA-85E5.10	L50R_T1	≥8	TBCD	MYH10	D988_M1	≥6.5
MIEN1	MAD1L1	35XC_M1	≥6.5	TBKBP1	CLPB	RZBM_M1	≥6.5
MITD1	ECT2	35XC_M1	≥8	TC2N	CATSPERB	WHDD_M1	≥8
MITF	FOXP1	8H0R_M1	≥6.5	TCF20	MYH9	EDTK_T1	≥8
MLEC	ACSF3	8HNA_T1	≥8	TCF7L1	AC009961.3	b46aa5c	≥8
MLL3	AC008132.1	TW0Z_T1	≥8	TCF7L1	PLA2R1	b46aa5c	≥6.5
MLL5	AKAP9	5PJH_M1	≥8	TCIRG1	ALDH3B2	HY35_T1	≥6.5
MLLT1	CATSPERD	Y5G9_T1	≥8	TCP11	NUDT3	59cb2ad	≥8
MMP26	AASDHPPPT	F11Y_T1	≥6.5	TCTN2	RILPL1	86DK_M1	≥6.5
MMP28	HSD17B12	b9b21b9	≥6.5	TDRD5	PTPRC	4WQ1_T1	≥8
MOGAT1	CUL3	b9b21b9	≥8	TDRD5	CDC42BPA	Q6FY_T1	≥8
MOXD1	HBS1L	231B_T1	≥8	TDRKH	GLDC	OLIZ_T1	≥6.5
MPDZ	LINC00583	51CU_M1	≥6.5	TEAD4	CACNA1C	HMXT_T1	≥8
MPP5	GPHN	YNSV_T1	≥8	TEAD4	ITFG2	YNSV_T1	≥8
MRPL1	C10orf57	QK84_M1	≥8	TEC	MIER3	WL6X_M1	≥6.5
MRPL11	CPT1A	NL3B_T1	≥8	TEKT3	ACACA	cf d2f24	≥8
MRPL21	C11orf74	0XC1_M1	≥6.5	TEN1	RIMS2	35XC_M1	≥8
MRPL45	FBXO28	Q6FY_T1	≥8	TESC	INPP4B	L50R_T1	≥6.5
MRPL48	MOCOS	4R5V_M1	≥8	TEX14	DCAKD	cf d2f24	≥6.5
MRS2	BTN3A3	T6Z1_T1	≥6.5	TEX2	RAD51C	cf d2f24	≥6.5
MS4A14	KDM2A	JVRW_M1	≥8	TEX28	BCAP31	PF9X_T1	≥6.5
MSI2	ARHGAP23	cf d2f24	≥8	TFG	GPR128	DBBB_M1	≥8
MSI2	BCAS3	TW0Z_T1	≥8	TFG	GPR128	NF9D_M1	≥8
MSRA	CNOT1	WL6X_M1	≥6.5	TFG	GPR128	Y5G9_T1	≥8
MTA3	AC079807.4	TX2S_T1	≥8	TFRC	SLC51A	dd3c42e	≥8
MTCH2	CRY2	PF9X_T1	≥8	TGFBRAP1	ANAPC1	Q6FY_T1	≥6.5
MTDH	LAPTM4B	T2VO_M1	≥8	TGS1	IPO9-AS1	TW0Z_T1	≥6.5
MTF1	MEAF6	B2HF_M1	≥8	TGS1	RNA5SP267	TW0Z_T1	≥6.5
MTMR3	KAT6B	L50R_T1	≥8	THADA	MYBL2	TX2S_T1	≥6.5
MTMR3	LIMK2	L50R_T1	≥6.5	THBS1	RP11-624L4.1	IUCQ_T1	≥6.5
MTMR4	CDR2L	B2HF_M1	≥6.5	THBS1	RP11-624L4.1	TX2S_T1	≥6.5
MTMR4	CDR2L	B2HF_T1	≥6.5	THBS1	RP11-624L4.1	YA4W_M1	≥6.5
MTOR	EXOSC10	B2HF_T1	≥8	THRA	PCGF2	WL6X_M1	≥6.5
MTUS1	FAM86A	dd3c42e	≥8	THRAP3	SKIL	XV6H_M1	≥6.5
MUC16	BRD4	WHDD_M1	≥6.5	THSD4	LRRC49	F7FD_M1	≥8
MUC16	CEP112	WHDD_M1	≥6.5	THSD4	FAH	HY35_T1	≥8
MX1	ABCG1	TX2S_T1	≥8	THSD4	CYP27C1	DBBB_M1	≥6.5
MYBPC1	ARL1	HMXT_T1	≥6.5	THSD4	IL16	HY35_T1	≥6.5

Continued on next page

Table S10 – continued from previous page

Gene1	Gene2	Sample	Score	Gene1	Gene2	Sample	Score
MYEOV	CCND1	FYVH_M1	≥8	THSD4	CYP27C1	QK84_M1	≥6.5
MYEOV	IGF1R	HY35_T1	≥6.5	THSD4	CYP27C1	XV6H_M1	≥6.5
MYH6	ERO1L	EDTK.T1	≥8	THUMPD2	LACE1	b46aa5c	≥6.5
MYO10	ENPP1	2RR2.T1	≥6.5	TIPIN	PLCB2	b46aa5c	≥8
MYO1D	ADORA2B	EDTK.T1	≥8	TJP1	AC009505.4	T6Z1_M1	≥8
MYO5B	ACAA2	L50R_T1	≥8	TLCD1	SGCZ	8H0R_M1	≥6.5
MYO7A	FAM168A	DR8V_T1	≥8	TLK1	HIBCH	WHDD_M1	≥8
MYO9A	IQCH	HY35_T1	≥8	TLK2	MAML3	b46aa5c	≥8
MYOM1	LPIN2	DMG3_M1	≥8	TLK2	METTL2B	HMXT_T1	≥8
MYOM3	LUZP1	59cb2ad	≥8	TLN1	LINC00032	LU50_M1	≥8
MYT1	C2orf83	TX2S_T1	≥8	TM4SF1	CP	HMXT_T1	≥8
NAA40	C12orf29	L50R_T1	≥8	TM7SF3	ITPR2	HMXT_T1	≥8
NAA40	ABCA4	L50R_T1	≥6.5	TMC2	PRCP	B2HF_M1	≥8
NAALADL2	GOLIM4	NF9D_M1	≥6.5	TMC2	PRCP	B2HF_T1	≥8
NADSYN1	C20orf94	B2HF_M1	≥6.5	TMCC1	AC079896.1	35XC_M1	≥6.5
NADSYN1	C20orf94	B2HF_T1	≥6.5	TMEFF2	DNAJC10	cfd2f24	≥6.5
NADSYN1	CCDC33	HY35_T1	≥6.5	TMEM100	NPEPPS	cfd2f24	≥8
NAT10	AC068858.1	0XC1_M1	≥8	TMEM100	RP11-	cfd2f24	≥6.5
					1407O15.2		
NAV3	ANKRD30A	Q6FY_T1	≥8	TMEM104	PRKCA	F11Y_T1	≥8
NAV3	ANKRD30A	QYXQ_T1	≥6.5	TMEM104	FLJ37644	B2HF_T1	≥6.5
NAV3	ANKRD30A	5Y1T_T1	≥6.5	TMEM117	MON2	b9b21b9	≥8
NAV3	ANKRD30A	7DTJ_T1	≥6.5	TMEM117	SCAF11	b9b21b9	≥6.5
NAV3	ANKRD30A	86DK_M1	≥6.5	TMEM131	C2orf15	Q6FY_T1	≥8
NAV3	ANKRD30A	NL3B_T1	≥6.5	TMEM132B	ITPR2	E65C_M1	≥8
NBEA	CASC3	I4ZX_T1	≥6.5	TMEM132B	PIGQ	5D6N_M1	≥6.5
NCKAP1	HSPD1	cfd2f24	≥8	TMEM14B	CDKAL1	T6Z1_T1	≥8
NCKAP5	MGAT5	HMXT_T1	≥8	TMEM14B	RP4-660H19.1	QYXQ_M1	≥6.5
NCOA1	ABCA10	b46aa5c	≥8	TMEM164	STX7	2RR2_T1	≥6.5
NCOA7	FBXL4	QYXQ_M1	≥8	TMEM167A	CTD-2001C12.1	35XC_M1	≥6.5
NCOA7	HEY2	HMXT_T1	≥6.5	TMEM182	SLC9A2	FYVH_M1	≥6.5
NDST3	FTO	LU50_M1	≥6.5	TMEM189	PRKCE	TX2S_T1	≥8
NDUFAF6	LRRC36	L50R_T1	≥8	TMEM19	NAP1L1	TW0Z_T1	≥8
NDUFB4	GTF2E1	cb6c764	≥6.5	TMEM213	PARP12	46DP_M1	≥6.5
NEBL	KIAA1217	4R5V_M1	≥8	TMEM214	FBXO8	0XC1_M1	≥8
NEBL	HK1	H9F4_M1	≥8	TMEM43	IRAK2	TW0Z_T1	≥8
NEBL	DDX11L1	ZS4T_T1	≥6.5	TMEM43	NEK10	TW0Z_T1	≥8
NEDD1	AKAP14	699525b	≥8	TMEM50B	DYRK1A	TX2S_T1	≥8
NEDD4	ANKRD30A	86DK_M1	≥6.5	TMEM55A	RAB11FIP1	YA4W_M1	≥8
NEK10	IRAK2	TW0Z_T1	≥6.5	TMEM63A	SUSD4	YA4W_M1	≥8
NEK11	C10orf68	HY35_T1	≥6.5	TMEM9	RP11-	TW0Z_T1	≥6.5
					470M17.2		
NEMF	LAMA4	EDTK.T1	≥8	TMOD3	PPFIA1	HY35_T1	≥6.5
NEMF	ARHGAP5	X0Z1_T1	≥6.5	TMOD3	RCE1	HY35_T1	≥6.5
NF1	GNA13	2RR2_T1	≥8	TMTC3	KITLG	b9b21b9	≥8
NF2	MTMR3	51CU_M1	≥8	TNFRSF10B	INTS9	RQX5_M1	≥8
NFASC	BRIP1	Q6FY_T1	≥8	TNFSF9	CAMSAP3	b9b21b9	≥6.5
NFIA	C3orf26	35XC_M1	≥6.5	TNKS	RP11-479G22.3	4R5V_M1	≥6.5
NFIB	MYB	Q4W1_T1	≥8	TNKS2	BTAF1	51CU_M1	≥8

Continued on next page

Table S10 – continued from previous page

Gene1	Gene2	Sample	Score	Gene1	Gene2	Sample	Score
NFIX	BRD4	Y5G9_T1	≥8	TNPO2	MACROD2	4c03c03	≥8
NFYA	FOXP4	PF9X_T1	≥8	TNRC6C	RNF157	LU50_M1	≥6.5
NHEJ1	DNPEP	51CU_M1	≥8	TNS3	NAT10	0XC1_M1	≥8
NIPBL	AC015820.1	5D6N_M1	≥6.5	TNS3	S100A10	bed845b	≥6.5
NIT1	DUSP10	Q6FY_T1	≥6.5	TNS4	KRT222	4R5V_T1	≥8
NLK	KRT18P55	T6Z1_M1	≥8	TOM1L1	C6orf183	cf2f24	≥6.5
NLK	LRRC37A3	2RR2_T1	≥8	TOM1L2	CD3D	AC72_T1	≥8
NLK	ADAP2	3fc2f6	≥6.5	TOM1L2	MPZL2	AC72_T1	≥8
NOD1	DDX56	B2HF_T1	≥8	TOM1L2	B9D1	AC72_T1	≥6.5
NOL11	ATP13A3	AEK9_T1	≥6.5	TOP2A	CASC3	QYXQ_M1	≥8
NOL11	ARHGAP24	TW0Z_T1	≥6.5	TOP2A	AC126365.1	QYXQ_M1	≥6.5
NOP2	NFIA	231B_T1	≥8	TOP2A	CACNB1	QYXQ_M1	≥6.5
NOTCH2NL	DNM3	LRU2_M1	≥6.5	TOPBP1	RP11-284G10.1	f1ae704	≥8
NOTCH3	CEP112	WHDD_M1	≥6.5	TOPORS-AS1	KRT13	DBBB_M1	≥8
NPAS1	DHX34	4c03c03	≥8	TOR1AIP2	SOAT1	cf2f24	≥8
NPEPPS	NF1	NL3B_T1	≥8	TP53BP2	PLA2G4A	TX2S_T1	≥8
NPIPL3	NDE1	ZS4T_T1	≥6.5	TP53I11	CAPRIN1	0XC1_M1	≥6.5
NPLOC4	ALYREF	HMXT_T1	≥8	TP53I11	LRRC4C	0XC1_M1	≥6.5
NPLOC4	HLF	B2HF_M1	≥6.5	TPD52	FABP4	X0Z1_T1	≥8
NPLOC4	HLF	B2HF_T1	≥6.5	TPD52	CSMD3	TW0Z_T1	≥6.5
NPLOC4	HGS	T2VO_M1	≥6.5	TPD52L1	NCOA7	HMXT_T1	≥8
NPSR1-AS1	MSI2	B2HF_M1	≥8	TPPP	BRD9	QYXQ_T1	≥6.5
NR2F6	BABAM1	4R5V_M1	≥6.5	TPST1	EYA2	ZS4T_T1	≥6.5
NR6A1	GSN	PF9X_T1	≥8	TPTE	AC008132.1	TW0Z_T1	≥8
NRCAM	EMCN	5PJH_M1	≥8	TPTE	MLL3	007M_M1	≥6.5
NRG1	ATP8A1	L1PK_T1	≥8	TPTE2P5	RP11-64P12.8	4R5V_T1	≥8
NRG1	MAK16	L50R_T1	≥6.5	TPTE2P5	TPTE2	6F41_T1	≥8
NRG3	MLL5	e45fa87	≥6.5	TPTE2P5	TPTE2	Q6FY_T1	≥8
NSMCE2	COL22A1	X0Z1_T1	≥8	TPTE2P5	RP11-64P12.8	ZCYX_M1	≥8
NSMCE2	CIR1P2	LRU2_M1	≥6.5	TPTE2P5	TPTE2	ZCYX_M1	≥8
NSMCE2	Metazoa_SR	LRU2_M1	≥6.5	TRAF3IP2-AS1	PTPRT	cf2f24	≥8
NSMCE4A	ATE1	L50R_T1	≥8	TRAP1	BCAR4	b46aa5c	≥6.5
NSRP1	EFCAB5	8H0R_M1	≥8	TRAPPC10	ERG	X0Z1_T1	≥8
NT5C1B	ATL2	4R5V_M1	≥6.5	TRAPPC10	FAM3B	X0Z1_T1	≥8
NT5C1B	MBD5	4R5V_M1	≥6.5	TRAPPC10	RP11-15M15.1	X0Z1_T1	≥8
NT5C3	COA1	L50R_T1	≥8	TRAPPC10	TFF3	X0Z1_T1	≥8
NTPCR	FLVCR1	cf2f24	≥8	TRAPPC8	RP11-746B8.1	8H0R_M1	≥6.5
NUDT12	KCNN2	007M_M1	≥6.5	TRAPPC9	AL137003.1	HMXT_T1	≥6.5
NUFIP2	CDK12	8H0R_M1	≥8	TRDMT1	CDC123	cf2f24	≥6.5
NUGGC	BMP1	699525b	≥6.5	TRHDE	ACP6	TW0Z_T1	≥8
NUP133	CDC42BPA	Q6FY_T1	≥8	TRIM2	FBXW7	HMXT_T1	≥8
NUP153	JARID2	WHDD_M1	≥8	TRIM36	CCDC112	HMXT_T1	≥8
NUP205	AGK	TX2S_T1	≥8	TRIM37	LINC00511	cf2f24	≥8
NUP210L	GATAD2B	HMXT_T1	≥8	TRIM37	RPS6KB1	cf2f24	≥8
NUP98	INPP4B	L50R_T1	≥8	TRIM37	SNHG16	cf2f24	≥8
NXPH1	KIAA1217	7FNO_M1	≥6.5	TRIM37	FLJ37644	2RR2_T1	≥8
NXPH3	CACNA1G	T6Z1_M1	≥6.5	TRIM37	HOXB-AS3	JVRW_M1	≥8
NYAP2	CUL3	QK84_M1	≥8	TRIM37	PPM1E	Q6FY_T1	≥8
NYAP2	FN1	TX2S_T1	≥8	TRIM37	TBC1D7	Q6FY_T1	≥8

Continued on next page

Table S10 – continued from previous page

Gene1	Gene2	Sample	Score	Gene1	Gene2	Sample	Score
OACYLP	C12orf49	L50R_T1	≥8	TRIM37	MARCH10	b9b21b9	≥6.5
ODZ2	CNOT6	D988_M1	≥8	TRIM37	RARA	cfdf2f24	≥6.5
OFCC1	ATG5	QYXQ_M1	≥8	TRIM44	LDLRAD3	OE5B_T1	≥8
OIT3	FAM149B1	YNSV_T1	≥8	TRIM60P19	MLL3	cfdf2f24	≥6.5
OMG	APPBP2	B2HF_M1	≥8	TRIM8	TACC2	SR1R_M1	≥6.5
OR13Z1P	HYDIN	TW0Z_T1	≥8	TRIO	ARHGEF3	E65C_M1	≥6.5
OR2Z1	GIPC1	E65C_M1	≥6.5	TRIP13	RP1-158P9.1	35XC_M1	≥6.5
OR5BB1P	NUMA1	8MNH_T1	≥6.5	TRMT2A	OR2J3	OE5B_T1	≥6.5
ORAOV1	CIT	L50R_T1	≥8	TRMT2A	OR2J3	T2VO_M1	≥6.5
ORAOV1	DDB1	L50R_T1	≥8	TRNT1	CNTN4	YNSV_T1	≥8
ORC4	GPD2	35XC_M1	≥6.5	TRPM7	LEO1	HY35_T1	≥8
ORMDL3	ACACA	35XC_M1	≥8	TRPM7	MAPK6	HY35_T1	≥6.5
OSBPL6	CIR1	TX2S_T1	≥8	TRPS1	SLC36A2	3b8237c	≥8
OSBPL6	AC073283.4	TX2S_T1	≥6.5	TRPS1	RP11-536K17.1	T2VO_M1	≥6.5
OSR2	KB-1047C11.2	TW0Z_T1	≥6.5	TSEN2	RP11-30J20.1	TW0Z_T1	≥6.5
OSTM1	DDX42	b46aa5c	≥8	TSEN54	GRB2	7FNO_M1	≥8
OTUD4	DOCK7	4R5V_M1	≥8	TSNAX	PTPRC	Q6FY_T1	≥6.5
OTUD6B	NECAB1	YA4W_M1	≥8	TSPAN14	DUPD1	46DP_M1	≥8
OXCT1	GCSHP1	IUCQ_T1	≥6.5	TSPAN14	C22orf45	HGX7_M1	≥6.5
OXNAD1	GHRL	YA4W_M1	≥8	TSPAN15	RP11-359E19.2	46DP_M1	≥6.5
OXR1	FAM49B	TC6T_T1	≥8	TSPAN5	FAM190A	WL6X_M1	≥8
OXR1	LARP1B	ZS4T_T1	≥8	TSPAN8	RP11-495P10.2	TW0Z_T1	≥6.5
PACSIN2	MKL1	WL6X_M1	≥6.5	TSR3	AC093515.1	TX2S_T1	≥6.5
PAFAH2	ARID1A	OE5B_T1	≥6.5	TTC16	SLC12A7	4R5V_M1	≥8
PAK1	MTL5	ZQC5_T1	≥8	TTC17	SS18	4R5V_M1	≥8
PAK1	C11orf49	HY35_T1	≥6.5	TTC28	THOC5	8MNH_T1	≥8
PAK1	CYP4Z1	TX2S_T1	≥6.5	TTC28	PIWI3	L50R_T1	≥8
PAK1	CPT1A	ZQC5_T1	≥6.5	TTC28	CERS4	Y5G9_T1	≥8
PAK7	JAG1	HMXT_T1	≥6.5	TTC28	CTA-85E5.10	L50R_T1	≥6.5
PAMR1	HIPK3	dd3c42e	≥6.5	TTC28	MYO18B	Y5G9_T1	≥6.5
PARK2	CNKSRS3	T6Z1_M1	≥8	TTC3	GART	TX2S_T1	≥8
PARM1	ALB	699525b	≥8	TTC3	HLCS	TX2S_T1	≥8
PARM1	LINC00504	699525b	≥6.5	TTC39B	OLAH	L50R_T1	≥6.5
PARP12	ATP6V0A4	46DP_M1	≥8	TTC39C	CCDC160	PF9X_T1	≥6.5
PBX1	CDC73	SR1R_M1	≥8	TTC6	MIPOL1	DMG3_M1	≥8
PBX1	F11R	SR1R_M1	≥8	TTC6	MIPOL1	007M_M1	≥8
PBX3	MAPKAP1	WHDD_M1	≥8	TTC6	MIPOL1	HY35_T1	≥8
PBX3	NEK6	WHDD_M1	≥6.5	TTC6	MIPOL1	WL6X_M1	≥8
PCBD1	KCNMA1	L50R_T1	≥8	TTC6	BMP4	T6Z1_M1	≥6.5
PCDH20	AL109763.2	F7FD_M1	≥6.5	TTI2	HMBOX1	L50R_T1	≥8
PCGF2	CLTC	cfdf2f24	≥8	TTI2	ADAM32	8MNH_T1	≥6.5
PCNT	NBEA	TX2S_T1	≥8	TTLL7	CDCA5	L50R_T1	≥8
PCNXL4	FUT8	231B_T1	≥8	TTTY14	MACROD1	L50R_T1	≥6.5
PCP4	DOPEY2	X0Z1_T1	≥8	TTYH2	BCAS3	Q6FY_T1	≥8
PCTP	HEATR6	F7FD_M1	≥8	TUBE1	LAMA4	8MNH_T1	≥8
PCTP	CCR7	WL6X_M1	≥6.5	TUBGCP3	IRS2	WHDD_M1	≥8
PDCD4	CITF22-92A6.1	HMXT_T1	≥6.5	TULP3	CACNA1C	HMXT_T1	≥8
PDE1C	MYT1	T2VO_M1	≥8	TULP4	EGFLAM	2RR2_T1	≥8
PDE3B	CLTC	2RR2_T1	≥8	TUSC3	RAPGEFL1	8H0R_M1	≥6.5

Continued on next page

Table S10 – continued from previous page

Gene1	Gene2	Sample	Score	Gene1	Gene2	Sample	Score
PDE4B	GNG12	35XC_M1	≥6.5	TWIST2	MSL3P1	T2VO_M1	≥6.5
PDE4DIP	KDM5B	T6Z1_T1	≥6.5	TWSG1	CEP192	cfdf2f24	≥6.5
PDE4DIP	NOTCH2	8H0R_M1	≥6.5	TXNDC9	TMEM87B	Q6FY_T1	≥8
PDE4DIP	NDUFS4	IUCQ_T1	≥6.5	TYW1	RABGEF1	59cb2ad	≥8
PDE7A	ATPBD4	F7FD_M1	≥6.5	U1	ENY2	35XC_M1	≥6.5
PDE7A	NDST1	HMXT_T1	≥6.5	U2AF2	CDC42EP5	75Z1_T1	≥8
PDIA2	IFT140	AEK9_T1	≥8	U6	RLF	f1ae704	≥8
PDIA4	DTX2P1-	ZCYX_M1	≥6.5	U6	TMCC1	35XC_M1	≥8
	UPK3BP1-						
	PMS2P11						
PDIA5	ITGB5	SR1R_M1	≥8	U6	RP11-127H5.1	35XC_M1	≥6.5
PDLIM7	LMAN2	ZS4T_T1	≥8	U6	PARD3B	EDTK_T1	≥6.5
PDS5B	CDK12	I4ZX_T1	≥8	U6	C10orf11	QK84_M1	≥6.5
PDS5B	NBEA	TX2S_T1	≥8	U6	NARS2	ZQG5_T1	≥6.5
PDSS2	AHI1	T6Z1_T1	≥8	U7	SVIL	4R5V_M1	≥6.5
PDSS2	ARMC2	cfdf2f24	≥8	UACA	RFWD3	HY35_T1	≥8
PDSS2	ERO1L	EDTK_T1	≥8	UBA1	SYAP1	QYXQ_M1	≥6.5
PDSS2	C6orf203	TW0Z_T1	≥6.5	UBAP1	DRAM1	QK84_M1	≥6.5
PDZD2	CERS6	RQX5_M1	≥6.5	UBAP2	ELOVL2	DMG3_M1	≥8
PDZD8	C14orf180	LU50_M1	≥8	UBAP2	B4GALT1	HMXT_T1	≥6.5
PDZRN3	FOXP1	8H0R_M1	≥8	UBAP2L	DENND4B	T6Z1_M1	≥6.5
PEX7	GRIK2	QYXQ_M1	≥8	UBC	UBB	cb6c764	≥8
PEX7	EYA4	T6Z1_T1	≥6.5	UBC	UBB	e64126c	≥8
PFDN2	F11R	DMG3_M1	≥6.5	UBE2G1	CTDSPL2	4R5V_M1	≥8
PFKFB2	CEP192	HMXT_T1	≥8	UBE2M	TRIM28	YNSV_T1	≥6.5
PFKFB3	AKR1C1	HMXT_T1	≥8	UBL3	TNFRSF19	WHDD_M1	≥8
PFKL	PCNT	TX2S_T1	≥8	UBL3	RP1-225E12.2	T6Z1_T1	≥6.5
PGAM1P2	PAK1	WHDD_M1	≥6.5	UBR4	CAMK2D	E65C_M1	≥6.5
PGS1	C17orf99	cb6c764	≥8	UBR5	AZIN1	59cb2ad	≥8
PHF20	AHCY	dd3c42e	≥8	UBXN2A	TARBP1	L1PK_T1	≥8
PHF20	ANO1	dd3c42e	≥6.5	UBXN2A	TARBP1	4R5V_M1	≥6.5
PHF20	FGF3	dd3c42e	≥6.5	UBXN2A	TARBP1	ZCYX_M1	≥6.5
PHF20L1	CA2	X0Z1_T1	≥8	UCHL5	GADD45A	TW0Z_T1	≥6.5
PHF3	EYS	EDTK_T1	≥6.5	UCP2	MYEOV	DR8V_T1	≥6.5
PHKB	LONP2	YA4W_M1	≥8	UCP2	P2RY6	DR8V_T1	≥6.5
PHTF1	PHGDH	4R5V_T1	≥6.5	UFD1L	CABIN1	Z2AO_T1	≥6.5
PICALM	MAPK10	Y5G9_T1	≥8	UFL1	AIM1	TW0Z_T1	≥8
PIGR	C18orf1	HMXT_T1	≥6.5	UGDH	RP11-63A11.1	cfdf2f24	≥8
PIR	CCDC3	cfdf2f24	≥6.5	UGGT2	GREB1	0XC1_M1	≥8
PITHD1	CUL4A	IUCQ_T1	≥8	UGT3A2	ADAMTS12	35XC_M1	≥8
PITPNC1	CA10	b9b21b9	≥8	UHRF1BP1L	SCYL2	OLIZ_T1	≥6.5
PITPNC1	NOL11	8H0R_M1	≥8	ULK4	RP11-187E13.2	5d6b06c	≥6.5
PITPNC1	B3GNTL1	2RR2_T1	≥6.5	ULK4	TRAK1	TW0Z_T1	≥6.5
PITPNC1	PIK3C2B	Q6FY_T1	≥6.5	UNC5C	BTNL9	OE5B_T1	≥6.5
PKHD1L1	KCNB2	35XC_M1	≥6.5	UNC5C	SPATA5	QK84_M1	≥6.5
PLA2G10	NDE1	ZS4T_T1	≥8	UNC5D	SUPT6H	cb6c764	≥8
PLCB1	C20orf94	3fcf2f6	≥6.5	UNC5D	PLEKHA2	cb6c764	≥6.5
PLCB4	C20orf94	3fcf2f6	≥6.5	UPF1	TJP1	TC6T_T1	≥6.5
PLD1	JHDM1D	TX2S_T1	≥8	UPF2	AIM1	L50R_T1	≥6.5

Continued on next page

Table S10 – continued from previous page

Gene1	Gene2	Sample	Score	Gene1	Gene2	Sample	Score
PLEKHA2	BAG4	FYVH_M1	≥6.5	UQCRC1	KIF13B	RQX5_M1	≥8
PLEKHA6	CD34	4WQ1_T1	≥8	UQCRC1	RBM6	RQX5_M1	≥8
PLEKHM2	ETV6	HMXT_T1	≥8	UQCRC1	RP11-521I2.3	RQX5_M1	≥6.5
PMEPA1	APMAP	SR1R_M1	≥6.5	URB1	RP11-347D21.1	X0Z1_T1	≥8
PNISR	COL10A1	QYXQ_M1	≥6.5	USB1	SGCZ	WL6X_M1	≥6.5
PNPO	MLLT6	T6Z1_M1	≥8	USH2A	TNRC18	FYVH_M1	≥8
POLA1	PHEX	0XC1_M1	≥8	USO1	RASSP6	DMG3_M1	≥8
POLB	EPB41L5	I4ZX_T1	≥8	USP1	CC2D1B	E65C_M1	≥8
POP4	ANKRD27	e64126c	≥8	USP15	PPM1H	T6Z1_T1	≥8
POU6F1	CBX5	af07947	≥8	USP24	GLIS1	TW0Z_T1	≥8
PPA1	LRRC3B	TW0Z_T1	≥8	USP25	AP000282.2	0E5B_T1	≥6.5
PPA1	AZI2	TW0Z_T1	≥6.5	USP25	AP000290.7	0E5B_T1	≥6.5
PPARGC1A	HTT	SR1R_M1	≥6.5	USP32	BAIAP2	cf2f24	≥8
PPFIA1	ADAM9	7DTJ_T1	≥8	USP32	CEP95	cf2f24	≥8
PPFIA1	NDUFCA2	DR8V_T1	≥8	USP32	PRKCA	cf2f24	≥8
PPFIA1	FAM102B	L50R_T1	≥6.5	USP32	RARA	cf2f24	≥8
PPFIBP1	FAR2	ZCYX_M1	≥8	USP32	BCAS3	B2HF_M1	≥8
PPIL4	KATNA1	0E5B_T1	≥8	USP32	BCAS3	B2HF_T1	≥8
PPM1D	AP2B1	QYXQ_M1	≥8	USP32	GPRC5C	Q6FY_T1	≥8
PPM1D	AMZ2	B2HF_T1	≥8	USP32	RPS6KB1	Q6FY_T1	≥8
PPM1D	EPCAM	b46aa5c	≥6.5	USP32	HDAC9	B2HF_M1	≥6.5
PPM1D	BRIP1	Q6FY_T1	≥6.5	USP32	ATXN1	Q6FY_T1	≥6.5
PPM1D	DDX42	Q6FY_T1	≥6.5	USP32	DCLK2	Q6FY_T1	≥6.5
PPM1E	ARHGEF1	WL6X_M1	≥8	USP36	TBCD	cf2f24	≥8
PPP1R12B	KCNMB4	TW0Z_T1	≥8	USP43	IFT122	SR1R_M1	≥8
PPP1R12B	MTMR11	TW0Z_T1	≥8	USP6	MIPEP	JVRW_M1	≥8
PPP1R21	AC078994.2	TX2S_T1	≥8	USP6	RPAIN	LU50_M1	≥8
PPP1R3B	AC093901.1	4R5V_M1	≥6.5	USP6NL	FAM188A	4c03c03	≥8
PPP1R9B	C17orf108	699525b	≥8	USP9X	ANXA13	615a439	≥8
PPP1R9B	MTMR4	699525b	≥8	UTP11L	AP000525.8	f1ae704	≥8
PPP2R5E	C14orf37	LU50_M1	≥6.5	UTP18	PIP4K2B	QYXQ_M1	≥8
PPP3CA	CISD2	B91A_M1	≥8	UTP6	TAOK1	8MNH_T1	≥8
PPP6R2	MAPK12	231B_T1	≥6.5	UTRN	PDE7B	007M_M1	≥8
PPP6R2	PLXNB2	HWX7_M1	≥6.5	UVRAG	ODZ4	e45fa87	≥8
PPP6R3	HSPH1	SR1R_M1	≥8	UVRAG	GRIK2	8MNH_T1	≥8
PPP6R3	C11orf80	WHDD_M1	≥8	UVRAG	LRP5	4WQ1_T1	≥6.5
PPP6R3	PDSS2	WHDD_M1	≥8	UVRAG	RP11-589C21.1	ZQC5_T1	≥6.5
PPT1	OR4N2	f1ae704	≥6.5	VAC14	COG4	YNSV_T1	≥8
PRCD	LASP1	DMG3_M1	≥6.5	VAMP1	ANKS3	HMXT_T1	≥6.5
PRDM1	LINC00085	T6Z1_T1	≥8	VANGL1	PDE4DIP	51CU_M1	≥8
PRDM1	ORAOV1	L50R_T1	≥8	VAPB	ANKRD60	2S2Q_T1	≥8
PRDM1	IL12RB2	QYXQ_M1	≥6.5	VAPB	CTCFL	0XC1_M1	≥6.5
PREP	7SK	cf2f24	≥6.5	VCL	RP11-745K9.1	46DP_M1	≥8
PREX1	CSE1L	HY35_T1	≥8	VIPR1	SCN5A	F7FD_M1	≥8
PREX1	KCNQ2	cb6c764	≥6.5	VMP1	RPS6KB1	B2HF_T1	≥8
PREX2	ACOX1	35XC_M1	≥8	VMP1	RP11-	cf2f24	≥6.5
					1018N14.5		
PRIM2	PREP	b46aa5c	≥6.5	VMP1	TRIM37	cf2f24	≥6.5
PRINS	NEBL	4R5V_M1	≥6.5	VMP1	HDAC9	B2HF_T1	≥6.5

Continued on next page

Table S10 – continued from previous page

Gene1	Gene2	Sample	Score	Gene1	Gene2	Sample	Score
PRKAB1	MED13L	L50R_T1	≥8	VPS13B	THOC1	2RR2_T1	≥8
PRKACB	ATE1	L50R_T1	≥8	VPS13D	KIAA1715	231B_T1	≥8
PRKAG2	GALNT11	372fc45	≥6.5	VPS13D	TNFRSF1B	YNSV_T1	≥8
PRKCA	BEND5	YNSV_T1	≥8	VPS35	RP11-613D13.4	9HTD_T1	≥6.5
PRKCB	ARFGEF2	SR1R_M1	≥6.5	VPS39	CSMD1	SR1R_M1	≥6.5
PRKCQ	ANKRD26	4c03c03	≥8	VPS72	BPTF	Q6FY_T1	≥6.5
PRKCQ	DIP2C	L50R_T1	≥8	VPS8	SET	DMG3_M1	≥8
PRKD2	ABCG1	TX2S_T1	≥6.5	VPS8	SMARCD3	3b8237c	≥6.5
PRKRIR	MRPL48	615a439	≥6.5	VTA1	RP11-561C5.3	YNSV_T1	≥6.5
PROCA1	ETV6	HMXT_T1	≥8	VTI1A	RP11-144G6.12	F7FD_M1	≥6.5
PRPF3	FMO5	HY35_T1	≥8	VWA7	BAG6	231B_T1	≥8
PRPF39	FAM179B	F7FD_M1	≥6.5	WDPBP	PDZD9	1ED9_T1	≥6.5
PRPF40A	ADAMTSL1	XV6H_M1	≥8	WDPBP	PDZD9	HY35_T1	≥6.5
PRRC2B	NUP214	007M_M1	≥8	WDPBP	PDZD9	Q4W1_T1	≥6.5
PRSS23	HSD17B12	I4ZX_T1	≥6.5	WDR11	FAM157B	YNSV_T1	≥6.5
PSEN1	AKAP6	KEQ4_T1	≥6.5	WDR11	FAM157C	YNSV_T1	≥6.5
PSIP1	MIR5007	007M_M1	≥6.5	WDR25	EML1	DR8V_T1	≥8
PSIP1	MIR5007	SR1R_M1	≥6.5	WDR26	CNIH3	Q6FY_T1	≥6.5
PSMA5	PRPF38A	E65C_M1	≥6.5	WDR43	PLB1	ZS4T_T1	≥8
PSMB7	PBX3	WHDD_M1	≥8	WDR67	FER1L6	L50R_T1	≥6.5
PSMD3	NXPH3	T6Z1_M1	≥8	WDR70	NXPH1	007M_M1	≥6.5
PTCHD4	DOPEY2	F7FD_M1	≥6.5	WDR70	NXPH1	2RR2_T1	≥6.5
PTDSS1	KCNU1	TW0Z_T1	≥8	WDR70	NXPH1	5PJH_M1	≥6.5
PTEN	PKHD1L1	DMG3_T1	≥8	WDR70	NXPH1	6F41_T1	≥6.5
PTEN	PLCE1	8HNA_T1	≥6.5	WDR70	NXPH1	AC72_T1	≥6.5
PTGFR	FAF1	35XC_M1	≥8	WDR70	NXPH1	NL3B_T1	≥6.5
PTK2	MMP1	TC6T_T1	≥8	WDR70	NXPH1	RQX5_M1	≥6.5
PTK2	KIF13B	X0Z1_T1	≥8	WEE1	EHF	WL6X_M1	≥6.5
PTK2	COL22A1	FHKD_T1	≥6.5	WHAMM	RP11-752G15.9	DMG3_M1	≥6.5
PTK2	DENND3	YNSV_T1	≥6.5	WHAMM	RP11-752G15.9	DMG3_T1	≥6.5
PTP4A1	ATG5	EDTK_T1	≥8	WHSC1L1	RGS20	b9b21b9	≥8
PTP4A1	MLIP	LU50_M1	≥6.5	WIFI1	RNF213	2S2Q_T1	≥8
PTPN1	AC009223.2	TX2S_T1	≥8	WIPF1	ANKRD30A	5D6N_M1	≥8
PTPN1	AC007317.1	TX2S_T1	≥6.5	WIPF2	RNF135	2RR2_T1	≥8
PTPN2	HMBOX1	cfd2f24	≥8	WIPF2	CDK12	I4ZX_T1	≥8
PTPN20B	BMS1P2	4R5V_T1	≥6.5	WIP1	CA10	JVRW_M1	≥8
PTPN20B	BMS1P2	WHDD_M1	≥6.5	WISP3	FAM117A	cfd2f24	≥6.5
PTPN3	ADAM17	WL6X_M1	≥8	WIZ	AATF	T6Z1_T1	≥8
PTPRB	COL19A1	F7FD_M1	≥6.5	WNT11	UVRAG	4R5V_M1	≥6.5
PTPRB	PPP1R12B	TW0Z_T1	≥6.5	WNT9B	NUDT4	DMG3_T1	≥6.5
PTPRC	GNG12	TW0Z_T1	≥8	WWP1	CSMD3	35XC_M1	≥8
PTPRD	ATG5	L50R_T1	≥8	WWP1	RP11-127H5.1	35XC_M1	≥8
PTPRD	CCDC64	L50R_T1	≥8	WWP1	U6	35XC_M1	≥8
PTPRD	MED13L	L50R_T1	≥8	WWP1	FABP12	TW0Z_T1	≥8
PTPRD	ABCA4	L50R_T1	≥6.5	WWP1	PXDNL	35XC_M1	≥6.5
PTPRD	ANO1	L50R_T1	≥6.5	XAGE3	RP11-167P23.2	ZS4T_T1	≥6.5
PTPRD	DNM1L	L50R_T1	≥6.5	XKR9	CYP7B1	35XC_M1	≥6.5
PTPRD	POLE	L50R_T1	≥6.5	XPO5	HELZ	af07947	≥8
PTPRG	CACNA1D	af07947	≥8	XPO5	GTPBP2	PF9X_T1	≥6.5

Continued on next page

Table S10 – continued from previous page

Gene1	Gene2	Sample	Score	Gene1	Gene2	Sample	Score
PTPRK	C6orf170	2RR2.T1	≥8	XPOT	NAP1L1	231B.T1	≥8
PTPRK	PEX7	YNSV.T1	≥8	XPR1	RP11-46A10.5	EDTK.T1	≥8
PTPRN2	NCAPG2	f1ae704	≥8	XRCC5	PECR	cb6c764	≥6.5
PTPRS	NFIC	TX2S.T1	≥8	XRRA1	UNC5D	372fc45	≥8
PTPRT	PPP1R1B	cfd2f24	≥8	XRRA1	AP3B1	HMXT.T1	≥6.5
PTPRT	PIGU	2S2Q.T1	≥8	XYLT2	SUPT6H	T6Z1.M1	≥6.5
PTPRT	AC005808.3	7DTJ.T1	≥6.5	Y_RNA	MAP3K7	2RR2.T1	≥6.5
PUM1	C1orf212	8MNH.T1	≥8	YARS2	KHDRBS2	E65C.M1	≥8
PUM1	C1orf94	8MNH.T1	≥8	YARS2	PTPRD	L50R.T1	≥6.5
PUM1	B3GNTL1	HMXT.T1	≥6.5	YEATS2	VPS8	86DK.M1	≥8
PVRL1	BCL9L	8H0R.M1	≥6.5	YEATS4	HOOK3	TW0Z.T1	≥8
PVT1	CA3	X0Z1.T1	≥8	YIPF1	ROR1	f1ae704	≥8
PVT1	KCNQ3	L50R.T1	≥6.5	YIPF1	TADA2A	35XC.M1	≥8
PWWP2A	FCHSD1	b46aa5c	≥6.5	YPEL2	SLC38A10	cfd2f24	≥8
PXDNL	NSMAF	35XC.M1	≥6.5	YPEL2	C7orf31	B2HF.T1	≥6.5
PXDNL	FAM150A	8MNH.T1	≥6.5	YY1AP1	ASH1L	8MNH.T1	≥8
PYGB	ENTPD6	af07947	≥8	ZBTB11	FNDC3B	35XC.M1	≥8
PYGB	CST7	SR1R.M1	≥8	ZBTB44	ACIN1	Y5G9.T1	≥8
PYGB	CSMD1	dd3c42e	≥6.5	ZC2HC1C	TMED10	8H0R.M1	≥8
PYGB	ADRA1D	L50R.T1	≥6.5	ZC3H11A	LAX1	4R5V.M1	≥6.5
PYROXD1	CTD-2547L16.1	b9b21b9	≥6.5	ZC3H7B	TTC28-AS1	L50R.T1	≥8
PYY2	KRT18P55	YNSV.T1	≥6.5	ZC3HAV1	RALGAPB	46DP.M1	≥8
QKI	PACRG	8HNA.T1	≥8	ZCCHC7	STIP1	8MNH.T1	≥8
QRSL1	ARHGAP10	b46aa5c	≥8	ZDHHC21	CCBL2	4R5V.M1	≥8
QRSL1	BCAS3	b46aa5c	≥8	ZDHHC21	ARMCX4	DR8V.T1	≥6.5
QRSL1	ITGB6	b46aa5c	≥6.5	ZFAND4	SGMS1	7FNO.M1	≥8
QSOX1	NEK7	4WQ1.T1	≥8	ZFC3H1	CTD-2547L16.1	b9b21b9	≥8
QSOX1	PTPRC	4WQ1.T1	≥8	ZFC3H1	TRIM37	TW0Z.T1	≥8
R3HDM2	OTOGL	RQX5.M1	≥8	ZFPL1	ZCCHC11	L50R.T1	≥8
R3HDM2	AC010887.1	46DP.M1	≥6.5	ZFR	SUB1	HMXT.T1	≥6.5
RAB10	KIF3C	231B.T1	≥6.5	ZFYVE9	GFRA1	L50R.T1	≥8
RAB22A	ACOT8	2S2Q.T1	≥8	ZGPAT	RTEL1	35XC.M1	≥6.5
RAB2A	CEBPG	231B.T1	≥8	ZHX2	RP11-758M4.1	X0Z1.T1	≥8
RAB2A	MCMDC2	F7FD.M1	≥6.5	ZKSCAN2	PHYHD1	T2VO.M1	≥6.5
RAB37	CA12	3fcb2f6	≥6.5	ZMAT3	HECTD1	TX2S.T1	≥6.5
RAB6A	CTD-2555I5.1	4WQ1.T1	≥6.5	ZMAT4	AP000487.6	7DTJ.T1	≥8
RAB6A	FCHSD2	DR8V.T1	≥6.5	ZMAT4	NARS2	ZQC5.T1	≥8
RAB7A	APH1B	FYVH.M1	≥8	ZMAT4	PPFIA1	7DTJ.T1	≥6.5
RABGAP1L	CNIH3	Q6FY.T1	≥8	ZMAT4	ERLIN2	EDTK.T1	≥6.5
RABGAP1L	KDM5B	YA4W.M1	≥8	ZMYM1	DLGAP3	8MNH.T1	≥8
RABGAP1L	NSL1	YA4W.M1	≥8	ZMYND11	CSMD3	YA4W.M1	≥8
RABGAP1L	CRB1	Q6FY.T1	≥6.5	ZMYND8	PTPRT	2S2Q.T1	≥8
RAD51B	PLCG2	HMXT.T1	≥8	ZNF117	SND1	e45fa87	≥8
RAD51B	NRXN3	IUCQ.T1	≥8	ZNF142	GLS	TX2S.T1	≥8
RAE1	MON2	2S2Q.T1	≥8	ZNF195	SUV420H1	EDTK.T1	≥6.5
RAF1	CHD1L	TW0Z.T1	≥8	ZNF20	KDM4B	Y5G9.T1	≥6.5
RALB	AC062020.2	4R5V.M1	≥8	ZNF248	PARD3	WHDD.M1	≥6.5
RALGAPA2	C16orf72	I4ZX.T1	≥8	ZNF257	SKAP1	2S2Q.T1	≥8
RALGAPB	MKLN1	46DP.M1	≥8	ZNF26	CPT1A	L50R.T1	≥8

Continued on next page

Table S10 – continued from previous page

Gene1	Gene2	Sample	Score	Gene1	Gene2	Sample	Score
RALGPS1	GOLGA1	4c03c03	≥6.5	ZNF326	DPYD	35XC.M1	≥8
RANBP10	CENPT	HMXT.T1	≥6.5	ZNF326	OSBPL11	4R5V.M1	≥8
RANBP17	FAF2	cfd2f24	≥8	ZNF331	ZNF114	75Z1.T1	≥8
RANBP17	HTR4	0E5B.T1	≥8	ZNF334	VMP1	cfd2f24	≥8
RANGAP1	P2RY4	L50R.T1	≥6.5	ZNF346	NSD1	8H0R.M1	≥8
RAP1A	PIGS	8H0R.M1	≥8	ZNF366	SKIV2L2	F7FD.M1	≥8
RAPGEF5	ITGB8	dd3c42e	≥6.5	ZNF37A	SIGLEC6	D988.M1	≥8
RARA	ABCA5	cfd2f24	≥8	ZNF420	PLD3	L50R.T1	≥6.5
RARA	NLK	8H0R.M1	≥8	ZNF43	ZNF208	A0GM.T1	≥6.5
RARA	LINC00365	I4ZX.T1	≥6.5	ZNF43	RP11-488L18.8	DBBB.M1	≥6.5
RARA	NBEA	I4ZX.T1	≥6.5	ZNF442	DNM2	4c03c03	≥8
RASAL2	GATC	L50R.T1	≥8	ZNF451	7SK	231B.T1	≥6.5
RASGEF1A	INPP5A	46DP.M1	≥8	ZNF488	RP11-292F22.7	8MNH.T1	≥6.5
RASL11A	LIMCH1	QK84.M1	≥6.5	ZNF512B	PDE1C	0E5B.T1	≥6.5
RASSF8	ERGIC2	b9b21b9	≥8	ZNF512B	PDE1C	T2VO.M1	≥6.5
RAVER1	LINC00460	T6Z1.T1	≥8	ZNF548	CREB5	L50R.T1	≥8
RB1	ENOX1	8HNA.T1	≥8	ZNF558	CEP112	WHDD.M1	≥6.5
RB1	FREM2	TX2S.T1	≥8	ZNF568	AY269186.2	46DP.M1	≥6.5
RB1CC1	EFCAB4B	dd3c42e	≥6.5	ZNF573	SNAP23	FYVH.M1	≥8
RBBP7	EEA1	L50R.T1	≥8	ZNF587	ZNF552	4ec8eca	≥8
RBFOX3	ABCA10	b46aa5c	≥6.5	ZNF587	NADKD1	F7FD.M1	≥8
RBM12	APP	2S2Q.T1	≥6.5	ZNF589	ARIH2	7DTJ.T1	≥8
RBM12B	FAM92A1	T2VO.M1	≥6.5	ZNF595	PINX1	46DP.M1	≥8
RBM14-RBM4	ANO1	HY35.T1	≥6.5	ZNF611	NLRP7	WL6X.M1	≥6.5
RBM19	PTPRD	L50R.T1	≥8	ZNF615	PHF12	WL6X.M1	≥8
RBM4	CTTN	HY35.T1	≥6.5	ZNF625	KDM4B	Y5G9.T1	≥6.5
RBM47	C4orf34	B91A.M1	≥8	ZNF649	ITSN1	TX2S.T1	≥8
RBPMS	KIF13B	cb6c764	≥8	ZNF652	CASC3	T6Z1.M1	≥8
RCC1	ANXA2	HMXT.T1	≥8	ZNF652	KRT18P55	T6Z1.M1	≥6.5
REEP1	EPAS1	H9F4.M1	≥8	ZNF665	CEACAM21	TX2S.T1	≥6.5
REEP3	FRMD4A	5PJH.M1	≥8	ZNF66P	EPS15L1	E65C.M1	≥6.5
REPS1	ACAP2	T6Z1.T1	≥6.5	ZNF674	KIAA1217	4c03c03	≥8
RERE	ERRFI1	HMXT.T1	≥8	ZNF677	AGAP4	F7FD.M1	≥6.5
RFPL4B	FAM117A	cfd2f24	≥6.5	ZNF697	PHTF1	4R5V.T1	≥6.5
RFWD3	GLG1	T2VO.M1	≥8	ZNF701	AC006293.3	TX2S.T1	≥6.5
RHOBTB3	ARSK	B2HF.T1	≥8	ZNF726	R3HDM1	5D6N.M1	≥6.5
RIMS2	C6orf203	2RR2.T1	≥6.5	ZNF761	GULP1	QYXQ.T1	≥6.5
RIMS2	C6orf203	TW0Z.T1	≥6.5	ZNF761	GULP1	5Y1T.T1	≥6.5
RLF	COL9A2	59cb2ad	≥8	ZNF761	TMEM8B	75Z1.T1	≥6.5
RLF	FAM183A	f1ae704	≥6.5	ZNF761	TMEM8B	86DK.M1	≥6.5
RNF103	DNAH5	RQX5.M1	≥8	ZNF761	TMEM8B	8HNA.T1	≥6.5
RNF168	FBXO45	699525b	≥8	ZNF761	GULP1	8MNH.T1	≥6.5
RNF169	CTD-2023N9.1	HMXT.T1	≥6.5	ZNF761	GULP1	9L95.T1	≥6.5
RNF185	ARMC3	cfd2f24	≥6.5	ZNF761	GULP1	F11Y.T1	≥6.5
RNF213	AC026188.1	f1ae704	≥8	ZNF761	TMEM8B	JVRW.M1	≥6.5
RNF213	ENDOV	86DK.M1	≥8	ZNF761	GULP1	PF9X.T1	≥6.5
RNF213	OGT	Q6FY.T1	≥8	ZNF761	TMEM8B	T2VO.M1	≥6.5
RNF4	GPM6A	WL6X.M1	≥8	ZNF761	GULP1	TW0Z.T1	≥6.5
RNF43	HEATR6	2RR2.T1	≥8	ZNF761	TMEM8B	VE5V.M1	≥6.5

Continued on next page

Table S10 – continued from previous page

Gene1	Gene2	Sample	Score	Gene1	Gene2	Sample	Score
RNF44	ATRIP	b46aa5c	≥6.5	ZNF761	TMEM8B	WHDD_M1	≥6.5
RNFT1	GRB2	Q6FY_T1	≥8	ZNF763	KIAA1671	Y5G9_T1	≥6.5
RNFT2	AP2B1	ZCYX_M1	≥6.5	ZNF783	ZNF212	OLIZ_T1	≥6.5
RNLS	DCUN1D5	Y5G9_T1	≥6.5	ZNF791	ZNF564	DMG3_M1	≥6.5
RNMT	C18orf1	HMXT_T1	≥6.5	ZNF808	KLK3	PF9X_T1	≥6.5
RNPEP	BCL9	TW0Z_T1	≥6.5	ZNF814	KCNQ2	e64126c	≥8
RNU7-14P	PTPRT	7DTJ_T1	≥8	ZNF816	L3MBTL1	TX2S_T1	≥8
ROBO1	ADAMTS12	35XC_M1	≥8	ZNF827	TRAPP11	YA4W_M1	≥8
ROBO1	LRRC63	AC72_T1	≥6.5	ZNF83	LRRC4B	75Z1_T1	≥8
ROBO2	GRHL2	TW0Z_T1	≥8	ZNRF3	CCDC117	b9b21b9	≥8
ROCK2	KRTAP24-1	SR1R_M1	≥6.5	ZNRF3	CHEK2	b9b21b9	≥8
RP11-101O21.1	BCAS3	Q6FY_T1	≥8	ZPLD1	NFKBIZ	DMG3_M1	≥8
RP11-1029J19.5	MNAT1	RZBM_M1	≥8	ZPLD1	NFKBIZ	WL6X_M1	≥6.5
RP11-1042B17.3	FUT8	7FNO_M1	≥6.5	ZRANB3	UGP2	LRU2_M1	≥8
RP11-107C16.2	INADL	L50R_T1	≥6.5	ZRANB3	CNTNAP2	4R5V_T1	≥6.5
RP11-1094H24.4	HEATR6	JVRW_M1	≥6.5	ZSCAN23	ARHGAP17	T2VO_M1	≥6.5
RP11-111M22.3	NARS2	4WQ1_T1	≥8	ZUFSP	MTUS1	AEK9_T1	≥6.5
RP11-112H10.4	LUC7L3	B2HF_M1	≥6.5	ZZZ3	GNG12	35XC_M1	≥8

Note: The order of fusion partner 5' and 3' is ignored to simplify comparison.

Table S11: Fusions identified across 13 different categories (score ≥ 6.5).

Sample ID	Gene1	Gene2	Score	Categorized gene	Category
FYVH_M1	AFF3	AC023672.1	≥ 6.5	AFF3	census gene (COSMIC)
5PJH_M1	AKAP9	ACTR3B	≥ 8	AKAP9	census gene (COSMIC)
QYXQ_M1	BRIP1	BCAS3	≥ 6.5	BRIP1	census gene (COSMIC)
86DK_M1	C12orf66	AFF3	≥ 6.5	AFF3	census gene (COSMIC)
B2HF_T1	CASP8	AP2S1	≥ 6.5	CASP8	census gene (COSMIC)
L50R_T1	CCND1	ANO1	≥ 6.5	CCND1	census gene (COSMIC)
e64126c	CCNE1	ANKRD27	≥ 8	CCNE1	census gene (COSMIC)
AC72_T1	CDH3	CDH1	≥ 8	CDH1	census gene (COSMIC)
EDTK_T1	CHN1	AC073465.3	≥ 8	CHN1	census gene (COSMIC)
YNSV_T1	COG5	ARNT	≥ 8	ARNT	census gene (COSMIC)
af07947	COL1A2	COL1A1	≥ 8	COL1A1	census gene (COSMIC)
HY35_T1	CRTC3	ARRDC4	≥ 6.5	CRTC3	census gene (COSMIC)
8MNH_T1	CUX1	CPA6	≥ 8	CUX1	census gene (COSMIC)
E65C_M1	CYLD	CNEP1R1	≥ 6.5	CYLD	census gene (COSMIC)
cfd2f24	CYTH1	ASPSCR1	≥ 8	ASPSCR1	census gene (COSMIC)
51CU_M1	DCP2	APC	≥ 8	APC	census gene (COSMIC)
HMXT_T1	DDX6	CTD-2216M2.1	≥ 6.5	DDX6	census gene (COSMIC)
Q6FY_T1	DENND1B	BRIP1	≥ 8	BRIP1	census gene (COSMIC)
WHDD_M1	DNM2	ADAMTS10	≥ 8	DNM2	census gene (COSMIC)
ZCYX_M1	DPP6	AKAP9	≥ 8	AKAP9	census gene (COSMIC)
L50R_T1	EPS15	ABCA4	≥ 8	EPS15	census gene (COSMIC)
35XC_M1	ERBB2	ACLY	≥ 6.5	ERBB2	census gene (COSMIC)
35XC_M1	ERBB2	ALG6	≥ 6.5	ERBB2	census gene (COSMIC)
0E5B_T1	ESR1	CCDC170	≥ 6.5	ESR1	census gene (COSMIC)
86DK_M1	ESR1	CCDC170	≥ 6.5	ESR1	census gene (COSMIC)
8H0R_M1	ESR1	CCDC170	≥ 6.5	ESR1	census gene (COSMIC)
DMG3_M1	ESR1	CCDC170	≥ 6.5	ESR1	census gene (COSMIC)
SR1R_M1	ESR1	CDH8	≥ 8	ESR1	census gene (COSMIC)
HMXT_T1	ETV6	BCL2L14	≥ 6.5	ETV6	census gene (COSMIC)
I4ZX_T1	ETV6	ANKS1B	≥ 8	ETV6	census gene (COSMIC)
ZCYX_M1	EZH2	ESCO1	≥ 8	EZH2	census gene (COSMIC)
cfd2f24	FASN	CDK12	≥ 8	CDK12	census gene (COSMIC)
DR8V_T1	FASTKD1	CREB1	≥ 8	CREB1	census gene (COSMIC)
4c03c03	FGF14	DNM2	≥ 6.5	DNM2	census gene (COSMIC)
F7FD_M1	FLCN	BTC	≥ 8	FLCN	census gene (COSMIC)
EDTK_T1	FOXO3	EYS	≥ 6.5	FOXO3	census gene (COSMIC)
cfd2f24	FYN	CDK12	≥ 6.5	CDK12	census gene (COSMIC)
WHDD_M1	GIPC1	DNM2	≥ 6.5	DNM2	census gene (COSMIC)
QYXQ_M1	HEATR6	BRIP1	≥ 8	BRIP1	census gene (COSMIC)
TW0Z_T1	HOOK3	C12orf28	≥ 6.5	HOOK3	census gene (COSMIC)
YA4W_M1	HOOK3	ADAM5	≥ 6.5	HOOK3	census gene (COSMIC)
TW0Z_T1	IL12RB2	CDC73	≥ 6.5	CDC73	census gene (COSMIC)
8H0R_M1	IVD	BUB1B	≥ 8	BUB1B	census gene (COSMIC)
L50R_T1	KAT6B	AP3M1	≥ 8	KAT6B	census gene (COSMIC)
QK84_M1	KAT6B	DLG5	≥ 6.5	KAT6B	census gene (COSMIC)
46DP_M1	KDM5A	CCDC77	≥ 6.5	KDM5A	census gene (COSMIC)
HMXT_T1	KIF5B	EPC1	≥ 8	KIF5B	census gene (COSMIC)
T6Z1_T1	LINC00460	CDK12	≥ 6.5	CDK12	census gene (COSMIC)

Continued on next page

Table S11 – continued from previous page

Sample ID	Gene1	Gene2	Score	Categorized gene	Category
D988_M1	LPP	HSD17B4	≥8	LPP	census gene (COSMIC)
WL6X_M1	LPP	AL133168.3	≥8	LPP	census gene (COSMIC)
35XC_M1	MAD1L1	ERBB2	≥6.5	ERBB2	census gene (COSMIC)
SR1R_M1	MAP2K4	IFT122	≥8	MAP2K4	census gene (COSMIC)
4R5V_T1	MAP3K1	ENC1	≥8	MAP3K1	census gene (COSMIC)
NF9D_M1	MECOM	GOLIM4	≥6.5	MECOM	census gene (COSMIC)
SR1R_M1	MECOM	EGFEM1P	≥8	MECOM	census gene (COSMIC)
8MNH_T1	MED1	CDK12	≥6.5	CDK12	census gene (COSMIC)
PF9X_T1	Metazoa_SRP	ATR	≥6.5	ATR	census gene (COSMIC)
0XC1_M1	METTL15	CREB3L1	≥6.5	CREB3L1	census gene (COSMIC)
L50R_T1	MGAT3	KAT6B	≥8	KAT6B	census gene (COSMIC)
8H0R_M1	MITF	FOXP1	≥6.5	FOXP1	census gene (COSMIC)
8H0R_M1	MITF	FOXP1	≥6.5	MITF	census gene (COSMIC)
5PJH_M1	MLL5	AKAP9	≥8	AKAP9	census gene (COSMIC)
Y5G9_T1	MLLT1	CATSPERD	≥8	MLLT1	census gene (COSMIC)
YNSV_T1	MPP5	GPHN	≥8	GPHN	census gene (COSMIC)
cfd2f24	MSI2	ARHGAP23	≥8	MSI2	census gene (COSMIC)
TW0Z_T1	MSI2	BCAS3	≥8	MSI2	census gene (COSMIC)
L50R_T1	MTMR3	KAT6B	≥8	KAT6B	census gene (COSMIC)
WHDD_M1	MUC16	BRD4	≥6.5	BRD4	census gene (COSMIC)
FYVH_M1	MYEOV	CCND1	≥8	CCND1	census gene (COSMIC)
b46aa5c	NCOA1	ABCA10	≥8	NCOA1	census gene (COSMIC)
2RR2_T1	NF1	GNA13	≥8	NF1	census gene (COSMIC)
51CU_M1	NF2	MTMR3	≥8	NF2	census gene (COSMIC)
Q6FY_T1	NFASC	BRIP1	≥8	BRIP1	census gene (COSMIC)
Q4W1_T1	NFIB	MYB	≥8	MYB	census gene (COSMIC)
Q4W1_T1	NFIB	MYB	≥8	NFIB	census gene (COSMIC)
Y5G9_T1	NFIX	BRD4	≥8	BRD4	census gene (COSMIC)
NL3B_T1	NPEPPS	NF1	≥8	NF1	census gene (COSMIC)
B2HF_M1	NPLOC4	HLF	≥6.5	HLF	census gene (COSMIC)
B2HF_T1	NPLOC4	HLF	≥6.5	HLF	census gene (COSMIC)
B2HF_M1	NPSR1-AS1	MSI2	≥8	MSI2	census gene (COSMIC)
L1PK_T1	NRG1	ATP8A1	≥8	NRG1	census gene (COSMIC)
L50R_T1	NRG1	MAK16	≥6.5	NRG1	census gene (COSMIC)
8H0R_M1	NUFIP2	CDK12	≥8	CDK12	census gene (COSMIC)
L50R_T1	NUP98	INPP4B	≥8	NUP98	census gene (COSMIC)
8MNH_T1	OR5BB1P	NUMA1	≥6.5	NUMA1	census gene (COSMIC)
WL6X_M1	PAC SIN2	MKL1	≥6.5	MKL1	census gene (COSMIC)
0E5B_T1	PAFAH2	ARID1A	≥6.5	ARID1A	census gene (COSMIC)
SR1R_M1	PBX1	CDC73	≥8	CDC73	census gene (COSMIC)
SR1R_M1	PBX1	CDC73	≥8	PBX1	census gene (COSMIC)
SR1R_M1	PBX1	F11R	≥8	PBX1	census gene (COSMIC)
cfd2f24	PCGF2	CLTC	≥8	CLTC	census gene (COSMIC)
2RR2_T1	PDE3B	CLTC	≥8	CLTC	census gene (COSMIC)
8H0R_M1	PDE4DIP	NOTCH2	≥6.5	NOTCH2	census gene (COSMIC)
8H0R_M1	PDE4DIP	NOTCH2	≥6.5	PDE4DIP	census gene (COSMIC)
IUCQ_T1	PDE4DIP	NDUFS4	≥6.5	PDE4DIP	census gene (COSMIC)
T6Z1_T1	PDE4DIP	KDM5B	≥6.5	PDE4DIP	census gene (COSMIC)
I4ZX_T1	PDS5B	CDK12	≥8	CDK12	census gene (COSMIC)

Continued on next page

Table S11 – continued from previous page

Sample ID	Gene1	Gene2	Score	Categorized gene	Category
8H0R_M1	PDZRN3	FOXP1	≥8	FOXP1	census gene (COSMIC)
Y5G9_T1	PICALM	MAPK10	≥8	PICALM	census gene (COSMIC)
HMXT_T1	PLEKHM2	ETV6	≥8	ETV6	census gene (COSMIC)
T6Z1_M1	PNPO	MLLT6	≥8	MLLT6	census gene (COSMIC)
ZCYX_M1	PPFIBP1	FAR2	≥8	PPFIBP1	census gene (COSMIC)
Q6FY_T1	PPM1D	BRIP1	≥6.5	BRIP1	census gene (COSMIC)
DMG3_M1	PRCD	LASP1	≥6.5	LASP1	census gene (COSMIC)
L50R_T1	PRDM1	ORAOV1	≥8	PRDM1	census gene (COSMIC)
QYXQ_M1	PRDM1	IL12RB2	≥6.5	PRDM1	census gene (COSMIC)
T6Z1_T1	PRDM1	LINC00085	≥8	PRDM1	census gene (COSMIC)
HMXT_T1	PROCA1	ETV6	≥8	ETV6	census gene (COSMIC)
007M_M1	PRRC2B	NUP214	≥8	NUP214	census gene (COSMIC)
007M_M1	PSIP1	MIR5007	≥6.5	PSIP1	census gene (COSMIC)
SR1R_M1	PSIP1	MIR5007	≥6.5	PSIP1	census gene (COSMIC)
8HNA_T1	PTEN	PLCE1	≥6.5	PTEN	census gene (COSMIC)
DMG3_T1	PTEN	PKHD1L1	≥8	PTEN	census gene (COSMIC)
F7FD_M1	PTPRB	COL19A1	≥6.5	PTPRB	census gene (COSMIC)
TW0Z_T1	PTPRB	PPP1R12B	≥6.5	PTPRB	census gene (COSMIC)
TW0Z_T1	PTPRC	GNG12	≥8	PTPRC	census gene (COSMIC)
L50R_T1	PTPRD	POLE	≥6.5	POLE	census gene (COSMIC)
af07947	PTPRG	CACNA1D	≥8	CACNA1D	census gene (COSMIC)
2RR2_T1	PTPRK	C6orf170	≥8	PTPRK	census gene (COSMIC)
YNSV_T1	PTPRK	PEX7	≥8	PTPRK	census gene (COSMIC)
b46aa5c	PWWP2A	FCHSD1	≥6.5	PWWP2A	census gene (COSMIC)
4WQ1_T1	QSOX1	PTPRC	≥8	PTPRC	census gene (COSMIC)
HMXT_T1	RAD51B	PLCG2	≥8	RAD51B	census gene (COSMIC)
IUCQ_T1	RAD51B	NRXN3	≥8	RAD51B	census gene (COSMIC)
TW0Z_T1	RAF1	CHD1L	≥8	RAF1	census gene (COSMIC)
0E5B_T1	RANBP17	HTR4	≥8	RANBP17	census gene (COSMIC)
cfd2f24	RANBP17	FAF2	≥8	RANBP17	census gene (COSMIC)
8H0R_M1	RARA	NLK	≥8	RARA	census gene (COSMIC)
cfd2f24	RARA	ABCAS5	≥8	RARA	census gene (COSMIC)
I4ZX_T1	RARA	LINC00365	≥6.5	RARA	census gene (COSMIC)
I4ZX_T1	RARA	NBEA	≥6.5	RARA	census gene (COSMIC)
8HNA_T1	RB1	ENOX1	≥8	RB1	census gene (COSMIC)
TX2S_T1	RB1	FREM2	≥8	RB1	census gene (COSMIC)
86DK_M1	RNF213	ENDOV	≥8	RNF213	census gene (COSMIC)
f1ae704	RNF213	AC026188.1	≥8	RNF213	census gene (COSMIC)
Q6FY_T1	RNF213	OGT	≥8	RNF213	census gene (COSMIC)
2RR2_T1	RNF43	HEATR6	≥8	RNF43	census gene (COSMIC)
TW0Z_T1	RNPEP	BCL9	≥6.5	BCL9	census gene (COSMIC)
615a439	RP11-11N9.4	NUMA1	≥8	NUMA1	census gene (COSMIC)
Q6FY_T1	RP11-311F12.1	LASP1	≥6.5	LASP1	census gene (COSMIC)
YNSV_T1	RP11-330L19.4	BUB1B	≥6.5	BUB1B	census gene (COSMIC)
TW0Z_T1	RP11-611E13.2	HOOK3	≥6.5	HOOK3	census gene (COSMIC)
8HNA_T1	RP11-76P2.3	PTEN	≥8	PTEN	census gene (COSMIC)
b46aa5c	RP11-93L9.1	BRIP1	≥8	BRIP1	census gene (COSMIC)
cb6c764	RP5-914P20.5	NFATC2	≥6.5	NFATC2	census gene (COSMIC)
D988_M1	RPL18	CDK12	≥6.5	CDK12	census gene (COSMIC)

Continued on next page

Table S11 – continued from previous page

Sample ID	Gene1	Gene2	Score	Categorized gene	Category
L50R_T1	RPS15AP5	FGFR2	≥6.5	FGFR2	census gene (COSMIC)
LRU2_M1	RPTOR	NF1	≥6.5	NF1	census gene (COSMIC)
2S2Q_T1	RUNX1	PPM1H	≥6.5	RUNX1	census gene (COSMIC)
b46aa5c	RUNX1	CCDC58	≥8	RUNX1	census gene (COSMIC)
b46aa5c	RUNX1	KPNA1	≥8	RUNX1	census gene (COSMIC)
HMXT_T1	RUNX1	BRE	≥8	RUNX1	census gene (COSMIC)
SR1R_M1	RUNX1	FARSB	≥8	RUNX1	census gene (COSMIC)
SR1R_M1	RUNX1	MOGAT1	≥6.5	RUNX1	census gene (COSMIC)
X0Z1_T1	RUNX1	AGPAT3	≥6.5	RUNX1	census gene (COSMIC)
L50R_T1	SDHAF2	C10orf47	≥8	SDHAF2	census gene (COSMIC)
TX2S_T1	SEC22B	NOTCH2	≥6.5	NOTCH2	census gene (COSMIC)
f1ae704	SEPT5	PPIL2	≥8	SEPT5	census gene (COSMIC)
AC72_T1	SEPT9	GRB2	≥8	SEPT9	census gene (COSMIC)
b9b21b9	SEPT9	CUEDC1	≥8	SEPT9	census gene (COSMIC)
b9b21b9	SEPT9	GDPD1	≥8	SEPT9	census gene (COSMIC)
4R5V_M1	SH3GL1	LRBA	≥8	SH3GL1	census gene (COSMIC)
7FNO_M1	SIPA1L3	CCNE1	≥8	CCNE1	census gene (COSMIC)
cfdf2f24	SKA2	RNF213	≥6.5	RNF213	census gene (COSMIC)
4R5V_M1	SLC25A17	MKL1	≥8	MKL1	census gene (COSMIC)
0XC1_M1	SMAD4	MAD2L1	≥8	SMAD4	census gene (COSMIC)
Y5G9_T1	SMARCA4	KANK3	≥8	SMARCA4	census gene (COSMIC)
Y5G9_T1	SMARCA4	PLA2G6	≥8	SMARCA4	census gene (COSMIC)
46DP_M1	SND1	CASD1	≥8	SND1	census gene (COSMIC)
2RR2_T1	SNTG1	CBLB	≥8	CBLB	census gene (COSMIC)
T6Z1_M1	SPAG9	NF1	≥6.5	NF1	census gene (COSMIC)
51CU_M1	SPEN	DDI2	≥8	SPEN	census gene (COSMIC)
2S2Q_T1	SPOP	GNA13	≥8	SPOP	census gene (COSMIC)
cfdf2f24	SPOP	RP11-429O1.1	≥6.5	SPOP	census gene (COSMIC)
T6Z1_M1	SPOP	HNF1B	≥6.5	SPOP	census gene (COSMIC)
T6Z1_M1	SPOP	MRPL45P2	≥6.5	SPOP	census gene (COSMIC)
T6Z1_M1	SPOP	RP11-192H23.4	≥6.5	SPOP	census gene (COSMIC)
T6Z1_M1	SPOP	RP11-697E22.2	≥6.5	SPOP	census gene (COSMIC)
86DK_M1	SRGAP1	AFF3	≥6.5	AFF3	census gene (COSMIC)
T6Z1_M1	STAT3	CDK12	≥8	CDK12	census gene (COSMIC)
T6Z1_M1	STAT3	CDK12	≥8	STAT3	census gene (COSMIC)
b46aa5c	STK39	BRIP1	≥6.5	BRIP1	census gene (COSMIC)
WHDD_M1	STXBP4	BRIP1	≥8	BRIP1	census gene (COSMIC)
b9b21b9	TADA2A	MSI2	≥8	MSI2	census gene (COSMIC)
WHDD_M1	TANC2	SMARCA4	≥6.5	SMARCA4	census gene (COSMIC)
HMXT_T1	TAOK1	KAT6A	≥6.5	KAT6A	census gene (COSMIC)
IUCQ_T1	TAOK1	CDK12	≥8	CDK12	census gene (COSMIC)
QYXQ_M1	TBC1D16	SPECC1	≥6.5	SPECC1	census gene (COSMIC)
EDTK_T1	TCF20	MYH9	≥8	MYH9	census gene (COSMIC)
4WQ1_T1	TDRD5	PTPRC	≥8	PTPRC	census gene (COSMIC)
DBBB_M1	TFG	GPR128	≥8	TFG	census gene (COSMIC)
NF9D_M1	TFG	GPR128	≥8	TFG	census gene (COSMIC)
Y5G9_T1	TFG	GPR128	≥8	TFG	census gene (COSMIC)
dd3c42e	TFRC	SLC51A	≥8	TFRC	census gene (COSMIC)
XV6H_M1	THRAP3	SKIL	≥6.5	THRAP3	census gene (COSMIC)

Continued on next page

Table S11 – continued from previous page

Sample ID	Gene1	Gene2	Score	Categorized gene	Category
X0Z1_T1	TRAPPC10	ERG	≥8	ERG	census gene (COSMIC)
HMXT_T1	TRIM2	FBXW7	≥8	FBXW7	census gene (COSMIC)
cfd2f24	TRIM37	RARA	≥6.5	RARA	census gene (COSMIC)
Q6FY_T1	TSNAX	PTPRC	≥6.5	PTPRC	census gene (COSMIC)
4R5V_M1	TTC17	SS18	≥8	SS18	census gene (COSMIC)
59cb2ad	UBR5	AZIN1	≥8	UBR5	census gene (COSMIC)
cfd2f24	USP32	RARA	≥8	RARA	census gene (COSMIC)
JVRW_M1	USP6	MIPEP	≥8	USP6	census gene (COSMIC)
LU50_M1	USP6	RPAIN	≥8	USP6	census gene (COSMIC)
51CU_M1	VANGL1	PDE4DIP	≥8	PDE4DIP	census gene (COSMIC)
DMG3_M1	VPS8	SET	≥8	SET	census gene (COSMIC)
F7FD_M1	VTI1A	RP11-144G6.12	≥6.5	VTI1A	census gene (COSMIC)
b9b21b9	WHSC1L1	RGS20	≥8	WHSC1L1	census gene (COSMIC)
2S2Q_T1	WIF1	RNF213	≥8	RNF213	census gene (COSMIC)
2S2Q_T1	WIF1	RNF213	≥8	WIF1	census gene (COSMIC)
I4ZX_T1	WIPF2	CDK12	≥8	CDK12	census gene (COSMIC)
TW0Z_T1	YEATS4	HOOK3	≥8	HOOK3	census gene (COSMIC)
e45fa87	ZNF117	SND1	≥8	SND1	census gene (COSMIC)
75Z1_T1	ZNF331	ZNF114	≥8	ZNF331	census gene (COSMIC)
8H0R_M1	ZNF346	NSD1	≥8	NSD1	census gene (COSMIC)
4c03c03	ZNF442	DNM2	≥8	DNM2	census gene (COSMIC)
b9b21b9	ZNRF3	CHEK2	≥8	CHEK2	census gene (COSMIC)
AEK9_T1	CTD-2194A8.2	BAD	≥8	BAD	ErbB signalling pathway
35XC_M1	ERBB2	ACLY	≥6.5	ERBB2	ErbB signalling pathway
35XC_M1	ERBB2	ALG6	≥6.5	ERBB2	ErbB signalling pathway
YNSV_T1	ERBB4	CYFIP1	≥6.5	ERBB4	ErbB signalling pathway
F7FD_M1	FLCN	BTC	≥8	BTC	ErbB signalling pathway
DMG3_T1	INTS8	ERBB4	≥6.5	ERBB4	ErbB signalling pathway
35XC_M1	MAD1L1	ERBB2	≥6.5	ERBB2	ErbB signalling pathway
SR1R_M1	MAP2K4	IFT122	≥8	MAP2K4	ErbB signalling pathway
YNSV_T1	MAPK8	FRMPD2	≥6.5	MAPK8	ErbB signalling pathway
TX2S_T1	MFSD6	MAPK10	≥8	MAPK10	ErbB signalling pathway
B2HF_T1	MTOR	EXOSC10	≥8	MTOR	ErbB signalling pathway
L1PK_T1	NRG1	ATP8A1	≥8	NRG1	ErbB signalling pathway
L50R_T1	NRG1	MAK16	≥6.5	NRG1	ErbB signalling pathway
e45fa87	NRG3	MLL5	≥6.5	NRG3	ErbB signalling pathway
HY35_T1	PAK1	C11orf49	≥6.5	PAK1	ErbB signalling pathway
TX2S_T1	PAK1	CYP4Z1	≥6.5	PAK1	ErbB signalling pathway
ZQC5_T1	PAK1	CPT1A	≥6.5	PAK1	ErbB signalling pathway
ZQC5_T1	PAK1	MTL5	≥8	PAK1	ErbB signalling pathway
HMXT_T1	PAK7	JAG1	≥6.5	PAK7	ErbB signalling pathway
WHDD_M1	PGAM1P2	PAK1	≥6.5	PAK1	ErbB signalling pathway
Y5G9_T1	PICALM	MAPK10	≥8	MAPK10	ErbB signalling pathway
YNSV_T1	PRKCA	BEND5	≥8	PRKCA	ErbB signalling pathway
SR1R_M1	PRKCB	ARFGEF2	≥6.5	PRKCB	ErbB signalling pathway
FHKD_T1	PTK2	COL22A1	≥6.5	PTK2	ErbB signalling pathway
TC6T_T1	PTK2	MMP1	≥8	PTK2	ErbB signalling pathway
X0Z1_T1	PTK2	KIF13B	≥8	PTK2	ErbB signalling pathway
YNSV_T1	PTK2	DENND3	≥6.5	PTK2	ErbB signalling pathway

Continued on next page

Table S11 – continued from previous page

Sample ID	Gene1	Gene2	Score	Categorized gene	Category
HMXT_T1	RAD51B	PLCG2	≥8	PLCG2	ErbB signalling pathway
TW0Z_T1	RAF1	CHD1L	≥8	RAF1	ErbB signalling pathway
Q6FY_T1	RNFT1	GRB2	≥8	GRB2	ErbB signalling pathway
B2HF_T1	RPS6KB1	BCAS3	≥8	RPS6KB1	ErbB signalling pathway
JVRW_M1	RPS6KB1	BAG4	≥6.5	RPS6KB1	ErbB signalling pathway
Q6FY_T1	RPS6KB1	CAMSAP2	≥8	RPS6KB1	ErbB signalling pathway
AC72_T1	SEPT9	GRB2	≥8	GRB2	ErbB signalling pathway
FYVH_M1	SGCZ	EIF4EBP1	≥6.5	EIF4EBP1	ErbB signalling pathway
YA4W_M1	SIN3A	NRG4	≥8	NRG4	ErbB signalling pathway
2RR2_T1	SNTG1	CBLB	≥8	CBLB	ErbB signalling pathway
b46aa5c	SOS1	RP6-65G23.3	≥8	SOS1	ErbB signalling pathway
TX2S_T1	SOS1	ARFGEF2	≥8	SOS1	ErbB signalling pathway
EDTK_T1	SOS2	NGDN	≥8	SOS2	ErbB signalling pathway
46DP_M1	SRC	METTL2B	≥6.5	SRC	ErbB signalling pathway
e45fa87	SRPK2	NRG3	≥8	NRG3	ErbB signalling pathway
cb6c764	TANC2	RPS6KB1	≥8	RPS6KB1	ErbB signalling pathway
F11Y_T1	TMEM104	PRKCA	≥8	PRKCA	ErbB signalling pathway
cfd2f24	TRIM37	RPS6KB1	≥8	RPS6KB1	ErbB signalling pathway
7FNO_M1	TSEN54	GRB2	≥8	GRB2	ErbB signalling pathway
E65C_M1	UBR4	CAMK2D	≥6.5	CAMK2D	ErbB signalling pathway
cfd2f24	USP32	PRKCA	≥8	PRKCA	ErbB signalling pathway
Q6FY_T1	USP32	RPS6KB1	≥8	RPS6KB1	ErbB signalling pathway
B2HF_T1	VMP1	RPS6KB1	≥8	RPS6KB1	ErbB signalling pathway
35XC_M1	ENY2	ADCY8	≥6.5	ADCY8	Estrogen signalling pathway
0E5B_T1	ESR1	CCDC170	≥6.5	ESR1	Estrogen signalling pathway
86DK_M1	ESR1	CCDC170	≥6.5	ESR1	Estrogen signalling pathway
8H0R_M1	ESR1	CCDC170	≥6.5	ESR1	Estrogen signalling pathway
DMG3_M1	ESR1	CCDC170	≥6.5	ESR1	Estrogen signalling pathway
SR1R_M1	ESR1	CDH8	≥8	ESR1	Estrogen signalling pathway
YNSV_T1	FAM49B	ADCY8	≥8	ADCY8	Estrogen signalling pathway
DR8V_T1	FASTKD1	CREB1	≥8	CREB1	Estrogen signalling pathway
0E5B_T1	GNAI3	FAM102B	≥8	GNAI3	Estrogen signalling pathway
699525b	GNAI3	C1orf101	≥8	GNAI3	Estrogen signalling pathway
0XC1_M1	METTL15	CREB3L1	≥6.5	CREB3L1	Estrogen signalling pathway
3fcf2f6	PLCB1	C20orf94	≥6.5	PLCB1	Estrogen signalling pathway
3fcf2f6	PLCB4	C20orf94	≥6.5	PLCB4	Estrogen signalling pathway
L50R_T1	PRKACB	ATE1	≥8	PRKACB	Estrogen signalling pathway
TW0Z_T1	RAF1	CHD1L	≥8	RAF1	Estrogen signalling pathway
Q6FY_T1	RNFT1	GRB2	≥8	GRB2	Estrogen signalling pathway
35XC_M1	SDCBP	ADCY8	≥6.5	ADCY8	Estrogen signalling pathway
AC72_T1	SEPT9	GRB2	≥8	GRB2	Estrogen signalling pathway
b46aa5c	SOS1	RP6-65G23.3	≥8	SOS1	Estrogen signalling pathway
TX2S_T1	SOS1	ARFGEF2	≥8	SOS1	Estrogen signalling pathway
EDTK_T1	SOS2	NGDN	≥8	SOS2	Estrogen signalling pathway
46DP_M1	SRC	METTL2B	≥6.5	SRC	Estrogen signalling pathway
DMG3_M1	STIP1	PLCB3	≥8	PLCB3	Estrogen signalling pathway
b46aa5c	TIPIN	PLCB2	≥8	PLCB2	Estrogen signalling pathway
HMXT_T1	TM7SF3	ITPR2	≥8	ITPR2	Estrogen signalling pathway
E65C_M1	TMEM132B	ITPR2	≥8	ITPR2	Estrogen signalling pathway

Continued on next page

Table S11 – continued from previous page

Sample ID	Gene1	Gene2	Score	Categorized gene	Category
7FNO_M1	TSEN54	GRB2	≥8	GRB2	Estrogen signalling pathway
L50R_T1	ZNF548	CREB5	≥8	CREB5	Estrogen signalling pathway
T6Z1_M1	ARL2	ANO1	≥8	ARL2	Ras superfamily
HMXT_T1	MYBPC1	ARL1	≥6.5	ARL1	Ras superfamily
231B_T1	RAB10	KIF3C	≥6.5	RAB10	Ras superfamily
2S2Q_T1	RAB22A	ACOT8	≥8	RAB22A	Ras superfamily
3fc2f6	RAB37	CA12	≥6.5	RAB37	Ras superfamily
4WQ1_T1	RAB6A	CTD-2555I5.1	≥6.5	RAB6A	Ras superfamily
DR8V_T1	RAB6A	FCHSD2	≥6.5	RAB6A	Ras superfamily
FYVH_M1	RAB7A	APH1B	≥8	RAB7A	Ras superfamily
4R5V_M1	RALB	AC062020.2	≥8	RALB	Ras superfamily
8H0R_M1	RAP1A	PIGS	≥8	RAP1A	Ras superfamily
QK84_M1	RASL11A	LIMCH1	≥6.5	RASL11A	Ras superfamily
B2HF_T1	RHOBTB3	ARSK	≥8	RHOBTB3	Ras superfamily
cfdf2f4	SRGAP2B	RAB25	≥8	RAB25	Ras superfamily
L50R_T1	SYDE2	RAB3B	≥6.5	RAB3B	Ras superfamily
FYVH_M1	SLC13A3	KLF12	≥6.5	SLC13A3	solute carrier family
L50R_T1	SLC16A12	RNFT2	≥6.5	SLC16A12	solute carrier family
2S2Q_T1	SLC16A7	METTL2A	≥6.5	SLC16A7	solute carrier family
YNSV_T1	SLC16A9	ANK3	≥8	SLC16A9	solute carrier family
59cb2ad	SLC17A8	GAS2L3	≥6.5	SLC17A8	solute carrier family
0XC1_M1	SLC1A2	C11orf49	≥8	SLC1A2	solute carrier family
372fc45	SLC22A20	ACAD11	≥6.5	SLC22A20	solute carrier family
I4ZX_T1	SLC24A3	AC005220.3	≥6.5	SLC24A3	solute carrier family
4R5V_M1	SLC25A17	MKL1	≥8	SLC25A17	solute carrier family
WHDD_M1	SLC25A26	ARHGAP21	≥8	SLC25A26	solute carrier family
LRU2_M1	SLC25A42	CCT6B	≥8	SLC25A42	solute carrier family
HIHE_T1	SLC26A3	CXCL14	≥6.5	SLC26A3	solute carrier family
YNSV_T1	SLC26A4	COG5	≥8	SLC26A4	solute carrier family
TX2S_T1	SLC29A3	ADK	≥8	SLC29A3	solute carrier family
Y5G9_T1	SLC2A12	PLEKHA7	≥8	SLC2A12	solute carrier family
L50R_T1	SLC30A8	RP11-157E21.1	≥6.5	SLC30A8	solute carrier family
H9F4_M1	SLC30A9	RP11-162G9.1	≥8	SLC30A9	solute carrier family
F7FD_M1	SLC35E3	FAM135A	≥8	SLC35E3	solute carrier family
L50R_T1	SLC35F4	CLTA	≥6.5	SLC35F4	solute carrier family
cb6c764	SLC38A10	RBPMS	≥8	SLC38A10	solute carrier family
Q6FY_T1	SLC39A11	BCAS3	≥8	SLC39A11	solute carrier family
WL6X_M1	SLC39A8	DEPDC5	≥6.5	SLC39A8	solute carrier family
615a439	SLC45A1	INADL	≥8	SLC45A1	solute carrier family
51CU_M1	SLC4A10	RBMS1	≥6.5	SLC4A10	solute carrier family
TX2S_T1	SLC4A10	C19orf77	≥6.5	SLC4A10	solute carrier family
TW0Z_T1	SLC6A11	ADAM18	≥8	SLC6A11	solute carrier family
TW0Z_T1	SLC6A6	RPRD2	≥8	SLC6A6	solute carrier family
SPJH_M1	SLCO1A2	NECAP1	≥6.5	SLCO1A2	solute carrier family
I4ZX_T1	SUMO1P1	SLC24A3	≥6.5	SLC24A3	solute carrier family
AC72_T1	TADA2A	SLC25A19	≥6.5	SLC25A19	solute carrier family
FYVH_M1	TMEM182	SLC9A2	≥6.5	SLC9A2	solute carrier family
3b8237c	TRPS1	SLC36A2	≥8	SLC36A2	solute carrier family
4R5V_M1	TTC16	SLC12A7	≥8	SLC12A7	solute carrier family

Continued on next page

Table S11 – continued from previous page

Sample ID	Gene1	Gene2	Score	Categorized gene	Category
cfd2f24	YPEL2	SLC38A10	≥8	SLC38A10	solute carrier family
YNSV_T1	COG5	ARNT	≥8	ARNT	HIF1 signalling pathway
35XC_M1	ERBB2	ACLY	≥6.5	ERBB2	HIF1 signalling pathway
35XC_M1	ERBB2	ALG6	≥6.5	ERBB2	HIF1 signalling pathway
HY35_T1	IGF1R	CCDC33	≥8	IGF1R	HIF1 signalling pathway
Y5G9_T1	INSR	FCER2	≥6.5	INSR	HIF1 signalling pathway
35XC_M1	MAD1L1	ERBB2	≥6.5	ERBB2	HIF1 signalling pathway
B2HF_T1	MTOR	EXOSC10	≥8	MTOR	HIF1 signalling pathway
HY35_T1	MYEOV	IGF1R	≥6.5	IGF1R	HIF1 signalling pathway
H9F4_M1	NEBL	HK1	≥8	HK1	HIF1 signalling pathway
HMXT_T1	PFKFB2	CEP192	≥8	PFKFB2	HIF1 signalling pathway
HMXT_T1	PFKFB3	AKR1C1	≥8	PFKFB3	HIF1 signalling pathway
TX2S_T1	PFKL	PCNT	≥8	PFKL	HIF1 signalling pathway
YNSV_T1	PRKCA	BEND5	≥8	PRKCA	HIF1 signalling pathway
SR1R_M1	PRKCB	ARFGEF2	≥6.5	PRKCB	HIF1 signalling pathway
HMXT_T1	RAD51B	PLCG2	≥8	PLCG2	HIF1 signalling pathway
B2HF_T1	RPS6KB1	BCAS3	≥8	RPS6KB1	HIF1 signalling pathway
JVRW_M1	RPS6KB1	BAG4	≥6.5	RPS6KB1	HIF1 signalling pathway
Q6FY_T1	RPS6KB1	CAMSAP2	≥8	RPS6KB1	HIF1 signalling pathway
FYVH_M1	SGCZ	EIF4EBP1	≥6.5	EIF4EBP1	HIF1 signalling pathway
HY35_T1	SHANK2	IGF1R	≥8	IGF1R	HIF1 signalling pathway
Y5G9_T1	SIAH1	INSR	≥6.5	INSR	HIF1 signalling pathway
T6Z1_M1	STAT3	CDK12	≥8	STAT3	HIF1 signalling pathway
cb6c764	TANC2	RPS6KB1	≥8	RPS6KB1	HIF1 signalling pathway
dd3c42e	TFRC	SLC51A	≥8	TFRC	HIF1 signalling pathway
F11Y_T1	TMEM104	PRKCA	≥8	PRKCA	HIF1 signalling pathway
cfd2f24	TRIM37	RPS6KB1	≥8	RPS6KB1	HIF1 signalling pathway
E65C_M1	UBR4	CAMK2D	≥6.5	CAMK2D	HIF1 signalling pathway
cfd2f24	USP32	PRKCA	≥8	PRKCA	HIF1 signalling pathway
Q6FY_T1	USP32	RPS6KB1	≥8	RPS6KB1	HIF1 signalling pathway
B2HF_T1	VMP1	RPS6KB1	≥8	RPS6KB1	HIF1 signalling pathway
F7FD_M1	CTD-2033D24.2	CACNG5	≥6.5	CACNG5	MAPK signalling pathway
WL6X_M1	DUSP4	CDCA2	≥6.5	DUSP4	MAPK signalling pathway
4c03c03	FGF14	DNM2	≥6.5	FGF14	MAPK signalling pathway
4R5V_M1	FGF14	COL4A1	≥8	FGF14	MAPK signalling pathway
SR1R_M1	FGF14	DNAJC3	≥6.5	FGF14	MAPK signalling pathway
L50R_T1	FGF19	EHD1	≥6.5	FGF19	MAPK signalling pathway
HWX7_M1	LAMTOR1	ARRB1	≥8	ARRB1	MAPK signalling pathway
SR1R_M1	MAP2K4	IFT122	≥8	MAP2K4	MAPK signalling pathway
4R5V_T1	MAP3K1	ENC1	≥8	MAP3K1	MAPK signalling pathway
OLIZ_T1	MAP3K5	LRRC16A	≥8	MAP3K5	MAPK signalling pathway
YNSV_T1	MAPK8	FRMPD2	≥6.5	MAPK8	MAPK signalling pathway
Q6FY_T1	MAPKAPK2	DENND1B	≥8	MAPKAPK2	MAPK signalling pathway
HMXT_T1	MAPKAPK3	HEMK1	≥6.5	MAPKAPK3	MAPK signalling pathway
NF9D_M1	MECOM	GOLIM4	≥6.5	MECOM	MAPK signalling pathway
SR1R_M1	MECOM	EGFEM1P	≥8	MECOM	MAPK signalling pathway
TX2S_T1	MFSD6	MAPK10	≥8	MAPK10	MAPK signalling pathway
2RR2_T1	NF1	GNA13	≥8	NF1	MAPK signalling pathway
Q6FY_T1	NIT1	DUSP10	≥6.5	DUSP10	MAPK signalling pathway

Continued on next page

Table S11 – continued from previous page

Sample ID	Gene1	Gene2	Score	Categorized gene	Category
2RR2_T1	NLK	LRRC37A3	≥8	NLK	MAPK signalling pathway
3fcf2f6	NLK	ADAP2	≥6.5	NLK	MAPK signalling pathway
T6Z1_M1	NLK	KRT18P55	≥8	NLK	MAPK signalling pathway
NL3B_T1	NPEPPS	NF1	≥8	NF1	MAPK signalling pathway
T6Z1_M1	NXPH3	CACNA1G	≥6.5	CACNA1G	MAPK signalling pathway
HY35_T1	PAK1	C11orf49	≥6.5	PAK1	MAPK signalling pathway
TX2S_T1	PAK1	CYP4Z1	≥6.5	PAK1	MAPK signalling pathway
ZQC5_T1	PAK1	CPT1A	≥6.5	PAK1	MAPK signalling pathway
ZQC5_T1	PAK1	MTL5	≥8	PAK1	MAPK signalling pathway
35XC_M1	PDE4B	GNG12	≥6.5	GNG12	MAPK signalling pathway
WHDD_M1	PGAM1P2	PAK1	≥6.5	PAK1	MAPK signalling pathway
dd3c42e	PHF20	FGF3	≥6.5	FGF3	MAPK signalling pathway
Y5G9_T1	PICALM	MAPK10	≥8	MAPK10	MAPK signalling pathway
B91A_M1	PPP3CA	CISD2	≥8	PPP3CA	MAPK signalling pathway
231B_T1	PPP6R2	MAPK12	≥6.5	MAPK12	MAPK signalling pathway
L50R_T1	PRKACB	ATE1	≥8	PRKACB	MAPK signalling pathway
YNSV_T1	PRKCA	BEND5	≥8	PRKCA	MAPK signalling pathway
SR1R_M1	PRKCB	ARFGEF2	≥6.5	PRKCB	MAPK signalling pathway
TW0Z_T1	PTPRC	GNG12	≥8	GNG12	MAPK signalling pathway
af07947	PTPRG	CACNA1D	≥8	CACNA1D	MAPK signalling pathway
TW0Z_T1	RAF1	CHD1L	≥8	RAF1	MAPK signalling pathway
8H0R_M1	RAP1A	PIGS	≥8	RAP1A	MAPK signalling pathway
8H0R_M1	RARA	NLK	≥8	NLK	MAPK signalling pathway
Q6FY_T1	RNFT1	GRB2	≥8	GRB2	MAPK signalling pathway
cb6c764	RP11-64C1.1	FLNB	≥6.5	FLNB	MAPK signalling pathway
L50R_T1	RPS15AP5	FGFR2	≥6.5	FGFR2	MAPK signalling pathway
DMG3_T1	RPS6KA1	KIAA1522	≥6.5	RPS6KA1	MAPK signalling pathway
JVRW_M1	RPS6KA4	KDM2A	≥6.5	RPS6KA4	MAPK signalling pathway
LRU2_M1	RPTOR	NF1	≥6.5	NF1	MAPK signalling pathway
AC72_T1	SEPT9	GRB2	≥8	GRB2	MAPK signalling pathway
b46aa5c	SOS1	RP6-65G23.3	≥8	SOS1	MAPK signalling pathway
TX2S_T1	SOS1	ARFGEF2	≥8	SOS1	MAPK signalling pathway
EDTK_T1	SOS2	NGDN	≥8	SOS2	MAPK signalling pathway
T6Z1_M1	SPAG9	NF1	≥6.5	NF1	MAPK signalling pathway
7FNO_M1	TAOK1	PCTP	≥8	TAOK1	MAPK signalling pathway
8MNH_T1	TAOK1	C17orf79	≥8	TAOK1	MAPK signalling pathway
HMXT_T1	TAOK1	KAT6A	≥6.5	TAOK1	MAPK signalling pathway
IUCQ_T1	TAOK1	CDK12	≥8	TAOK1	MAPK signalling pathway
TW0Z_T1	TAOK3	RNFT2	≥8	TAOK3	MAPK signalling pathway
WL6X_M1	TBC1D3G	NTF4	≥6.5	NTF4	MAPK signalling pathway
HMXT_T1	TEAD4	CACNA1C	≥8	CACNA1C	MAPK signalling pathway
F11Y_T1	TMEM104	PRKCA	≥8	PRKCA	MAPK signalling pathway
QYXQ_M1	TOP2A	CACNB1	≥6.5	CACNB1	MAPK signalling pathway
TX2S_T1	TP53BP2	PLA2G4A	≥8	PLA2G4A	MAPK signalling pathway
7FNO_M1	TSEN54	GRB2	≥8	GRB2	MAPK signalling pathway
HMXT_T1	TULP3	CACNA1C	≥8	CACNA1C	MAPK signalling pathway
TW0Z_T1	UCHL5	GADD45A	≥6.5	GADD45A	MAPK signalling pathway
cfd2f24	USP32	PRKCA	≥8	PRKCA	MAPK signalling pathway
8MNH_T1	UTP6	TAOK1	≥8	TAOK1	MAPK signalling pathway

Continued on next page

Table S11 – continued from previous page

Sample ID	Gene1	Gene2	Score	Categorized gene	Category
2RR2_T1	Y_RNA	MAP3K7	≥6.5	MAP3K7	MAPK signalling pathway
35XC_M1	ZZZ3	GNG12	≥8	GNG12	MAPK signalling pathway
5D6N_M1	CIR1	CERS6	≥6.5	CIR1	Notch signalling pathway
WHDD_M1	NOTCH3	CEP112	≥6.5	NOTCH3	Notch signalling pathway
TX2S_T1	OSBPL6	CIR1	≥8	CIR1	Notch signalling pathway
HMXT_T1	PAK7	JAG1	≥6.5	JAG1	Notch signalling pathway
8H0R_M1	PDE4DIP	NOTCH2	≥6.5	NOTCH2	Notch signalling pathway
KEQ4_T1	PSEN1	AKAP6	≥6.5	PSEN1	Notch signalling pathway
WL6X_M1	PTPN3	ADAM17	≥8	ADAM17	Notch signalling pathway
FYVH_M1	RAB7A	APH1B	≥8	APH1B	Notch signalling pathway
TX2S_T1	SEC22B	NOTCH2	≥6.5	NOTCH2	Notch signalling pathway
b46aa5c	TLK2	MAML3	≥8	MAML3	Notch signalling pathway
B2HF_T1	CASP8	AP2S1	≥6.5	CASP8	P53 signalling pathway
L50R_T1	CCND1	ANO1	≥6.5	CCND1	P53 signalling pathway
e64126c	CCNE1	ANKRD27	≥8	CCNE1	P53 signalling pathway
F11Y_T1	CRY2	CD82	≥8	CD82	P53 signalling pathway
PF9X_T1	Metazoa_SRPP	ATR	≥6.5	ATR	P53 signalling pathway
FYVH_M1	MYEOV	CCND1	≥8	CCND1	P53 signalling pathway
B2HF_T1	PPM1D	AMZ2	≥8	PPM1D	P53 signalling pathway
b46aa5c	PPM1D	EPCAM	≥6.5	PPM1D	P53 signalling pathway
Q6FY_T1	PPM1D	BRIP1	≥6.5	PPM1D	P53 signalling pathway
Q6FY_T1	PPM1D	DDX42	≥6.5	PPM1D	P53 signalling pathway
QYXQ_M1	PPM1D	AP2B1	≥8	PPM1D	P53 signalling pathway
8HNA_T1	PTEN	PLCE1	≥6.5	PTEN	P53 signalling pathway
DMG3_T1	PTEN	PKHD1L1	≥8	PTEN	P53 signalling pathway
8HNA_T1	RP11-76P2.3	PTEN	≥8	PTEN	P53 signalling pathway
2RR2_T1	SESN1	FOXJ3	≥8	SESN1	P53 signalling pathway
b46aa5c	SESN1	CCDC162P	≥8	SESN1	P53 signalling pathway
Y5G9_T1	SIAH1	INSR	≥6.5	SIAH1	P53 signalling pathway
7FNO_M1	SIPA1L3	CCNE1	≥8	CCNE1	P53 signalling pathway
B2HF_M1	SPATA20	PPM1D	≥8	PPM1D	P53 signalling pathway
IUCQ_T1	THBS1	RP11-624L4.1	≥6.5	THBS1	P53 signalling pathway
TX2S_T1	THBS1	RP11-624L4.1	≥6.5	THBS1	P53 signalling pathway
YA4W_M1	THBS1	RP11-624L4.1	≥6.5	THBS1	P53 signalling pathway
RQX5_M1	TNFRSF10B	INTS9	≥8	TNFRSF10B	P53 signalling pathway
TW0Z_T1	UCHL5	GADD45A	≥6.5	GADD45A	P53 signalling pathway
TX2S_T1	ZMAT3	HECTD1	≥6.5	ZMAT3	P53 signalling pathway
b9b21b9	ZNRF3	CHEK2	≥8	CHEK2	P53 signalling pathway
L50R_T1	CCND1	ANO1	≥6.5	CCND1	PI3K-Akt-mTor signalling pathway
e64126c	CCNE1	ANKRD27	≥8	CCNE1	PI3K-Akt-mTor signalling pathway
2S2Q_T1	COL1A2	CASD1	≥8	COL1A2	PI3K-Akt-mTor signalling pathway
af07947	COL1A2	COL1A1	≥8	COL1A1	PI3K-Akt-mTor signalling pathway
af07947	COL1A2	COL1A1	≥8	COL1A2	PI3K-Akt-mTor signalling pathway
0XC1_M1	COL24A1	APBB3	≥6.5	COL24A1	PI3K-Akt-mTor signalling pathway
NF9D_M1	COL6A5	ACTL6A	≥6.5	COL6A5	PI3K-Akt-mTor signalling pathway
AEK9_T1	CTD-2194A8.2	BAD	≥8	BAD	PI3K-Akt-mTor signalling pathway
4c03c03	EFNA1	C1orf167	≥8	EFNA1	PI3K-Akt-mTor signalling pathway
DR8V_T1	FASTKD1	CREB1	≥8	CREB1	PI3K-Akt-mTor signalling pathway
4c03c03	FGF14	DNM2	≥6.5	FGF14	PI3K-Akt-mTor signalling pathway

Continued on next page

Table S11 – continued from previous page

Sample ID	Gene1	Gene2	Score	Categorized gene	Category
4R5V_M1	FGF14	COL4A1	≥8	COL4A1	PI3K-Akt-mTor signalling pathway
4R5V_M1	FGF14	COL4A1	≥8	FGF14	PI3K-Akt-mTor signalling pathway
SR1R_M1	FGF14	DNAJC3	≥6.5	FGF14	PI3K-Akt-mTor signalling pathway
L50R_T1	FGF19	EHD1	≥6.5	FGF19	PI3K-Akt-mTor signalling pathway
TX2S_T1	FN1	AC007563.5	≥6.5	FN1	PI3K-Akt-mTor signalling pathway
EDTK_T1	FOXO3	EYS	≥6.5	FOXO3	PI3K-Akt-mTor signalling pathway
TC6T_T1	G6PC3	FMNL1	≥6.5	G6PC3	PI3K-Akt-mTor signalling pathway
HMXT_T1	GNB1	AC004996.1	≥8	GNB1	PI3K-Akt-mTor signalling pathway
SR1R_M1	GNB1	AJAP1	≥6.5	GNB1	PI3K-Akt-mTor signalling pathway
5d6b06c	HACE1	COL6A3	≥6.5	COL6A3	PI3K-Akt-mTor signalling pathway
HY35_T1	IGF1R	CCDC33	≥8	IGF1R	PI3K-Akt-mTor signalling pathway
Y5G9_T1	INSR	FCER2	≥6.5	INSR	PI3K-Akt-mTor signalling pathway
4R5V_T1	ITGB5	GOLM1	≥6.5	ITGB5	PI3K-Akt-mTor signalling pathway
6F41_T1	ITGB5	GOLM1	≥6.5	ITGB5	PI3K-Akt-mTor signalling pathway
TDDP_T1	ITGB5	GOLM1	≥6.5	ITGB5	PI3K-Akt-mTor signalling pathway
WHDD_M1	ITGB5	GOLM1	≥6.5	ITGB5	PI3K-Akt-mTor signalling pathway
WL6X_M1	ITGB5	GOLM1	≥6.5	ITGB5	PI3K-Akt-mTor signalling pathway
b9b21b9	KITLG	CEP290	≥6.5	KITLG	PI3K-Akt-mTor signalling pathway
L50R_T1	KITLG	HAUS6	≥6.5	KITLG	PI3K-Akt-mTor signalling pathway
0XC1_M1	METTL15	CREB3L1	≥6.5	CREB3L1	PI3K-Akt-mTor signalling pathway
372fc45	MICAL1	ITGA11	≥6.5	ITGA11	PI3K-Akt-mTor signalling pathway
B2HF_T1	MTOR	EXOSC10	≥8	MTOR	PI3K-Akt-mTor signalling pathway
FYVH_M1	MYEOV	CCND1	≥8	CCND1	PI3K-Akt-mTor signalling pathway
HY35_T1	MYEOV	IGF1R	≥6.5	IGF1R	PI3K-Akt-mTor signalling pathway
EDTK_T1	NEMF	LAMA4	≥8	LAMA4	PI3K-Akt-mTor signalling pathway
Q4W1_T1	NFIB	MYB	≥8	MYB	PI3K-Akt-mTor signalling pathway
TX2S_T1	NYAP2	FN1	≥8	FN1	PI3K-Akt-mTor signalling pathway
35XC_M1	PDE4B	GNG12	≥6.5	GNG12	PI3K-Akt-mTor signalling pathway
SR1R_M1	PDIA5	ITGB5	≥8	ITGB5	PI3K-Akt-mTor signalling pathway
dd3c42e	PHF20	FGF3	≥6.5	FGF3	PI3K-Akt-mTor signalling pathway
LU50_M1	PPP2R5E	C14orf37	≥6.5	PPP2R5E	PI3K-Akt-mTor signalling pathway
YNSV_T1	PRKCA	BEND5	≥8	PRKCA	PI3K-Akt-mTor signalling pathway
SR1R_M1	PRKCB	ARFGEF2	≥6.5	PRKCB	PI3K-Akt-mTor signalling pathway
8HNA_T1	PTEN	PLCE1	≥6.5	PTEN	PI3K-Akt-mTor signalling pathway
DMG3_T1	PTEN	PKHD1L1	≥8	PTEN	PI3K-Akt-mTor signalling pathway
FHKD_T1	PTK2	COL22A1	≥6.5	PTK2	PI3K-Akt-mTor signalling pathway
TC6T_T1	PTK2	MMP1	≥8	PTK2	PI3K-Akt-mTor signalling pathway
X0Z1_T1	PTK2	KIF13B	≥8	PTK2	PI3K-Akt-mTor signalling pathway
YNSV_T1	PTK2	DENNND3	≥6.5	PTK2	PI3K-Akt-mTor signalling pathway
TWOZ_T1	PTPRC	GNG12	≥8	GNG12	PI3K-Akt-mTor signalling pathway
b46aa5c	QRSL1	ITGB6	≥6.5	ITGB6	PI3K-Akt-mTor signalling pathway
TWOZ_T1	RAF1	CHD1L	≥8	RAF1	PI3K-Akt-mTor signalling pathway
dd3c42e	RAPGEF5	ITGB8	≥6.5	ITGB8	PI3K-Akt-mTor signalling pathway
Q6FY_T1	RNFT1	GRB2	≥8	GRB2	PI3K-Akt-mTor signalling pathway
8HNA_T1	RP11-76P2.3	PTEN	≥8	PTEN	PI3K-Akt-mTor signalling pathway
WHDD_M1	RP5-1029K10.2	PKN1	≥8	PKN1	PI3K-Akt-mTor signalling pathway
L50R_T1	RPS15AP5	FGFR2	≥6.5	FGFR2	PI3K-Akt-mTor signalling pathway
DMG3_T1	RPS6KA1	KIAA1522	≥6.5	RPS6KA1	PI3K-Akt-mTor signalling pathway
B2HF_T1	RPS6KB1	BCAS3	≥8	RPS6KB1	PI3K-Akt-mTor signalling pathway

Continued on next page

Table S11 – continued from previous page

Sample ID	Gene1	Gene2	Score	Categorized gene	Category
JVRW_M1	RPS6KB1	BAG4	≥6.5	RPS6KB1	PI3K-Akt-mTor signalling pathway
Q6FY_T1	RPS6KB1	CAMSAP2	≥8	RPS6KB1	PI3K-Akt-mTor signalling pathway
cfd2f24	RPTOR	DUS1L	≥8	RPTOR	PI3K-Akt-mTor signalling pathway
LRU2_M1	RPTOR	NF1	≥6.5	RPTOR	PI3K-Akt-mTor signalling pathway
2S2Q_T1	RRAGC	MACF1	≥6.5	RRAGC	PI3K-Akt-mTor signalling pathway
AC72_T1	SEPT9	GRB2	≥8	GRB2	PI3K-Akt-mTor signalling pathway
FYVH_M1	SGCZ	EIF4EBP1	≥6.5	EIF4EBP1	PI3K-Akt-mTor signalling pathway
b9b21b9	SH2D4A	KITLG	≥8	KITLG	PI3K-Akt-mTor signalling pathway
HY35_T1	SHANK2	IGF1R	≥8	IGF1R	PI3K-Akt-mTor signalling pathway
Y5G9_T1	SIAH1	INSR	≥6.5	INSR	PI3K-Akt-mTor signalling pathway
7FNO_M1	SIPA1L3	CCNE1	≥8	CCNE1	PI3K-Akt-mTor signalling pathway
231B_T1	SKI	PRKCZ	≥8	PRKCZ	PI3K-Akt-mTor signalling pathway
b46aa5c	SOS1	RP6-65G23.3	≥8	SOS1	PI3K-Akt-mTor signalling pathway
TX2S_T1	SOS1	ARFGEF2	≥8	SOS1	PI3K-Akt-mTor signalling pathway
EDTK_T1	SOS2	NGDN	≥8	SOS2	PI3K-Akt-mTor signalling pathway
cb6c764	TANC2	RPS6KB1	≥8	RPS6KB1	PI3K-Akt-mTor signalling pathway
IUCQ_T1	THBS1	RP11-624L4.1	≥6.5	THBS1	PI3K-Akt-mTor signalling pathway
TX2S_T1	THBS1	RP11-624L4.1	≥6.5	THBS1	PI3K-Akt-mTor signalling pathway
YA4W_M1	THBS1	RP11-624L4.1	≥6.5	THBS1	PI3K-Akt-mTor signalling pathway
F11Y_T1	TMEM104	PRKCA	≥8	PRKCA	PI3K-Akt-mTor signalling pathway
b9b21b9	TMTC3	KITLG	≥8	KITLG	PI3K-Akt-mTor signalling pathway
cfd2f24	TRIM37	RPS6KB1	≥8	RPS6KB1	PI3K-Akt-mTor signalling pathway
7FNO_M1	TSEN54	GRB2	≥8	GRB2	PI3K-Akt-mTor signalling pathway
8MNH_T1	TUBE1	LAMA4	≥8	LAMA4	PI3K-Akt-mTor signalling pathway
cfd2f24	USP32	PRKCA	≥8	PRKCA	PI3K-Akt-mTor signalling pathway
Q6FY_T1	USP32	RPS6KB1	≥8	RPS6KB1	PI3K-Akt-mTor signalling pathway
B2HF_T1	VMP1	RPS6KB1	≥8	RPS6KB1	PI3K-Akt-mTor signalling pathway
L50R_T1	ZNF548	CREB5	≥8	CREB5	PI3K-Akt-mTor signalling pathway
35XC_M1	ZZZ3	GNG12	≥8	GNG12	PI3K-Akt-mTor signalling pathway
AEK9_T1	CTD-2194A8.2	BAD	≥8	BAD	Ras signalling pathway
4c03c03	EFNA1	C1orf167	≥8	EFNA1	Ras signalling pathway
4R5V_T1	EXOC2	EFHC1	≥6.5	EXOC2	Ras signalling pathway
4c03c03	FGF14	DNM2	≥6.5	FGF14	Ras signalling pathway
4R5V_M1	FGF14	COL4A1	≥8	FGF14	Ras signalling pathway
SR1R_M1	FGF14	DNAJC3	≥6.5	FGF14	Ras signalling pathway
L50R_T1	FGF19	EHD1	≥6.5	FGF19	Ras signalling pathway
HMXT_T1	GNB1	AC004996.1	≥8	GNB1	Ras signalling pathway
SR1R_M1	GNB1	AJAP1	≥6.5	GNB1	Ras signalling pathway
D988_M1	HTR7	CYP7B1	≥8	HTR7	Ras signalling pathway
HY35_T1	IGF1R	CCDC33	≥8	IGF1R	Ras signalling pathway
Y5G9_T1	INSR	FCER2	≥6.5	INSR	Ras signalling pathway
b9b21b9	KITLG	CEP290	≥6.5	KITLG	Ras signalling pathway
L50R_T1	KITLG	HAUS6	≥6.5	KITLG	Ras signalling pathway
TW0Z_T1	KSR2	FBXO21	≥6.5	KSR2	Ras signalling pathway
YNSV_T1	MAPK8	FRMPD2	≥6.5	MAPK8	Ras signalling pathway
TX2S_T1	MFSD6	MAPK10	≥8	MAPK10	Ras signalling pathway
HY35_T1	MYEOV	IGF1R	≥6.5	IGF1R	Ras signalling pathway
2RR2_T1	NF1	GNA13	≥8	NF1	Ras signalling pathway
NL3B_T1	NPEPPS	NF1	≥8	NF1	Ras signalling pathway

Continued on next page

Table S11 – continued from previous page

Sample ID	Gene1	Gene2	Score	Categorized gene	Category
HY35_T1	PAK1	C11orf49	≥6.5	PAK1	Ras signalling pathway
TX2S_T1	PAK1	CYP4Z1	≥6.5	PAK1	Ras signalling pathway
ZQC5_T1	PAK1	CPT1A	≥6.5	PAK1	Ras signalling pathway
ZQC5_T1	PAK1	MTL5	≥8	PAK1	Ras signalling pathway
HMXT_T1	PAK7	JAG1	≥6.5	PAK7	Ras signalling pathway
35XC_M1	PDE4B	GNG12	≥6.5	GNG12	Ras signalling pathway
WHDD_M1	PGAM1P2	PAK1	≥6.5	PAK1	Ras signalling pathway
dd3c42e	PHF20	FGF3	≥6.5	FGF3	Ras signalling pathway
Y5G9_T1	PICALM	MAPK10	≥8	MAPK10	Ras signalling pathway
ZS4T_T1	PLA2G10	NDE1	≥8	PLA2G10	Ras signalling pathway
TX2S_T1	PLD1	JHDM1D	≥8	PLD1	Ras signalling pathway
L50R_T1	PRKACB	ATE1	≥8	PRKACB	Ras signalling pathway
YNSV_T1	PRKCA	BEND5	≥8	PRKCA	Ras signalling pathway
SR1R_M1	PRKCB	ARFGEF2	≥6.5	PRKCB	Ras signalling pathway
8HNA_T1	PTEN	PLCE1	≥6.5	PLCE1	Ras signalling pathway
TW0Z_T1	PTPRC	GNG12	≥8	GNG12	Ras signalling pathway
HMXT_T1	RAD51B	PLCG2	≥8	PLCG2	Ras signalling pathway
TW0Z_T1	RAF1	CHD1L	≥8	RAF1	Ras signalling pathway
4R5V_M1	RALB	AC062020.2	≥8	RALB	Ras signalling pathway
8H0R_M1	RAP1A	PIGS	≥8	RAP1A	Ras signalling pathway
dd3c42e	RAPGEF5	ITGB8	≥6.5	RAPGEF5	Ras signalling pathway
L50R_T1	RASAL2	GATC	≥8	RASAL2	Ras signalling pathway
Q6FY_T1	RNFT1	GRB2	≥8	GRB2	Ras signalling pathway
L50R_T1	RPS15AP5	FGFR2	≥6.5	FGFR2	Ras signalling pathway
LRU2_M1	RPTOR	NF1	≥6.5	NF1	Ras signalling pathway
dd3c42e	RUFY1	RAPGEF5	≥6.5	RAPGEF5	Ras signalling pathway
AC72_T1	SEPT9	GRB2	≥8	GRB2	Ras signalling pathway
b9b21b9	SH2D4A	KITLG	≥8	KITLG	Ras signalling pathway
HY35_T1	SHANK2	IGF1R	≥8	IGF1R	Ras signalling pathway
Y5G9_T1	SIAH1	INSR	≥6.5	INSR	Ras signalling pathway
Y5G9_T1	SMARCA4	PLA2G6	≥8	PLA2G6	Ras signalling pathway
b46aa5c	SOS1	RP6-65G23.3	≥8	SOS1	Ras signalling pathway
TX2S_T1	SOS1	ARFGEF2	≥8	SOS1	Ras signalling pathway
EDTK_T1	SOS2	NGDN	≥8	SOS2	Ras signalling pathway
T6Z1_M1	SPAG9	NF1	≥6.5	NF1	Ras signalling pathway
8MNH_T1	STEAP1B	RAPGEF5	≥8	RAPGEF5	Ras signalling pathway
F11Y_T1	TMEM104	PRKCA	≥8	PRKCA	Ras signalling pathway
b9b21b9	TMTc3	KITLG	≥8	KITLG	Ras signalling pathway
TX2S_T1	TP53BP2	PLA2G4A	≥8	PLA2G4A	Ras signalling pathway
7FNO_M1	TSEN54	GRB2	≥8	GRB2	Ras signalling pathway
cfd2f24	USP32	PRKCA	≥8	PRKCA	Ras signalling pathway
35XC_M1	ZZZ3	GNG12	≥8	GNG12	Ras signalling pathway
B2HF_T1	BCAS3	AC005682.8	≥6.5	BCAS3	oncogene (UniProt)
Q6FY_T1	BCAS3	ABCA8	≥8	BCAS3	oncogene (UniProt)
QYXQ_M1	BRIP1	BCAS3	≥6.5	BCAS3	oncogene (UniProt)
L50R_T1	CCND1	ANO1	≥6.5	CCND1	oncogene (UniProt)
cfd2f24	CYTH1	ASPSCR1	≥8	ASPSCR1	oncogene (UniProt)
HMXT_T1	DDX6	CTD-2216M2.1	≥6.5	DDX6	oncogene (UniProt)
L50R_T1	EPS15	ABCA4	≥8	EPS15	oncogene (UniProt)

Continued on next page

Table S11 – continued from previous page

Sample ID	Gene1	Gene2	Score	Categorized gene	Category
HMXT.T1	ETV6	BCL2L14	≥6.5	ETV6	oncogene (UniProt)
I4ZX.T1	ETV6	ANKS1B	≥8	ETV6	oncogene (UniProt)
EDTK.T1	FOXO3	EYS	≥6.5	FOXO3	oncogene (UniProt)
cfd2f24	FYN	CDK12	≥6.5	FYN	oncogene (UniProt)
NF9D_M1	MECOM	GOLIM4	≥6.5	MECOM	oncogene (UniProt)
SR1R_M1	MECOM	EGFEM1P	≥8	MECOM	oncogene (UniProt)
Q6FY_T1	MERTK	C2orf15	≥8	MERTK	oncogene (UniProt)
Y5G9_T1	MLLT1	CATSPERD	≥8	MLLT1	oncogene (UniProt)
TW0Z_T1	MSI2	BCAS3	≥8	BCAS3	oncogene (UniProt)
FYVH_M1	MYEOV	CCND1	≥8	CCND1	oncogene (UniProt)
FYVH_M1	MYEOV	CCND1	≥8	MYEOV	oncogene (UniProt)
HY35_T1	MYEOV	IGF1R	≥6.5	MYEOV	oncogene (UniProt)
b46aa5c	NCOA1	ABCA10	≥8	NCOA1	oncogene (UniProt)
Q4W1_T1	NFIB	MYB	≥8	MYB	oncogene (UniProt)
B2HF_M1	NPLOC4	HLF	≥6.5	HLF	oncogene (UniProt)
B2HF_T1	NPLOC4	HLF	≥6.5	HLF	oncogene (UniProt)
WL6X_M1	PACSin2	MKL1	≥6.5	MKL1	oncogene (UniProt)
SR1R_M1	PBX1	CDC73	≥8	PBX1	oncogene (UniProt)
SR1R_M1	PBX1	F11R	≥8	PBX1	oncogene (UniProt)
dd3c42e	PHF20	FGF3	≥6.5	FGF3	oncogene (UniProt)
Y5G9_T1	PICALM	MAPK10	≥8	PICALM	oncogene (UniProt)
HMXT.T1	PLEKHM2	ETV6	≥8	ETV6	oncogene (UniProt)
T6Z1_M1	PNPO	MLLT6	≥8	MLLT6	oncogene (UniProt)
YNSV_T1	PRKCA	BEND5	≥8	PRKCA	oncogene (UniProt)
HMXT.T1	PROCA1	ETV6	≥8	ETV6	oncogene (UniProt)
007M_M1	PRRC2B	NUP214	≥8	NUP214	oncogene (UniProt)
b46aa5c	QRSL1	BCAS3	≥8	BCAS3	oncogene (UniProt)
TW0Z_T1	RAF1	CHD1L	≥8	RAF1	oncogene (UniProt)
8H0R_M1	RARA	NLK	≥8	RARA	oncogene (UniProt)
cfd2f24	RARA	ABCA5	≥8	RARA	oncogene (UniProt)
I4ZX_T1	RARA	LINC00365	≥6.5	RARA	oncogene (UniProt)
I4ZX_T1	RARA	NBEA	≥6.5	RARA	oncogene (UniProt)
8HNA_T1	RB1	ENOX1	≥8	RB1	oncogene (UniProt)
TX2S_T1	RB1	FREM2	≥8	RB1	oncogene (UniProt)
86DK_M1	RNF213	ENDOV	≥8	RNF213	oncogene (UniProt)
f1ae704	RNF213	AC026188.1	≥8	RNF213	oncogene (UniProt)
Q6FY_T1	RNF213	OGT	≥8	RNF213	oncogene (UniProt)
TW0Z_T1	RNPEP	BCL9	≥6.5	BCL9	oncogene (UniProt)
Q6FY_T1	RP11-101O21.1	BCAS3	≥8	BCAS3	oncogene (UniProt)
2S2Q_T1	RP11-522N14.1	BCAS3	≥8	BCAS3	oncogene (UniProt)
L50R_T1	RP3-486B10.1	MYEOV	≥8	MYEOV	oncogene (UniProt)
L50R_T1	RPS15AP5	FGFR2	≥6.5	FGFR2	oncogene (UniProt)
B2HF_T1	RPS6KB1	BCAS3	≥8	BCAS3	oncogene (UniProt)
2S2Q_T1	RUNX1	PPM1H	≥6.5	RUNX1	oncogene (UniProt)
b46aa5c	RUNX1	CCDC58	≥8	RUNX1	oncogene (UniProt)
b46aa5c	RUNX1	KPNA1	≥8	RUNX1	oncogene (UniProt)
HMXT.T1	RUNX1	BRE	≥8	RUNX1	oncogene (UniProt)
SR1R_M1	RUNX1	FARSB	≥8	RUNX1	oncogene (UniProt)
SR1R_M1	RUNX1	MOGAT1	≥6.5	RUNX1	oncogene (UniProt)

Continued on next page

Table S11 – continued from previous page

Sample ID	Gene1	Gene2	Score	Categorized gene	Category
X0Z1_T1	RUNX1	AGPAT3	≥6.5	RUNX1	oncogene (UniProt)
HY35_T1	SEMA4B	AKAP13	≥6.5	AKAP13	oncogene (UniProt)
4R5V_M1	SH3GL1	LRBA	≥8	SH3GL1	oncogene (UniProt)
cfd2f24	SKA2	RNF213	≥6.5	RNF213	oncogene (UniProt)
231B_T1	SKI	PRKCZ	≥8	SKI	oncogene (UniProt)
4R5V_M1	SLC25A17	MKL1	≥8	MKL1	oncogene (UniProt)
Q6FY_T1	SLC39A11	BCAS3	≥8	BCAS3	oncogene (UniProt)
46DP_M1	SRC	METTL2B	≥6.5	SRC	oncogene (UniProt)
HMXT_T1	TAOK1	KAT6A	≥6.5	KAT6A	oncogene (UniProt)
QYXQ_M1	TBC1D16	SPECC1	≥6.5	SPECC1	oncogene (UniProt)
DBBB_M1	TFG	GPR128	≥8	TFG	oncogene (UniProt)
NF9D_M1	TFG	GPR128	≥8	TFG	oncogene (UniProt)
Y5G9_T1	TFG	GPR128	≥8	TFG	oncogene (UniProt)
F11Y_T1	TMEM104	PRKCA	≥8	PRKCA	oncogene (UniProt)
X0Z1_T1	TRAPPC10	ERG	≥8	ERG	oncogene (UniProt)
2RR2_T1	TRIM37	FLJ37644	≥8	TRIM37	oncogene (UniProt)
b9b21b9	TRIM37	MARCH10	≥6.5	TRIM37	oncogene (UniProt)
cfd2f24	TRIM37	LINC00511	≥8	TRIM37	oncogene (UniProt)
cfd2f24	TRIM37	RARA	≥6.5	RARA	oncogene (UniProt)
cfd2f24	TRIM37	RARA	≥6.5	TRIM37	oncogene (UniProt)
cfd2f24	TRIM37	RPS6KB1	≥8	TRIM37	oncogene (UniProt)
cfd2f24	TRIM37	SNHG16	≥8	TRIM37	oncogene (UniProt)
JVRW_M1	TRIM37	HOXB-AS3	≥8	TRIM37	oncogene (UniProt)
Q6FY_T1	TRIM37	PPM1E	≥8	TRIM37	oncogene (UniProt)
Q6FY_T1	TRIM37	TBC1D7	≥8	TRIM37	oncogene (UniProt)
4R5V_M1	TTC17	SS18	≥8	SS18	oncogene (UniProt)
Q6FY_T1	TTYH2	BCAS3	≥8	BCAS3	oncogene (UniProt)
DR8V_T1	UCP2	MYEOV	≥6.5	MYEOV	oncogene (UniProt)
B2HF_M1	USP32	BCAS3	≥8	BCAS3	oncogene (UniProt)
B2HF_T1	USP32	BCAS3	≥8	BCAS3	oncogene (UniProt)
cfd2f24	USP32	PRKCA	≥8	PRKCA	oncogene (UniProt)
cfd2f24	USP32	RARA	≥8	RARA	oncogene (UniProt)
JVRW_M1	USP6	MIPEP	≥8	USP6	oncogene (UniProt)
LU50_M1	USP6	RPAIN	≥8	USP6	oncogene (UniProt)
cfd2f24	VMP1	TRIM37	≥6.5	TRIM37	oncogene (UniProt)
DMG3_M1	VPS8	SET	≥8	SET	oncogene (UniProt)
YNSV_T1	WDR11	FAM157B	≥6.5	WDR11	oncogene (UniProt)
YNSV_T1	WDR11	FAM157C	≥6.5	WDR11	oncogene (UniProt)
b9b21b9	WHSC1L1	RGS20	≥8	WHSC1L1	oncogene (UniProt)
2S2Q_T1	WIF1	RNF213	≥8	RNF213	oncogene (UniProt)
TW0Z_T1	ZFC3H1	TRIM37	≥8	TRIM37	oncogene (UniProt)
8H0R_M1	ZNF346	NSD1	≥8	NSD1	oncogene (UniProt)
E65C_M1	CYLD	CNEP1R1	≥6.5	CYLD	gene ssuppressor (UniProt)
51CU_M1	DCP2	APC	≥8	APC	gene ssuppressor (UniProt)
4c03c03	EFNA1	C1orf167	≥8	EFNA1	gene ssuppressor (UniProt)
F7FD_M1	FLCN	BTC	≥8	FLCN	gene ssuppressor (UniProt)
HMXT_T1	hsa-mir-4763	PDCD4	≥6.5	PDCD4	gene ssuppressor (UniProt)
TW0Z_T1	IL12RB2	CDC73	≥6.5	CDC73	gene ssuppressor (UniProt)
HMXT_T1	INPP5K	DPH1	≥6.5	DPH1	gene ssuppressor (UniProt)

Continued on next page

Table S11 – continued from previous page

Sample ID	Gene1	Gene2	Score	Categorized gene	Category
8H0R_M1	IVD	BUB1B	≥8	BUB1B	gene ssuppressor (UniProt)
WL6X_M1	MFHAS1	CHD9	≥6.5	MFHAS1	gene ssuppressor (UniProt)
WL6X_M1	MFHAS1	GPT2	≥8	MFHAS1	gene ssuppressor (UniProt)
dd3c42e	MTUS1	FAM86A	≥8	MTUS1	gene ssuppressor (UniProt)
2RR2_T1	NF1	GNA13	≥8	NF1	gene ssuppressor (UniProt)
51CU_M1	NF2	MTMR3	≥8	NF2	gene ssuppressor (UniProt)
NL3B_T1	NPEPPS	NF1	≥8	NF1	gene ssuppressor (UniProt)
SR1R_M1	PBX1	CDC73	≥8	CDC73	gene ssuppressor (UniProt)
HMXT_T1	PDCD4	CITF22-92A6.1	≥6.5	PDCD4	gene ssuppressor (UniProt)
8HNA_T1	PTEN	PLCE1	≥6.5	PTEN	gene ssuppressor (UniProt)
DMG3_T1	PTEN	PKHD1L1	≥8	PTEN	gene ssuppressor (UniProt)
8H0R_M1	RAP1A	PIGS	≥8	RAP1A	gene ssuppressor (UniProt)
dd3c42e	RB1CC1	EFCAB4B	≥6.5	RB1CC1	gene ssuppressor (UniProt)
HMXT_T1	RERE	ERRFI1	≥8	ERRFI1	gene ssuppressor (UniProt)
3fc2f6	RP11-1407O15.2	BRMS1	≥8	BRMS1	gene ssuppressor (UniProt)
YNSV_T1	RP11-330L19.4	BUB1B	≥6.5	BUB1B	gene ssuppressor (UniProt)
8HNA_T1	RP11-76P2.3	PTEN	≥8	PTEN	gene ssuppressor (UniProt)
dd3c42e	RP11-93K22.11	MTUS1	≥6.5	MTUS1	gene ssuppressor (UniProt)
QYXQ_M1	RP3-453D15.1	FRK	≥6.5	FRK	gene ssuppressor (UniProt)
LRU2_M1	RPTOR	NF1	≥6.5	NF1	gene ssuppressor (UniProt)
T6Z1_T1	SASH1	PCMT1	≥8	SASH1	gene ssuppressor (UniProt)
T6Z1_M1	SPAG9	NF1	≥6.5	NF1	gene ssuppressor (UniProt)
TW0Z_T1	UFL1	AIM1	≥8	UFL1	gene ssuppressor (UniProt)
YA4W_M1	ZMYND11	CSMD3	≥8	ZMYND11	gene ssuppressor (UniProt)
46DP_M1	ZNF595	PINX1	≥8	PINX1	gene ssuppressor (UniProt)
b9b21b9	ZNRF3	CHEK2	≥8	CHEK2	gene ssuppressor (UniProt)
AEK9_T1	ZUFSP	MTUS1	≥6.5	MTUS1	gene ssuppressor (UniProt)

Note: The order of fusion partner 5' and 3' is ignored to simplify comparison.

Table S12: Mutations of CYP, SULT and UGT family genes.

Gene	Sample_ID	Chromosome	Position	Reference	Alternative
CYP11B2	E65C_M1	8	143995706	C	T
CYP21A2	DBBB_M1	6	32007327	A	G
CYP24A1	TM97_T1	20	52775638	G	C
CYP26C1	E65C_M1	10	94821792	G	C
CYP26C1	T2VO_M1	10	94828310	G	C
CYP26C1	OE5B_T1	10	94828310	G	C
CYP27A1	b9b21b9	2	219646928	G	C
CYP2C8	ZS4T_T1	10	96800708	T	A
CYP2R1	9HTD_T1	11	14900848	T	A
CYP2U1	E65C_M1	4	108853211	G	C
CYP3A5	E65C_M1	7	99264265	C	G
CYP51A1	EDTK_T1	7	91743002	G	A
SULT1A1	E65C_M1	16	28619801	G	A
SULT1C4	8HNA_T1	2	108999642	G	T
UGT1A7	3b8237c	2	234590789	C	T
UGT2B17	4R5V_M1	4	69431337	C	T
UGT2B7	AC72_T1	4	69964380	T	A

“_T1” indicates primary tumors and the remaining are refractory tumors.

Bibliography

- [1] Bert Vogelstein and Kenneth W Kinzler. The multistep nature of cancer. *Trends in genetics*, 9(4):138–141, 1993. 1.1
- [2] Carlo M Croce. Oncogenes and cancer. *New England Journal of Medicine*, 358(5):502–511, 2008. 1.1
- [3] Felix Mitelman, Bertil Johansson, and Fredrik Mertens. The impact of translocations and gene fusions on cancer causation. *Nature Reviews Cancer*, 7(4):233–245, 2007. 1.1
- [4] Fredrik Mertens, Bertil Johansson, Thoas Fioretos, and Felix Mitelman. The emerging complexity of gene fusions in cancer. *Nature Reviews Cancer*, 15(6):371–381, 2015. 1.1, 1.4, 1.7, 1.3, 1.4, 1.6, 4.2
- [5] Cancer Genome Atlas Network et al. Comprehensive molecular portraits of human breast tumours. *Nature*, 490(7418):61–70, 2012. 1.2
- [6] Weiyi Toy, Yang Shen, Helen Won, Bradley Green, Rita A Sakr, Marie Will, Zhiqiang Li, Kinisha Gala, Sean Fanning, Tari A King, et al. ESR1 ligand-binding domain mutations in hormone-resistant breast cancer. *Nature genetics*, 45(12):1439–1445, 2013. 1.2, 1.2, 1.2, 1.6
- [7] Dan R Robinson, Yi-Mi Wu, Pankaj Vats, Fengyun Su, Robert J Lonigro, Xuhong Cao, Shanker Kalyana-Sundaram, Rui Wang, Yu Ning, Lynda Hodges, et al. Activating ESR1 mutations in hormone-resistant metastatic breast cancer. *Nature genetics*, 45(12):1446–1451, 2013. 1.2, 1.2, 1.6, 3.1.2, 4.3.2, 4.3.3
- [8] William D Foulkes, Ian E Smith, and Jorge S Reis-Filho. Triple-negative breast cancer. *New England journal of medicine*, 363(20):1938–1948, 2010. 1.2
- [9] Steven A Narod. Breast cancer in young women. *Nature reviews Clinical oncology*, 9(8):460–470, 2012. 1.2

- [10] Aron Goldhirsch, Eric P Winer, AS Coates, RD Gelber, Martine Piccart-Gebhart, B Thürlimann, H-J Senn, Kathy S Albain, Fabrice André, Jonas Bergh, et al. Personalizing the treatment of women with early breast cancer: highlights of the St Gallen International Expert Consensus on the Primary Therapy of Early Breast Cancer 2013. *Annals of oncology*, 24(9):2206–2223, 2013. 1.2
- [11] Christina Curtis, Sohrab P Shah, Suet-Feung Chin, Gulisa Turashvili, Oscar M Rueda, Mark J Dunning, Doug Speed, Andy G Lynch, Shamith Samarajiwa, Yinyin Yuan, et al. The genomic and transcriptomic architecture of 2,000 breast tumours reveals novel subgroups. *Nature*, 486(7403):346–352, 2012. 1.2
- [12] Shantanu Banerji, Kristian Cibulskis, Claudia Rangel-Escareno, Kristin K Brown, Scott L Carter, Abbie M Frederick, Michael S Lawrence, Andrey Y Sivachenko, Carrie Sougnez, Lihua Zou, et al. Sequence analysis of mutations and translocations across breast cancer subtypes. *Nature*, 486(7403):405–409, 2012. 1.2, 1.2, 1.4
- [13] Matthew J Ellis, Li Ding, Dong Shen, Jingqin Luo, Vera J Suman, John W Wallis, Brian A Van Tine, Jeremy Hoog, Reece J Goiffon, Theodore C Goldstein, et al. Whole-genome analysis informs breast cancer response to aromatase inhibition. *Nature*, 486(7403):353–360, 2012. 1.2
- [14] Michael S Lawrence, Petar Stojanov, Craig H Mermel, James T Robinson, Levi A Garraway, Todd R Golub, Matthew Meyerson, Stacey B Gabriel, Eric S Lander, and Gad Getz. Discovery and saturation analysis of cancer genes across 21 tumour types. *Nature*, 505(7484):495–501, 2014. 1.2, 3.1.2
- [15] Philip J Stephens, Patrick S Tarpey, Helen Davies, Peter Van Loo, Chris Greenman, David C Wedge, Serena Nik-Zainal, Sancha Martin, Ignacio Varela, Graham R Bignell, et al. The landscape of cancer genes and mutational processes in breast cancer. *Nature*, 486(7403):400–404, 2012. 1.2
- [16] Kornelia Polyak and Otto Metzger Filho. Snapshot: Breast cancer. *Cancer Cell*, 22(4):562 – 562.e1, 2012. 1.1
- [17] Steffi Oesterreich and Nancy E Davidson. The search for ESR1 mutations in breast cancer. *Nature genetics*, 45(12):1415–1416, 2013. 1.3
- [18] Shuzhen Liu, Judy-Anne W Chapman, Margot J Burnell, Mark N Levine, Kathleen I Pritchard, Timothy J Whelan, Hope S Rugo, Kathy S Albain, Edith A Perez, Shakeel Virk, et al. Prognostic and predictive investigation of PAM50 intrinsic subtypes in the

- NCIC CTG MA. 21 phase III chemotherapy trial. *Breast cancer research and treatment*, 149(2):439–448, 2015. 1.2
- [19] Joel S Parker, Michael Mullins, Maggie CU Cheang, Samuel Leung, David Voduc, Tammi Vickery, Sherri Davies, Christiane Fauron, Xiaping He, Zhiyuan Hu, et al. Supervised risk predictor of breast cancer based on intrinsic subtypes. *Journal of clinical oncology*, 27(8):1160–1167, 2009. 1.2
- [20] Soonmyung Paik, Steven Shak, Gong Tang, Chungyeul Kim, Joffre Baker, Maureen Cronin, Frederick L Baehner, Michael G Walker, Drew Watson, Taesung Park, et al. A multigene assay to predict recurrence of tamoxifen-treated, node-negative breast cancer. *New England Journal of Medicine*, 351(27):2817–2826, 2004. 1.2
- [21] Soonmyung Paik, Gong Tang, Steven Shak, Chungyeul Kim, Joffre Baker, Wanseop Kim, Maureen Cronin, Frederick L Baehner, Drew Watson, John Bryant, et al. Gene expression and benefit of chemotherapy in women with node-negative, estrogen receptor-positive breast cancer. *Journal of clinical oncology*, 24(23):3726–3734, 2006. 1.2
- [22] Laura J Van't Veer, Hongyue Dai, Marc J Van De Vijver, Yudong D He, Augustinus AM Hart, Mao Mao, Hans L Peterse, Karin van der Kooy, Matthew J Marton, Anke T Witteveen, et al. Gene expression profiling predicts clinical outcome of breast cancer. *nature*, 415(6871):530–536, 2002. 1.2
- [23] Laura J van't Veer, Soonmyung Paik, and Daniel F Hayes. Gene expression profiling of breast cancer: a new tumor marker. *Journal of clinical oncology*, 23(8):1631–1635, 2005. 1.2
- [24] Christos Sotiriou and Lajos Pusztai. Gene-expression signatures in breast cancer. *New England Journal of Medicine*, 360(8):790–800, 2009. 1.2
- [25] H Raza Ali, Oscar M Rueda, Suet-Feung Chin, Christina Curtis, Mark J Dunning, SAJR Aparicio, and Carlos Caldas. Genome-driven integrated classification of breast cancer validated in over 7,500 samples. *Genome Biol*, 15(8):431, 2014. 1.2
- [26] Minju Ha and V Narry Kim. Regulation of microRNA biogenesis. *Nature reviews Molecular cell biology*, 15(8):509–524, 2014. 1.2
- [27] Eleni van Schooneveld, Hans Wildiers, Ignace Vergote, Peter B Vermeulen, Luc Y Dirix, and Steven J Van Laere. Dysregulation of microRNAs in breast cancer and their potential role as prognostic and predictive biomarkers in patient management. *Breast Cancer Research*, 17(1):21, 2015. 1.2

- [28] Li Ma, Julie Teruya-Feldstein, and Robert A Weinberg. Tumour invasion and metastasis initiated by microRNA-10b in breast cancer. *Nature*, 449(7163):682–688, 2007. 1.2
- [29] Galina Gabriely, Nadiya M Teplyuk, and Anna M Krichevsky. Context effect: microRNA-10b in cancer cell proliferation, spread and death. *Autophagy*, 7(11):1384–1386, 2011. 1.2
- [30] Heidi Dvinge, Anna Git, Stefan Gräf, Mali Salmon-Divon, Christina Curtis, Andrea Sottoriva, Yongjun Zhao, Martin Hirst, Javier Armisen, Eric A Miska, et al. The shaping and functional consequences of the microRNA landscape in breast cancer. *Nature*, 497(7449):378–382, 2013. 1.2
- [31] Tatiana Borodina, James Adjaye, and Marc Sultan. A strand-specific library preparation protocol for RNA sequencing. *Methods Enzymol*, 500:79–98, 2011. 1.2, 2.1
- [32] Marc Sultan, Simon Dökel, Vyacheslav Amstislavskiy, Daniela Wuttig, Holger Sültmann, Hans Lehrach, and Marie-Laure Yaspo. A simple strand-specific RNA-Seq library preparation protocol combining the Illumina TruSeq RNA and the dUTP methods. *Biochemical and biophysical research communications*, 422(4):643–646, 2012. 1.2, 2.1
- [33] O Alejandro Balbin, Rohit Malik, Saravana M Dhanasekaran, John R Prensner, Xuhong Cao, Yi-Mi Wu, Dan Robinson, Rui Wang, Guoan Chen, David G Beer, et al. The landscape of antisense gene expression in human cancers. *Genome research*, 25(7):1068–1079, 2015. 1.2
- [34] Douglas L Black. Mechanisms of alternative pre-messenger RNA splicing. *Annual review of biochemistry*, 72(1):291–336, 2003. 1.2
- [35] Jeyanthy Eswaran, Anelia Horvath, Sucheta Godbole, Sirigiri Divijendra Reddy, Prakriti Mudvari, Kazufumi Ohshiro, Dinesh Cyanam, Sujit Nair, Suzanne AW Fuqua, Kornelia Polyak, et al. RNA sequencing of cancer reveals novel splicing alterations. *Scientific reports*, 3, 2013. 1.2
- [36] Dimitrios Zardavas, José Baselga, and Martine Piccart. Emerging targeted agents in metastatic breast cancer. *Nature Reviews Clinical Oncology*, 10(4):191–210, 2013. 1.2, 1.4
- [37] Marta Persson, Ywonne Andrén, Joachim Mark, Hugo M Horlings, Fredrik Persson, and Göran Stenman. Recurrent fusion of MYB and NFIB transcription factor genes in carcinomas of the breast and head and neck. *Proceedings of the National Academy of Sciences*, 106(44):18740–18744, 2009. 1.2, 3.3.7.16, 3.17
- [38] Marick Laé, Paul Fréneaux, Xavier Sastre-Garau, Olfa Chouchane, Brigitte Sigal-Zafrani, and Anne Vincent-Salomon. Secretory breast carcinomas with ETV6-NTRK3 fusion gene

- belong to the basal-like carcinoma spectrum. *Modern Pathology*, 22(2):291–298, 2009. 1.2
- [39] Dan R Robinson, Shanker Kalyana-Sundaram, Yi-Mi Wu, Sunita Shankar, Xuhong Cao, Bushra Ateeq, Irfan A Asangani, Matthew Iyer, Christopher A Maher, Catherine S Grasso, et al. Functionally recurrent rearrangements of the MAST kinase and Notch gene families in breast cancer. *Nature medicine*, 17(12):1646–1651, 2011. 1.2, 1.6, 3.3.7.4, 4.3.2
- [40] Jamunarani Veeraraghavan, Ying Tan, Xi-Xi Cao, Jin Ah Kim, Xian Wang, Gary C Chamness, Sourindra N Maiti, Laurence JN Cooper, Dean P Edwards, Alejandro Contreras, et al. Recurrent ESR1–CCDC170 rearrangements in an aggressive subset of oestrogen receptor-positive breast cancers. *Nature communications*, 5, 2014. 1.2, 3.3.7.6, 4.3.3
- [41] Juan-Miguel Mosquera, Sonal Varma, Chantal Pauli, Theresa Y MacDonald, Jossie J Yashinski, Zsuzsanna Varga, Andrea Sboner, Holger Moch, Mark A Rubin, and Sandra J Shin. MAGI3-AKT3 fusion in breast cancer amended. *Nature*, 520(7547):E11–E12, 2015. 1.2
- [42] Francesco Abate, Sakellarios Zairis, Elisa Ficarra, Andrea Acquaviva, Chris H Wiggins, Veronique Frattini, Anna Lasorella, Antonio Iavarone, Giorgio Inghirami, and Raul Rabadan. Pegasus: a comprehensive annotation and prediction tool for detection of driver gene fusions in cancer. *BMC systems biology*, 8(1):97, 2014. 1.3, 1.3, 1.6
- [43] Thomas Helleday, Saeed Eshtad, and Serena Nik-Zainal. Mechanisms underlying mutational signatures in human cancers. *Nature Reviews Genetics*, 15(9):585–598, 2014. 1.3
- [44] Karin G Hermans, Ronald van Marion, Herman van Dekken, Guido Jenster, Wytske M van Weerden, and Jan Trapman. TMPRSS2: ERG fusion by translocation or interstitial deletion is highly relevant in androgen-dependent prostate cancer, but is bypassed in late-stage androgen receptor-negative prostate cancer. *Cancer research*, 66(22):10658–10663, 2006. 1.3
- [45] Sven Perner, Francesca Demichelis, Rameen Beroukhim, Folke H Schmidt, Juan-Miguel Mosquera, Sunita Setlur, Joelle Tchinda, Scott A Tomlins, Matthias D Hofer, Kenneth G Pienta, et al. TMPRSS2: ERG fusion-associated deletions provide insight into the heterogeneity of prostate cancer. *Cancer research*, 66(17):8337–8341, 2006. 1.3
- [46] Sameer Jhavar, Alison Reid, Jeremy Clark, Zsofia Kote-Jarai, Timothy Christmas, Alan Thompson, Christopher Woodhouse, Christopher Ogden, Cyril Fisher, Cathy Corbishley, et al. Detection of TMPRSS2-ERG translocations in human prostate cancer by expression

- profiling using GeneChip Human Exon 1.0 ST arrays. *The Journal of Molecular Diagnostics*, 10(1):50–57, 2008. 1.3
- [47] Anthony JF Griffiths, Susan R Wessler, Richard C Suzuki, Lewontin, William M Gelbart, David T, Jeffrey H Miller, et al. *An introduction to genetic analysis*. 8th edition, 2005. 1.5
- [48] Yuesheng Jin, Fredrik Mertens, Carl-Magnus Kullendorff, et al. Fusion of the tumor-suppressor gene CHEK2 and the gene for the regulatory subunit B of protein phosphatase 2 PPP2R2A in childhood teratoma. *Neoplasia*, 8(5):413–418, 2006. 1.3
- [49] Peter J Campbell, Philip J Stephens, Erin D Pleasance, Sarah O’Meara, Heng Li, Thomas Santarius, Lucy A Stebbings, Catherine Leroy, Sarah Edkins, Claire Hardy, et al. Identification of somatically acquired rearrangements in cancer using genome-wide massively parallel paired-end sequencing. *Nature genetics*, 40(6):722–729, 2008. 1.4
- [50] Andrew McPherson, Fereydoun Hormozdiari, Abdalnasser Zayed, Ryan Giuliany, Gavin Ha, Mark GF Sun, Malachi Griffith, Alireza Heravi Moussavi, Janine Senz, Nataliya Melnyk, et al. deFuse: an algorithm for gene fusion discovery in tumor RNA-Seq data. *PLoS Comput Biol.* 1.4, 1.1, 1.5, 1.9, 1.10, 1.11, 2.2.3, 3.2.3
- [51] Somasekar Seshagiri, Eric W Stawiski, Steffen Durinck, Zora Modrusan, Elaine E Storm, Caitlin B Conboy, Subhra Chaudhuri, Yinghui Guan, VasanthaRajan Janakiraman, Bijay S Jaiswal, et al. Recurrent R-spondin fusions in colon cancer. *Nature*, 488(7413):660–664, 2012. 1.4
- [52] Christian Steidl, Sohrab P Shah, Bruce W Woolcock, Lixin Rui, Masahiro Kawahara, Pedro Farinha, Nathalie A Johnson, Yongjun Zhao, Adele Telenius, Susana Ben Neriah, et al. MHC class II transactivator CIITA is a recurrent gene fusion partner in lymphoid cancers. *Nature*, 471(7338):377–381, 2011. 1.4, 2.3
- [53] Joachim Weischenfeldt, Ronald Simon, Lars Feuerbach, Karin Schlangen, Dieter Weichenhan, Sarah Minner, Daniela Wuttig, Hans-Jörg Warnatz, Henning Stehr, Tobias Rausch, et al. Integrative genomic analyses reveal an androgen-driven somatic alteration landscape in early-onset prostate cancer. *Cancer cell*, 23(2):159–170, 2013. 1.4, 3.3.2, 3.8
- [54] Julio C Ricarte-Filho, Sheng Li, Maria ER Garcia-Rendueles, Cristina Montero-Conde, Francesca Voza, Jeffrey A Knauf, Adriana Heguy, Agnes Viale, Tetyana Bogdanova, Geraldine A Thomas, et al. Identification of kinase fusion oncogenes in post-Chernobyl radiation-induced thyroid cancers. *The Journal of clinical investigation*, 123(11):4935, 2013. 1.4, 3.2

- [55] Zhao-Shi Bao, Hui-Min Chen, Ming-Yu Yang, Chuan-Bao Zhang, Kai Yu, Wan-Lu Ye, Bo-Qiang Hu, Wei Yan, Wei Zhang, Johnny Akers, et al. RNA-seq of 272 gliomas revealed a novel, recurrent PTPRZ1-MET fusion transcript in secondary glioblastomas. *Genome research*, 24(11):1765–1773, 2014. 1.4, 3.2
- [56] Henrik Lilljebjörn, Helena Ågerstam, Christina Orsmark Pietras, Marianne Rissler, Hans Ehrencrona, L Nilsson, Johan Richter, and Thoas Fioretos. RNA-seq identifies clinically relevant fusion genes in leukemia including a novel MEF2D/CSF1R fusion responsive to imatinib. *Leukemia*, 28(4):977–979, 2014. 1.4
- [57] Cancer Genome Atlas Research Network et al. Comprehensive molecular characterization of clear cell renal cell carcinoma. *Nature*, 499(7456):43–49, 2013. 1.4, 2.3
- [58] Saravana M Dhanasekaran, O Alejandro Balbin, Guoan Chen, Ernest Nadal, Shanker Kalyana-Sundaram, Jincheng Pan, Brendan Veeneman, Xuhong Cao, Rohit Malik, Pankaj Vats, et al. Transcriptome meta-analysis of lung cancer reveals recurrent aberrations in NRG1 and Hippo pathway genes. *Nature communications*, 5, 2014. 1.4
- [59] Juliann Chmielecki, Aimee M Crago, Mara Rosenberg, Rachael O'Connor, Sarah R Walker, Lauren Ambrogio, Daniel Auclair, Aaron McKenna, Michael C Heinrich, David A Frank, et al. Whole-exome sequencing identifies a recurrent NAB2-STAT6 fusion in solitary fibrous tumors. *Nature genetics*, 45(2):131–132, 2013. 1.4
- [60] Daehwan Kim and Steven L Salzberg. TopHat-Fusion: an algorithm for discovery of novel fusion transcripts. *Genome Biol*, 12(8):R72, 2011. 1.1
- [61] Marcus Kinsella, Olivier Harismendy, Masakazu Nakano, Kelly A Frazer, and Vineet Bafna. Sensitive gene fusion detection using ambiguously mapping RNA-Seq read pairs. *Bioinformatics*, 27(8):1068–1075, 2011. 1.1
- [62] Yang Li, Jeremy Chien, David I Smith, and Jian Ma. FusionHunter: identifying fusion transcripts in cancer using paired-end RNA-seq. *Bioinformatics*, 27(12):1708–1710, 2011. 1.1
- [63] Andrea Sboner, Lukas Habegger, Dorothee Pflueger, Stephane Terry, David Z Chen, Joel S Rozowsky, Ashutosh K Tewari, Naoki Kitabayashi, Benjamin J Moss, Mark S Chee, et al. FusionSeq: a modular framework for finding gene fusions by analyzing paired-end RNA-sequencing data. *Genome Biol*, 11(10):R104, 2010. 1.1
- [64] Richard W Francis, Katherine Thompson-Wicking, Kim W Carter, Denise Anderson, Ursula R Kees, and Alex H Beesley. FusionFinder: a software tool to identify expressed gene fusion candidates from RNA-Seq data. *PloS one*, 7(6):e39987, 2012. 1.1

- [65] Huanying Ge, Kejun Liu, Todd Juan, Fang Fang, Matthew Newman, and Wolfgang Hoeck. FusionMap: detecting fusion genes from next-generation sequencing data at base-pair resolution. *Bioinformatics*, 27(14):1922–1928, 2011. 1.1, 2.2.3
- [66] Wenlong Jia, Kunlong Qiu, Minghui He, Pengfei Song, Quan Zhou, Feng Zhou, Yuan Yu, Dandan Zhu, Michael L Nickerson, Shengqing Wan, et al. SOAPfuse: an algorithm for identifying fusion transcripts from paired-end RNA-Seq data. *Genome Biol*, 14:R12, 2013. 1.1, 2.2.3
- [67] Matthew K Iyer, Arul M Chinnaiyan, and Christopher A Maher. ChimeraScan: a tool for identifying chimeric transcription in sequencing data. *Bioinformatics*, 27(20):2903–2904, 2011. 1.1
- [68] Ken Chen, John W Wallis, Cyriac Kandoth, Joelle M Kalicki, Karen L Mungall, Andrew J Mungall, Steven J Jones, Marco A Marra, Timothy J Ley, Elaine R Mardis, et al. BreakFusion: targeted assembly-based identification of gene fusions in whole transcriptome paired-end sequencing data. *Bioinformatics*, 28(14):1923–1924, 2012. 1.1
- [69] Yan W Asmann, Asif Hossain, Brian M Necela, Sumit Middha, Krishna R Kalari, Zhifu Sun, High-Seng Chai, David W Williamson, Derek Radisky, Gary P Schroth, et al. A novel bioinformatics pipeline for identification and characterization of fusion transcripts in breast cancer and normal cell lines. *Nucleic acids research*, 39(15):e100–e100, 2011. 1.1
- [70] Rocco Piazza, Alessandra Pirola, Roberta Spinelli, Simona Valletta, Sara Redaelli, Vera Magistroni, and Carlo Gambacorti-Passerini. FusionAnalyser: a new graphical, event-driven tool for fusion rearrangements discovery. *Nucleic acids research*, page gks394, 2012. 1.1
- [71] Wandaliz Torres-García, Siyuan Zheng, Andrey Sivachenko, Rahulsimham Vegeña, Qianghu Wang, Rong Yao, Michael F Berger, John N Weinstein, Gad Getz, and Roel GW Verhaak. PRADA: pipeline for RNA sequencing data analysis. *Bioinformatics*, 30(15):2224–2226, 2014. 1.1, 1.4, 2.3
- [72] K Yoshihara, Q Wang, W Torres-Garcia, S Zheng, R Vegeña, H Kim, and RGW Verhaak. The landscape and therapeutic relevance of cancer-associated transcript fusions. *Oncogene*, 2014. 1.4, 1.2, 1.8, 3.2.5, 4.3.3
- [73] Matteo Carrara, Marco Beccuti, Fulvio Lazzarato, Federica Cavallo, Francesca Cordero, Susanna Donatelli, and Raffaele A Calogero. State-of-the-art fusion-finder algorithms sensitivity and specificity. *BioMed research international*, 2013, 2013. 1.4

- [74] Ben Langmead, Cole Trapnell, Mihai Pop, and Steven L Salzberg. Ultrafast and memory-efficient alignment of short DNA sequences to the human genome. *Genome Biol*, 10(3):R25, 2009. 1.5
- [75] Jianmin Wang, Charles G Mullighan, John Easton, Stefan Roberts, Sue L Heatley, Jing Ma, Michael C Rusch, Ken Chen, Christopher C Harris, Li Ding, et al. CREST maps somatic structural variation in cancer genomes with base-pair resolution. *Nature methods*, 8(8):652–654, 2011. 2.2.1
- [76] Tobias Rausch, Thomas Zichner, Andreas Schlattl, Adrian M Stütz, Vladimir Benes, and Jan O Korbel. DELLY: structural variant discovery by integrated paired-end and split-read analysis. *Bioinformatics*, 28(18):i333–i339, 2012. 2.2.1
- [77] Heng Li and Richard Durbin. Fast and accurate long-read alignment with Burrows-Wheeler transform. *Bioinformatics*, 26(5):589–595, March 2010. 2.2.2
- [78] Heng Li, Bob Handsaker, Alec Wysoker, Tim Fennell, Jue Ruan, Nils Homer, and Gabor Marth et al. The Sequence Alignment/Map (SAM) Format and SAMtools. *Bioinformatics*, 25(16):2078–2079, Aug 2009. 2.2.2
- [79] David TW Jones, Natalie Jäger, Marcel Kool, Thomas Zichner, Barbara Hutter, Marc Sultan, Yoon-Jae Cho, Trevor J Pugh, Volker Hovestadt, Adrian M Stütz, et al. Dissecting the genomic complexity underlying medulloblastoma. *Nature*, 488(7409):100–105, 2012. 2.2.2
- [80] Daniel C Koboldt, Qunyuan Zhang, David E Larson, Dong Shen, Michael D McLellan, Ling Lin, Christopher A Miller, Elaine R Mardis, Li Ding, and Richard K Wilson. VarScan 2: somatic mutation and copy number alteration discovery in cancer by exome sequencing. *Genome research*, 22(3):568–576, 2012. 2.2.2
- [81] Andy Rimmer, Hang Phan, Iain Mathieson, Zamin Iqbal, Stephen RF Twigg, Andrew OM Wilkie, Gil McVean, Gerton Lunter, WGS500 Consortium, et al. Integrating mapping-, assembly-and haplotype-based approaches for calling variants in clinical sequencing applications. *Nature genetics*, 46(8):912–918, 2014. 2.2.2
- [82] David S DeLuca, Joshua Z Levin, Andrey Sivachenko, Timothy Fennell, Marc-Danie Nazaire, Chris Williams, Michael Reich, Wendy Winckler, and Gad Getz. RNA-SeQC: RNA-seq metrics for quality control and process optimization. *Bioinformatics*, 28(11):1530–1532, 2012. 2.2.3

- [83] Alexander Dobin, Carrie A Davis, Felix Schlesinger, Jorg Drenkow, Chris Zaleski, Sonali Jha, Philippe Batut, Mark Chaisson, and Thomas R Gingeras. STAR: ultrafast universal RNA-seq aligner. *Bioinformatics*, 29(1):15–21, 2013. 2.2.3
- [84] Simon Anders, Paul Theodor Pyl, and Wolfgang Huber. HTSeq—A Python framework to work with high-throughput sequencing data. *Bioinformatics*, page btu638, 2014. 2.2.3
- [85] Andreas Untergasser, Ioana Cutcutache, Triinu Koressaar, Jian Ye, Brant C Faircloth, Maito Remm, and Steven G Rozen. Primer3-new capabilities and interfaces. *Nucleic acids research*, 40(15):e115–e115, 2012. 2.2.3
- [86] Nasim Ahmadiyeh, Mark M Pomerantz, Chiara Grisanzio, Paula Herman, Li Jia, Vanessa Almendro, Housheng Hansen He, Myles Brown, X Shirley Liu, Matt Davis, et al. 8q24 prostate, breast, and colon cancer risk loci show tissue-specific long-range interaction with MYC. *Proceedings of the National Academy of Sciences*, 107(21):9742–9746, 2010. 3.1.1
- [87] Sarina Sulong, Anthony V Moorman, Julie AE Irving, Jonathan C Strefford, Zoe J Konn, Marian C Case, Lynne Minto, Kerry E Barber, Helen Parker, Sarah L Wright, et al. A comprehensive analysis of the CDKN2A gene in childhood acute lymphoblastic leukemia reveals genomic deletion, copy number neutral loss of heterozygosity, and association with specific cytogenetic subgroups. *Blood*, 113(1):100–107, 2009. 3.1.1
- [88] Cynthia X Ma, Tomás Reinert, Izabela Chmielewska, and Matthew J Ellis. Mechanisms of aromatase inhibitor resistance. *Nature Reviews Cancer*, 15(5):261–275, 2015. 3.1.1, 4.3.3
- [89] Yoshiaki Ito, Suk-Chul Bae, and Linda Shyue Huey Chuang. The RUNX family: developmental regulators in cancer. *Nature Reviews Cancer*, 15(2):81–95, 2015. 3.1.1
- [90] Geneviève Deblois and Vincent Giguère. Oestrogen-related receptors in breast cancer: control of cellular metabolism and beyond. *Nature Reviews Cancer*, 13(1):27–36, 2013. 3.1.1
- [91] Giovanni Ciriello, Michael L Gatza, Andrew H Beck, Matthew D Wilkerson, Suhn K Rhie, Alessandro Pastore, Hailei Zhang, Michael McLellan, Christina Yau, Cyriac Kandoth, et al. Comprehensive Molecular Portraits of Invasive Lobular Breast Cancer. *Cell*, 163(2):506–519, 2015. 3.1.2
- [92] C Palmieri, B Rudraraju, M Monteverde, L Lattanzio, O Gojis, R Brizio, O Garrone, M Merlano, N Syed, C Lo Nigro, et al. Methylation of the calcium channel regulatory subunit $\alpha 2\delta$ -3 (CACNA2D3) predicts site-specific relapse in oestrogen receptor-positive primary breast carcinomas. *British journal of cancer*, 107(2):375–381, 2012. 3.1.2

- [93] Young Seok Ju, Won-Chul Lee, Jong-Yeon Shin, Seungbok Lee, Thomas Bleazard, Jae-Kyung Won, Young Tae Kim, Jong-Il Kim, Jin-Hyoung Kang, and Jeong-Sun Seo. A transforming KIF5B and RET gene fusion in lung adenocarcinoma revealed from whole-genome and transcriptome sequencing. *Genome research*, 22(3):436–445, 2012. 3.2
- [94] Xiaoke Wang, Krista L Bledsoe, Rondell P Graham, Yan W Asmann, David S Viswanatha, Jean E Lewis, Jason T Lewis, Margaret M Chou, Michael J Yaszemski, Jin Jen, et al. Recurrent PAX3-MAML3 fusion in biphenotypic sinonasal sarcoma. *Nature genetics*, 46(7):666–668, 2014. 3.2
- [95] David TW Jones, Barbara Hutter, Natalie Jäger, Andrey Korshunov, Marcel Kool, Hans-Jörg Warnatz, Thomas Zichner, Sally R Lambert, Marina Ryzhova, Dong Anh Khuong Quang, et al. Recurrent somatic alterations of FGFR1 and NTRK2 in pilocytic astrocytoma. *Nature genetics*, 45(8):927–932, 2013. 3.2
- [96] Kristian W Pajtler, Hendrik Witt, Martin Sill, David TW Jones, Volker Hovestadt, Fabian Kratochwil, Khalida Wani, Ruth Tatevossian, Chandanamali Punchihewa, Pascal Johann, et al. Molecular Classification of Ependymal Tumors across All CNS Compartments, Histopathological Grades, and Age Groups. *Cancer cell*, 27(5):728–743, 2015. 3.2, 3.3.6
- [97] Jeong-Sun Seo, Young Seok Ju, Won-Chul Lee, Jong-Yeon Shin, June Koo Lee, Thomas Bleazard, Junho Lee, Yoo Jin Jung, Jung-Oh Kim, Jung-Young Shin, et al. The transcriptional landscape and mutational profile of lung adenocarcinoma. *Genome research*, 2012. 3.2
- [98] Feng-Yang Zong, Xing Fu, Wen-Juan Wei, Ya-Ge Luo, Monika Heiner, Li-Juan Cao, Zhaoyuan Fang, Rong Fang, Daru Lu, Hongbin Ji, et al. The RNA-binding protein QKI suppresses cancer-associated aberrant splicing. *PLoS Genet*, 10(4):e1004289, 2014. 3.2.5
- [99] Helen R Dawe, Helen Farr, Neil Portman, Michael K Shaw, and Keith Gull. The Parkin co-regulated gene product, PACRG, is an evolutionarily conserved axonemal protein that functions in outer-doublet microtubule morphogenesis. *Journal of cell science*, 118(23):5421–5430, 2005. 3.2.5
- [100] M Trautmann, E Sievers, S Aretz, D Kindler, S Michels, N Friedrichs, M Renner, J Kirfel, S Steiner, S Huss, et al. SS18-SSX fusion protein-induced Wnt/β-catenin signaling is a therapeutic target in synovial sarcoma. *Oncogene*, 33(42):5006–5016, 2014. 3.3.1
- [101] Melker Göransson, Mattias K Andersson, C Forni, Anders Ståhlberg, Carola Andersson, A Olofsson, R Mantovani, and Pierre Åman. The myxoid liposarcoma FUS-DDIT3 fusion

- oncoprotein deregulates NF- κ B target genes by interaction with NFKBIZ. *Oncogene*, 28(2):270–278, 2009. 3.3.1
- [102] Nele Vanlangenakker, T Vanden Berghe, and Peter Vandenabeele. Many stimuli pull the necrotic trigger, an overview. *Cell Death & Differentiation*, 19(1):75–86, 2012. 3.3.2
- [103] Arthur Lau, Karim Khan, Alex Pavlosky, Ziqin Yin, Xuyan Huang, Aaron Haig, Weihua Liu, Bhagi Singh, Zhu-Xu Zhang, and Anthony M Jevnikar. Serine Protease Inhibitor-6 Inhibits Granzyme B–Mediated Injury of Renal Tubular Cells and Promotes Renal Allograft Survival. *Transplantation*, 98(4):402–410, 2014. 3.3.3
- [104] Yu-Zhang Jiang, Qian-Hui Li, Jian-Qiang Zhao, and Jun-Ji Lv. Identification of a novel fusion gene (HLA-E and HLA-B) by RNA-seq analysis in esophageal squamous cell carcinoma. *Asian Pacific journal of cancer prevention: APJCP*, 15(5):2309–2312, 2013. 3.3.4
- [105] Pedro G Ferreira, Pedro Jares, Daniel Rico, Gonzalo Gómez-López, Alejandra Martínez-Trillo, Neus Villamor, Simone Ecker, Abel González-Pérez, David G Knowles, Jean Monlong, et al. Transcriptome characterization by RNA sequencing identifies a major molecular and clinical subdivision in chronic lymphocytic leukemia. *Genome research*, 24(2):212–226, 2014. 3.3.5
- [106] Richard Pearson, Jacqueline Fleetwood, Sally Eaton, Merlin Crossley, and Shisan Bao. Krüppel-like transcription factors: a functional family. *The international journal of biochemistry & cell biology*, 40(10):1996–2001, 2008. 3.3.6
- [107] Matthew Parker, Kumarasamypet M Mohankumar, Chandanamali Punchihewa, Ricardo Weinlich, James D Dalton, Yongjin Li, Ryan Lee, Ruth G Tatevossian, Timothy N Phoenix, Radhika Thiruvenkatam, et al. C11orf95-RELA fusions drive oncogenic NF-[kgr] B signalling in ependymoma. *Nature*, 506(7489):451–455, 2014. 3.3.7
- [108] Wei Ma, Claudia Baumann, and Maria M Viveiros. NEDD1 is crucial for meiotic spindle stability and accurate chromosome segregation in mammalian oocytes. *Developmental biology*, 339(2):439–450, 2010. 3.3.8
- [109] Anne Beghin, Stéphane Belin, Rouba Hage Sleiman, Stéphanie Brunet Manquat, Sophie Goddard, Eric Tabone, Lars P Jordheim, Isabelle Treilleux, Marie-France Poupon, Jean-Jacques Diaz, et al. ADP ribosylation factor like 2 (Arl2) regulates breast tumor aggressivity in immunodeficient mice. *PloS one*, 4(10), 2009. 3.3.8.1
- [110] Anne Béghin, Eva-Laure Matera, Stephanie Brunet-Manquat, and Charles Dumontet. Expression of Arl2 is associated with p53 localization and chemosensitivity in a breast cancer cell line. *Cell Cycle*, 7(19):3074–3082, 2008. 3.3.8.2

- [111] YX Yin, F Shen, H Pei, Y Ding, Hua Zhao, Min Zhao, and Q Chen. Increased expression of Rab25 in breast cancer correlates with lymphatic metastasis. *Tumor Biology*, 33(5):1581–1587, 2012. 3.3.7.1
- [112] Qing Li and Yan Shu. Role of solute carriers in response to anticancer drugs. *Molecular and Cellular Therapies*, 2(1):15, 2014. 3.3.7.2, 4.3.3
- [113] Manuele Rebsamen, Lorena Pochini, Taras Stasyk, Mariana EG de Araújo, Michele Galluccio, Richard K Kandasamy, Berend Snijder, Astrid Fauster, Elena L Rudashevskaya, Manuela Bruckner, et al. SLC38A9 is a component of the lysosomal amino acid sensing machinery that controls mTORC1. *Nature*, 519(7544):477–481, 2015. 3.3.7.2
- [114] Tayebeh Oghabi Bakhshairesh, Marzie Armat, Dariush Shanehbandi, Simin Sharifi, Behzad Baradaran, Mohammad Saeed Hejazi, and Nasser Samadi. Arsenic Trioxide Promotes Paclitaxel Cytotoxicity in Resistant Breast Cancer Cells. *Asian Pacific journal of cancer prevention: APJCP*, 16(13):5191, 2015. 3.3.7.5
- [115] Umberto Galderisi, Francesco Paolo Jori, and Antonio Giordano. Cell cycle regulation and neural differentiation. *Oncogene*, 22(33):5208–5219, 2003. 3.3.7.5
- [116] Yu Zhang, Jian Yao, Lin Huan, Junwei Lian, Chuanyang Bao, Yan Li, Chao Ge, Jinjun Li, Ming Yao, Linhui Liang, et al. GNAI3 inhibits tumor cell migration and invasion and is post-transcriptionally regulated by miR-222 in hepatocellular carcinoma. *Cancer letters*, 356(2):978–984, 2015. 3.3.7.6
- [117] Nguyen Thi Thuy Phuong, Sung Chul Lim, Young Mi Kim, and Keon Wook Kang. Aromatase induction in tamoxifen-resistant breast cancer: Role of phosphoinositide 3-kinase-dependent CREB activation. *Cancer letters*, 351(1):91–99, 2014. 3.3.7.6
- [118] Jun-Yang Lou, Fernanda Laezza, Benjamin R Gerber, Maolei Xiao, Kathryn A Yamada, Hali Hartmann, Ann Marie Craig, Jeanne M Nerbonne, and David M Ornitz. Fibroblast growth factor 14 is an intracellular modulator of voltage-gated sodium channels. *The Journal of physiology*, 569(1):179–193, 2005. 3.3.7.7
- [119] Srivatcha Naragoni, Shireesha Sankella, Kinesha Harris, and Wesley G Gray. Phytoestrogens regulate mRNA and protein levels of guanine nucleotide-binding protein, beta-1 subunit (GNB1) in MCF-7 cells. *Journal of cellular physiology*, 219(3):584–594, 2009. 3.3.7.7
- [120] Kelley C Larson, Michael P Draper, Maciej Lipko, and Michal Dabrowski. Gng12 is a novel negative regulator of LPS-induced inflammation in the microglial cell line BV-2. *Inflammation research*, 59(1):15–22, 2010. 3.3.7.7

- [121] Johan Lennartsson and Lars Rönnstrand. Stem cell factor receptor/c-Kit: from basic science to clinical implications. *Physiological reviews*, 92(4):1619–1649, 2012. 3.3.7.7
- [122] OO Seminog and MJ Goldacre. Age-specific risk of breast cancer in women with neurofibromatosis type 1. *British journal of cancer*, 112(9):1546–1548, 2015. 3.3.7.7
- [123] Zahi Mitri, Tina Constantine, and Ruth O'Regan. The HER2 receptor in breast cancer: pathophysiology, clinical use, and new advances in therapy. *Cancer research and practice*, 2012, 2012. 3.3.7.8
- [124] Hoiseon Jeong, Jinkyung Kim, Youngseok Lee, Jae Hong Seo, Sung Ran Hong, and Aeree Kim. Neuregulin-1 induces cancer stem cell characteristics in breast cancer cell lines. *Oncology reports*, 32(3):1218–1224, 2014. 3.3.7.8
- [125] WY Leung, Ioannis Roxanis, Helen Sheldon, Francesca M Buffa, Ji-Liang Li, Adrian L Harris, and Anthony Kong. Combining lapatinib and pertuzumab to overcome lapatinib resistance due to NRG1-mediated signalling in HER2-amplified breast cancer. *Oncotarget*, 6(8):5678–5694, 2015. 3.3.7.8
- [126] YH Park, HT Shin, HH Jung, YL Choi, T Ahn, K Park, A Lee, IG Do, JY Kim, JS Ahn, et al. Role of HER2 mutations in refractory metastatic breast cancers: targeted sequencing results in patients with refractory breast cancer. *Oncotarget*, 2015. 3.3.7.8
- [127] Sangmin Kim, Jeongmin Lee, Se Kyung Lee, Soo Youn Bae, Jiyoung Kim, Minkuk Kim, Won Ho Kil, Seok Won Kim, Jeong Eon Lee, and Seok Jin Nam. Protein kinase C- α downregulates estrogen receptor- α by suppressing c-Jun phosphorylation in estrogen receptor-positive breast cancer cells. *Oncology reports*, 31(3):1423–1428, 2014. 3.3.7.8
- [128] Christy C Ong, Sarah Gierke, Cameron Pitt, Meredith Sagolla, Christine K Cheng, Wei Zhou, Adrian M Jubb, Laura Strickland, Maike Schmidt, Sergio G Duron, et al. Small molecule inhibition of group I p21-activated kinases in breast cancer induces apoptosis and potentiates the activity of microtubule stabilizing agents. *Breast Cancer Research*, 17(1):59, 2015. 3.3.7.8
- [129] Daniel Lietha, Xinming Cai, Derek FJ Ceccarelli, Yiqun Li, Michael D Schaller, and Michael J Eck. Structural basis for the autoinhibition of focal adhesion kinase. *Cell*, 129(6):1177–1187, 2007. 3.3.7.8
- [130] Farnaz Bahrami-B, Parvin Ataie-Kachoie, Mohammad H Pourgholami, and David L Morris. p70 Ribosomal protein S6 kinase (Rps6kb1): an update. *Journal of clinical pathology*, pages jclinpath–2014, 2014. 3.3.7.9

- [131] Rachel L Yamnik, Alla Digilova, Daphne C Davis, Z Nilly Brodt, Christopher J Murphy, and Marina K Holz. S6 kinase 1 regulates estrogen receptor α in control of breast cancer cell proliferation. *Journal of Biological Chemistry*, 284(10):6361–6369, 2009. 3.3.7.9
- [132] Karin Beelen, Mark Opdam, Tesa M Severson, Rutger HT Koornstra, Andrew D Vincent, Jelle Wesseling, Jettie J Muris, EM Berns, Jan B Vermorken, Paul J van Diest, et al. Phosphorylated p-70S6K predicts tamoxifen resistance in postmenopausal breast cancer patients randomized between adjuvant tamoxifen versus no systemic treatment. *Breast Cancer Res*, 16(1):R6, 2014. 3.3.7.9
- [133] Gray Pearson, Fred Robinson, Tara Beers Gibson, Bing-e Xu, Mahesh Karandikar, Kevin Berman, and Melanie H Cobb. Mitogen-activated protein (MAP) kinase pathways: regulation and physiological functions 1. *Endocrine reviews*, 22(2):153–183, 2001. 3.3.7.10
- [134] Manabu Futamura, Hirofumi Arakawa, Koichi Matsuda, Toyomasa Katagiri, Shigetoyo Saji, Yoshio Miki, and Yusuke Nakamura. Potential role of BRCA2 in a mitotic checkpoint after phosphorylation by hUBR1. *Cancer research*, 60(6):1531–1535, 2000. 3.3.7.11
- [135] Darren J Baker, Meelad M Dawlaty, Tobias Wijshake, Karthik B Jeganathan, Liviu Malureanu, Janine H van Ree, Ruben Crespo-Diaz, Santiago Reyes, Lauren Seaburg, Virginia Shapiro, et al. Increased expression of BubR1 protects against aneuploidy and cancer and extends healthy lifespan. *Nature cell biology*, 15(1):96–102, 2013. 3.3.7.11
- [136] Anupama E Gururaj, Caroline Holm, Göran Landberg, and Rakesh Kumar. Breast Cancer-Amplified Sequence 3, a Target of Metastasis-Associated Protein 1, Contributes to Tamoxifen Resistance in Premenopausal Patients with Breast Cancer. *Cell cycle*, 5(13):1407–1410, 2006. 3.3.7.12
- [137] Anupama E Gururaj, Rajesh R Singh, Suresh K Rayala, Caroline Holm, Petra den Hollander, Hao Zhang, Seetharaman Balasenthil, Amjad H Talukder, Goran Landberg, and Rakesh Kumar. MTA1, a transcriptional activator of breast cancer amplified sequence 3. *Proceedings of the National Academy of Sciences*, 103(17):6670–6675, 2006. 3.3.7.12
- [138] Aaron G Lewis, James Flanagan, Anna Marsh, Gulietta M Pupo, Graham Mann, Amanda B Spurdle, Geoffrey J Lindeman, Jane E Visvader, Melissa A Brown, Georgia Chenevix-Trench, et al. Mutation analysis of FANCD2, BRIP1/BACH1, LMO4 and SFN in familial breast cancer. *Breast Cancer Research*, 7(6):R1005, 2005. 3.3.7.13
- [139] Dimitrios Balafoutas, Axel Zur Hausen, Sebastian Mayer, Marc Hirschfeld, Markus Jaeger, Dominik Denschlag, Gerald Gitsch, Achim Jungbluth, and Elmar Stickeler. Cancer testis

- antigens and NY-BR-1 expression in primary breast cancer: prognostic and therapeutic implications. *BMC cancer*, 13(1):271, 2013. 3.3.7.14
- [140] Wenwen Wu, Ko Sato, Ayaka Koike, Hiroyuki Nishikawa, Hirotaka Koizumi, Ashok R Venkitaraman, and Tomohiko Ohta. HERC2 is an E3 ligase that targets BRCA1 for degradation. *Cancer research*, 70(15):6384–6392, 2010. 3.3.7.14
- [141] Daniel J Klein, Caroline F Thorn, Zeruesenay Desta, David A Flockhart, Russ B Altman, and Teri E Klein. PharmGKB summary: tamoxifen pathway, pharmacokinetics. *Pharmacogenetics and genomics*, 23(11):643–647, 2013. 3.3.7.15, S8
- [142] M Whirl-Carrillo, EM McDonagh, JM Hebert, Li Gong, K Sangkuhl, CF Thorn, RB Altman, and Teri E Klein. Pharmacogenomics knowledge for personalized medicine. *Clinical Pharmacology & Therapeutics*, 92(4):414–417, 2012. 3.3.7.15, S7
- [143] Jan A Burger, Meike Burger, and Thomas J Kipps. Chronic lymphocytic leukemia B cells express functional CXCR4 chemokine receptors that mediate spontaneous migration beneath bone marrow stromal cells. *Blood*, 94(11):3658–3667, 1999. 4.2
- [144] Bikash Debnath, Shili Xu, Fedora Grande, Antonio Garofalo, and Nouri Neamati. Small molecule inhibitors of CXCR4. *Theranostics*, 3(1):47, 2013. 4.2
- [145] Paul Labhart, Sudipan Karmakar, Eleni M Salicru, Brian S Egan, Vassilios Alexiadis, Bert W O’Malley, and Carolyn L Smith. Identification of target genes in breast cancer cells directly regulated by the SRC-3/AIB1 coactivator. *Proceedings of the National Academy of Sciences of the United States of America*, 102(5):1339–1344, 2005. 4.3.2
- [146] Loren W Runnels, Lixia Yue, and David E Clapham. The TRPM7 channel is inactivated by PIP2 hydrolysis. *Nature cell biology*, 4(5):329–336, 2002. 4.3.2
- [147] Jeroen Middelbeek, Arthur J Kuipers, Linda Henneman, Daan Visser, Ilse Eidhof, Remco van Horssen, Bé Wieringa, Sander V Canisius, Wilbert Zwart, Lodewyk F Wessels, et al. TRPM7 is required for breast tumor cell metastasis. *Cancer research*, 72(16):4250–4261, 2012. 4.3.2
- [148] Lidia Nieto, Inga M Tharun, Mark Balk, Hans Wienk, Rolf Boelens, Christian Ottmann, Lech-Gustav Milroy, and Luc Brunsvelde. Estrogen receptor folding modulates csrc kinase sh2 interaction via a helical binding mode. *ACS chemical biology*, 2015. 4.3.3
- [149] Nissim Hay and Nahum Sonenberg. Upstream and downstream of mTOR. *Genes & development*, 18(16):1926–1945, 2004. 4.3.3

- [150] Eijiro Yamada, Shuichi Okada, Tsugumichi Saito, Kihachi Ohshima, Minoru Sato, Takafumi Tsuchiya, Yutaka Uehara, Hiroyuki Shimizu, and Masatomo Mori. Akt2 phosphorylates Synip to regulate docking and fusion of GLUT4-containing vesicles. *The Journal of cell biology*, 168(6):921–928, 2005. 4.3.3
- [151] Pablo Garrido, Javier Morán, Ana Alonso, Segundo González, and Celestino González. 17β -estradiol activates glucose uptake via GLUT4 translocation and PI3K/Akt signaling pathway in MCF-7 cells. *Endocrinology*, 154(6):1979–1989, 2013. 4.3.3
- [152] Veronica Wendy Setiawan, Susan E Hankinson, Graham A Colditz, David J Hunter, and Immaculata De Vivo. HSD17B1 gene polymorphisms and risk of endometrial and breast cancer. *Cancer Epidemiology Biomarkers & Prevention*, 13(2):213–219, 2004. 4.3.3
- [153] Simon Anders and Wolfgang Huber. Differential expression analysis for sequence count data. *Genome biol*, 11(10):R106, 2010. S3

List of Figures

1.1	Key signalling pathways in breast cancer based on somatically mutated genes	3
1.2	Top mutated and amplified genes in metastatic breast cancers	4
1.3	ESR1 mutation in metastatic breast cancer	5
1.4	Targeting agents under clinical development	8
1.5	Different types of chromosomal rearrangements	9
1.6	Different categories of gene fusions	10
1.7	Number of newly reported fusions from 1982 to 2014	12
1.8	Copy number variance of each fusion partner gene identified by PRADA	14
1.9	Method of fusion detection in deFuse	16
1.10	Relative importance of 11 features in deFuse adaboost classifier	16
1.11	ROC curve of adaboost probability in deFuse	17
2.1	Example of quality control of an RNA-seq sample	21
2.2	Overview of data flow in RNA-seq analysis	22
2.3	171 paired-end RNA-seq samples from 15 different entities.	24
3.1	Copy number variance in primary and refractory breast tumors	28
3.2	Distribution of base substitutions in breast cancer	28
3.3	SNVs and Indels in primary breast tumors	29
3.4	SNVs and Indels in refractory breast tumors	30
3.5	SNVs and Indels in list of genes from estrogen pathway in breast primary and refractory tumors	32
3.6	Tumor DNA allele variance and tumor allele expression	33
3.7	The number of recurrent fusions in 15 different entities	34
3.8	Identified fusion genes and recovery rate of validated fusions among different tools	36

3.9	ConfFuse score and recovery rate in 96 published samples	37
3.10	Comparison of probability predicted by deFuse and confidence score by confFuse in 96 published RNA-seq samples	39
3.11	18 high-confidence fusions validated by RT-PCR followed by Sanger sequencing .	40
3.12	Comparison of different fusion detection tools in 22 GBM	41
3.13	Validated fusions in 22 GBM based on known fusions and DNA-seq supporting evidence	43
3.14	Plot of 12 recurrent fusions (score ≥ 6.5) in 48 GBM samples	46
3.15	Gene expression of GLI1 in 75 samples	48
3.16	Number of fusions scored ≥ 6.5 (top) and ≥ 8 (bottom) in 135 lymphoma samples	49
3.17	Plot of 29 recurrent fusion genes scored ≥ 6.5 in 135 lymphoma samples	51
3.18	Number of fusions identified in CLL samples from ICGC and HIPO-005 project .	52
3.19	Structures of gene fusions CXCR4:PTMA and CXCR4:GNAS, and Sanger sequencing of fusion boundaries	55
3.20	Structures of eight validated fusions in CLL	56
3.21	Expression of novel regions located CXCR4 upstream	57
3.22	Expression of CXCR4 and non-annotated regions	58
3.23	Correlation coefficient between CXCR4 and non-annotated regions	59
3.24	Novel expressed regions in ependymoma	60
3.25	Fusion-involved genes in Her2 breast cancer pathway	65
3.26	Fusion-involved genes in the MAPK signalling pathway	67
3.27	Example of fusion leading to abnormal exon expression in 5' fusion partner . .	71
3.28	Example of fusion leading to abnormal exon expression in 3' fusion partner .	72
3.29	Examples of potential fusion proteins (intra-chromosome) in two primary tumors	74
3.30	Genomic distributions of high confidence fusions across tumor entities . .	76
S1	The number of read pairs in 96 published paired-end RNA-seq samples from seven different studies	86
S2	Mapping quality control of 98 breast RNA-seq samples in HIPO-017	90
S3	Multidimensional scaling of 106 breast tumor RNA-seq samples	91
S4	Number of fusions in 118 breast tumors	92
S5	Novel non-annotated region in upstream of gene HSD17B4	93
S6	Example of required computer resource in running deFuse	93

S7	Estrogen metabolism in the liver	94
S8	Tamoxifen metabolism in the liver	95

List of Tables

1.1	An overview of different fusion detection tools based on RNA-seq data	11
1.2	RNA-seq data set from 13 different tumor types in TCGA	12
1.3	Number of known/identified gene fusions in different neoplasia subtypes	13
2.1	The weights of single and combined features in confFuse scoring algorithm.	25
3.1	Mutations of calcium channel, voltage-dependent, alpha subunits (CACNA)	31
3.2	The recovery of validated fusions for deFuse, confFuse-6.5 and confFuse-8	35
3.3	The recovery of validated fusions in fusionMap	36
3.4	The recovery of validated fusions in soapFuse.	37
3.5	High-confidence fusion genes in 27 INFORM samples	42
3.6	Recurrent fusion genes identified in HIPO-028 sarcoma samples.	43
3.7	Fusions with recurrent partners (score ≥ 8) in 83 sarcoma samples	44
3.8	24 high-confidence fusion genes identified in 11 early-onset prostate cancer	45
3.9	Recurrent fusions ($n=12$, score ≥ 6.5) in 48 GBM samples	47
3.10	29 recurrent fusion genes (score ≥ 6.5) in 135 lymphoma samples	50
3.11	Nine validated fusion in lymphoma samples	50
3.12	Recurrent fusions in CLL samples from HIPO-005 and ICGC projects	53
3.13	15 fusions validated by RT-PCR and Sanger sequencing in three CLL samples	55
3.14	Distribution of fusion genes identified in 118 breast tumors across 13 different functional categories	61
3.15	Recurrent rearrangements of fusion partner genes found in the list of census genes (COSMIC)	68
3.16	Recurrent fusions in 118 breast tumor samples	69
3.17	Potential fusion proteins (inter-chromosome) identified by confFuse in 118 breast tumor samples	70

3.18 Potential fusion proteins (intra-chromosome) identified by confFuse in 118 breast tumor samples	73
S1 Sequenced-read length of seven published studies	86
S2 Validated fusions from 96 paired-end RNA-seq samples in seven published studies	86
S3 Validation results of three breast tumor samples	96
S4 Fusions identified in 83 sarcoma samples	98
S5 Fusions identified in 84 prostate cancer	112
S6 Fusions identified in 48 GBM samples	116
S7 Fusions identified in 135 lymphomas samples	121
S8 Fusions identified in 114 CLL samples from HIPO-005	125
S9 Fusions identified in 25 ependymoma samples	133
S10 Fusions identified in 118 breast tumor samples	134
S11 Fusions identified across 13 different categories	153
S12 Mutations of CYP, SULT and UGT family genes	169